Physical-Chemical Properties and Sorption Characteristics of Peat

Presented for the Degree of Ph.D. by

Domenico M.S. Delicato, B.A.

Under the Supervision of Dr. Odilla Finlayson,

School of Chemical Sciences,

Dublin City University

July 1996

I hereby certify that this material, which I now submit for assessment on the program of study leading to the award of Ph.D. is entirely my own work and has not been taken from the work of others save and to the extent that such work has been cited and acknowledged within the text of my work

Signed: Domenico Delicato ID No.: 91701082

Date: 23/9/96

Table of Contents

Abstract

The physicochemical properties of peat fibre, peat moss and two processed forms of peat moss were studied The properties examined included thermal analysis (by TGA and DSC), IR spectroscopy and the zero point of charge From DSC analysis it was found that the ignition point for the peat materials occurred at about 200°C Above this temperature there were three exothermic peaks recorded, the first at c 333°C corresponded to the decomposition of cellulose, the second at c 438°C to the decomposition of bitumens and/or humic substance and the third at c 479°C to the decomposition of lignin

The surface area of the peat fibre was measured by methylene blue dye adsorption, N_2 adsorption and the negative adsorption of chloride ions The surface areas measured by the three methods were 307, 2 3 and 0 05 $m^2\ g^{-1}$ respectively The variation in surface areas was in keeping with the large differences in surface areas which have been reported for SOM

The sorption of a series of alcohols from vapour and aqueous phase by peat fibre was also studied It was found that the sorption of alcohols from the vapour phase decreased in the order ethanol > 2-propanol > 1-butanol > 1-pentanol while the sorption from the aqueous phase decreased in the order 1-hexanol > 1-pentanol > 1-butanol > 2-propanol > ethanol The results were inconclusive, but suggested that the sorption from the vapour phase was principally by adsorption followed by absorption into the interior of the peat, while the sorption from the aqueous phase was principally by adsorption

A lab-scale biofilter was set up to eliminate ethanol vapour from an artificial waste gas stream using peat fibre as the filter material After about 80 days of operation over 80 % of the ethanol vapour (inlet concentration c 76 g dm^{-3}) was being eliminated The elimination capacity was calculated to be c 61 g $dm^{-3}\ h^{-1}$ and the critical gas constant to be c 60 g dm^{-3}

Acknowledgements

It's amazed me the number of people who want to be acknowledged in this thesis not one ! However, I'm not one to be intimidated by such a hostile response, so without further ado I'll roll on the credits

Firstly, I would like to thank my supervisor Dr Odilla Finlayson for all her help, encouragement and advice which she has given me through out my four years at DCU I would also like to acknowledge the help of Dr B Quilty and her students in the Biology Department, and to Dr I Shannahan for her help with the biofiltration project I also want to thank Bord na Mona for their financial support and for supplying materials, equipment and advice during the course of my work

To my fellow inmates in AG20, Mick Tiernan and Mick O'Brien for all their help (lack of, that is), crack(ed in the head) and putting up with me for so long without resorting to physical violence (well almost never)

I would like to thank the technicians and post-grads in the Chemistry Department for giving me such an 'interesting' time at DCU

Thanks to the members of the self-help group, Pat (who was never there, but still managed to turn the office into his laundry room), Ciaran (who is offensively nice) and John for his help and advice (whether wanted or not)

Finally, but by no means last, I want to thank my parents and family for their help, encouragement, financial assistance and for generally annoying me until I got it done

Introduction

Peat is an organic soil which is derived from decayed vegetative matter that has built up in areas of poor water drainage It is a complex, heterogeneous material which can vary considerably in its chemical composition and physical properties In general, peat, along with other forms of soil organic matter (SOM), is an amorphous material with a poorly defined structural arrangement As a result, there is considerable difficulty in estimating the surface area of peat materials and in determining the sorption mechanism of peat for the uptake of organic compounds This thesis is concerned basically with measuring the surface area of peat fibre using three different methods of surface area determination, and in examining its sorption mechanism for the uptake of a series of alcohols from the vapour and aqueous phases A separate project, which is reported in Chapter 4, examines the use of peat fibre as the filter bed material of a biofilter for the elimination of ethanol from an artificial waste gas stream

A brief overview of soil discussing its formation, classification and its major constituents, is given in Chapter 1 In particular, this introductory chapter describes in Sections 1 2 to 1 4 the structure and physical properties of the soil mineral and organic matter fractions of soil which are of relevance to the proceeding chapters

Chapter 2 begins by describing the formation, classification, chemical composition and physical properties of peat in Sections 2 1 1 to 2 3 1 The thermal analysis of peat is reviewed in Section 2 3 2 in relation to the decomposition of the various components of peat The experimental section (Sections 2 5 to 2 5 2) presents and discusses the results from the analysis of peat fibre, peat moss and two processed forms of peat moss The physiochemical properties which are reported in this chapter are relevant to the surface area measurements that are described in Chapter 3 The physicochemical properties of the peat materials examined included their pH, moisture, ash content, point of zero charge, thermal analysis (by DSC and TGA), SEM studies and IR spectroscopy

The results from the determination of the surface area of peat fibre and its sorption mechanism for the uptake of a series of alcohols are reported in Chapter 3 This chapter begins by describing the various forces of adsorption and absorption which are responsible for the uptake of organic compounds by soil The methods used for measuring the surface area of the soil mineral and organic matter fractions are discussed in Sections 3 2 to 3 2 3 In particular, attention is drawn to the operationally defined nature of surface area when dealing with soil materials The sorption of non-ionic organic compounds by SOM from aqueous and non-aqueous

phases are reviewed in Sections 3 3 1 and 3 3 2, while their sorption from the vapour phase is examined in Section 3 3 3 The experimental section of this chapter, Section 3 5 2 1, compares and discusses the results of the three methods used to estimate the surface area of peat fibre The three methods used were the adsorption of N_2 using the single point BET method, the adsorption of methylene blue from aqueous solution and the negative adsorption of chloride ions from aqueous solution The results from the sorption of a series of alcohols from the vapour and aqueous phases are presented in Section 3 5 2 2 The results of the sorption studies are examined and their implications for the sorption mechanism of peat fibre for its uptake of alcohols from the vapour and aqueous phases are discussed

Chapter 4 examines the use of biofiltration for the elimination of contaminants from waste gas streams It begins by briefly describing in Section 4 1 the physical, chemical, thermal and biological methods which are presently available for the treatment of waste gases Section 4 2 describes in detail the various operational parameters which are important for the efficient running of a biofilter Sections 4 4 and 4 5 review the elimination of organic and inorganic compounds from waste gases, under various headings of volatile organic compounds (VOCs) and volatile inorganic compounds (VICs) The experimental section (Section 4 7) presents results from a lab-scale biofilter, which used peat fibre as the filter material, for the elimination of ethanol vapour from an artificial gas stream

Chapter 1

General Overview of Soil and Its Major Constituents

1 Introduction

Soil is a mixture of finely divided components consisting of weathered rock, gas, water and organic matter, in varying proportions It is a naturally occurring body of material which covers most of the upper crust of the earth as a continuum On average soil covers the bed rock to a depth of 2 m but its thickness can vary considerably from less than 1 m to depths of up to 50 m in some areas Due to different environmental factors which acted on a particular soil during its formation no two soils are identical in their exact composition or physicochemical properties The environmental factors responsible for the formation of a soil include the parent rock from which it was derived, the climatic conditions under which the soil formed, its relationship to the local water table, its age, and the growth and activity of plants and animals

Soil is important in sustaining life Apart from supplying vegetation with the nutrients that are required for growth, soil also has an important role in a number of natural cycles, such as the recycling of carbon, nitrogen and sulphur (1, 2)

This chapter discusses the origin and formation of soils and their major inorganic and organic constituents The classification, structure, chemical characterisation, and physical properties of soils which are relevant to this work are also discussed

1 1 The Formation and Classification of Soils

(a) Formation

The formation of a particular soil is due to (i) the combined action of a number of different physical and chemical processes, which are collectively referred to as weathering, and (ii) to biological activity which is carried out by soil organisms, such as burrowing animals (e g worms) and soil micro-organisms These processes and some of their principal mechanisms of action are summarised in Table 1 1

Through the combined action of weathering and biological activity consolidated bed rock is gradually transformed into soil Soil formation is a slow process and it involves several stages of development, which are usually occurring concurrently Initially, there is fragmentation of the parent rock by physical weathering, which includes the abrasive action of running water wind and the freeze-thaw cycle Further action on the soil can occur *in situ* or it can involve the

Table 1 1 The Weathering and Biological Processes Occurring in Soil

Process	Mechanism of action
Physical	Abrasive processes leading to the break-up of bed-rock by the action of water, wind, glacial movement and the freeze-thaw cycle
Chemical	Transformation of primary minerals to secondary minerals by hydration, hydrolysis, oxidation, reduction, complexation, dissolution
Biological	Action is principally on organic matter by decomposition, transformation

of the soil by running water, gravity, or glacial movement to sites distant from the parent rock As the accumulation of rock debris occurs it is acted on further by chemical and biological processes This results m the transformation of the original minerals present in the parent rock, which are referred to as the primary minerals, into new mineral compounds that are termed the secondary minerals It is the dominance of one or more of the weathering/biological processes which results in the formation of a particular soil type, e g desert soils which consist mainly of sand and very little organic matter in arid climates, or peat soils which consist mainly of organic matter which has built up under water logged conditions It should be noted that the formation of a particular soil is a dynamic process Any change in the environmental conditions may alter the dominant weathering process, resulting in the development of a new soil type

The end product of weathering is the differentiation of the soil into various layers, termed horizons The horizons run parallel to the surface and are distinguished from one another by the dominance of one or more of the weathering/biological processes within a particular layer making it different from the horizons above and below it Both the presence and thickness of a horizon is variable, and is usually a characteristic of a particular soil type Up to five principal horizons called O, A, B, C and R can be distinguished, see Table 1 2 (1)

The O-horizon is the topmost layer of the soil and consists of organic matter debris In well drained soils the O-horizon is usually about 2 to 5 cm in thickness It represents the accumulation of dead organic matter from plant and animal sources which are at various stages of decomposition Peat soils, which are typically between 3 and 15 m in depth, are composed almost exclusively of this horizon

Table 1 2 The Principal Soil Horizons (1)

Horizon	Description
O	Organic horizon, composed of dead organic residues at various stages of decomposition
A	Accumulation of washed down organic matter, horizon of highest biological activity, removal of dissolved and suspended materials by water percolation
B	Horizon of maximum transformation of mineral constituents
C	Broken up bed-rock, very little weathering except for the accumulation of salts and oxides from upper horizons
R	Unweathered bed-rock

The A-horizon is immediately below the O-horizon Its dark colouring is due to the accumulation of organic matter which has been washed down from the layer above it by downwardly percolating water This is the horizon of maximum biological activity due to its high levels of organic matter, water and oxygen

The B-horizon is the transitional horizon between A and C and it represents the level of maximum mineral deposition The formation of minerals in this horizon is primarily due to the action to chemical weathering

The C-horizon is the layer of fragmented rock immediately above the bed-rock The rock fragments have undergone very little weathering

The R-horizon refers to the unaltered bed rock of the soil, which has not been altered by weathering

The process which results in the formation of the various soil horizons can be divided into the following (1)

(i) gains to the soil, which include the addition of new organic material to the top layer of the soil and also the addition of oxygen and water through oxidation and hydration processes In addition, gains may be due to the precipitation of dissolved salts and deposition of suspended material in water from the adjacent water tables,

(ii) losses of material, this occurs through the removal of dissolved and suspended material by the downward percolation of water and their dispersion to adjacent areas through the water table,

(iii) transfers between horizons, these can be as a result of the downward movement of water depositing materials from higher horizons into lower ones Also, it can be from the activity of burrowing animals which can mix soil components between layers, or, as a result of plants absorbing nutrients such as cations through their roots from lower horizons and returning them at the top layer by the loss of leaves,

(iv) transformation of soil components, this is a result of the processes of chemical weathering, and results in the break-up of the primary minerals and their deposition as secondary minerals

(b) Classification

Since 1975 the standard classification system used by the United States Department of Agriculture (USDA) has been based on the measurement of the physical and chemical properties of the soil *in situ* (1, 2) This system has the advantage of being able to broadly classify a soil of unknown origin into a particular order on the basis of its properties There are 10 orders of soil recognised in this system which are summarised in Table 1 3

The full classification of a soil requires statement of its order, suborder, great group, subgroup, family, and series (1, 2) A complete discussion of the USDA classification system falls beyond the scope of this work However, a brief definition of each of these levels of categorisation is outlined as follows

(i) the soil order broadly groups those soils together which were formed under similar conditions and which are similar in their horizon profile and the level of horizon development In addition, it also distinguishes, between mineral and organic soils,

(ii) the suborder (of which there are over 40) is a subdivision of the soil order It subdivides soils belonging to the same soil order into different groups based on various physicals characteristics such as pH, moisture content, temperature and the presence of other distinguishing soil properties,

Table 1.3 **The Soil Orders According to the USDA System (1)**

Order	General description
Alfisols	Soils with grey to brown surface horizons, medium to high base supply, with horizons of clay accumulation, usually moist, but may be dry during summer
Aridisols	Soils with pedogenic horizons, low in organic matter and usually dry
Entisols	Soils without pedogenic horizons
Histosols	Organic soils (peats and mucks)
Inceptisols	Soils that are usually moist, with pedogenic horizons of alteration of parent materials but not of illuviation
Mollisols	Soils with nearly black, organic-rich surface horizons and high base supply
Oxisols	Soils with residual accumulation of inactive clays, free oxides, kaolin, and quartz, mostly tropical
Spodosols	Soils with accumulations of amorphous materials in subsurface horizons
Ultisols	Soils that are usually moist, with horizons of clay accumulation and low supply of base
Vertisols	Soils with high contents of swelling clays and wide deep cracks during some seasons

(iii) the great group category groups soils together on the basis of having similar horizons in the same sequence to one another and which also share similar moisture and temperature characteristics,

(iv) the subgroup narrows the classification of the soils further by grouping those soils that are most similar in their major great group properties together,

(v) the family category of classification characterise the soils principally on their mineralogy and physical properties for plant growth,

(vi) the series is the lowest category in soil taxonomy, and it refers to the common name of a soil type The series name is usually taken from a town or region where the soil was first described

1.2 Soil Minerals

Inorganic materials comprise the dominant fraction of most soil types The most important groups are the silicates, aluminosilicates, the metal oxides and metal hydroxides, carbonates, and sulphates These minerals are formed from the weathered parent bed-rock materials The minerals may be classified as being either primary minerals, if they are derived directly from the parent rock, i e they have not undergone any chemical transformations, or as secondary mmerals if they are products of chemical weathering

Most minerals exist as crystalline solids and in particular as polymer type structures composed of repeating units of single or mixed compounds A mineral soil is referred to as being crystalline if the repeating structure extends over a distance of at least 3 nm (3) If the repeating structure does not extend over this distance the soil is said to be an amorphous mineral soil

The two most important repeating units found in mineral soils are

(i) the silica tetrahedral unit, SiO_4^{4-} (the oxygens at the corner of the tetrahedron are called apical oxygens),

(ii) the octahedral MX_6^{m-6b} unit, where M^{m+} is a metal cation, usually Al or Mg, and X^{b-} represents an anion

The tetrahedral and octahedral structures can exist in polymerised form to give the sheet structures shown in Figure 1 1 (3) The sheet of silica tetrahedrons is formed by the sharing of apical oxygens anions of the basic tetrahedral unit The octahedral sheet is formed by the sharing of edge oxygens If all the possible cation sites are filled in the octahedral sheet the sheet is said to be trioctahedral However, usually only two thirds of the possible sites are occupied by metal cations and in this case the sheet is referred to as dioctahedral, see Figure 1 1

Both of these sheet structures combine further to form an important group of minerals called the phyllosilicates (or aluminosilictes), which are commonly referred to as the clay minerals, clay soils or just clays The clays are formed by the joining of the tetrahedral and octahedral sheet structures through the sharing of the apical oxygen anions of the tetrahedral sheet (3), see Figure 1 2

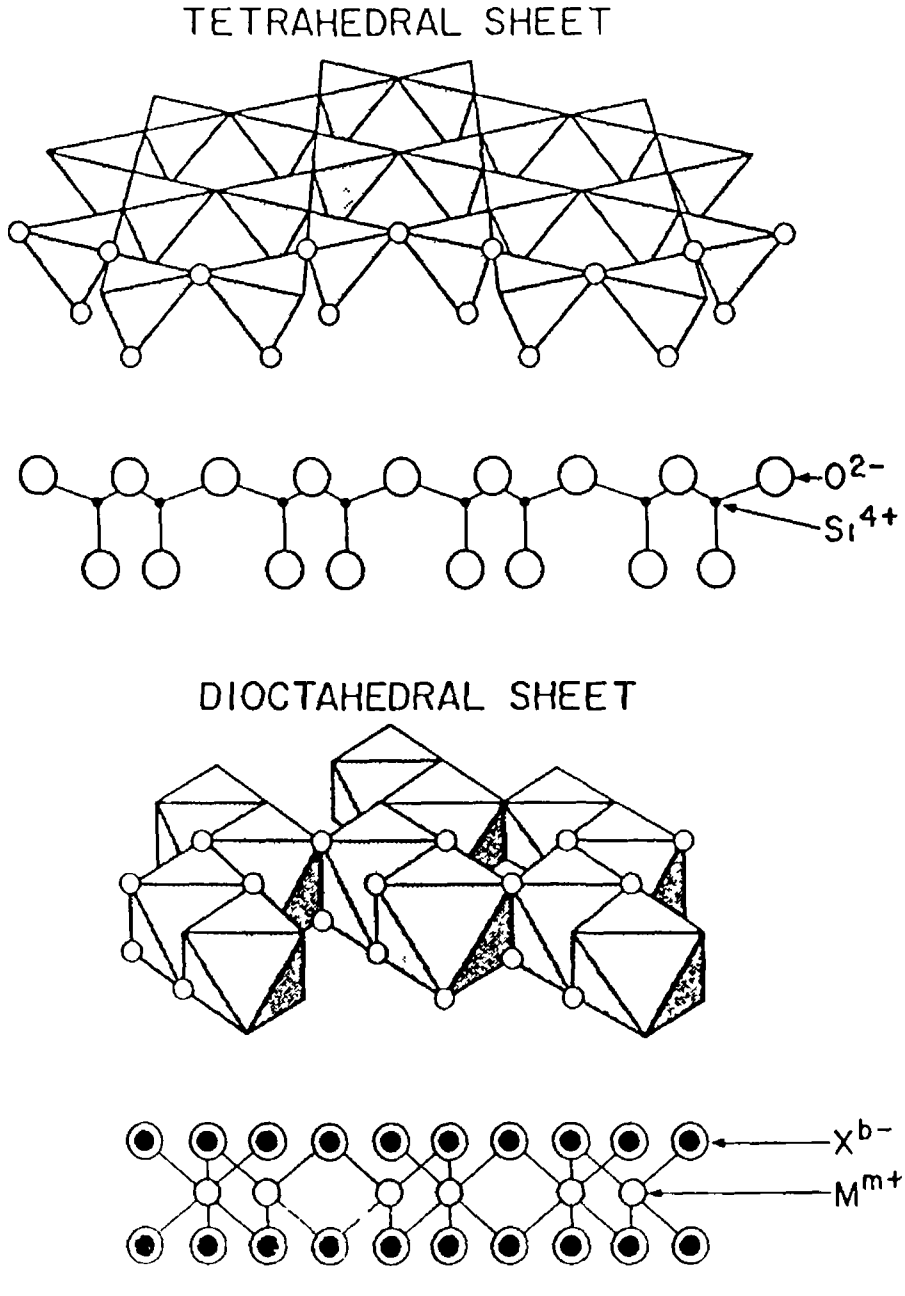

Figure 1.1 **The Sheet Polymeric Structure of the Silica Tetrahedral SiO_4^{4-} Unit and the Metal Octahedral MX_6^{m-6b} Unit (3)** Note The open circles at the polyhedral vertices in each perspective view are shown directly below in a projection along the crystallogtaphic *a* axis

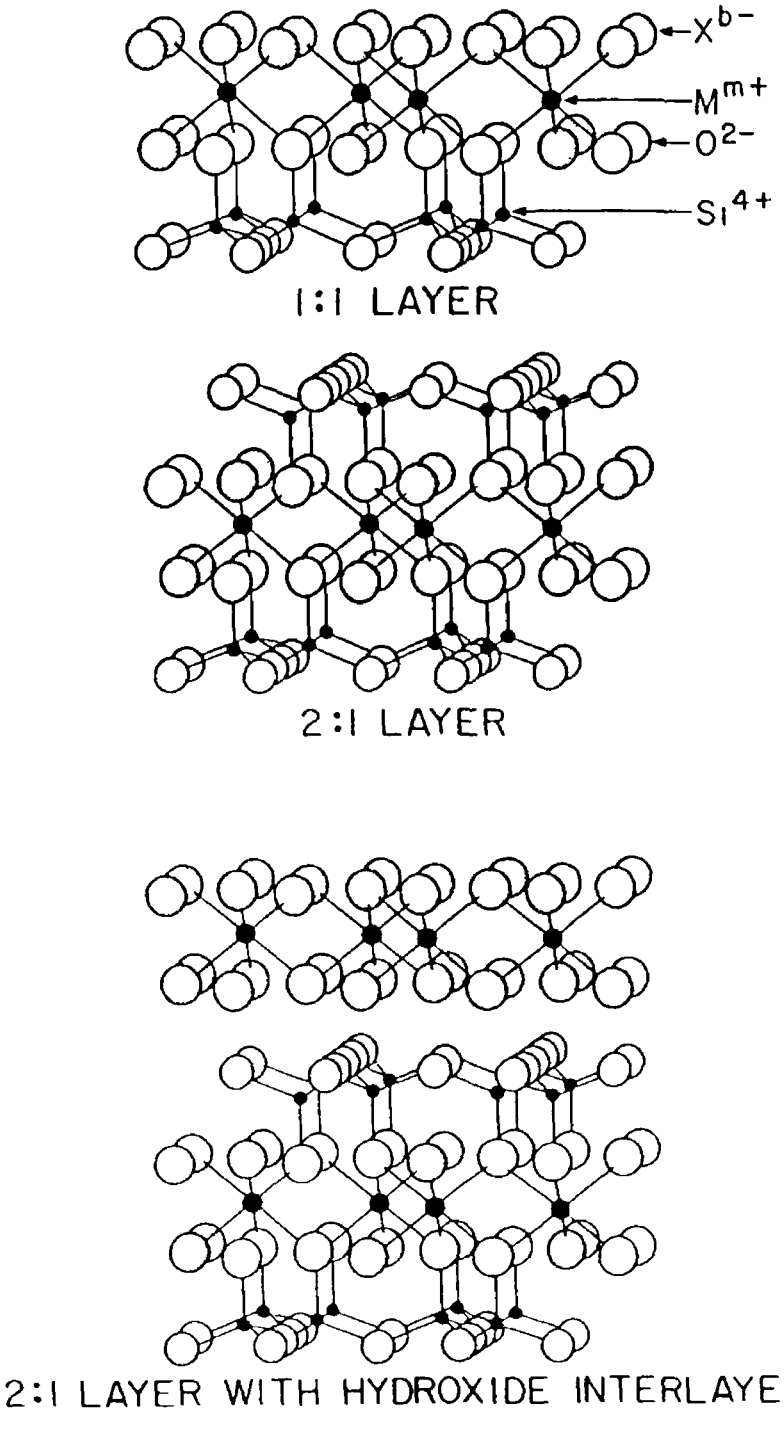

Figure 1.2 The Three Layer Types for Pollysilicates Structures in Soils (3)

Note All shown here are dioctahedral with hydroxy groups shown as shaded circles

The clays are distinguished into three layer types by the ratio of tetrahedral sheets to octahedral sheets, these are the 1 1 clays, the 2 1 clays, and the 2 1 clays with hydroxyl interlayers, see Figure 1 2 The clays are further divided into five groups based on the amount of isomorphic substitution of the central cation which has occurred, see Table 1 4 Isomorphic substitution refers to the replacing of the central cation by a second cation of similar size, but not necessarily of the same valency, without seriously distorting the crystal structure during the formation of the clay Examples of isomorphic substitution include the replacement of Si^{4+} by Al^{3+} in the tetrahedral position, or the replacement of Al^{3+} by Mg^{2+} in the octahedral position As a result of isomorphic substitution the charges present in the cell-unit may no longer sum to zero and there is a net negative charge on the clay This is referred to as the permanent charge of the clay It is usually balanced by the presence of adsorbed cations, such as K^+ or Ca^{2+}, at the external surface of the clay particle, or between the layers (i e the interlayer positions) A second charge, referred to as the pH-dependent charge, is due to the protonation/deprotonation of surface hydroxyl groups, and as the name suggests, varies with the pH of the clay's environment Each layer type will now be discussed below

Table 1 4 The Classification of the Clays (3)

Layer type	Group	Layer charge	Chemical formula coefficients			
			a	b	c	c'
1 1	Kaolinite	< 0 01	-	-	-	-
2 1	Smectite[a]	0 5-1 2	8	3 2	c+c'~0 2	
2 1	Vermiculite	1 2-1 8	7	3	0 5	-
2 1	Mica (illitic)	1 4-2 0	6 8	3	c+c'~0 25	
2 1[b]	Chlorite	variable	2 4	8 4	0 5	1 5

Note [a] Principally montmorillonite [b] With hydroxide interlayers

(a) 1 1 Clays

The 1 1 layer type consists of one tetrahedral sheet and one octahedral sheet and has the following unit cell formula

$$[Si]_4(Al)_4O_{10}(OH)_{10}$$

where the cation in the square brackets is in the tetrahedral co-ordination position and the cation in the parentheses is in the octahedral co-ordination position An example of the 1 1 clays is the kaolinite group This group has usually undergone very little isomorphic substitution, and as a result they have a very small permanent negative charge associated with them The arrangement of oxygen and hydroxide planes on opposing faces of the interlayer gives rise to hydrogen bonding between the sheets, see Figure 1 3 This bonding is strong enough to prevent the intrusion of water and cations into the interlayer regions As a result the adsorption of ions, organic compounds, etc , is confined to the external surfaces of these clays (2, 3)

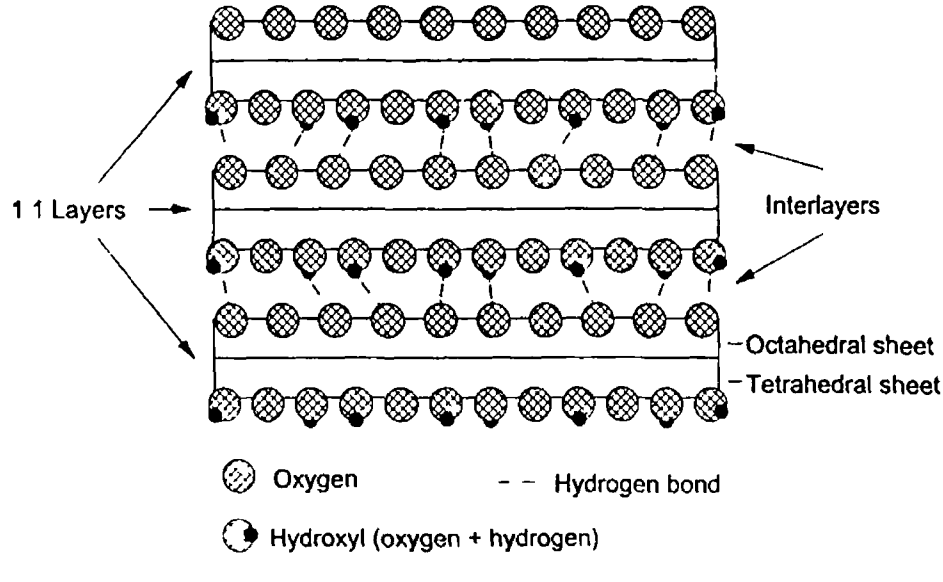

Figure 1.3 The Hydrogen Bonding of Adjacent 1.1 Layers (2)

(b) 2 1 Clays

The 2 1 layer types consist of one octahedral sheet which is sandwiched between two tetrahedral sheets as shown in Figure 1 2 They have the general unit formula

$$M_x [Si_a Al_{8-a}] (Al_b Fe(III)_c Fe(II)_{c'} Mg_{4-b-c-c'}) O_{20}(OH)_4$$

where M represents one mole of cation charge on the surface layer and a, b, c and c' are the stoichiometric coefficients The layer charge, x is given by Equation 1 1,

$$x = 12 - a - b - c \qquad \text{Equation 1 1}$$

where a, b, c are coefficients given in Table 1 4, and x is the number of moles of net electron charge per unit cell that is produced by isomorphic substitution

There are three layer groups within the 2 1 layer type, these are the mica, vermiculite and smectite groups The 2 1 groups are distinguished by differences in their layer charge which is found to decrease in the order mica > vermiculite > smectite In addition the vermiculites are distinguished from the smectites in that the former has more isomorphic substitution in its tetrahedral sheet (3)

Unlike the 1 1 clays, the opposite facing surfaces of 2 1 clays are composed only of oxygen (2, 3) As a result, the adjacent layers are held weakly together by van der Waals forces and by their mutual attraction for interlayer cations The weaker forces of attraction give rise to the swelling phenomena of 2 1 clays under water saturated conditions in the soil The swelling is due to the ability of the water molecules to gain access to the interlayer regions of the clay and force the sheets apart, see Figure 1 4 (2) The strength of the attraction between the adjacent layers has been found to decrease with increasing isomorphic substitution in the clay, and with increasing size of the hydrated interlayer cations (3) The swelling of the clay results in large increases in its surface area when fully swollen This in turn has important consequences for the determination of surface area of the clays which is discussed further in Chapter 3

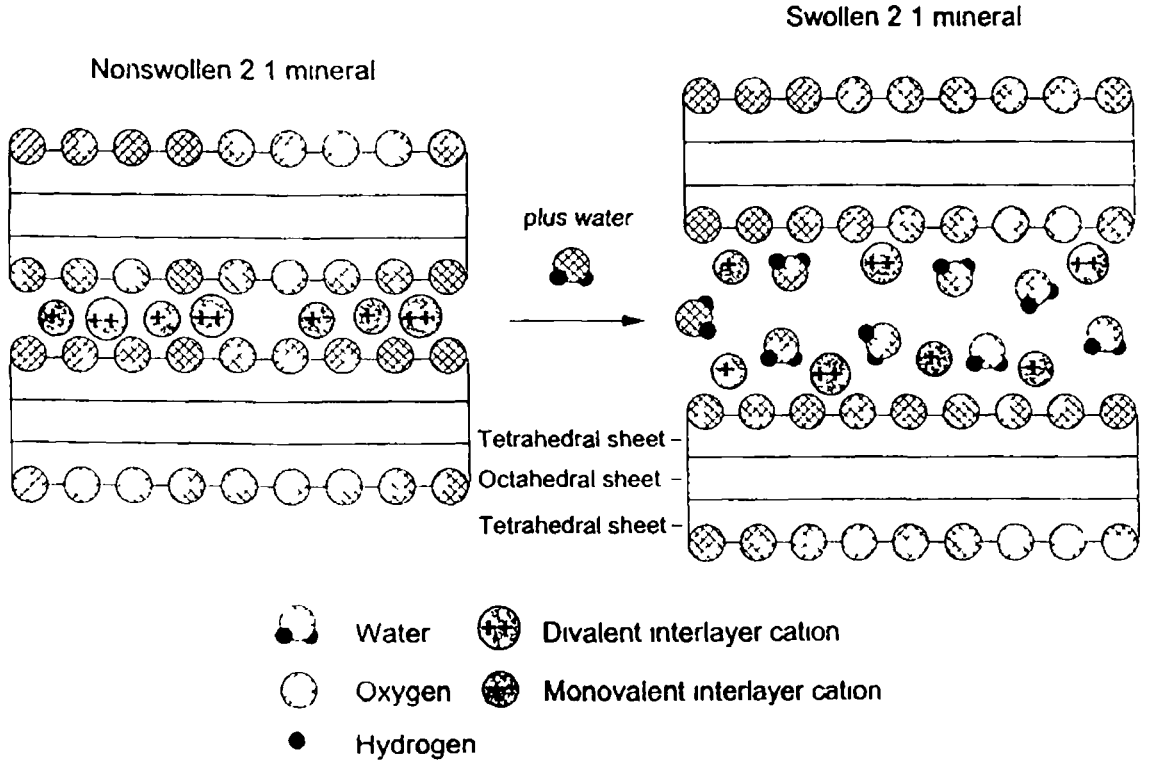

Figure 1 4 Swelling in a 2 1 Clay Mineral (2)

(c) 2 1 Clays with Hydroxide Interlayers

The 2 1 layer type with hydroxide interlayer is represented by the chlorite group The unit cell formula for chlorite is

$$[Si_aAl_{8-a}] (Al_b Fe(III)_c Mg_{c'}) O_{20}(OH)_{16}$$

The octahedrally co-ordinated metal cations are present in two sheets, namely in the 2 1 sheet structure as $M(OH)_2O_4^{m-10}$, where M^{m+} can be Al^{3+}, Fe^{3+} or Mg^{2+}, and in the interlayer sheet mainly as $Al(OH)_6^{3-}$

In addition to the clays there are numerous other minerals present in soil These mainly consist of octahedrally co-ordinated metal cations, which like the phyllosilicates, are present as sheet structures In particular the metals aluminium, iron and magnesium predominate because of their abundance in the earth's crust and due to their low water solubility in most soils A list of the most widespread minerals found in soil is given in Table 1 5 The structure of two of the most common minerals, goethite and gibbsite, are shown in Figure 1 5

Table 1 5 The Metal Oxides, Oxyhydroxides and Hydroxides Commonly Found in Mineral Soils (3)

Name	Formula	Name	Formula
Anatase	TiO_2	Hematite[a]	α-Fe_2O_3
Birnessite	$Na_{0.7}Ca_{0.3}Mn_7O_{14}$ 2 8 H_2O	Ilmenite	$FeTiO_3$
Boehmite[a]	γ-AlOOH	Lepidocrocite[a]	γ-FeOOH
Ferrihydrite	Fe_2O_3 2FeOOH 2 6 H_2O	Lithiophorite	$(Al,Li)MnO_2(OH)_2$
Gibbsite[a]	γ-$Al(OH)_3$	Maghemite[a,b]	γ-Fe_2O_3
Goethite[a]	α-FeOOH	Magnetite[b]	$FeFe_2O_4$

Note ([a]) The γ denotes cubic close-packing of anions, and the α denotes hexagonal close-packing ([b]) Some of the Fe(III) ions are in tetrahedral co-ordination

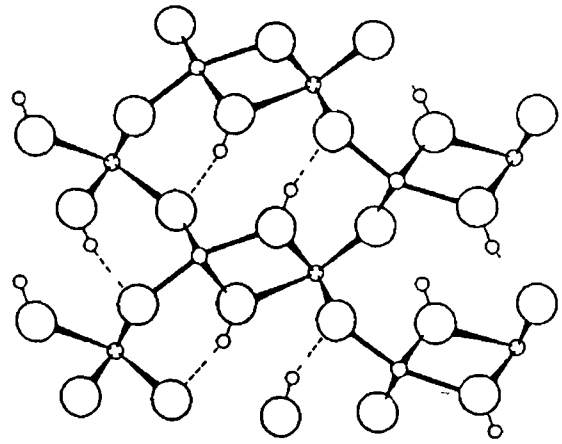

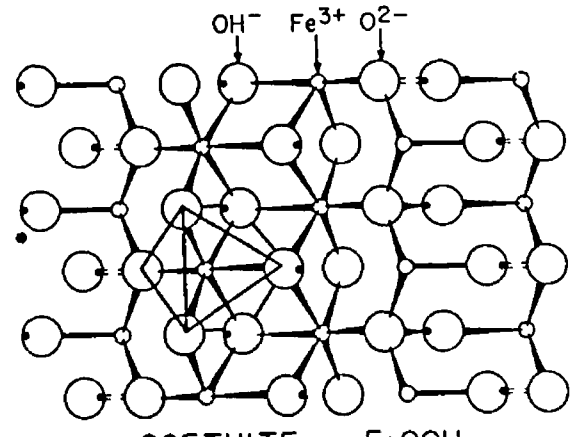

GOETHITE, α-FeOOH

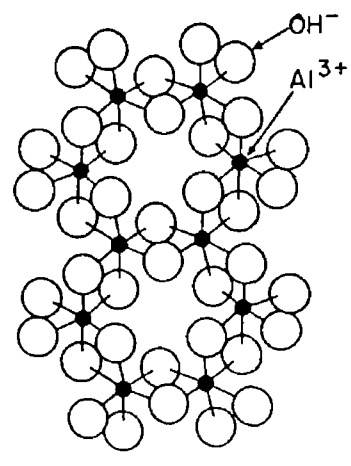

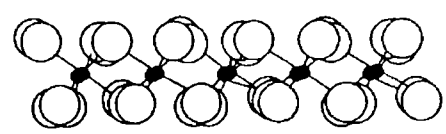

GIBBSITE, γ-Al(OH)$_3$

Figure 1 5 **The Structure of Goethite and Gibbsite (3)** Note The structure of goethite and gibbsite are shown projected along the crystallographic c axis (upper) and a axis (lower) Hydrogen bonds in goethite are indicated by dashed lines, and an $FeO_3(OH)_3$ octahedron is outlined in the a axis projection

1.3 Soil Organic Matter

The organic matter content of mineral soil usually accounts for only 1 to 5 % of the soil's dry weight However, for the organic soils, such as peat, the organic matter content varies from 20 % to over 99 % of the soil's dry weight All the organic matter in soil is collectively referred to as soil organic matter (SOM) Thus, SOM is composed of plant, animal and microbial residues which are at various stages of decomposition The highly decomposed fraction of SOM, which is the most abundant and most stable form of organic matter present in soil, consists of the humic and fulvic acids (which are discussed in detail in the following sections) This fraction of SOM is collectively referred to as the humic substances (other names include humus or humates) In fact the humic substances account for 70 to 80 % of the organic matter found in mineral soils For this reason the humic substances have received the greatest attention by soil scientists, and most of the knowledge concerning SOM is derived from the study of humic and fulvic acids (4)

1 3 1 The Formation of Humic Substances

The formation of humic substances is a complex process that is still poorly understood It is thought that they are derived mainly from vegetative matter which has undergone extensive decomposition and transformation in the soil, see Figure 1 6 (3) It is known that the synthesis of the humic substances does involve the formation of phenolic compounds which are themselves derived from the decomposition of proteins, carbohydrates and lignin In particular, soil micro-organisms are thought to play an important part in the formation of the humic substances both in the breakdown of the vegetative matter and in the formation of the phenolic precursors of the humic substances (4, 5)

The organic matter residues which contribute to humic substances (and SOM formation) can be classified into the following groups

(i) the plant carbohydrates, such as cellulose, hemicellulose, pectin, and chitin (chitin is a major cell wall component of fungi),
(ii) lignin, and the lignin like materials,
(iii) nitrogen containing compounds, which consist mainly of amino acids derived from micro-organisms,
(iv) microbial cell wall components, in particular peptidoglycan, and other microbial synthesised materials such as melanin and aspergillin

A more detailed description of these materials is given in Section 2 2 1 in relation to their contribution to the formation of peat soils

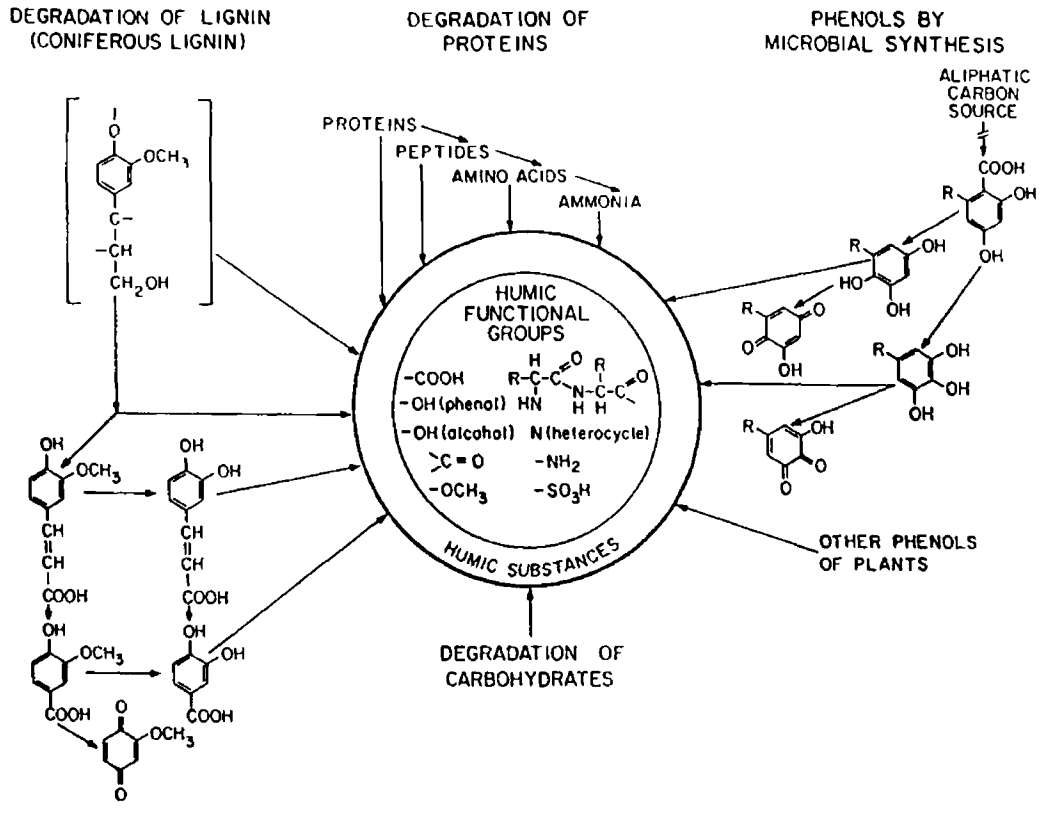

Figure 1.6 The Degradation of Plant Residues and the Formation of Humic Substances (5)

Several hypotheses have been proposed to explain the synthesis of humic substances (4) which are as follows

(i) the plant alteration hypothesis, which suggests that the more resistant plant materials, notably lignin, are only superficially altered to form the humic substances According to this theory the high-molecular weight humic acids and humins are the first to be formed These are subsequently degraded to form the fulvic acids which are further oxidised to CO_2 and H_2O However, this hypothesis is doubtful since it is known that Antarctic humic substances (which are similar to humic substances found elsewhere) are formed from mosses which contain little if any lignin (6),

(ii) the chemical polymerisation hypothesis The soil-micro-organisms break down the plant materials, and synthesise phenols and ammo compounds which are eventually released into the surrounding environment These compounds are subsequently oxidised and polymerised to form the humic substances There are two possible mechanisms which have been proposed to describe the formation of the humic substances (5)

- the browing mechanism, this involves the reaction of an amino compound with a sugar residue, a generalised pathway for this mechanism is shown in Figure 1 7 The resultant amino-sugar compound undergoes rearrangement

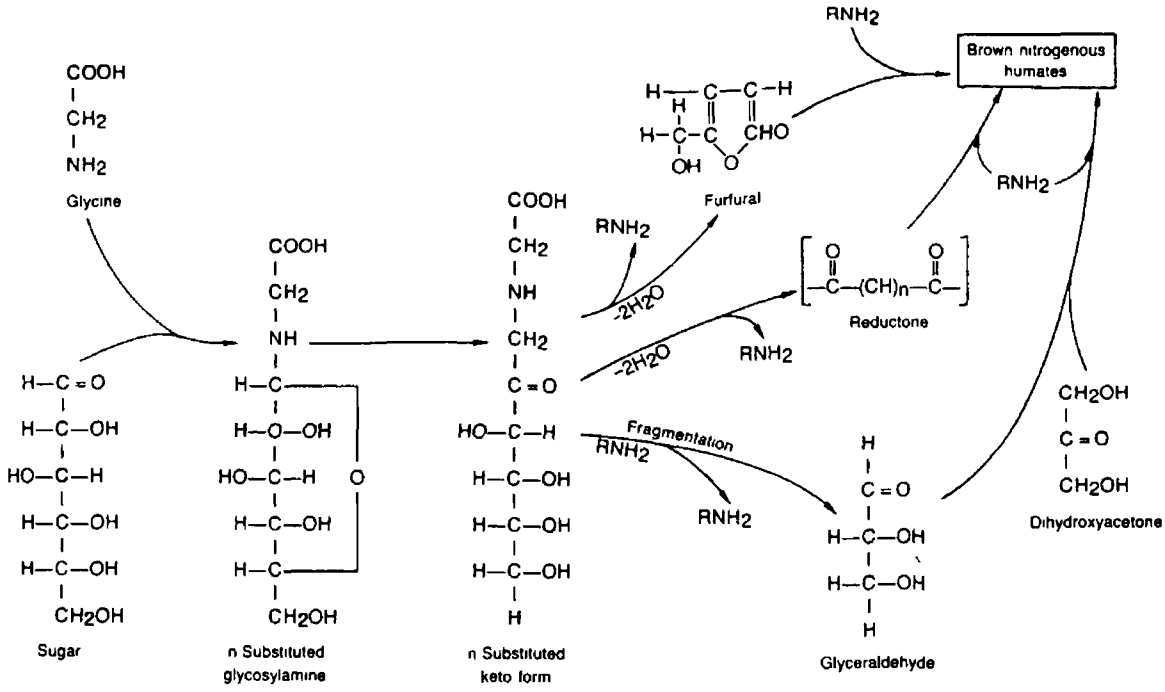

Figure 1 7 **The Browing Mechanism for the Formation of Humic Substances (5)** Note The reaction presented here is between an amino acid (glycine) and a sugar, other amino compounds or reducing sugars can be involved

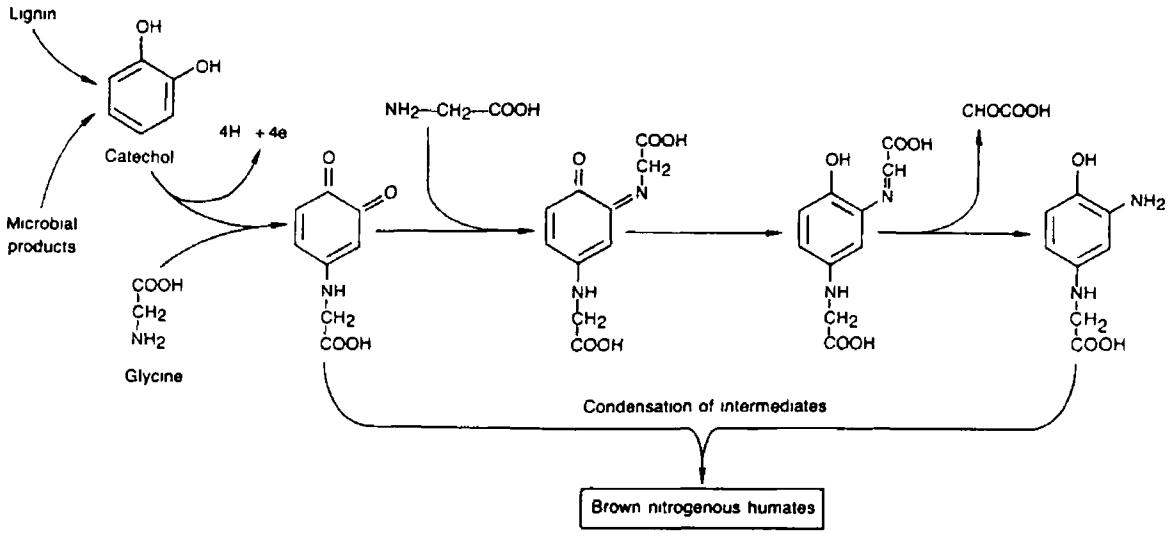

Figure 1 8 **The Polyphenol Mechanism for the Formation of Humic Substances (5)**

and fragmentation to form three intermediate types three-carbon aldehydes and ketones, reductones, and furfurals These compounds can react further with other amino-compounds to form the humic substances

- the polyphenol mechanism, this involves the reaction of an amino compound with a phenolic residue, which is derived from lignin or from microbial residues The mechanism, which is shown schematically in Figure 1 8, shows the reaction of a phenol (catechol) and an amino compound (glycine) to form an aminoqumone intermediate, which further condenses to form nitrogen humates

(iii) the cell autolysis hypothesis, which suggests that the humic substances are the products of the autolysis of plant and microbial cells which condense and polymerise via free radicals,

(iv) the microbial synthesis hypothesis This hypothesis suggests that the soil micro-organisms utilise the plant materials as a carbon and energy source for the synthesis of intercellular high-molecular weight humic substances, or humic-like substances such as melanin and aspergillin These represent the first stages of humic formation and are further degraded to humic acids, fulvic acids and ultimately to CO_2 and H_2O

It is difficult to determine which of the above four hypotheses is the most likely It is probable that all four processes are occurring simultaneously and that under particular conditions one or more of them dominates The overall trend appears to be the initial formation of the high-molecular weight humic substances, i e humic acids and humins, which are in turn oxidised to the lower molecular weight constituents (fulvic acids) and finally to CO_2 and H_2O

1 3 2 The Characterisation of Humic Substances

In appearance the humic substances are dark in colour, they are amorphous, acidic and hydrophilic, and are known to contain flexible molecular polyelectrolytes Their structure is thought to be based on an aromatic ring structure Prior to analysis, the organic fraction must be separated from the rest of the soil substances This is usually done by extraction with dilute alkali solutions, usually NaOH or $Na_4P_2O_7$ Once extracted, they can be further divided into three fractions based on their solubility in alkali and acidic solutions (4)

(i) the humic acids, which are soluble in alkali solutions but precipitate out of solution once it is acidified,

(ii) the fulvic acids, which remain in solution once the humic acids have been precipitated out by the addition of acid,

(iii) humin, which is the remaining humic substance which is neither soluble in acidic nor alkali solutions It is thought that its insolubility is due to its strong adsorption onto the surfaces of clay minerals

Numerous methods of analysis have been applied to the study of the humic and fulvic acids, both non-degradative and degradative methods and these are discussed in the following sections In contrast to the well characterised structures of the mineral fraction of soil, there is considerable disagreement about the structure of SOM, except that it is very complex and quite variable in its composition (2, 4)

The elemental composition and the general characteristics of "model" humic and fulvic acid (the humins are similar in composition to the humic acids) are shown in Table 1 6

Table 1.6 The Elemental Composition and Other Characteristics of "Model" Humic and Fulvic Acid (4)

Characteristic	Humic acid	Fulvic acid
Element (%)		
Carbon	56 2	45 7
Hydrogen	4 7	5 4
Nitrogen	3 2	2 1
Sulphur	0 8	1 9
Oxygen	35 5	44 8
Total	100 4	99 7
Functional groups (meq g^{-1})		
Total acidity	6 7	10 3
COOH	3 6	8 2
Phenolic OH	3 9	3 0
Alcoholic OH	2 6	6 1
Quinone C=O and		
Ketone C=O	2 9	2 7
OCH_3	0 6	0 8
E_4/E_6	4 8	9 6

From a study of Table 1 6 it can be seen that

- humic acid contains about 10 % more carbon and about 10 % less oxygen than fulvic acid,
- both the fulvic and humic acids contain similar amounts of nitrogen, sulphur and hydrogen,
- the total acidity and COOH content of fulvic acid is higher than that of humic acid,
- both the fulvic and humic acids contain similar amounts of phenolic OH, ketone and quinone C=O and OCH_3 groups, but the fulvic acids have a higher amount of alcoholic OH groups,
- the E_4/E_6 ratio (the ratio of absorbency at 465 nm to 665 nm) is about 2 times larger for the fulvic acids This indicates that the particle size of fulvic acids is smaller than that of the humic acids (see next section)

1.3 2 1 Non-Degradative Methods

Analysis of humic substances can be divided into non-degradative and degradative methods This body of work is extensive and only a brief summary of the results is presented here For an in-depth review of these methods the reader is referred to Schmtzer (4)

The non-degradative methods that have been used include the following various types of spectrophotometry, spectroscopy, x-ray analysis, electron microscopy, colloid-chemical and electrochemical methods (4)

(i) UV-visible spectra of fulvic and humic acids are characteristically featureless, with no maxima or minima, and show a gradual increase in the absorbency with increasing wavelength The optical density ratio at 465 nm and 665 nm, termed the E_4/E_6 ratio, is used to characterise humic and fulvic acid extracts According to Chen *et al* (7) the E_4/E_6 ratio is

- primarily related to the particle size of the humate molecule It was found that the ratio is inversely related to the particle size
- is affected by pH The E_4/E_6 ratio was found to increase as the pH was increased from pH 1 to 6, and to reach a maximum between pH 6 and 8 Above pH 8 there was a gradual decline in the E_4/E_6 ratio
- correlates with the concentration of free radicals, and the oxygen, carbon, COOH, and the total acidity levels
- is independent of the humic or fulvic acid concentration, at least in the range studied (100 to 500 ppm)

- it does not appear to be related to the relative concentration of condensed aromatic ring structures

(ii) the IR spectra of the humic substances tend to show broad adsorption bands (due to overlapping), and an abundance of oxygen containing functional groups, see Figure 1 9 (4) The main adsorption bands are 3,400 cm^{-1} (hydrogen-bonded OH), 2,900 cm^{-1} (aliphatic C-H stretch), 1,725 cm^{-1} (C=O of COOH, C=O stretch of ketonic C=O), 1630 cm^{-1} (aromatic C=C, hydrogen-bonded C=O of carbonyl of quinone, COO^-), 1,450 cm^{-1} (aliphatic C-H), 1,400 cm^{-1} (COO^-, aliphatic C-H), 1,200 cm^{-1} (C-O stretch of OH-deformation of COOH) and 1,050 cm^{-1} (Si-O of silicate impurities),

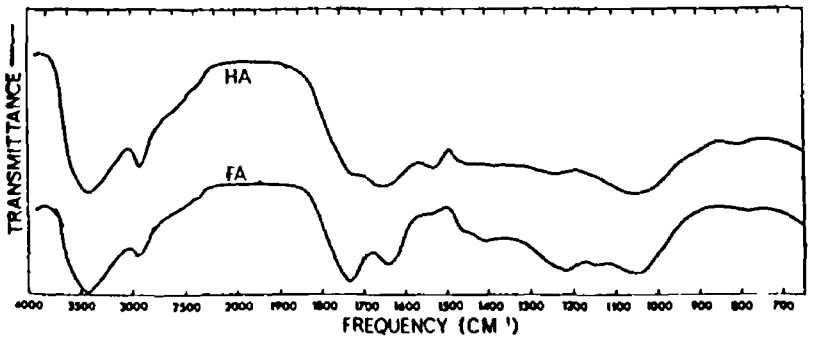

Figure 1.9 IR Spectra of Humic Substances (4)
Note HA humic acid, FA fulvic acid

(iii) SEM analysis of fulvic acids by Chen and Schnitzer (8) demonstrated the influence of pH on the physical structure of humic substances It was found that at low pH levels (pH 2) fulvic acid appeared as elongated bundles of fibres which formed a relatively open structure, see Figure 1 10 (a, b) As the pH was increased (pH 4 to 7) there was a gradual change in the physical appearance of the fibres they became thinner and more finely woven, and the overall structure became sponge-like, Figure 1 10 (c to j) Above pH 7, there was a distinct change in the structural arrangement of the fulvic acid By pH 8 (Figure 1 10 k, l) the structure became sheet-like in appearance, and the sheets thickened as the pH was increased, by pH 10 homogeneous grains were visible, Figure 1 10 (m, n)

Similar structural changes were observed for humic acids, but due to their lower solubility, it occurred over a narrower pH range (pH 6 to 10) The physical change in appearance of the fulvic and humic acids was explained as follows at the lower pH levels, the fulvic acids (or humic acids) aggregated due to intermolecular forces of attraction, such as hydrogen-bonding and van der

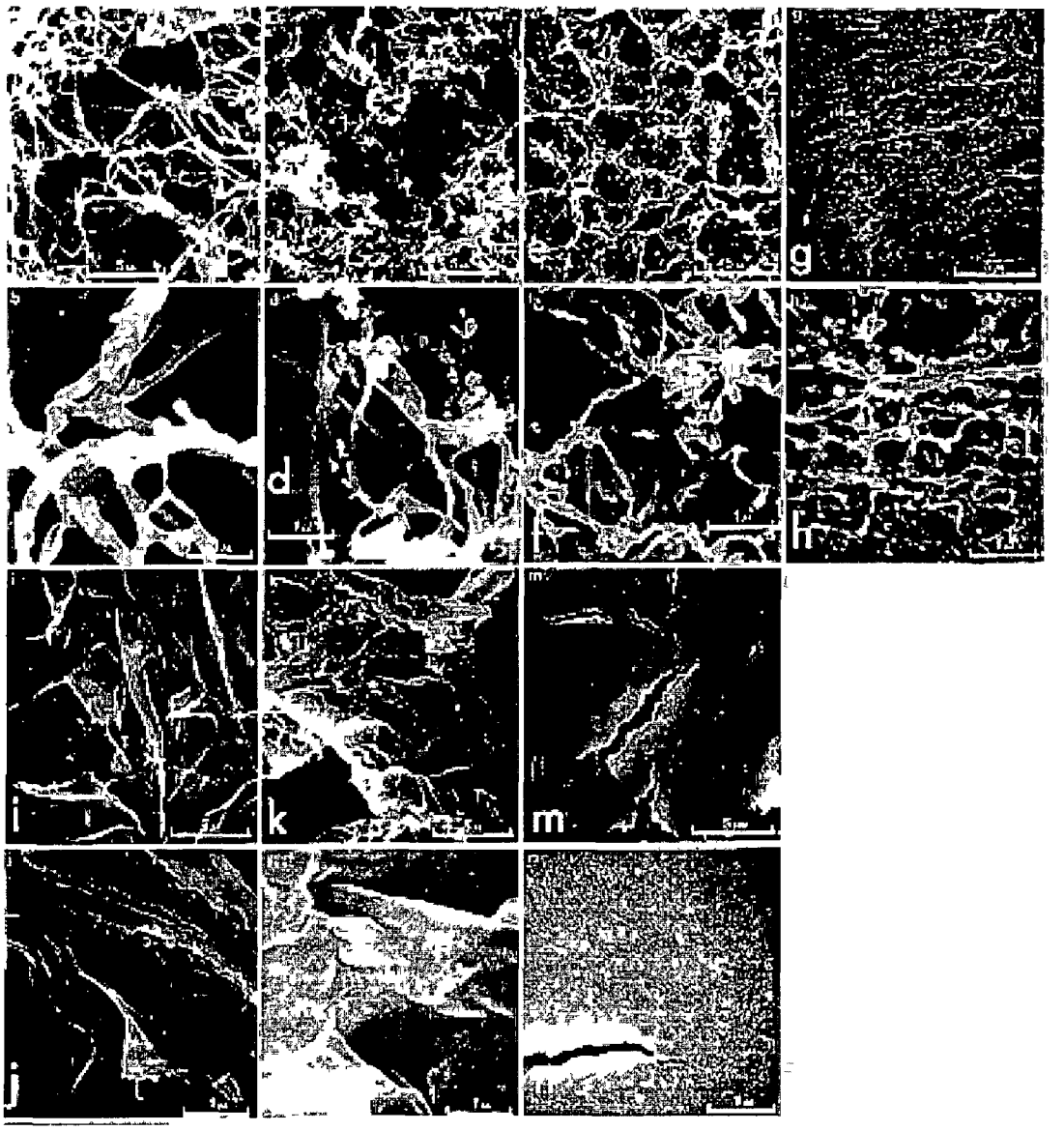

Figure 1 10 Scanning Electron Micrographs of Fulvic Acid at Various pHs (10) Note a, b at pH 2, c, d at pH 4, e, f at pH 6, g, h at pH 8, i, j at pH 9, k, l at pH 10

Waals forces This allowed for the formation of the elongated structures seen by SEM As the pH was increased these forces of attraction became weaker due to the increasing ionisation of the COOH and phenolic OH groups, which lead to mutual repulsion between the molecules As a result the molecular arrangement became smaller and smaller but better oriented, which lead to the formation of sheet-like structures and the appearance of homogeneous grains at the higher pH levels,

(iv) both ^{13}C and ^{1}H-NMR have been carried out on humic substances Grant (9) concluded from the ^{1}H-NMR analysis of a humus fraction extracted from a Podzol that $CH_3(CH_2)_n$ structures were present along with various environments of $CH_2(CO)$, CH_2-NH-, carbohydrate H-C-O, and only a small amount of aromatic protons He reported that 72 % of the H-C groups occurred in $CH_3(CH_2)_n$ structures, while 6% occurred in carbohydrates and less than 2 % as aromatic protons Ruggiero *et al* (10) concluded, from ^{13}C-NMR and ^{1}H-NMR analysis on humic substances extracted from an Andosol, that aromatic structures were much more significant It was noted that strong absorption between 7 4 and 8 8 ppm of ^{1}H-NMR spectra indicated the presence of aromatic protons It was concluded that the percentage of protons present in aromatic structures was as follows, fulvic acid 20 %, humic acid 19 % (10) However, these values decreased to fulvic acid < 12% and humic acid 14 % for humic substances extracted by oxidative extraction methods,

(v) X-ray analysis and electron spin resonance (ESR) studies were carried out by Eltantawy and Baverez (11) X-ray diffraction of the humic substances studied showed diffraction bands at 3 6, 2 1 and 1 2 Å, which were attributed to the presence of aromatic layers or graphite-like layers, and also a band at 7 5 Å

which indicated the presence of a non-aromatic fraction An ESR signal at G ~ 2 indicated the presence of free radicals, which are thought to be important in polymerisation-depolymerisation reactions of humic substances, and with reactions with other organic compounds The level and stability of free radicals were found to increase with increasing pH,

(vi) viscosity measurements were carried out by Chen and Schnitzer (12) to examine the effects of pH on particle shape and dimensions, particle weight, and polyelectrolyte behaviour It was found that fulvic and humic acids behaved like flexible, linear polyelectrolytes At low pH levels (pH 1 to 1 5 for fulvic acids and pH 7 for humic acids), the humic substances behaved as uncharged polymers At higher pH levels both the fulvic and humic acids exhibited strong

polyelectrolyte characteristics It was concluded from analysis of the results that the particles of humic substance were rod shaped in structure,

(vii) various methods for measuring the molecular weights of humic and fulvic acids have been used These methods include viscosity, gel filtration, and sedimentation (4) The various methods have yielded a wide variation in values from a few hundred for fulvic acids to several million for humic acids For instance, using gel filtration, weight-averaged molecular weights (Mw) of 300 to > 200,000 have been reported for soil humic acids For humic and fulvic acids extracted from marine sediments Mw ranging from 700 to >2,000,000 have been reported, and for humic acids extracted from natural waters Mw varied from < 700 to 50,000 (4)

1.3 2 2 Degradative Methods

The degradative methods of analysis which have been used include oxidative and reductive degradation, hydrolysis, irradiation, thermal analysis, and biological degradation (4)

(i) oxidative degradation of unmethylated and methylated humic substances has been carried out under various acidic and alkali conditions, using such oxidative compounds as $KMnO_4$, CuO, H_2O_2, and others (4) The derivatives of humic and fulvic acid oxidation can be divided into three general classes

- aliphatic carboxylic compounds, mainly n-fatty acids of n-C_{16} and n-C_{18}, and also di- and tri-carboxylic acids,
- benzenepolycarboxylic acids, particularly the tri-, tetra-, penta- and hexa-forms,
- phenolic acids, mainly those with between 1 and 3 OH groups and between 1 and 5 COOH groups

The data in Table 1 7 shows the major chemical constituent of "model" fulvic and humic acid, determined from the oxidative breakdown products of the humic and fulvic acids From Table 1 7 it can be seen that

- humic acid contains similar amounts of aliphatic and phenolic structures but a greater amount of benzenecarboxylic acid structures
- fulvic acid contains similar amounts of aliphatic and benzenecarboxylic structures and higher percentage of phenolic structures
- both materials contain approximately equal proportions of aliphatic and aromatic structures Thus, according to Schnitzer (4), the "model" humic

Table 1.7 **The Major Chemical Structures in "Model" Humic and Fulvic Acid (4)**

Major product	Humic acid (%)	Fulvic acid (%)
Aliphatic	24 0	22 2
Phenolic	20 3	30 2
Benzenecarboxylic	32 0	23 0
Total	76 3	75 4
Benzenecarboxylic/Phenolic ratio	1 6	0 8
Aromaticity	69	71

and fulvic acid are very similar in chemical composition except that the fulvic acid is richer in phenolic but poorer in benzenecarboxylic structures than the humic acid

(ii) reductive degradation of humic and fulvic acids that have been carried out include Zn-distillation, Na-amalgam reduction, hydrogenation and hydrogenolysis (4) The main products of reductive methods have been polycyclic aromatic hydrocarbons (4, 6) The results of the reductive methods have tended to be poor and according to Schnitzer (4) are to be doubted He has suggested that the reaction conditions used may be too severe in some cases, and excessive bond breakage and molecular rearrangement may have occurred Thus, the degradative products may bare no resemblance to the actual structures found in the humic substances Some of the compounds which have been identified include the following naphthalenes, anthracenes, phenanthrenes, 2,3-benzofluorene, 1,2-benzofluorene, fluoranthene, 1,2-benzanthracene, chysene, triphenylene, pyrene, methyl pyrenes, perylene, 1,2-benzopyrene, 3,4-benzopyrene, 1,12-benzopyrene, coronene, naphta (2',3' 1,2) pyrene, and carbazole

(iii) thermal methods of analysis used to study fulvic and humic acids include thermogravimetry, differential thermogravimetry, differential thermal analysis, and pyrolysis-gas chromatography Schnitzer and Hoffman (13) found that fulvic and humic acid samples heated in air showed

- an increase in their elemental carbon content with an increase in temperature, while the elemental oxygen content decreases Charred samples heated to 540°C contained both elemental carbon and hydrogen, but no oxygen

- that the phenolic OH groups were more stable to heating than the COOH groups, but that both were degraded between 250° and 400°C Also, that these two functional groups were found to be more stable in fulvic acids than in humic acids

(iv) biological methods have been used to study the humic substances Enzyme degradation was considered to be a more promising technique than other degradation methods, since there was less likely to be molecular rearrangement Majumdar and Rao (14) used the enzymes pronase and hemicellulase to degrade fulvic acids The enzymes released several of the ammo acids found in fulvic acid (valine, alanine, tryptophane, serine, glycine, glutamic acid and aspartic acid) and carbohydrates (galactose and arabinose), while leaving the fulvic acid core untouched It was concluded that the carbohydrate and amino acid portions are present as side chains which are attached to an aromatic core and not as bridging units between the aromatic cores

1 3 2 3 The Structure of Humic Substances

It is surprising that after such intensive study as noted above that the structure of humic substances still remains unclear This is partially due to the complex nature of the material and because of disagreements about the interpretation of results, particularly those gained from degradation studies Several possible structures have been proposed for the humic substances based on their chemical composition and their behaviour in solution

Haworth (6) considered the structure of humic acid to consist of a complex aromatic core to which were attached, either chemically or physically, polysaccharides, proteins, simple phenols, and metals, see Figure 1 11

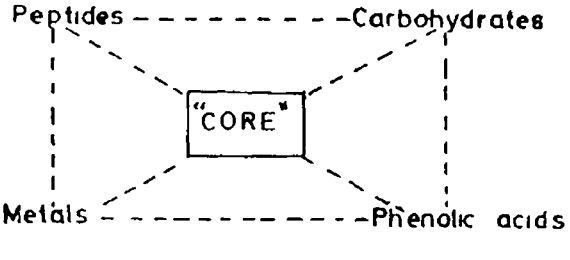

Figure 1 11 **The Schematic Structure of Humic Acid as Proposed by Haworth (6)**

With regard to the nature of the core, the ESR spectra of an ortho-benzoquinone polymer was found to be remarkably similar to that of an acid boiled humic acid, though not to be identical (6) The structure of the ortho-benzoquinone polymer was unclear though there was evidence of polyphenyl linkages, see Figure 1 12, and possibly diphenyl ether (dibenzofruran) groups

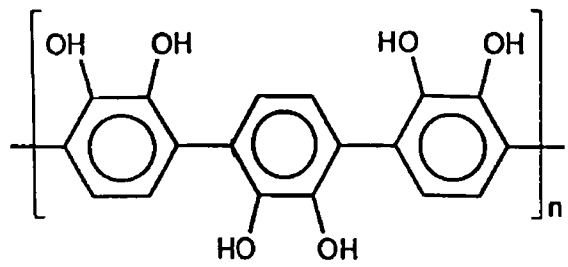

Figure 1 12 Possible Polyphenyl Linkages of SOM Core (6)

Majumdar and Rao (14) concluded from enzyme-degradation studies on fulvic acids that the carbohydrates and amino acids which were present existed as long side chains attached to aromatic cores These long chain structures were not considered to act as bridging units between the aromatic cores

Schnitzer (4) concluded that up to 50 % of the aliphatic structures in humic and fulvic acids existed as n-fatty acids which were covalently joined to the phenolic OH groups through ester linkages, see Figure 1 13

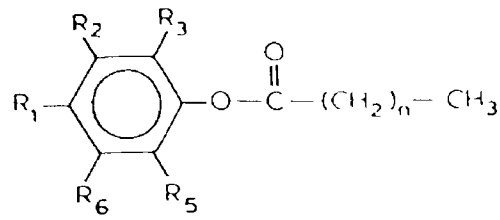

Figure 1 13 Structure of Phenol-Fatty Acid Esters in Humic and Fulvic Acids Proposed by Schnitzer (4) Note R_1 = COOH or $COCH_3$ or OH, R_2 = H or OH or COOH, R_3 = H or OH or OCH_3 or COOH, R_4 = OH esterified to fatty acid, R_5 = H or OH of OCH_3, R_6 = H or $COOCH_3$ For the humic acids n = 14 to 16, for fulvic acids n = 14,15,16, and 18

According to Schnitzer (4) the remaining aliphatics were "loosely" bound to the aromatic core by physical adsorption The basic "building block" of the humic substances was concluded to be phenolic and benzenecarboxylic acid units, see Figure 1 14 This model could explain the flexible nature of the humic substances which shows dependence on the pH of their environment At low pH levels the fulvic and humic acids aggregate to form elongated fibres, through various attractive forces such as hydrogen bonding, van der Waals forces, hydrophobic interactions between aromatic rings, etc As the pH increases these forces become weaker due to the ionisation of the phenolic OH and COOH groups This results in an electrostatic repulsion between the molecules, so that the molecular arrangements become increasingly smaller but better oriented, see Figure 1 10

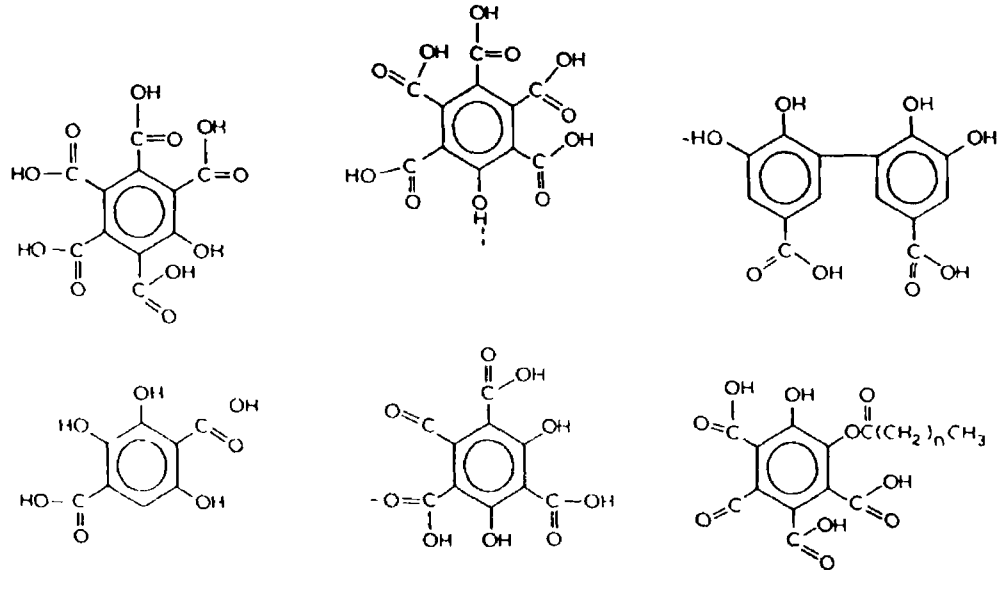

Figure 1 14 Structure of Fulvic Acid as Proposed by Schnitzer (4)

Ghosh and Schnitzer (15) investigated the macromolecular arrangement of humic and fulvic acids They reported that the structural arrangement of the humic substances was dependent on three main factors, namely the humic substance concentration, the pH of the solution, and the ionic strength of the solution It was found that humic substances behaved as rigid, spherical, colloid structures in solutions containing high concentrations of the sample (> 35-50 x10^{-4} g cm^{-3}), or for lower concentrations of sample when the pH is low (< pH 3 5), or in the presence of high concentrations of neutral electrolytes (> 0 05 M), see Figure 1 15 In contrast, it was observed that the humic substances behaved like flexible, linear colloids at low sample concentrations provided that the ionic strength was relatively low (< 0 05 M), or that the pH of the solution was not too low (> pH 3 5) The former case represents the normal conditions found in soils

Fulvic acid	Electrolyte (NaCl) Concentration (M)					pH				
Concentration	0 001	0 005	0 01	0 05	0 1	2 0	3 5	6 5	8 0	9 5
Low										
High										

(a) Fulvic Acid

Humic acid	Electrolyte (NaCl) Concentration (M)					pH				
Concentration	0 001	0 005	0 01	0 05	0 1	2 0	3 5	6 5	8 0	9 5
Low										
High										

(b) Humic Acid

Figure 1 15 **Model Macromolecular Structures for (a) Fulvic and (b) Humic Acids (15)**

More complicated models for the structure of humic substances have also been proposed, such as the structure shown in Figure 1 16 (16) This model is of a loosely associated, three-dimensional macro-molecule consisting of a number of flexible side chains that interlink the aromatic units These linkages include aliphatic chains, sugar residues, amino acids, and co-ordinated metal ions In summary, none of the models which have been discussed are completely satisfactory, but they do reflect the complexity and transient arrangement of the humic substances and SOM in general

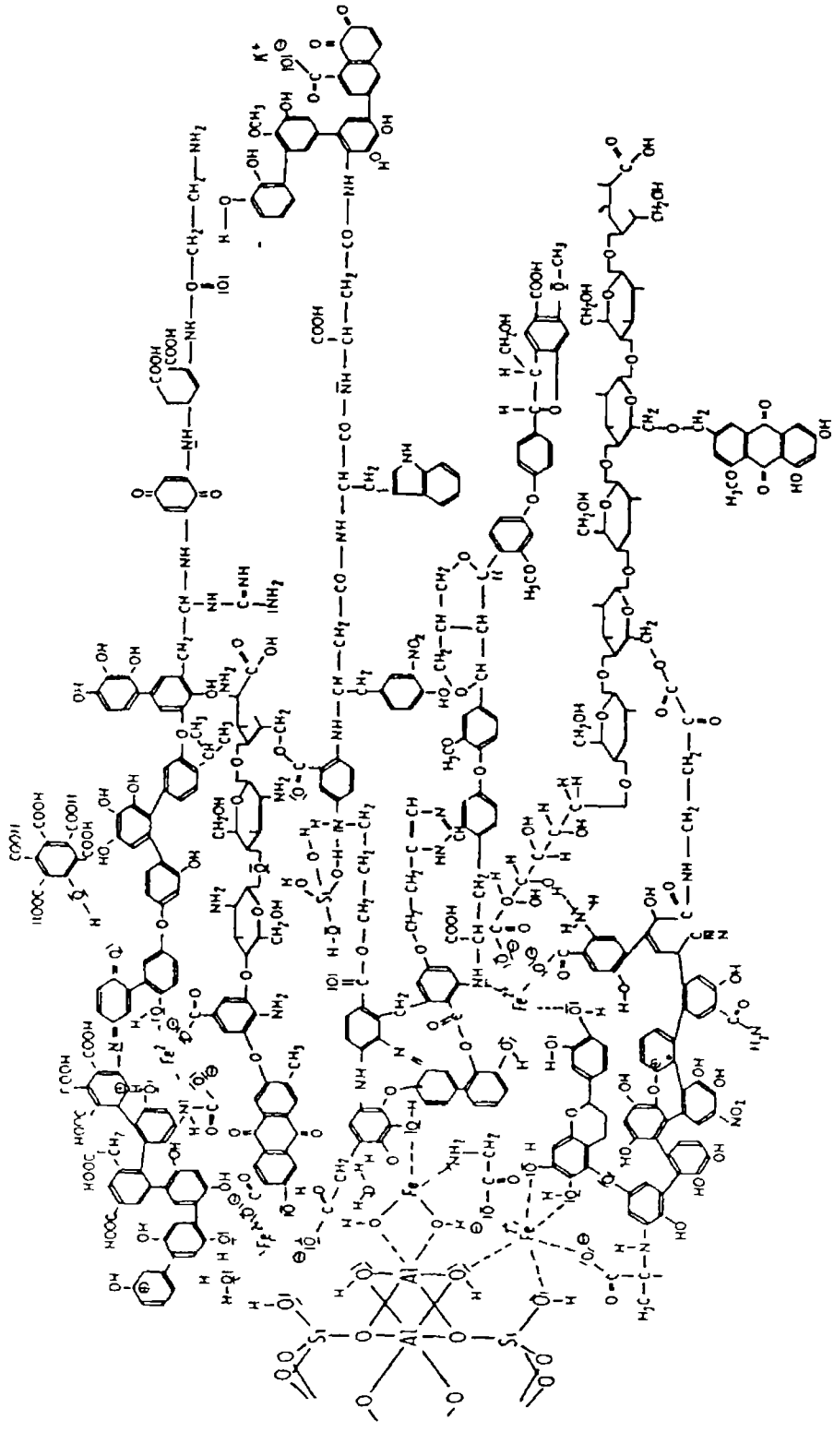

Figure 1.16 A Complex Model for the Structure of Humic Substances (16)

1 4 The Surface Properties of Soil

In aqueous solution the surfaces of both the mineral and organic fractions of the soil are usually charged The sign and magnitude of the surface charge has important consequences for the physicochemical properties of the soil, specifically in relation to its water and nutrient holding capacity for plant growth In particular, the surface charge influences the cation exchange capacity (CEC) and anion exchange capacity (AEC) of the soil, its colloidal stability and its aggregation properties

1 4 1 The Surface Charge of Soil Constituents

It has already been mentioned in Section 1 2 that the intrinsic surface charge of the minerals arise from two sources, the first is the permanent surface charge which arises from isomorphic substitution, and the second is the ionisation of the functional groups present at the surface of the clay, i e the pH-dependent charge The pH-dependent charge is also important for the organic matter fraction For the minerals the most important functional group present is the hydroxyl group which is found on the surfaces of clays, amorphous silicate materials, and on metal oxides, oxyhydroxides and hydroxides Similarly, for the SOM the two principal functional groups are the carboxyl and the phenolic OH groups In general the surface charge is determined by the adsorption of H^+ and OH^- ions This is known to be the case for the metallic oxides and it has been suggested to be probably the case for the other mineral and organic components of the soil (17)

As a result of the adsorption of H^+ and OH^- ions, the surface of the soil can become positively or negatively charged depending on the pH of the aqueous solution Thus, the sign and the magnitude of the surface charge is a pH-dependent quantity It can be seen from Equations 1 2 and 1 3, that at low pH values a positively charged surface will develop from the protonation of the surface functional groups,

$$>Al\text{-}OH + H^+ \rightarrow Al\text{-}OH_2^+ \qquad \text{Equation 1 2}$$

$$R\text{-}COOH + H^+ \rightarrow R\text{-}COOH_2^+ \qquad \text{Equation 1 3}$$

whereas at high pH values (Equation 1 4 and 1 5) the deprotonation of the functional groups will result in the formation of a negative charge on the surface

$$>Al\text{-}OH + OH^- \rightarrow Al\text{-}O^- + H_2O \qquad \text{Equation 1 4}$$

$$R\text{-}COOH + OH^- \Rightarrow R\text{-}COO^- + H_2O \qquad \text{Equation 1 5}$$

The surface charge of the soil is the sum of several distinct surface charge densities (3) which are as follows

(i) the permanent surface charge density, σ_0, which is due to isomorphic substitution occurring in the clay minerals,

(ii) the net protons charge density, σ_H Thus, the intrinsic surface charge density, σ_{in}, of the soil is given by the relationship $\sigma_0 + \sigma_H = \sigma_{in}$,

(iii) the inner-sphere complex charge density, σ_{IS}, which is equal to the net total surface charge of adsorbed ions (other than H^+ and OH^-) which have formed inner-sphere complexes with the surface functional groups An inner-sphere complex forms when an ion is bound directly to the surface functional group In such instances there are no molecules of the bathing solvent (i e water) interposed between the functional group and the adsorbed ion An example of an inner-sphere complex can be seen in Figure 1 17(a) which illustrates the adsorption of the K^+ cation directly to the surface of a vermiculite clay with no water molecules between the cation and the surface

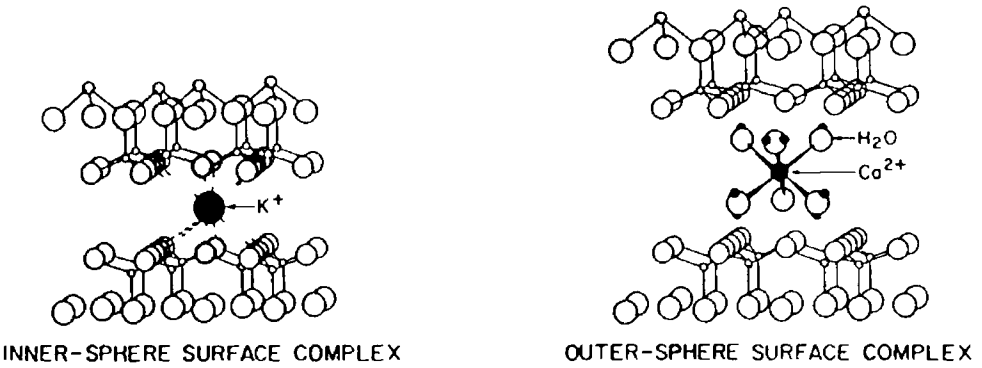

Figure 1 17 **Surface Complexes between Metal Cations and the Surface of 2 1 Phyllosilicates (3)**

On the other hand, an outer-sphere complex occurs when there is at least one solvent molecule in between the adsorbed ion and the surface functional group This can be seen in Figure 1 17(b) which shows an outer-sphere complex formed between the hydrated $Ca(H_2O)^{2+}_6$ ion and the surface of a montmorillonite clay, the water molecules are interposed between the Ca^{2+} ion

and the clay surface As a general rule outer-sphere complexes involve electrostatic bonding mechanisms and are consequently less stable than inner-sphere complexes which involve either ionic or covalent bonding,

(iv) the outer-sphere complex charge density, σ_{os}, which is equal to the total surface charge of the ions that have formed outer-sphere complexes with the surface functional groups

Thus, the overall surface charge density of the soil, σ_{sc}, can be expressed by the following equation

$$\sigma_{sc} = \sigma_o + \sigma_H + \sigma_{is} + \sigma_{os} \qquad \text{Equation 1 6}$$

Each of the terms on the right hand side of Equation 1 6 can be either positive or negative depending on the environmental conditions of the soil and in general their sum will not equal zero However, balancing the surface charge is an associated opposite charge in the solution close to the surface of the soil which give rise to the electric double layer (or the diffused double layer) The opposite charge is due to the swarm of ions in solution close to the surface of the soil particles which have not formed complexes with the surface functional groups This counter charge is referred to as the dissociated charge density, σ_d The dissociated charge is equal in magnitude but opposite in sign to the overall surface charge density, i e $\sigma_d + \sigma_{sc} = 0$ The overall balance of surface charge can be expressed by the following equation

$$\sigma_o + \sigma_H + \sigma_{is} + \sigma_{os} + \sigma_d = 0 \qquad \text{Equation 1 7}$$

This is a fundamental conservation law that must be satisfied by the electric field interface of any soil

1 4 2 The Point of Zero Charge

It follows from the previous section that for a particular soil there will exist a characteristic pH value at which the surface charge, or the sum of the surface charges, will be zero, this is referred to as the point of zero charge (The point of zero charge is also referred to as the zero point charge, or the isoelectric point where it is measured by electrokinetic methods) Below the point of zero charge there is an excess of positively charged functional groups, thus, the surface of the soil is positively charged Conversely, above the point of zero charge of the soil there is an

excess of negative charges at the surface of the soil so the surface is negatively charged

The point of zero charge can be measured by several techniques such as potentiometric titration or by electrophoretic mobility methods, these are described in several sources (3, 16, 18) Sposito (3) noted that there are several distinct points of zero charge which can be distinguished for mineral surfaces, these are summarised in Table 1 8

Table 1 8 Definition of Points of Zero Charge (3)

Name	Defining equation
Point of zero charge (PZC)	$\sigma_d = 0$
Point of zero net proton charge (PZNPC)	$\sigma_H = 0$
Point of zero salt effect (PZSE)	$(\delta \sigma_H / \delta I)_T = 0^a$
Point of zero net charge (PZNC)	$\sigma_{os} + \sigma_d = 0$

Note [a] I is the ionic strength of the background electrolyte solution and T the absolute temperature

Sposito (3) defined the points of zero charge as follows

(i) the conventional point of zero charge (PZC), this is the pH at which the net surface charge is equal to zero, i e $\sigma_d = 0$ In electrokinetic experiments this is known as the isoelectric point,

(ii) the point of zero net proton charge (PZNPC) is the pH at which the surface charge density of protons (σ_H) is zero The PZNPC can be measured by potentiometric titration provided that only proton-selective functional groups are being titrated,

(iii) the point of zero salt effect (PZSE), this is the pH value for the common point of intersection of several titration curves of σ_H versus pH at several fixed ionic strengths,

(iv) the point of zero net charge (PZNC) is the pH of the solution at which the difference between the CEC and AEC is zero

As can be seen the various points of zero charge are not identical and their values can differ significantly from each other for the same soil sample Sposito (3)

has noted that in some instances the various points of zero charge can be equivalent, two general conditions where equivalence amongst the points of zero charge usually occurs are

(i) if a soil is suspended in a background solution of a 1 1 electrolyte whose cations and anions form only outer-sphere surface complexes (ions such as Na^+ and Cl^- usually form outer-sphere complexes) then the PZC, the PZNC and the PZSE for the soil are likely to be equal,

(ii) if a soil is suspended in an 1 1 electrolyte solution as in case (i) which contains ions which are adsorbed specifically, then the PZC and the PZSE are likely to be equal In this case the PZC changes relative to its value as determined by case (i) and the sign of the change is the same as the sign of the valence of the specifically adsorbing ion

The points of zero charge of mineral soils and soil organic matter will now be discussed

(a) Points of Zero Charge of Mineral Soils

For mineral soils there are considerable data available for the points of zero charge, see references quoted in Sposito (3) Table 1 9 compares the points of zero charge for several soil minerals (3)

Table 1 9 **A Comparison of the Points of Zero Charge for Several Different Soil Minerals Suspended in Solutions of 1 1 Electrolytes (3)**

Mineral	PZC	PZNPC	PZSE	PZNC
Alon (γ-AlO_3)	8 7	8 2	8 5	-
Birnessite (δ-MnO_2)	1 7	2 2	2 3	1 9
Calcite ($CaCO_3$)	10	-	9 5	-
Corundum (α-Al_2O_3)	9 1	9 1	-	-
Goethite (α-FeOOH)	6 1	7 7	7 3	-
Hematite (α-Fe_2O_3)	-	8 4	8 5	-
Hydroxyapatite ($Ca_5(PO_4)_3OH$)	7 5	-	7 6	-
Kaolinite ($Si_4Al_4O_{10}(OH_8)$)	4 7	-	-	4 8
Quartz (α-SiO_2)	2 0	-	2 9	-

As can be seen from Table 1 9, the points of zero charge for a particular mineral are not usually found to be identical, but are generally close to each other For example, the various points of zero charge for birnessite vary from pH 1 7 to 2 3 and goethite from pH 6 1 to 7 7 In the case of corundum it can be seen that PZC = PZNPZ = pH 9 1

(b) Point of Zero Charge of Soil Organic Matter

Information concerning the surface charge of soil organic matter such as peat is extremely limited in the literature (Indeed, the lack of information would suggest there is some difficulty in obtaining point of zero charge values for SOM, this point is returned to in Section 2 5 2) It was reported by van Raij and Peech (17) that the point of zero charge of Oxisol and Alfisol mineral soils was influenced by their organic matter content The surface charge of the two soils was measured by potentiometric titration This involved the titration of the soil sample with acid and base solutions (in this case NaOH and HCl) for several concentrations of a 1 1 electrolyte solution (1 0, 0 1, 0 01 and 0 001 M NaCl) Thus, strictly speaking the point of zero charge measured by the authors would be the PZSE The pH value at which the titration curves intersect was taken to be the point of zero charge It was observed that the point of intersection of the titration curves decreased to lower pH vales with increasing organic matter content (see Table 1 10 and Figure 1 18), i e the point of zero charge decreased with increasing organic matter content of the soil

Table 1 10 The Zero Point Charge For Oxisol and Alfisol Soils as a Function of Their Organic Matter Content (17)

Soil Order	Sample[a]	OC[b] (%)	pH		pH of PZC[d]	Position of PZC[e]
			H_2O	KCl[c]		
Oxisol	Acrohumox-A_p	1 9	4 9	4 1	3 6	0 4 acid side
	Acrohumox-B_2	0 3	4 9	4 3	4 2	0 7 acid side
	Acrorthox-A_p	2 5	5 3	4 7	3 9	1 3 acid side
	Acrorthox-B_2	0 7	5 9	6 0	6 2	0 2 alkali side
Alfisol	Tropudalf-A_p	2 3	6 3	5 4	3 4	1 8 acid side
	Tropudalf-B_2	1 0	6 7	5 9	3 8	1 3 acid side

Note ([a]) the subscript p denotes ploughing or other disturbance of the A horizon had occurred, while the subscript 2 indicates these samples are sub-horizons of the B horizon ([b]) OC, organic matter, ([c]) in 1M KCl, ([d]) calculated from the titration curves in Figure 1 18, ([e]) with respect to the pH at 0 addition of acid or base

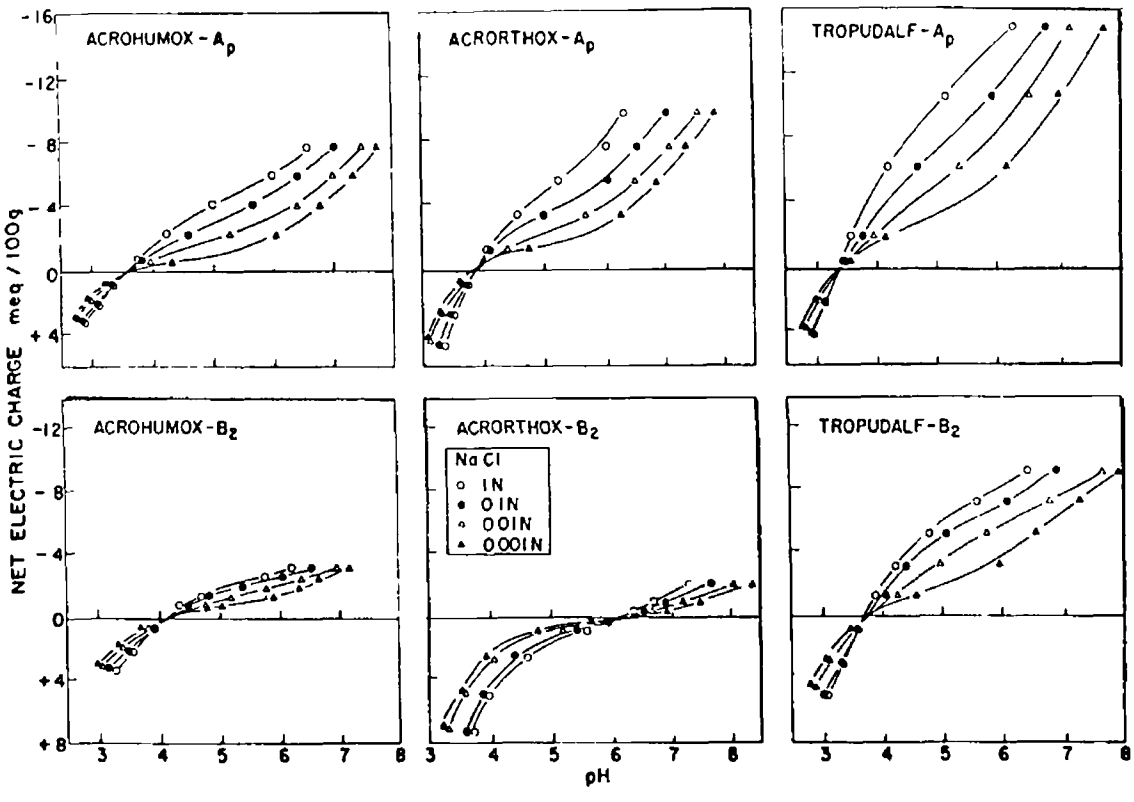

Figure 1 18 The Net Electrical Charge of Soils as Determined By Potentiometric Titration (17)

Since the only difference in the soil samples examined was their organic matter content, van Raij and Peech (17) concluded that the lower pH of the point of zero charge for the A_p horizons was attributed to their higher organic matter content, see Table 1 10 The only exception to this observation was one of the Oxisol samples (Acrorthox-B_2) In this instance the higher point of zero charge was attributed to a high content of iron oxides and gibbsite in the soil sample which shifted the point of zero charge to higher pH values In general it was concluded that the presence of iron and aluminium oxides will tend to increase the point of zero charge to higher pH values, while the presence of clays with permanent or structural negative charges or organic matter will tend to shift the point of zero charge to lower pH values

In addition, van Raij and Peech (17) noted the influence of the point of zero charge on the pH of the sample measured in water and 1 M KCl solution, see Table 1 10 above If the pH of a soil is found to be higher in the KCl solution than in water (as it was for the Acrorthox-B_2 sample) then the pH of the sample lies on the positive side of the point of zero charge, and consequently the soil has a net positive charge

associated with it On the other hand, if the pH of the soil in the KCl solution is lower than its pH in water (as was found for the other soil samples) then the pH of the soil lies to the negative side of the point of zero charge and the soil carries a net negative charge In addition a large difference between the pH values measured in water and the KCl solution indicates that the pH of the soil lies several units away from the point of zero charge

Morais *et al* (19) also noted that the pH value for the point of zero charge for several tropical soils decreased with increasing organic matter content of the sample

Sparks (20) stated that the humic substances of soil organic matter are a major source of pH-dependent charge in soils, see Table 1 11 The functional groups which interact with cations include the acidic groups, carbonyl groups, and the alcoholic hydroxyls The acidic groups are the source of most of the exchange capacity of SOM in general Carboxyl groups account for up to 50 % of the CEC of SOM, and 30 % of CEC at pH 7 can be divided between quinonic, phenolic and enolic hydroxyls (20)

Table 1 11 Functional Group Content of SOM and Hydrolysis Products (20)

Functional group	Humic acids (μmol g^{-1})	Fulvic acids (μmol g^{-1})	Humins (μmol g^{-1})	pKa
Total acidity	4 4-10	5 1-14 2	4 1-5 9	-
Carboxyl	1 5-5 7	2 5-11 2	1 3-3 8	0 2-6 2
Phenolic OH	2 1-5 7	2 6-5 3	1 8-4 0	4-10
Alcoholic OH	0 2-3 5	0 1-4 9	2 0-5 7	6 5-7 5
Carbonyl	0 5-4 4	1 1-5 0	0 3-3 7	-
Methoxyl	0 3-1 2	0 3-1 2	0 3-0 4	>7

Chang and Choi (21) reported on the surface charge of soil organic matter The organic soils studied were Peat A (Yeong yang peat) with an organic matter content of 43 3 % and Peat B (Peong tack peat) (53 7 % OM) the general physical properties of the two peats studied are shown in Table 1 12 The acidic group content and the pKa of the two peat samples were initially examined The point of zero charge was determined from potentiometric titration (with NaOH in 1, 0 1 and 0 001 M NaCl solution) The titration curves for the two peat samples, see Figure 1 19, were found to intersect between pH 4 15 and 4 4 for Peat A and between pH 3 8 and 4 0 for Peat B

Table 1.12 Properties of the Peat Samples Studied by Chang and Choi (21)

Property	Peat A	Peat B
Depth of sample (cm)	280	0-10
pH[a] (H_2O)	6.4	4.3
(KCl)	5.6	4.0
Organic matter (%)	43.3	53.7
Carbon/ Nitrogen ratio	270.4	40.31
CEC (meq 100 g^{-1})	74.5	78.6

Note: [a] solution: sample = 2.5:1, concentration of KCl solution not stated.

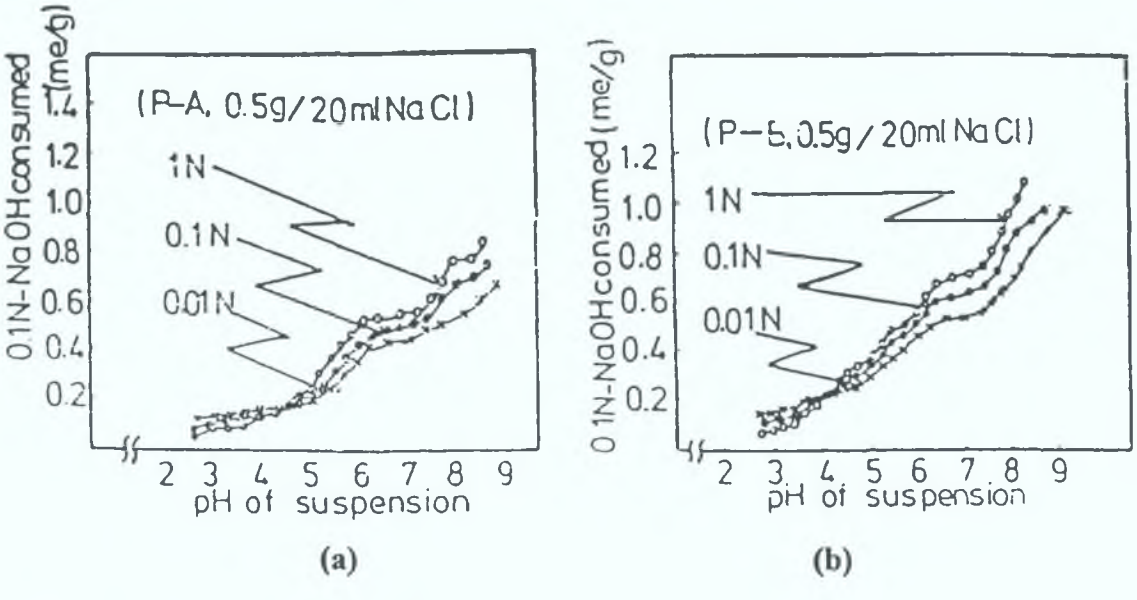

Figure 1.19 Determination of the Point of Zero Charge for Peat A (21)
Note: (a) Peat A; (b) Peat B

The authors conclude that the point of zero charge occurred at about pH 4 for both peats. The results for both peat samples is shown are Table 1.13. It was concluded that at lower pH values the positive charge on the samples may result from the protonation of the hydrous oxides present in the peats. At higher pH values desorption of protons from uncomplexed phenolic and carboxylic functional groups of organic matter may be the major contributor to the negative charge. Therefore, the point of zero charge of the peats was considered to be the result of the overall mineral and organic content of the peat. However, the authors note that the peats studied contained sizeable amounts of quartz, while illite, kaolinite, hydrated-halloysite and feldspars were present only in trace amounts. Thus, it was suggested that the magnitude of the surface charge measured for the peats was primarily dependent on the dissociation constant of the functional acidic groups of the organic matter.

Table 1.13 Results for Peat Soils Studied by Chang and Choi (21)

Property	Peat Sample	
	A	B
Total acidity (meq g^{-1})	0 973	1 257
Weakly acidic groups (meq g^{-1})	0 426	0 588
pKa_1	3 95	4 05
Very weakly acidic groups (meq g^{-1})	0 547	0 699
pKa_2	9 51	8 60
Point of zero charge	4 15-4 4	3 8-4 0

1.5 Summary

This introductory chapter has briefly discussed the formation of soil and broadly outlined its classification In particular, it has discussed the various physical and chemical properties of the clay mineral and organic matter fractions of the soil which are of relevance to the following chapters of this thesis The peat fibre and the other peat materials which are discussed in the following chapters are organic matter soils, and thus belong to the Histosol group Chapter 2 is concerned with the characterisation of the peat materials and discusses the point of zero charge, the thermal decomposition and the IR spectroscopy of the peat samples examined Chapter 3 is concerned with the measurement of the surface area of the peat samples and the sorption of organic compounds by the peat As will be discussed in the relevant chapters the surface area and sorptive properties of solid materials are interrelated properties This is particularly the case for soil constituents where the structural and physical properties of the clay minerals and soil organic matter have important consequences for what constitutes their surface area and their sorption mechanism

16 References

(1) McGraw and Hill, Encyclopedia of Science and Technology, 7ed , McGraw and Hill, (1992)

(2) Hassett, J J and Banwart, W L , Soils and Their Environment, Prentice-Hall, (1992)

(3) Sposito, G , The Surface Chemistry of Soil, Oxford University Press, (1984)

(4) Schnitzer, M , Humic Substances. Chemistry and Reactions, in Soil Organic Matter, (Schnitzer, M and Khan, S U , eds) pp 1-65, (1978)

(5) Paul, E A , Soil Microbiology and Biochemistry, pp 91-114, Academic Press, (1989)

(6) Haworth R D , Soil Sci., 111(1), 71-79 (1971)

(7) Chen, Y Senesi, N and Schnitzer, M , Soil Sci. Soc. Am J., 41, 352-358 (1977)

(8) Chen, Y and Schnitzer, M , Soil Sci. Soc. Am. J., 40, 682-686 (1976)

(9) Grant, D , Nature, 270, 709-710 (1977)

(10) Ruggiero, P , Interesse, F S and Sciacovelli, O , Geochemica. Cosmo. Acta, 43, 1771-1775 (1979)

(11) Eltantawy, I M and Baverez, M , Soil Sci Soc Am J , 42, 903-905 (1978)

(12) Chen, Y and Schnitzer, M , Soil Sci Soc. Am. J., 40, 866-872 (1976)

(13) Schnitzer, M and Hoffman, I , Soil Sci. Soc Proc., 28, 520-525 (1964)

(14) Majumdar, S K and Rao, C V N , J. Soil Sci., 29, 489-497 (1978)

(15) Ghosh, K and Schnitzer, M , Soil Sci., 129, 266-276 (1980)

(16) Kleinhempel, Albtecht Thear Archives, 14, 3-14 (1970) *opt cit* in Buffle, J , Complexation Reactions in Aquatic Systems, An Analytical Approach, Ellis Hirwood Limited, (1988)

(17) van Raij, B and Peech, M , Soil Sci Soc Amer , Proc , 36, 587-593 (1972)

(18) Schofield, R K , J Soil Sci , 1, 1-8 (1949)

(19) Morais, F I, Page, A L and Lund, L J , Soil Sci Soc Amer J, 40, 521-527 (1976)

(20) Sparks, D L , Soil Physical Chemistry, CRC Press, (1986)

(21) Chang, S M and Choi, J , J Korean Agricultural Chemical Society, 30(1), 1-8 (1987)

Chapter 2

Peat Soils

2 Introduction

Peat is an organic soil which is formed by the accumulation of decayed vegetative matter that has formed in areas of poor water drainage Under the United States Department of Agriculture (USDA) classification system peat belongs to the organic group of soils referred to as the Histosols, see Chapter 1, Table 1 3 (1) Deposits of peat vary from the small pockets of organic soil that are to be found by the banks of rivers and lakes, to the larger areas of peat land, which are referred to as bogs in this work, but are also known by several other names, including moors, fens, swamps, etc (2) The depth of a peat deposit can vary considerably, from as little as 30 cm (the minimum thickness of peat soil required for the area to be classified as a bog) to depths in excess of 50 to 70 m (2) However, on average most bogs are between 3 to 15 m in depth It can be seen from Table 2 1 that significant deposits are to be found in the high latitudes of the Northern Hemisphere, where large areas of peat have accumulated over the last 10,000 to 12,000 years (2) In addition, large peat deposits are to be found in tropical and subtropical regions such as Brazil and Indonesia (3)

The principal uses of peat are as a fuel and as a source of raw materials for the chemical industry As a fuel, peat is considered to be a very young coal Compared to coal, it is a poor energy source, typically oven-dried peat has a heating value of 5300 Kcal kg^{-1} compared to bituminous coal which has a heating values of 7300 Kcal kg^{-1} (2) World reserves of peat are estimated to be about 0 89 $x10^{12}$ tonnes compared to coal reserves of 7 6 $x10^{12}$ tonnes (2) Peat reserves in Ireland are estimated to be about 4 72 $x10^{9}$ tonnes (which corresponds to about 0 5 % of the World's resources) and Ireland is the second biggest producer of peat in the world after the former USSR (2)

It should be noted that a wide spectrum of organic soils are grouped under the peat classification These soils vary considerably in their physical and chemical properties, ranging from the sphagnum and fibrous peats which contain the remains of recognisable plant and moss species, to the highly decomposed plant residues which make up the muck soils

This chapter discusses the formation of peat and the various classification systems used to characterise it In particular, it is concerned with the various physical and chemical properties of peat and the influence of the state of decomposition on these properties

Table 2 1 **World's Peat Resources[a] (3)**

Country/Region	Area (hectares x 10^6)	Dry Weight (tonne x 10^9)
Canada	150 00	600 0
Former USSR[b]	92 30	302 00
USA	59 64	238 56
Indonesia	17 00	68 00
Finland	10 40	41 60
Sweden	7 00	28 00
South America	6 176	24 70
China	4 159	12 64
Africa	3 803	15 21
Norway	3 00	12 00
West Indies and Central America	2 888	11 55
Malaysia	2 500	10 00
United Kingdom	1 58	6 32
Ireland	1 18	4 72
Germany	1 11	4 44
Iceland	1 00	4 00
Other Far Eastern Countries	0 431	1 72
Netherlands	0 28	1 12
Japan	0 25	1 00
New Zealand	0 15	0 60
Denmark	0 12	0 48
Italy	0 12	0 48
France	0 09	0 36
Bangladesh	0 06	0 24
Switzerland	0 055	0 22
Austria	0 022	0 088
Belgium	0 018	0 072
Australia	0 015	0 060
Luxembourg	0 0002	0 0008
Total	273 05	878 18

Note [a] 1988 estimate [b] Values for region formerly occupied by USSR are the largest values given by Fuchsman (2)

2 1 The Formation and Classification of Peat Soils

The formation of peat soils and the various systems which are used to classify them are discussed in this section

2 1 1 The Formation of Peat

The development of an area of bogland is due to the accumulation of dead vegetative matter in areas of poor water drainage The two processes of bog formation are (4)

(i) lakefill, where the accumulation of plant material gradually forms a mat of dead matter which expands in area to fill the lake,

(ii) swamping, which occurs in areas of poor water drainage, such as marshes, where the build up of the dead vegetative matter gradually expands in area

Within the bog environment, the dead plant matter is gradually transformed into peat due to the process of humification, or decomposition These two terms tend to be used interchangeably, however, the term humification more correctly refers to the decomposition of the plant matter and its transformation from its original plant character to the organic residues found in organic soils (2) In particular humification refers to the formation of humic substances which are the most abundant and most stable form of soil organic matter, see Chapter 1

The formation of peat is basically due to the fact that the rate of accumulation of plant material in the bog is faster than its rate of decomposition As a result there is a gradual build up of semi-decayed vegetative matter at various stages of decomposition, this material is referred to as peat For a well-established bog, the rate of peat deposition is usually about 3 cm per 100 years (2) This rate does vary depending on several factors such as, seasonal conditions, the location of the bog, the plant species present, etc

The slow rate of decomposition is a result of the water logged environment of the bog which severely inhibits the process of decay as carried out by soil micro-organisms The most rapid rate of decomposition is confined to the top few centimetres of the bog At this depth the level of oxygen is high enough for

decomposition to be carried out by micro-organisms, mainly by aerobic and facultative bacteria

The more readily degradable materials are the first to be removed from newly dead vegetative matter These consist of the water soluble components of the plant cell, such as the simple sugars, nucleic acids and proteins The materials which make up the cell wall of the plant, such as cellulose, pectins, hemicellulose, lignin, etc , are more resistant to decay They are attacked by the soil micro-organisms at a much slower rate compared to the plant cellular components The first cell wall constituents to be removed include cellulose and pectins, due to their simple structures which make them accessible to microbial attack Lignin is more resistant to decay than the other cell wall components and as a consequence its rate of removal is much slower than the other materials

As the remaining plant residues are slowly compressed by the addition of new plant matter from above, the overall rate of decomposition begins to slow down This is due to the lower oxygen levels available to the soil micro-organisms at subsurface levels, and because of the increasing difficulty of degrading the cell wall material which remains, an increasing proportion of which is ligmn The resistant materials are slowly removed by the action of anaerobic bacteria below the surface of the bog, these bacteria may be'active to depths of up to 1 m below the surface

The rate of biological activity declines with increasing depth from the surface of the bog as does the rate of humification of the peat Very deep down in the peat (below 3 to 5 m) all biological activity has virtually stopped, and the residual plant materials are no longer subject to the action of biological decomposition However, the transformation of the peat has not stopped Under the slowly increasing pressure of the new layers being laid down above it, the peat undergoes the slow chemical transformation process which eventually leads to the formation of coal over geological time It can be seen from Figure 2 1, which illustrates the transformation of peat into coal on the geological time scale, that the percentage of elemental carbon increases over time from about 40 % in peat to greater than 90 % in anthracite coal Whereas the percentage of oxygen decreases from about 40 % in peat to about 2 % in anthracite, similarly the level of 'volatile matter' is observed to decrease from about 80 % in peat to about 5 % in anthracite (4)

Occurring simultaneously to the decomposition of the plant matter is the formation of the humic substances, i e the humic and fulvic acids As previously described in Chapter 1, the mechanism of their formation is uncertain It has been suggested that they are the result of microbial synthesis, or that they are the remains

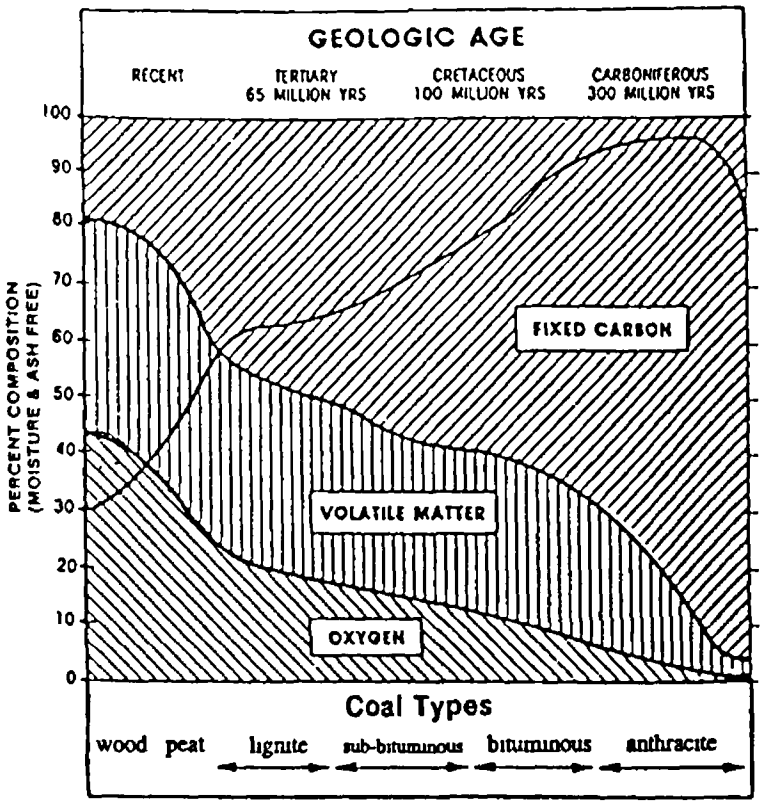

Figure 2.1 Comparison Between Peat and Older Coals (4)

of transformed plant residues (in particular lignin) However, whichever is the case, the proportion of humic substances present in peat soils has been found to increase with the increasing state of humification of the peat (2), this is discussed further in Section 2 2 1

2 1 2 The Classification of Peat

There are several different systems currently in use for the classification of peat These systems are based on such characteristics as the geology of the peat deposit, its botanical content, or its physiochemical properties (2 4)

The characteristic of greatest importance in a peat deposit from a geological perspective is its relationship to the water table of the surrounding mineral soil (2) This relationship results in the division of bogs into three broad categories, namely low-moor, transitional-moor, and high-moor peats In the low-moor and transitional-moor deposits, the water level in the bog is continuous with the water table of the adjacent mineral soil, the low-moors being somewhat wetter than the transitional-moors The high-moor peats are raised significantly higher than the surrounding water table and they tend to be the driest of the three types of moor

The botanical classification system of peat soils is based on the identification of the major plant species present in the peat The botanical classification system has been developed in greatest detail in Russia, and a total of 38 different classes are recognised (2) The system is based on the three main groups namely the low-moor, transitional-moor, and high-moor peats, and is further divided into six subgroups woody, woody-grassy, woody-mossy, grassy, grassy-mossy, and mossy Within each subgroup the peat is classified by the nature of the dominant plant species present

Botanical classification is relatively straight forward for the undecomposed peats, but identification of plant residues becomes progressively more difficult with increasing degree of decomposition or depth of the sample In addition, there can be significant changes in the plant species present in the peat deposit with increasing depth in the bog The botanical classification is applied mainly to the peats of the northern-temperate regions, and is not applicable to the peats found in tropical and semi-tropical areas, which contain different types of vegetation, such as mangroves and cypresses For the high-moor peat the principal species which may be present include the mosses (*Sphagnum*), which are the most common, and cotton grass (*Eriophorum*) The low-moor peat contain plants such as the fondiferous mosses (*Hypnum*), reeds (*Phragmites*) and sedges (*Carex*) Also, present are woody plants, such as alder (*Alnus*), willow (*Salix*) birch (*Betula*), and conifers The transitional-moors have variable mixtures of the above species

Neither the geological nor the botanical classification systems are completely satisfactory for the characterisation of peat soils These systems do not consider the nature of the peat material itself, and in particular ignore the state of humification of the peat which does significantly influence the nature and properties of the organic soil The most useful classification systems are based on the physiochemical properties of the peat, one of the most important physiochemical characteristics being the degree of decomposition of the soil sample (2)

A widely employed classification system in Europe is the von Post scale of humification (2, 5), a modified version of which is presented in Table 2 2 The von Post system defines 10 degrees of humification from H 1 for the slightly decomposed peats which contain recognisable plant residues to H 10 for the highly decomposed varieties which are usually referred to as mucks This is a subjective classification system and experience is required in its use The basic procedure is that a sample of the fresh peat is squeezed between the fingers of a clenched fist and note is taken of the amount and colour of water pressed from the hand and the consistency of the

Table 2 2 **The von Post System of Peat Humification (5)**

Degree of decomposition	Nature of water expressed on squeezing	Proportion of peat extruded between fingers	Nature of plant residues	Description
H 1	Clear, colourless	None	Unaltered, fibrous, elastic	Undecomposed
H 2	Almost clear, yellow-brown	None	Almost unaltered	Almost undecomposed
H 3	Slight turbid, brown	None	Most remains easily identifiable	Very slightly decomposed
H 4	Turbid, brown	None	Most remains identifiable	Slightly decomposed
H 5	Strongly turbid, contains a little peat in suspension	Very little	Bulk of remains difficult to identify	Moderately well decomposed
H 6	Muddy, much peat in suspension	One third	Bulk of remains unidentifiable	Well decomposed
H 7	Strongly muddy	One half	Relatively few remains identifiable	Strongly decomposed
H 8	Thick mud, little free water	Two thirds	Only resistant roots, fibres and bark, etc , identifiable	Very strongly decomposed
H 9	No free water	Almost all	Practically no identifiable remains	Almost completely decomposed
H 10	No free water	All	Completely amorphous	Completely decomposed

residue remaining between the fingers The results are compared to the descriptions, listed in Table 2 2, and the humification value of the sample is thus decided

The International Peat Society (IPS) proposed a contracted version of the von Post scale in 1976 (4) This divided the various degrees of decomposition of the peat into three broad states of decomposition, namely R 1 (equivalent to H 1 to H 3 on the von Post scale), R 2 (H 4 to H 6), and R 3 (H 7 to H 10)

In North America the USDA system divides peat into four suborders of the Histosol group, namely fibrist, folist, hemist and saprist (1, 4) An organic soil is classified into one of the subgroups based on a number of its characteristics, such as the identity of the major plant species present, its state of decomposition, and the degree of water saturation

(i) the fibrists comprise the least decomposed peats and fall in the H 1 to H 3 range on the von Post scale The fibrists consist of recogmsable plant fibres of sphagnum and other mosses,

(ii) the folists (H 1 to H 3) contain forest material intermixed with rock debris Both the folists and the fibrists subgroups are young peats which have undergone very little decomposition and contain very little inorganic material They are usually not saturated with water, but a combination of rainfall, mist and low temperatures keep the soils wet,

(iii) the hemists (H 4 to H 6) are composed of the partially decomposed remains of plant matter, the majority coming from reeds and sedges The hemists are generally well saturated for most of the year,

(iv) the saprists (H 7 to H 10), which are also known as the muck soils, are the most decomposed organic soils, none of the original plant materials which remain are recognisable The saprists are nearly always water saturated for most of the year

In Ireland, the USDA classification system has been adapted to suit Irish peat soils (24) The basic modifications have been at the family and series levels of the Histosol order to emphasise climatic and anthropic factors which are important in the Irish context

More quantitative methods for measuring the degree of decomposition have been summarised by Fuchsman (2) These include the Russian system of

microscopic estimation of the degree of decomposition This method consists of preparing thin layers of peat on microscopic slides and examining them at 100 to 140 times magnification The portion of visible solids that do not have fibrous structures is estimated to within 5 % A decomposition value of between 0 to 25 % by this method is equivalent to H 1 to H 5 5 on the von Post scale, and a range of 25 to 60 % decomposition falls between H 5 5 to H 10 A high degree of skill is required before accurate and reproducible results can be obtained by this method (2)

A second Russian procedure for measuring the degree of decomposition is the GOST method (2) A fresh sample of peat is placed on a 25 μm sieve and gently washed with water The water slurry passing through the sieve is collected, centrifuged, and the volume of solids measured This is compared to the unsieved peat, and the ratio of the two values is used as a measure of the state of decomposition of the sample (the manner in which the data is presented and its relationship with other humification scales such as the von Post scale was not stated)

A German method is based on dissolution of hemicellulose and cellulose by sulphuric acid and measuring the undissolved residue (2) The amount of residue remaining is expressed as a percentage of ash-free peat and is designated as the r-value The r-value is used to indicate the degree of decomposition of the peat, it is related to the von Post scale by the relationship H = (r/6 1) - 2 3 A comparison of the various classification systems is presented in Table 2 3

Table 2 3 A Comparison of the Various Classification Systems for Peat Soils to the von Post Scale of Humification

System	Scale									
von Post	H1	H2	H3	H4	H5	H6	H7	H8	H9	H10
IPS	R 1			R 2			R 3			
USDA	fibrist, folist			hemist			saprist			
Russian	0-25 %					25-60 %				
r-value	0 57	0 70	0 87	1 03	1 20	1 36	1 52	1 67	1 85	2 02

2 2 The Chemical Composition of Peat

Typically, in a sample of fresh peat about 80 to 90 % of the sample weight is accounted for by water (2) The solid material in peat accounts for only 10 to 20 % of the weight of the sample The solid is nearly all organic matter, with only 2 to 10 % of the solid material being inorganic

2 2.1 Organic Materials

The organic residues present in peat are derived mainly from vegetative matter, and to a lesser extent from microbial sources (2, 6) Peat contains an enormous number of organic compounds, thus, it should be appreciated that the chemical composition of peat is complex In addition, the composition of the peat can vary considerably from bog to bog, and even within the same bog the chemical composition can change with depth

The state of decomposition of the peat strongly influences its organic composition The change in the elemental composition of peat as a function of its state of decomposition is shown in Table 2 4 As can be seen, as the peat decomposes there is about a 10 % increase in its carbon content, from an initial value of about 50 % (H 1 to H 3) to about 60 % (H 8 to H 10), due to microbial degradation of the vegetative matter The percentage of oxygen decreases by about 10 % with increasing humification of the sample, from about 43 % (H 1 to H 3) to about 33% (H 8 to H 10) There are smaller increases in the percentages of nitrogen and sulphur with increasing state of decomposition while the percentage content of hydrogen remains roughly static

Table 2 4 Percentage Elemental Composition of Peat as a Function of Humification (2)

Element	H 1 to H 3	H 4 to H 7	H 8 to H 10
Carbon (%)	48-53	56-58	59-63
Hydrogen (%)	5 0-6 1	5 5-6 1	5 1-6 1
Oxygen (%)	40-46	34-39	31-34
Nitrogen (%)	0 5-1 0	0 8-1 1	0 9-1 9
Sulphur (%)	0 1-0 2	0 1-0 3	0 2-0 5

Note The values in Table 2 4 refer to the percentage of each element in the dry organic material fraction of the sample

As decomposition proceeds, the relative abundance of the various organic matter constituents decreases (4), see Table 2 4 The readily degraded materials, such as cellulose and hemicellulose, are the first to be attacked by the soil micro-organisms, and it can be seen that the levels of these materials drops to almost nothing in the highly decomposed peats (H 9 to H 10) The more resistant materials,

particularly lignin, are degraded at a slower rate, with the result that considerable amounts of these materials remain even in the highly decomposed mucks

However, it is not just loss of materials from the peat that is occurring during the process of humification The levels of bitumens and humic acids can be seen to increase (see Table 2 5), and in the highly decomposed samples the humic acids can account for up to 60 % of the organic matter present The amount of nitrogen containing compounds, which are derived from microbial sources, is also seen to increase, see Table 2 5

Table 2 5 Percentage of Various Organic Matter Constituents in Peat of Varying Degrees of Humification (%, Dry Basis) (4)

Organic material	H 1 to H 2	H 5 to H 6	H 9 to H 10
Cellulose (%)	15-20	5-15	-
Hemicellulose (%)	15-30	10-25	0-1
Lignin (%)	5-40	5-30	5-20
Humic acids (%)	0-5	20-30	50-60
Bitumens (%)	1-10	5-15	5-20
Nitrogen compounds (%)	3-14	5-20	5-25

The plant material from which the peat is derived does have some influence on the chemical composition of the peat, though it is not as influential as the level of humification Some indication of the influence of plant origin on peat composition can be seen from Table 2 6 (2) This table compares the composition of peatland plants to the composition of low-moor (sedges and forests) peats and high-moor (moss) peats to which such plants give rise Proceeding from plant to peat composition it can be seen that characteristic changes occur In particular, the decomposition of the carbohydrate fractions, noticeably the cellulose, is greatest in the sedge and forest derived peats, while the more resistant lignin comprises a larger percentage of the forest derived peats than other peat types

The organic matter constituents which make up the peat are varied, and for convenience the major constituents have been divided into four broad groups, namely bitumens, carbohydrates, lignin and lignin-like materials, and humic substances (2) The division of the peat constituents into the four groups is based on the solubility of the various groups in organic and aqueous solvents

Table 2 6 **A Comparison of Peat Plants and Peat Soils (%, Dry Basis) (2)**

	Sedges		Mosses		Forest	
	Plant	Peat	Plant	Peat	Plant[a]	Peat
Ether-soluble	1-3	1-3	1-5	2-6	4	3
Water-soluble	3-13	2-3	4-8	ND[b]	15	N[b]
Hemicelluloses	12-31	0	21-25	12-19	17	3
Lignins[c]	21-42	38-46	7-12	25-52	30	61
Proteins[d]	4-15	22-23	4-6	5-6	3	14
Ash	3-5	10-13	3-4	1-2	5	4
Total	93-98	88-91	73-86	73-87	90	90

Note ([a]) Oak leaves, ([b]) ND not determined, ([c]) including humic acids, ([d]) assuming all nitrogen present to be protein

(1) bitumens The bitumens are those components of peat which are soluble in hot, nonpolar organic solvents and can thereby be isolated from the rest of the peat which remains undissolved The bitumens are a large group of heterogeneous compounds which include esters, organic acids, alcohols, hydrocarbons, aromatics, sterols, etc The proportion of bitumens extracted from peat does vary with peat type (2) The yield of bitumens also increases with increasing state of decomposition of the peat, as can be seen from Table 2 5 In addition, the yield of bitumens varies with the solvent used for extraction Various organic solvents are used, ranging from petroleum ether which only dissolves a small amount of the organic compounds present in peat, to stronger solvents, such as benzene, chlorinated hydrocarbons, ethers, ketones, esters, alcohols, organic acids, and binary mixes such as benzene-ethanol which dissolve most of the bitumens present in the peat The bitumens can be further divided into subgroups, again based on their solubility in organic solvents (2) These subgroups are

- resins, which are extractable in low-boiling point alcohols at room temperature,
- waxes, which are soluble in aliphatic hydrocarbons,
- asphalts, which are insoluble in both light petroleum ether, and in hot methanol,

(ii) carbohydrates The carbohydrates are the largest fraction of organic matter present in peat (2) They are divided into two broad groups based on their aqueous solubility

- the water soluble and easily hydrolysed carbohydrates, such as hemicellulose, pectin and some of the glycosides
- the water-insoluble and difficult to hydrolyse carbohydrates, which consist of cellulose only

The following are the major carbohydrates found in peat (2)

- pectin, which is extracted from peat by hot water Pectin is a linear chain of galacturonic acid units, linked by 1,4-α bonding, see Figure 2 2

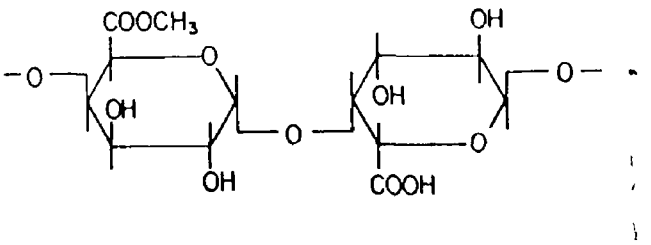

Figure 2.2 Structure of Pectin (2)

- hemicellulose, which is soluble in mildly alkali solution, and is precipitated by re-acidification The hemicelluloses are the carbohydrates present in the largest proportion in most peats Their origin is uncertain, the hemicelluloses found in peat are thought to be partially derived from plant matter, but may also originate from microbial sources Hemicellulose is a complex material, consisting of 200 to 300 sugar units linked to form long chains The sugar units found in hemicellulose are glucose, fructose, mannose, galactose, xylose, arabinose, rhamnose, glucuronic acid, galacturomc acid, O-methylated sugars and glucosamine From Table 2 5 it can be seen that the level of hemicellulose decreases with increasing state of decomposition of the peat
- cellulose, which is insoluble in water It is a linear polymer of glucose containing as many as 10,000 sugar units, joined by 1,4-β linkages, Figure 2 3

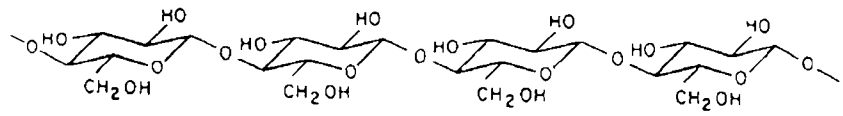

Figure 2.3 Structure of Cellulose (7)

- chitin, which is found in the cell walls of fungi, and is a linear polymer of N-acetylglucosamine, see Figure 2 4,

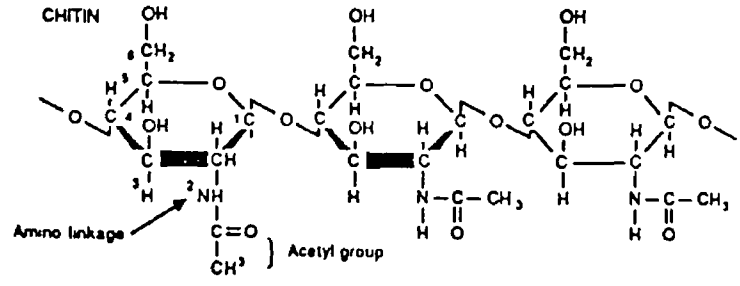

Figure 2.4 Structure of Chitin (6)

(iii) the lignin and lignin-like materials The fundamental unit of the lignin structure is that of a phenol substituted in the para-position by an n-propyl chain, and in one or both ortho-positions by a methoxyl group, see Figure 2 5 The lignin units are linked in a variety of ways to form a complex macromolecular structure The basic function of lignin is to give support to the plant, and as a result of its complex structure to protect the living plant from biological attack from micro-organisms Due to the resistance of lignin to decay, the proportion of lignin increases with the degree of decomposition of the sample,

Sphagnum moss does not contain true lignin, but contains sphagnol, a material which is closely analogous to lignin (2, 8) In sphagnol, p-hydroxyphenylpropyl units replace the methoxy containing guaiacyl units found in the lignins of the higher plants, see Figure 2 6,

(iv) the humic substances have already been discussed in Chapter 1, it only remains to be added that humic substances are not found in living plants, and their presence in peat is due to the processes of humification

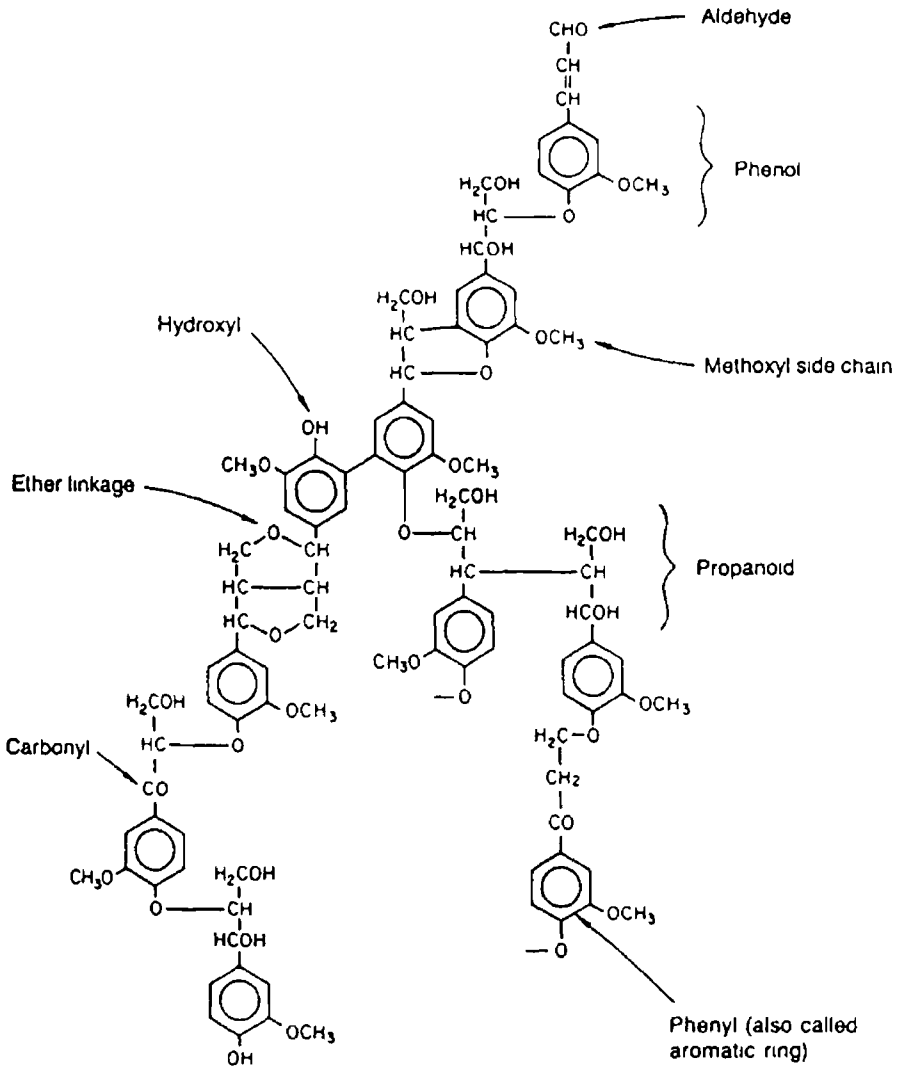

Figure 2.5 Generalised Structure for Lignin (6)

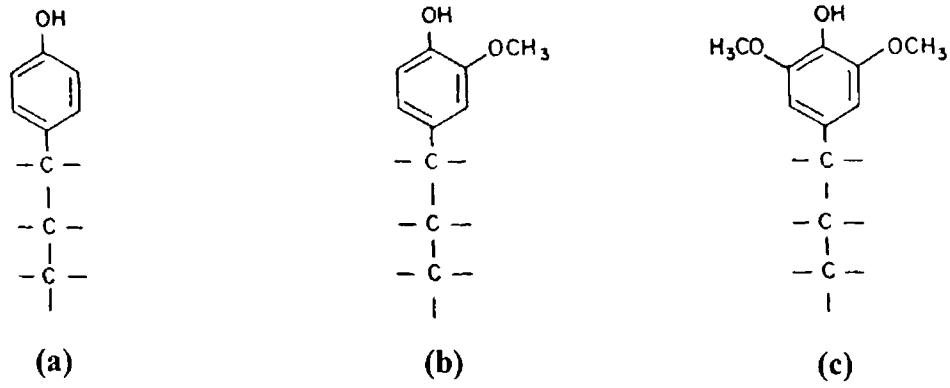

Figure 2.6 Comparison of Lignin and Lignin like Materials (2)

Note (a) para-hydroxyphenylpropane (presumed structural unit of sphagnol), (b) guaiacyl-propane (lignin structural unit), (c) syringylpropane (lignin structural unit)

2 2 2 Inorganic Materials

Ignoring water, the inorganic fraction of peat usually accounts for only 2 to 10 % of the dry weight of the sample, for the highly decomposed mucks this can increase to about 60 % of the dry weight (2) The inorganic composition of peat varies considerably from region to region (4) Table 2 7 compares the amount of elements found in the ash of peat samples from Germany, Finland, Canada and the United States It can be seen from the table that the amount of a particular inorganic species present varies considerably between regions

Table 2 7 Ash Composition of Peats from Various Countries[a] (4)

Material	Germany (%)	Finland (%)	Canada (%)	United States (%)
CaO	2 0-45 0	1 5-4 6	1 3-42 7	2 3-47 8
Al_2O_3	1 0-11 0	1 3-5 1	3 3-23 1	5 1-16 6
SiO_2	10 0-45 0	50 0-72 0	7 9-38 8	42 0-91 2
Fe_2O_3	1 5-5 5	4 6-7 1	2 4-11 6	0 3-8 9
S	-	0 2	0 01-0 75	-
MgO	1 0-20 0	-	1 3-27 8	0 5-7 0
MnO	0 1-0 3	-	0 1-0 2	-
K_2O	0 1-2 5	-	0 4-2 8	0 2-2 8
Na_2O	0 2-5 0	-	0 3-2 0	0 1-2 9
P_2O_5	1 0-3 0	2 3-4 2	0 0-2 6	-

Note [a] Percentage composition of ash (moisture free basis)

In general the total inorganic content of the peat (which is usually expressed in terms of the ash content of the sample) is greatly influenced by the following two factors

(i) the relationship between the peat deposit and the local water table, from Table 2 7 it can be seen that the ash content of peat samples decreases in the following order, low-moor (7 6 % ash), transitional-moor (6 6 % ash) and high-moor peat (2 4 % ash) This trend may be explained by recalling from Section 2 1 2 that the water table of the low-moor and transitional-moor deposits overlap with the water table of the adjacent mineral soil As a result, the water is relatively rich in inorganic materials which can be transferred to the low-moor and transitional-moor peats On the other hand, the lower inorganic content of the high-moor peat is due to the fact that this bog type is above the local water

Table 2 8 **The Variation in the Inorganic Content of Peat with the State of Decomposition (4)**

Ash and element	Peat type		
	Saprist (muck)	Hemist	Fibrist
Fe	1 73 %	0 4 %	0 08 %
Be	1 90	0 20	0 01
Pd	17 33	2 09	1 24
Ga	9 84	0 58	0 78
Mg	0 49 %	0 44 %	0 10 %
Y	12 33	1 39	0 11
Nd	33 52	4 27	0 54
Ca	0 60 %	0 24 %	0 09 %
Cd	NS	0 87	1 03
Zn	30 18	9 70	0 39
Ti	0 11 %	0 007 %	0 001 %
Co	6 39	0 69	0 15
Zr	109 32	5 55	1 08
Mn	312 90	176 00	35 57
Cr	40 05	3 59	1 33
Sc	8 55	0 79	0 08
Si	14 54 %	0 51 %	0 07 %
Ag	0 09	0 02	0 007
Cu	22 60	7 82	1 50
Sn	3 19	0 37	0 07
Al	4 87 %	0 21 %	0 03 %
La	20 17	3 03	0 34
Sr	110 31	35 54	13 3
Na	1 15 %	0 05 %	0 03 %
Mo	0 82	0 48	0 10
K	1 25 %	0 57 %	0 008 %
B	35 41	8 23	2 67
Nb	7 37	3 67	0 07
P	0 80 %	0 35 %	0 01 %
Ba	237 99	22 60	6 06
Ni	16 81	2 38	1 14
V	39 98	2 67	0 43
Ce	46 04	13 80	0 58
Yb	2 68	0 20	0 008
Total ash	57 4 %	4 9 %	1 25 %

Note Ash is moisture free The elements obtained from the ash are calculated on a whole-sample basis and are give in ppm unless indicated in percent

table As a result, its main source of inorganic material is from rain or snow which have relatively low concentrations of inorganic materials (2),

(ii) the state of decomposition of the peat, Table 2 8 (4) shows the total percentage ash content of peat samples taken from a bog site which contained three peat layers, each at a distinct stage of decomposition, namely a muck (well decomposed saprist peat) overlaid with a hemist peat layer and a fibrist peat layer respectively As can be seen from Table 2 8 the ash content of the peat increases with increasing state of decomposition of the peat in the order, fibrist peat (1 25 % ash), hemist peat (4 9 % ash) and saprist peat (57 4 % ash) This trend is related to the cation exchange capacity of the peat (see Section 2 3 1) which increases with the state of decomposition of the peat, and therefore the ability of the peat to retain cationic species also increases with decomposition (5)

2 3 The Physical Properties of Peat

The physical properties of peat are dependent on the state of decomposition of the peat and to a lesser extent on the plant matter from which it was derived The general physical properties which have been reported in the literature are mainly related with the application of the peat for horticultural purposes (4, 5) Thus, physical properties concerning the structure of the peat, its porosity and pore distribution, density, the water permeability and water retention capacity, and the acidity and cation exchange capacity of peat are discussed

2 3 1 Bulk Physical Properties of Peat

In appearance, the physical structure of peat ranges from the relatively undecomposed mats of well-preserved plant remains to the amorphous mucks containing highly decomposed organic residues From Table 2 9, which shows some of the general physical properties of various peat materials, it can be seen that the density of peat increases with increasing humification of the sample, while the fibrous content of the material is found to decrease with increasing degree of decomposition

Table 2 9 **Physical Properties of Various Peats (4)**

von Post Scale	H 1 to H 3			H 4 to H 6	H 7 to H 10
Peat type	Sphagnum moss	Hypnum moss	Reed sedge	Partly decomposed peat humus	Decomposed humus
Property					
pH	3 2-4 0	5 0-7 0	4 0-7 0	4 0-7 5	3 5-8 0
Density (kg m^{-3})	48-80	64-96	80-96	112-192	280-480
Maximum water content (%)	90	90-92	90-92	80-90	80-90
Average fibre content (%)	85-95	80-85 .	70-80	40-60	10-20

Peat is a very porous material, particularly the peat mosses, with total pore volume accounting from 85 to over 98 % of its volume (5) This is quite large when it is considered that mineral soils have pore volumes of 50 to 70 % The pore size distribution in peat is divided between the macropores, which are those pores above 0 03 mm in diameter, and the micropores which are below this value (5) As can be seen from Table 2 10 the percentage of the peat's volume occupied by micropores is found to increase with increasing humification of the sample while the percentage of macropores decreases As a result of its high porosity, peat has a large water retention capacity, it has been found that the fibrous peats can hold up to 15 to 20 times their own dry weight in water, while the amorphous types can hold from 4 to 8 times their dry weight equivalent (5)

Table 2 10 **The Percentage Macropore and Micropore Distribution in Various Peat Types (5)**

Peat type	Micropores (%)	Macropores (%)
Coarse sphagnum moss peat[a]	18	78
Medium-coarse sphagnum moss peat[a]	29	66
Fine, dark sphagnum moss peat[b]	43	50
Black peat[c]	50	39

Note On van Post scale ([a]) H1-H3, ([b]) H3-H6, ([c]) H6-H10

It can be seen from Table 2 9 that peat tends to be acidic in nature (5) This is due to the presence of a wide range of acidic functional groups which are able to release H^+ into the surrounding peat environment In particularly, the carboxyl (COOH) and phenolic hydroxyl (OH) groups are responsible for the acidic character of peat These acidic groups are present at the surface of large undecomposed peat particles or in the increasing amounts of humic substances which are found in peat as humification proceeds As a result, peat has a larger capacity to adsorb OH^- ions compared to other soil types This can be seen from Figure 2 7 which shows the adsorption of NaOH per 100 g of soil versus the equilibrium pH of the solution It can be seen from the figure that the peat soils (sedge peat, bryales peat and light sphagnum peat) have higher capacities for the adsorption of NaOH than the silt, heavy clay and mould samples (8)

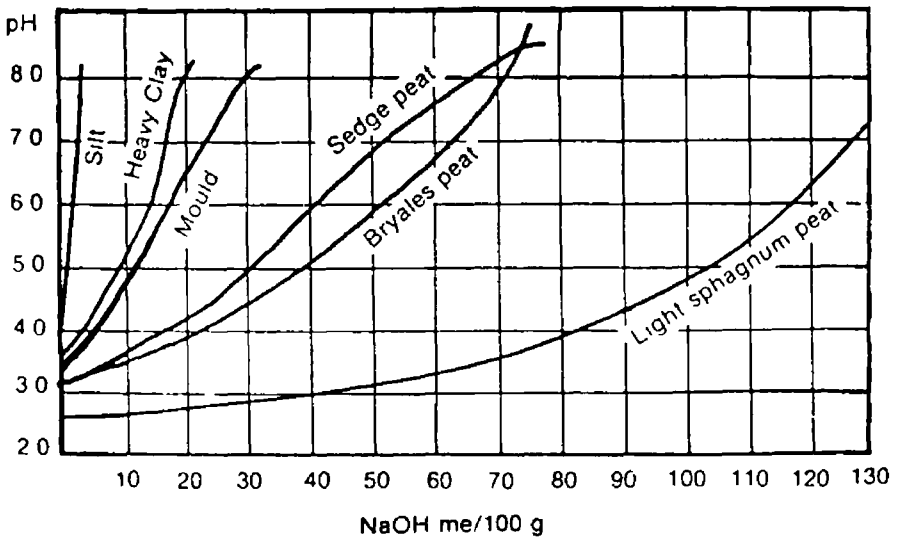

Figure 2 7 **A comparison of the Adsorption of NaOH by Various Soil Types (8)**

In general the high-moor peats tend to be the most acidic having pH values of 3 to 5 The transitional peats have pH values of 3 5 to 6, while the low-moor peats have pH values of between 4 to 7 5

As a consequence of the large number of acidic groups present in peat, it has a large capacity to attract and retain positively charged ions at its surface The capacity of a soil to retain cations is called the cation exchange capacity (CEC) which is usually expressed as milliequivalents per 100 grams (meq $100g^{-1}$) of air-dried material or as milliequivalents per litre of fresh peat (meq dm^{-3}) The cations which are adsorbed on the surface of the peat are termed exchangeable cations and the process of interchange between the adsorbed cations and those in solution is called

cation exchange CEC is pH-dependent and it must be determined at a fixed pH, usually pH 7 The CEC of peat has been found to increase generally with increasing degree of decomposition and is dependent on the plant species from which it was derived, see Table 2 11 In contrast to the large CEC of peat, its ability to take up anions is very low (5)

Table 2 11 The CEC of Different Peat Types and Peat-Forming Plants (5)

Species/Peat type	CEC	
	meq $100g^{-1}$	meq dm^{-3}
Sphagnum fuscum	140	80
Sphagnum papillosum	110	60
Sphagnum suspidatum	90	45
Undecomposed sphagnum moss peat	130	80
Sphagnum-sedge peat	110	60
Sedge peat	80	40
Highly decomposed black peat	160	240

2.3 2 Thermal Characterisation of Peat

The thermal analysis of peat has involved the use of several different techniques which can be divided into the following categories

(i) those which measure weight loss (or gain) to the peat sample with heating These consist of thermogravimetric analysis (TG or TGA) which measured the weight loss to the sample directly and differential thermogravimetric analysis (DTG) which measures the rate of weight loss to the peat sample,

(ii) those which measure the endothermic/exothermic activity of the peat sample with heating Differential scanning calorimetry (DSC) and differential thermal analysis (DTA) belong to this category Both of these techniques measure the endothermic/exothermic activity of the sample, they differ only in the instrument design,

(iii) measurement of the gas evolved by the sample on heating by evolved gas analysis (EGA) The gases usually measured are CO, CO_2 and H_2O

Schnitzer and Hoffman (9) examined the differential thermogravimetric (DTG) curves of 22 Canadian organic soils as a means of assessing the degree of humification of the sample The 22 soils examined were classified into three groups, namely peats, mucky peats and mucks, which were of increasing state of decomposition The DTG results are shown in Figure 2 8

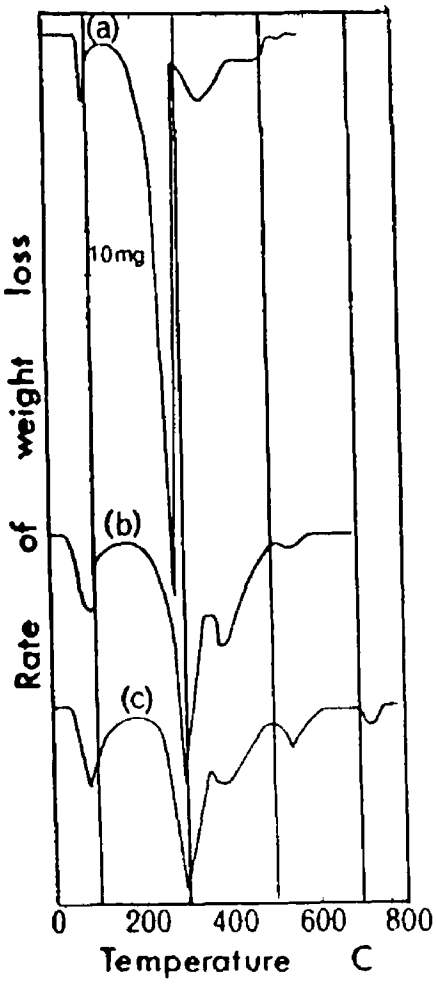

Figure 2 8 DTG Curves for the Decomposition of Canadian Organic Soils (9)
Note (a) peat, (b) mucky peat, (c) muck

The results of Figure 2 8 can be summarised as follows,

(i) the initial peak maxima on all three DTG curves occurred near 100°C and represented water evaporation from the soil samples,

(ii) the height and broadness of the peak maxima near 280°C were found to be inversely related to the state of decomposition of the sample For the peat samples the peak maximum at 270°C was long and narrow in shape, for the mucky peats this peak was shorter and broader while for the muck samples the

peak maximum had shifted to 290°C and was smaller and broader still The sharpness of the 270°C peak for the peat samples suggested that the organic matter fraction responsible for this peak was more homogeneous than the fraction present in the mucky peat and muck samples The identity of the 280°C peak was subsequently identified by Schnitzer and Hoffman (10) as being due to the thermal decomposition of the cellulose fraction of the peat The decomposition of the lignin fraction of the peat gave only a poorly defined peak at 280°C, which was considered to be due to the presence of cellulose impurities in the samples, and a second larger peak maximum at 480°C

(iii) the peak at 370°C was found to be not solely related to the degree of humification of the sample, but it was observed to become more prominent with increasing state of decomposition of the sample The organic matter fraction of the soil responsible for this peak was not identified

(iv) the smaller peak maxima for the mucky peat and muck samples at 540°C was considered to be due to decomposition of Ca-organic matter complexes, while the peak at 720°C on the muck DTG curves was due to the decomposition of carbonates

Levesque and Dinel (11) reported on DTG and DTA (differential thermal analysis) curves of four peat soils chosen for their botanical composition and degree of decomposition, see Table 2 12 In addition to the peat samples, the thermal analysis of holocellulose, humic and fulvic acids and several peat forming plants and mosses were also studied to compare with those of the original samples (Holocellulose is a mixed category of substances, comprising principally of cellulose and hemicellulose [2]) The objectives of Levesque and Dinel (11) were to determine the usefulness of thermal analysis as a method for characterising various peats and in particular to investigate the claim of Schnitzer and Hoffman (9, 10) that a positive correlation existed between the size and shape of the peak maximum near 300°C and the state of decomposition of the peat on DTG curves They also examined if the DTG and DTA curves gave any indication of the vegetative origin of the peat (i e was it derived from plant or moss)

The results of the DTG curves for the four soils are shown in Figure 2 9 It can be seen from the figure that apart from the peak maxima located at 60°C for the peat samples which corresponded to water loss, there were three main regions of weight loss observed as follows

Table 2 12 Composition and Properties of the Four Peat Soils[a] Studied by Levesque and Dinel (11)

Parameter	Peat[a]			
	Gatineau	Cochrane	Clothilde	Ormstown
Peat material formed from	Sphagnum	Sedge-fen	Woody-fen	Sedge-fen
Carbon (%)	44 1	51 2	48 7	52 9
Nitrogen (%)	0 86	2 79	3 41	2 12
C/N ratio	51 3	18 5	14 3	25 0
Phosphorus (μg/g)	197	353	394	535
Ash (%)	6 4	6 2	10 9	7 1
pH	3 3	5 0	5 3	3 3
Cellulose (%)	13 5	6 9	3 3	6 6
Holocellulose (%)	50	20	10	16
Fibre content (%)	65 6	49 2	42 1	29 6
Optical density (465nm) of P_2O_7 extract (0 025M)	0 17	0 23	0 24	0 65
Calorific value (cal g^{-1})	4772	4670	4316	4772

Note [a] peat soils are arranged in order of increasing decomposition This was based on their fibre content (which decreased with increasing degree of decomposition) and on the optical density at 465 nm (which increased with increasing degree of decomposition)

(i) the first at 275° to 325°C with peak maxima at about 300°C This region of weight loss was the most prominent, it was concluded that it corresponded to the thermal decomposition of the readily degradable materials such as cellulose The area under this peak was found not to correlate with the degree of decomposition of the peats, for instance the peak for the Ormstown sample (the most decomposed peat) did not differ greatly from the peak for the Gatineau sample (the least decomposed of the peats),

(ii) the second region was between 360° to 460°C with a peak maxima at about 400°C This peak maxima was concluded to be due to the thermal decomposition of humic substances present in the peat samples (see later)

(iii) the third region was between 500° to 560°C, which was associated with the thermal decomposition of the non-hydrolyzable residues The lack of thermal activity of the Ormstown peat (Curve 4 in Figure 2 9) above 420°C was considered to be a result of its botanical origin (derived mainly from *Carex* and *Eriophorum* species) and its relatively well decomposed state

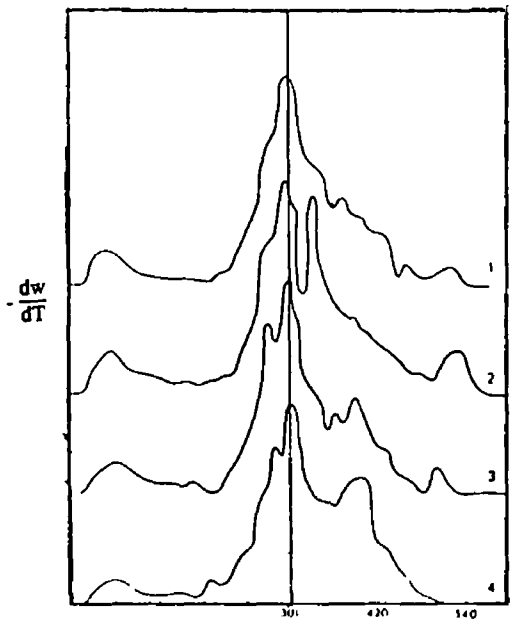

Figure 2 9 DTG Curves of Various Peat Materials (11) Note heating rate 2°C min^{-1}, Curve-1 Cochrane, Curve-2 Clothilde, Curve-3 Gatineau, Curve-4 Ormstown

The DTG curves of the hollocellulose fraction of the four peats are shown in Figure 2 10 (11) A sharp peak at 300°C was observed in the curves for all four peats studied Secondary peaks in the 375° to 500°C range were less clearly defined, for the Cochrane and the Gatineau peats the secondary peak maximum was located at 450°C, for the Clothilde and Ormstown it occurred at about 500°C

The DTG curves for the humic and fulvic acid fractions which were obtained from a chernozemic A1 horizon are shown in Figure 2 11 (11) The humic acid showed two peak maxima, the first at 280°C and a more prominent peak at 460°C The fulvic acid had two sharp peak maxima at 360°C and 385°C, the last peak coincided with one of the secondary peaks of the humic acid

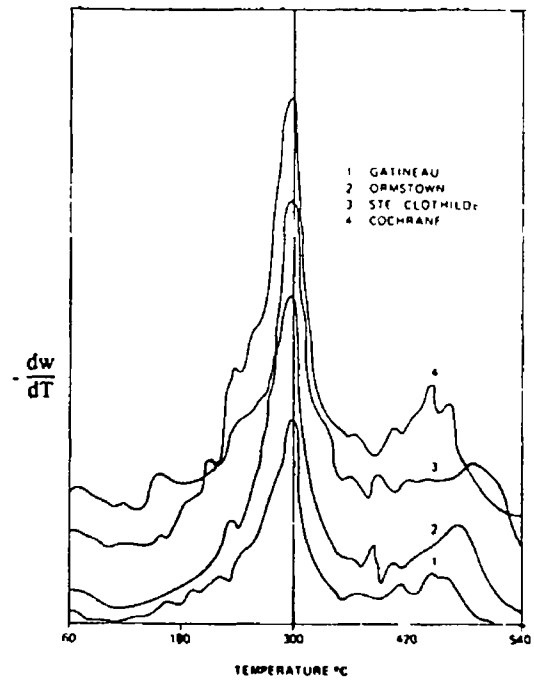

Figure 2.10 **DTG Curves for the Holocellulose Fraction of the Four Peat Materials (11)**

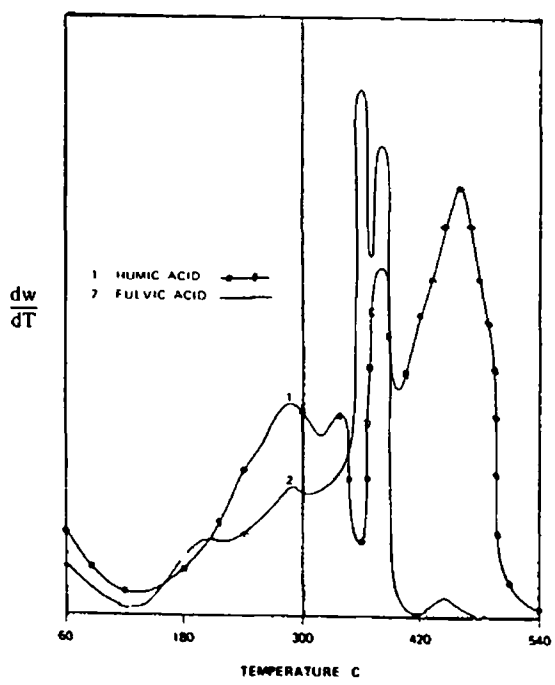

Figure 2.11 **DTG Curves for Humic and Fulvic Acid Fractions (11)**

DTG for peat-forming plants (species of *Typha*, *Carex*, *Alnus* and *Juncus*) and mosses (species of *Sphagnum*, *Polytrichum*, *Hypnum* and *Drepanocladus*) were also examined (11) For the mosses studied the peak pattern was complex with broad peaks observed around 300°C and an undifferentiated portion around 420°C, see Figure 2 12 (11) The DTG curves for the Sphagnum and Hypnum mosses did show some similarities, particularly around 420°C A comparison of the DTG curves for the mosses with the original peat soils indicated some similarity between the Sphagnum curve and the Gatineau peat, which is derived from Sphagnum mosses Also, some similarity was found between the Polytrichum curve and the Cochrane peat which is derived from several mosses including Polytrichum

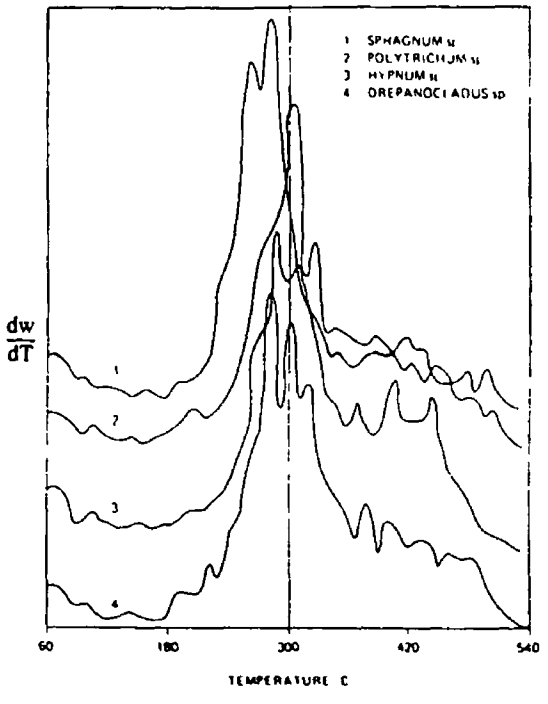

Figure 2.12 DTG Curves for Peat-Forming Mosses (11)

The DTG curves for the peat-forming plants differed from one another in general shape, particularly in the 275° to 325°C region, however they did share a common undifferentiated region of their curves between 380° to 480°C, see Figure 2 13 (11) The most prominent peak for the plants occurred above 300°C In general the DTG curves obtained for the peat-forming plants were found to have little similarity with the curves for the peat soils

The results of the DTA curves for the four peat soils are shown in Figure 2 14 The DTA curves showed three well defined exothermic peaks, which were as follows

(i) the first at 250° to 375°C with the maximum at 320° to 340°C,

(ii) a second peak at 375° to 450°C with the maximum at 418° to 432°C,

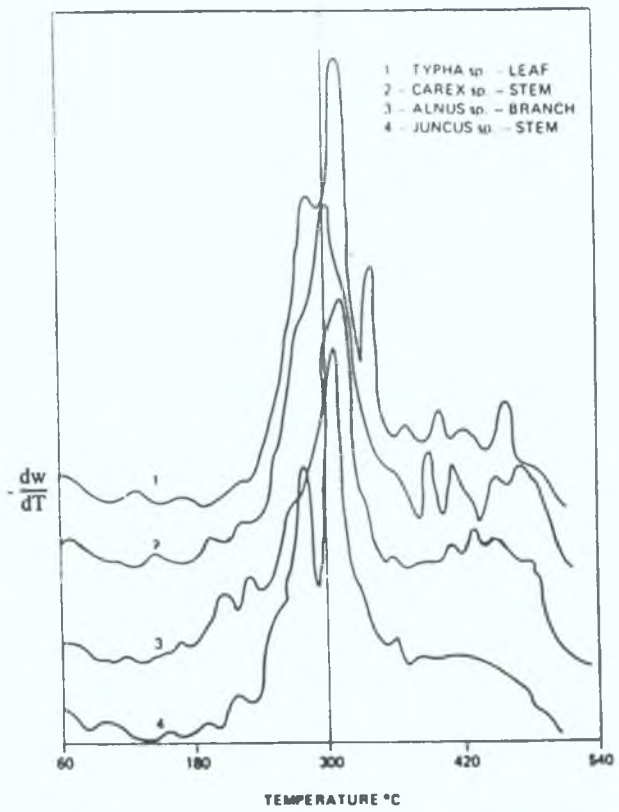

Figure 2.13 **DTG Curves for Peat-Forming Plants (11)**

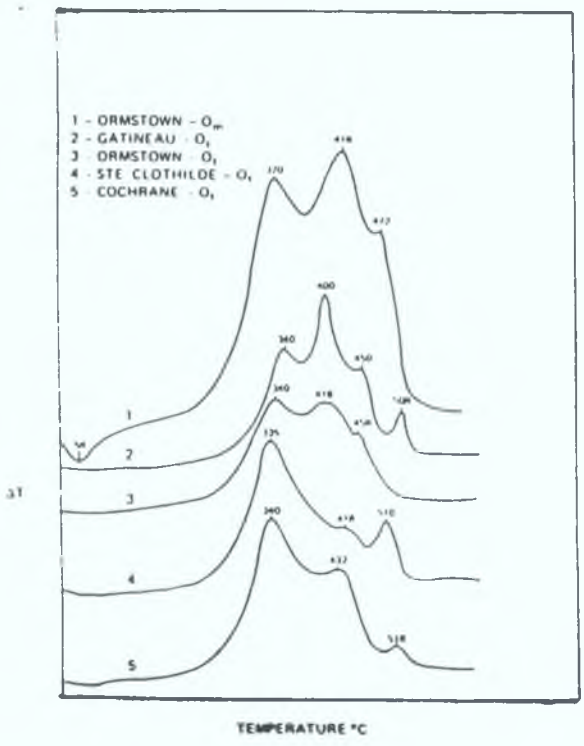

Figure 2.14 **DTA Curves for Various Peat Materials (11)** Note: Curve-1 Ormstown-O_m; Curve-2 Gatineau-O_f; Curve-3 Ormstown-O_f; Curve 4 Clothilde-O_f; Curve-5 Cochrane-O_f, where the O_m and O_f suffixes indicate that the sample was taken from a moderately decomposed peat layer (O_m) or a fibrist layer (O_f), i.e. layer has undergone little decomposition.

(iii) the third peak at 450° to 525°C with the maximum at 472° to 518°C
The Gatineau sample (curve 2) differed from the other three peats in having a four peak pattern with the additional prominent peak at 400°C In general the results of the DTA curves were found to correlate closely to the DTG curve pattern It was also observed from a comparison of the Ormstown O_m and O_f layers that an increase in the state of decomposition of the peat also increased the size of the second (ii) peak (The O_m and O_f suffixes indicate that the sample was taken from a moderately decomposed peat layer (O_m) or a fibrist layer (O_f), i e layer has undergone little decomposition)

Levesque and Dinel (11) conclude that specific features of the DTG curves could not be readily correlated to the dominant plant or moss species from which the peat originated, or be related to specific chemical components of the peat However, the DTG curve could be used to give a rough approximation of the complexity of the botanical source of the peat In addition the height of the 300°C peak could be used as an approximation of the degree of decomposition of the peat sample as it reflects the concentration of more readily degradable compounds

Ranta *et al* (12) reported on the simultaneous thermal analysis of a Finnish raised bog sphagnum peat (H 7 on the von Post scale, 36 % according to GOST method) and on its extracts (bitumens, readily hydrolyzable and water-soluble components, humic acids and lignin) using TG, DTG, DTA and evolved gas analysis (EGA) for the detection of released H_2O and CO_2 from the sample The results of the thermal analysis of the peat sample are shown in Figure 2 15 (12)

It can be seen from the TG curve in Figure 2 15 that weight loss began at c 200°C The DTA results showed three peak maxima at 300°C, 344°C, and 386°C which closely corresponded to peak maxima on the DTG curve at 281°C, 341°C and 400°C respectively The EGA curve showed that the evolution of CO_2 (negative peak on the EGA curve) was greatest at about 344°C The ignition temperature (the temperature at which exothermic activity became detectable) of the peat sample was determined to be 228°C from inspection of the DTA curve

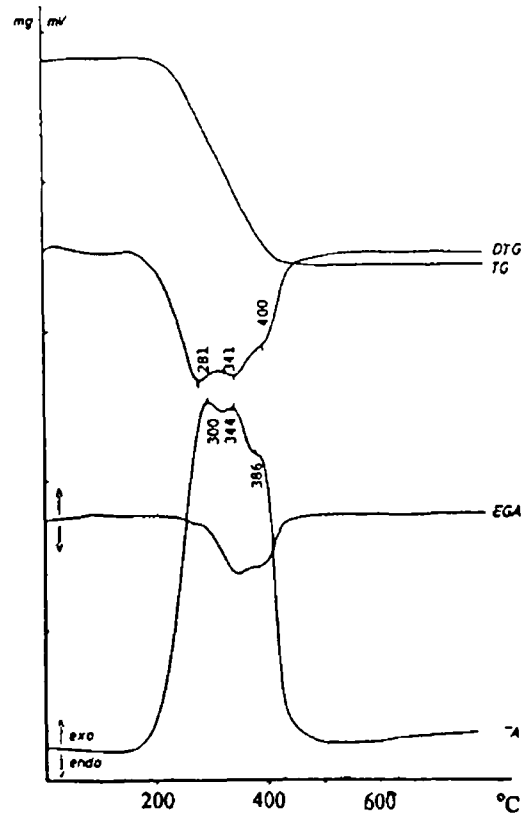

Figure 2 15 Thermal Curves for Peat Heated in Air Atmosphere (12)

Ranta *et al* (12) attempted to assign the various peak maxima of the original peat sample to specific peat components This was carried out by comparing the thermal decomposition curves of the peat sample to the curves for the various peat extracts The peat extracts examined consisted of the bitumens, easily hydrolyzable and water-soluble substances, humic acids and lignin The results obtained from the analysis of these peat extracts are shown in Figures 2 16 to 2 19 The results may be summarised as follows

(i) four bitumen fractions were examined, these were extracted from the peat using four different solvents, namely benzene-ethanol, benzene, petroleum ether and n-hexane The bitumen extracts were found to give different peak maxima on the DTA curves (see Table 2 13) but all extracts showed three exothermic peaks The DTA curve shown in Figure 2 16 was obtained for the bitumen extracted in hexane, the three peak maxima observed for this bitumen extract were at 363°, 429°, and 513°C It was found that the intensity of the first peak at c 363°C was dependent on the extraction solvent used

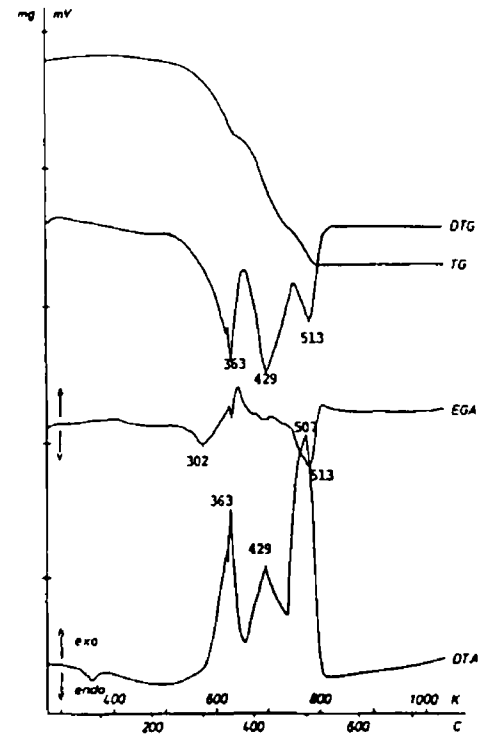

Figure 2 16 **Thermal Curves of Peat Bitumen (extracted with Hexane) (12)**

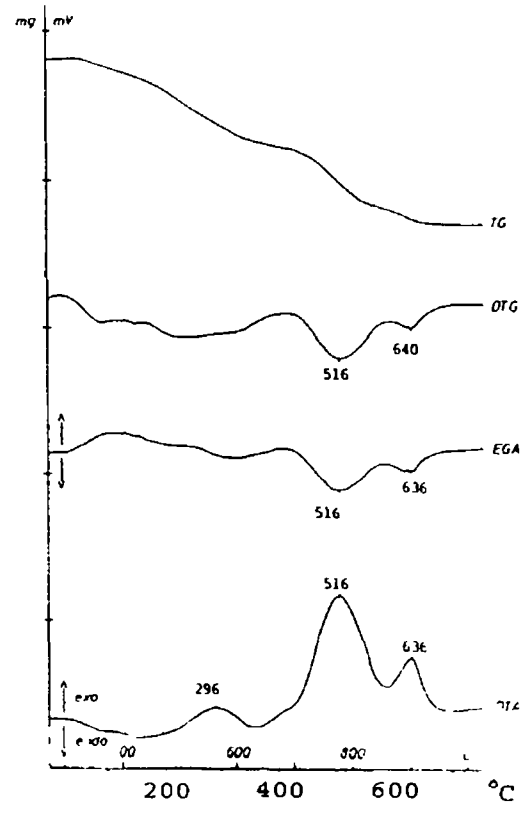

Figure 2 17 **Thermal Curves of Easily Hydrolyzable and Water-Soluble Materials (12)**

Table 2 13 **DTG and DTA Peak Maxima for Bitumen Extracts (12)**

Extracting solvent	Ignition point (°C)	DTG peak maxima (°C)			DTA peak maxima (°C)		
		I	II	III	I	II	III
Benzene-ethanol	300	331	416	515	331	416	505
Benzene	311	357	432	509	358	420	504
Petroleum ether	305	353	432	500	353	432	496
n-Hexane	305	358	429	513	358	421	507

(ii) for the easily hydrolyzable and water-soluble substances (see Figure 2 17) the DTA curve showed three peak maxima at 296°C, 516°C and 636°C respectively This corresponded closely to the DTG curve which showed peak maxima at 516°C and 640°C and the evolution of CO_2 (negative peaks) on the EGA curve occurred at 516°C and 636°C,

(iii) for the humic acids the DTA curve showed exothermic peaks at 332°, 426° and 504°C, each peak being successively larger than the previous one, see Figure 2 18 The DTG peak maxima were located at 426°C and 500°C which correspond closely to the DTA peaks From the EGA curve it was observed that the evolution of CO_2 was at a maximum at 426°C and 515°C,

(iv) for the lignin fraction of the peat the DTA curve showed a small exothermic peak at 153°C, but the curve was dominated by a single, large peak maximum at 470°C, see Figure 2 19 The DTG curve showed peak maxima at 90°C, 220°C and 470°C, while from the EGA curve it could be seen that a positive peak corresponding to water evolution occurred at 140°C while CO_2 evolution was observed at 214°C and 467°C

The major peaks of the exothermic curves from the DTA results are presented in Table 2 14 Ranta *et al* (12) made little comment on their results and it is difficult to assign the peak maxima of the various peat extracts examined with the peak maxima of the original peat sample It was concluded by the authors that the humic acid fraction seemed to be the most important with respect to the total energy of combustion (it accounted for 40 to 60 % of the energy released), the lignin/cellulose materials (about 25 %) and the readily hydrolyzable components (15 %), with the bitumens (2 %) the least important

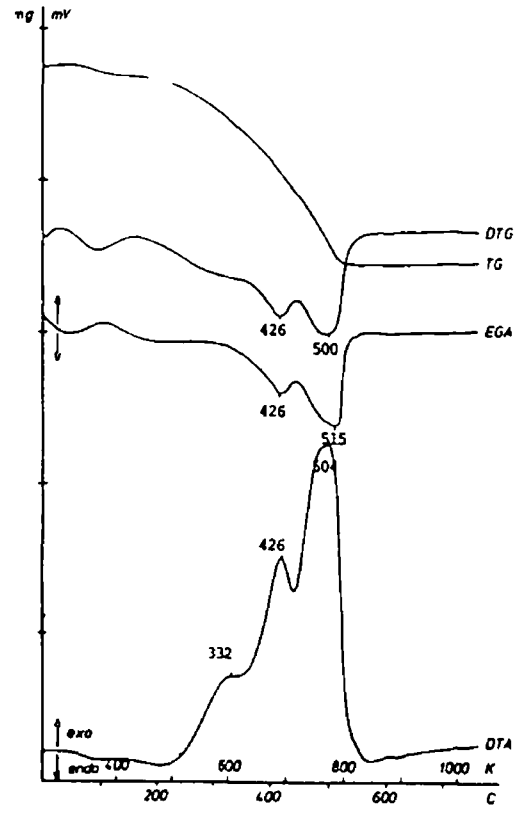

Figure 2 18 Thermal Curves of Humic acids (12)

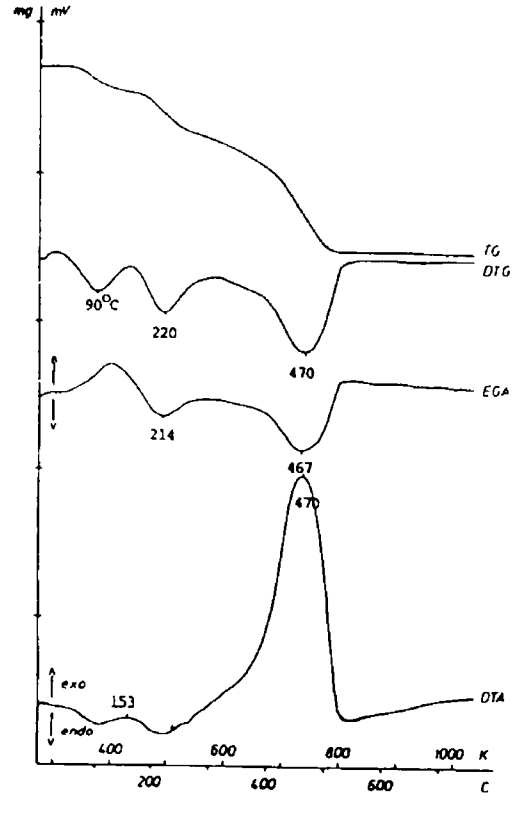

Figure 2 19 Thermal Curves of Peat Lignin (12)

Table 2 14 **Temperature and Ignition Points in Exothermic Reactions for Different Extracted Components of Peat (12)**

Component	Ignition point (°C)	DTA exotherms (°C)			
		I	II	III	IV
Peat sample (not extracted)	228	300	344	386	-
Bitumen[a]	305	350	425	505	-
Readily hydrolyzable and water soluble components	194	296	-	516	636
Humic acids	242	332	426	504	-
Lignin	239	-	-	470	-

Note ([a]) bitumen values in the table are the mean values of the four bitumen extracts listed in Table 2 12

Atanasov and Rustschev (13) reported on TG and DTA curves obtained for several peat samples taken from different depths (0 to 420 cm) from the same location, see Table 2 15 This was to investigate the effects of combustible peat mass (CPM) quantity on the thermal degradation of the peat The peat samples were initially heated in an oxygen atmosphere to determine the ash content of the peat and thus their CPM quantity which was calculated by the relationship CPM = (100 - A), where A is the percentage ash remaining after combustion of the sample The results of the TG and DTA curves are shown in Figure 2 20 (13)

Table 2 15 **The Combustible Peat Mass Content and the Temperatures of Ignition and Combustion of Peat Samples (13)**

Sample	Description of peat	Age of peat (years)[a]	Depth of sample (cm)	Ignition point (°C)	Combustion point (°C)	CPM[b]
a	sedge peat	-	0	220	300	84 6
b	sedge peat	1360	70	220	305	74 2
c	sedge peat	2380	140	230	300	69 6
d	sedge peat	-	210	220	320	47 3
e	sedge peat	3130	280	200	330	41 8
f	peat mixed with rotten slime	-	350	220	335	35 6
g	lake rotten slime	6500-7000	420	210	330	15 4

Note Samples were heated in an oxygen atmosphere ([a]) years before present ([b]) CPM calculated from the residual weight of the sample after heating to 500°C

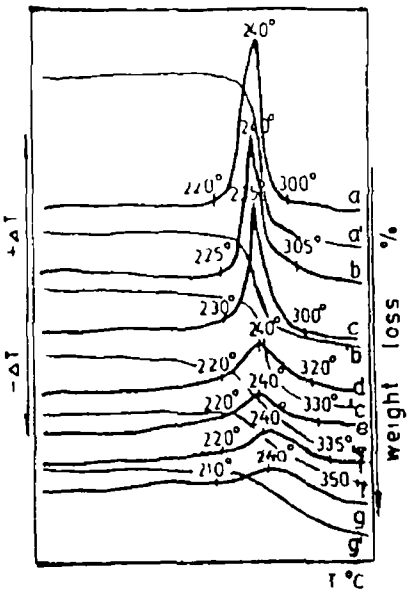

Figure 2 20 DTA and TG Curves for Peat Samples Taken from Different Depths Heated in an Oxygen Atmosphere (13)

The results presented in Table 2 15 show that the peat samples had similar temperatures of ignition (210° to 230°C) and combustion (300° to 350°C) in spite of the large differences in the CPM values, which varied from 83 6 % for the surface sample to 15 4 % for the sample taken from 420 cm below the surface (The temperature of ignition and combustion of the peat samples were defined as the temperature at which the exothermic peak began and ended respectively on the DTA curve) The size of the exothermic peak was also observed to decrease with increasing depth of the sample, this corresponded to the decrease in the amount of combustible peat material available The slope of the TG curve (i e the rate of weight loss) was also observed to decrease in the temperature range 210° to 350°C with increasing depth of the peat sample

Atanasov and Rustschev (13) subsequently examined the combustion of the peat samples in air The DTA curves for the samples are shown in Figure 2 21 Three exothermic peaks were visible, located at 230° to 240°C, 280° to 290°C and 360° to 375°C The increase in depth of the sample (a to g) and the resultant decrease in the CPM was compared to the decrease in the size of the exothermic peaks, and a shift of the peak maxima to lower temperatures The exothermic effects noted in the temperature range 280° to 375°C were considered to be characteristic of samples with high combustible mass contents The exothermic activity was due to (i) the release of volatile compounds, (ii) the decomposition of oxygen-containing compounds and (iii) decarboxylation and dehydroxylation reactions Identification of the peat components which were responsible for the various peak maxima was not stated by the authors, but they had previously suggested that the peak at c 375°C

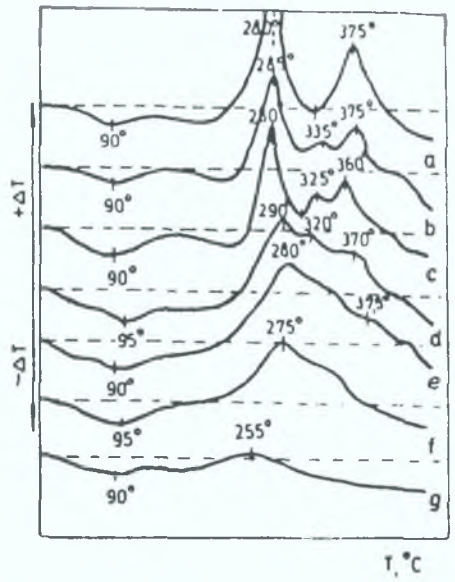

Figure 2.21 **DTA and TG Curves for Peat Samples Taken from Different Depths Heated in Air (13)**

disappeared with the removal of the bitumen and humic fractions of the peat samples (14).

Fuchsman (2) summarised the results of the thermal decomposition of peat. In general on heating peat in the low temperature range up to 280°C in the absence of air there is no loss of organic matter from the sample up to 170°C. Between 170° and 180°C decomposition has been reported to begin and to increase with increasing temperature of the sample. H_2O is released along with CO_2 which is evolved at a maximum rate in the temperature range 200° to 250°C, and CO reaches its maximum rate of evolution between 250° and 280°C. The chemical changes which occur in the heated peat consist mainly of the loss of elemental oxygen as H_2O, CO_2 and CO, and in particular the decarboxylation of the carboxylic groups in the hemicellulose and humic acids, especially in the temperature range 200° to 250°C. The general trend is a reduction in the fraction of water soluble and the easily-hydrolysable materials, and an increase in the level of aromatic, cyclic and unsaturated organic compounds. By 300°C there is a general breakdown in the carbohydrate structure.

The remaining aromatic structures of the decarboxylated humic acids and the lignin materials begin to breakdown in the 300° to 400°C range. The evolved gases from heated samples contain mainly H_2O and CO_2, and small amounts of NH_3 and acetic acid in this temperature range (2). Bitumens and other organic residues are reported to decompose in the temperature range 340° to 500°C. By 500°C carbonisation of the peat is virtually completed though small amounts of gas evolution have been reported for temperatures up to 700°C (2).

2 4 Summary

Peat is an organic soil which is found in large deposits throughout the world It is formed from the build up of semi-decayed vegetative matter that has accumulated in areas of poor water drainage Peat may be considered to be a very young coal which over the geological time scale is eventually transformed into anthracite It is a complex material which can vary considerably in its composition This variation is partially due to the vegetation from which it is derived, but more significantly it is due to the state of decomposition of the deposit Peat is a rich source of organic materials and in particular it contains sizeable quantities of lignin, bitumens and humic acids The thermal decomposition of peat is complex which reflects its varied composition and state of decomposition

The following experimental section examines the physicochemical properties of peat fibre and three other peat materials In particular it reports on the thermal analysis of the peat materials by TG and DSC, and follows the thermal decomposition of the peat fibre by IR spectroscopy

2 5 Aims of Experimental Work

In this section results from the characterisation of the physicochemical properties of four peat materials are presented In particular results from the thermal analysis of peat fibre and the determination of its point of zero charge are presented and discussed The experimental work carried out can be divided into the following categories

(i) general physical properties of the four peat materials This involved the determination of the pH, the density, the ash content and the moisture content of the peat samples This category also included SEM studies of peat fibre and peat moss, and IR spectroscopy of unheated and heated peat fibre samples,

(ii) point of zero charge determination of the peat fibre, which was measured by acid/base titration with different electrolyte concentrations,

(iii) thermal analysis using DSC and TGA

The peat materials examined in this work are used by Bord na Mona as filter materials in several of their pilot and commercially available biological filtration systems (such as the biofilters which is discussed in Chapter 4) Broadly speaking the peat used in such systems is in a relatively undecomposed state (typically H 1 to H 3 on the von Post scale) and usually consists of either peat fibre and/or peat moss mixed with 'bulking agents' such as heather The PMA and PMG samples (see below) are processed forms of peat moss which have been examined by Bord na Mona as filter materials

2 5 1 Experimental Details

(a) Materials Used

The peat samples examined were supplied by Bord na Mona, Environmental Division, Newbridge, Co Kildare The four peat materials used were the following

(i) peat fibre (PF), which in its untreated state is composed of a dense mat of fibrous material made up from the remains of dead plant matter It was dark brown to black in colour and moist to the touch Under a light microscope it was determined that the PF was composed mainly of plant residues from grasses and sedges and that there was very little woody plant material present in the sample The length and diameter of the fibres examined under the microscope were found to be variable The fibres consisted of strands with diameters of between 0 025 to 0 1 cm and lengths of 0 5 to 3 0 cm From its

appearance it was estimated that the PF has undergone relatively little decomposition and it was judged to have a humification value of H 2 to H 3 according to the von Post scale,

(ii) peat moss (PM), which consisted of large fragments of plant materials mainly derived from sphagnum moss It was similar in colour and moisture content to the PF, but lacked its fibrous nature Its degree of decomposition was judged to be H 1 to H 3 on the von Post scale,

(iii) a processed form of PM, referred to in this work as PMA PMA consisted of milled PM, mixed with water and areolight (an organic binding agent) in the ratio 1 to 4 respectively In its untreated state the PMA was supplied in the form of small, tubular shaped granules with diameters of about 0 5 cm and lengths of 0 5 to 2 cm,

(iv) a second processed form of granulated PM, referred to as PMG The PMG consisted of milled PM which had been compressed into spherical shaped granules with diameters of 0 2 to 0 3 cm

(b) General Physical Measurements

Pre-treatment

Pre-treatment of the peat materials was adapted from Puustjarvi (14) and the standard methods described by the AOAC (25) This consisted of first drying the peat in air, at 20°C for 24 hours to remove excess moisture The peat was then cut and ground using a mortar and pestle before it was sieved to obtain several different size fractions The mesh sizes used were 1000-750 μm, 750-500 μm, 500-180 μm, 180-90 μm and 90-45 μm Size fractionating consisted of shaking the peat sample for 10 minutes on stacked sieves, after which time the amount of peat retained by each of the lower sieves was collected and stored in sealed containers

Moisture Content

The moisture content of the peat samples was measured as follows, about 2 g of the peat sample (500-180 μm) was measured into a dry, pre-weighed crucible, and placed in an oven at 110°C (14) The sample was removed periodically and allowed to cool to room temperature in a desiccator before being re-weighed This procedure was repeated until a constant final weight was achieved The weight loss to the

sample was considered to be equivalent to the moisture content of the peat The moisture content was expressed as a percentage value of the unheated peat sample

pH

The pH of the peat materials was measured by adding an amount of unheated peat sample (500-180 μm) equivalent to 10 g of the dried peat to 90 g of distilled water (15) The suspension was then stirred for one hour and the final pH of the solution measured using a Corning pH 240 meter

Ash Content

Ash contents were determined by measuring about 5 g of the oven-dried peat (500-180 μm) into a dry, pre-weighed crucible (14) The sample was then heated at 1000°C for 20 hours in a muffle furnace The ashed sample was then cooled to room temperature in a desiccator before being re-weighed The ash content was expressed as a percentage of the dry weight of the peat

(c) Electronmicroscopy

Scanning electron microscopy (SEM) studies were carried out on PF and PM samples using a Philips 505 scanning electron microscope For the studies the 500-180 μm size fraction of the peat samples was used Pre-treatment of the peat materials consisted of mounting the sample on an aluminium stub followed by evaporating a thin film of gold over the samples to produce an electron conducting surface

(d) Point of Zero Charge Determination

The procedure used for the determination of the point of zero charge of the PF was adapted from the method described by van Raij and Peech (16) The method used was as follows to 0 75 g of oven dried PF (500-180 μm) was added NaCl solution (the background electrolyte), H_2O and either 0 1 M NaOH or 0 1 M HCl in appropriate amounts to make up a final volume of 15 cm^3 The final concentrations of the background electrolyte used were either 1 0, 0 1 and 0 01 M NaCl The sample bottles were stoppered and gently shaken for 24 hours The pH of the suspension was subsequently measured using a Corning pH meter, with measurements taken while continually stirring the solution

The amount of H^+ or OH^- adsorbed by the PF at a given pH value was taken to be equal to the amount of HCl or NaOH added to the solution less the amount of HCl or NaOH required to bring the same volume and the same concentration of NaCl solution, but without the peat sample, to the same pH The point of zero charge was considered to be the common intersection point of the titration curves

(e) FT-IR Spectroscopy

FT-IR spectroscopy of the peat was adapted from Schnitzer and Hoffman (17) IR spectra of unheated and heated PF samples were recorded in the 4000 to 500 cm^{-1} range using an Perkin-Elmer 2000 FT-IR spectrophotometer Samples were analysed as 1 5 % peat (w/w) KBr discs using 0 7 g of the PF/KBr mix in each disc The heated peat samples were prepared by heating in a muffle furnace at 50°C intervals from 150° to 1000° C inclusive The peat was held at each temperature for 2 hours, after which 1 g of sample was removed before proceeding to the next temperature

(f) Thermal Analysis

Thermal analysis of the peat materials consisted of thermal gravimetric analysis (TGA) using a Stanton Redcroft TG-750 thermoballance, and differential scanning calometry (DSC) using a Stanton Redcroft DSC-700 analyser For both studies 5 to 6 mg of sample was heated at the rate of 10°C min^{-1} under a nitrogen gas flow of 20 cm^3 min^{-1} The resultant weight loss or exothermic/endothermic activity of the sample was recorded using a twin pen Linseis chart recorder

2 5 2 Results And Discussion

(a) General Peat Characteristics

The general physical properties of the peat materials studied are presented in Table 2 16

Table 2 16 Characteristics of Peat Materials Studied

Parameter	PF	PM	PMA	PMG
Moisture content (%)	16 8	14 9	13 9	11 9
pH	4 3	3 6	3 0	4 2
Ash content (%)	1 1	1 8	1 1	1 6

Note The values shown are the averaged values for sample measurements For all four samples moisture measurements were ± 2 %, pH values were ± 0 3 pH units, ash content values were ± 0 2 %

It can be seen from Table 2 16 that the general physicochemical properties of the peat material examined were as follows

(i) all the samples had similar moisture contents ranging from 12 % for PMG to 17 % for PF and low ash contents ranging from 1 % for PF and PMG to 1 8 % for PM In particular, the moisture contents of the PF (16 8 %) and PM (14 9 %) were lower than would be expected for samples taken directly from the field, which would typically have moisture contents of 30 to 60 % (4) The lower moisture contents for these samples was due to the pre-treatment of the peat particularly the air-drying overnight before sieving The ash contents reflect the relatively undecomposed state of the peat samples Undecomposed peats typically have ash contents of 1 to 2 %, which is in contrast to the ash content of the highly decomposed peats which can be as high as 60 % in some instances (2),

(ii) the pH of the PF and the PMG were similar at about pH 4 3 The pH of the PM and the PMG were found to be more acidic at pH 3 6 and 3 0

(b) Scanning Electron Microscopy

Micrographs of the PF and PM samples are shown in Figure 2 22 and Figure 2 23 respectively Figures 2 22 (a) and 2 22 (b) show single PF strands under low magnification The ribbed, vascular structures which can be seen to run the length of the fibre, are the remains of the phylum and xylem vessels of the living plant In addition, it can be seen that decomposition to the fibre has resulted in the breaking up of its surface resulting in the formation of holes and cavities on its surface At higher magnification (Figure 2 22 (c)), the surface of the PF is seen to be relatively smooth and featureless in areas which have suffered little from the effects of decay

Figure 2 23 (a) shows a fragment of PM under low magnification This fragment of moss is quite characteristic for PM samples in general, and it can be readily seen that the structure of PM is very different from that of PF In appearance the fragment is amorphous, lacking the ribbed appearance of the PF, and its surface is not smooth but covered in holes and small cavities These cavities can be seen more clearly under higher magnification in Figure 2 23 (b)

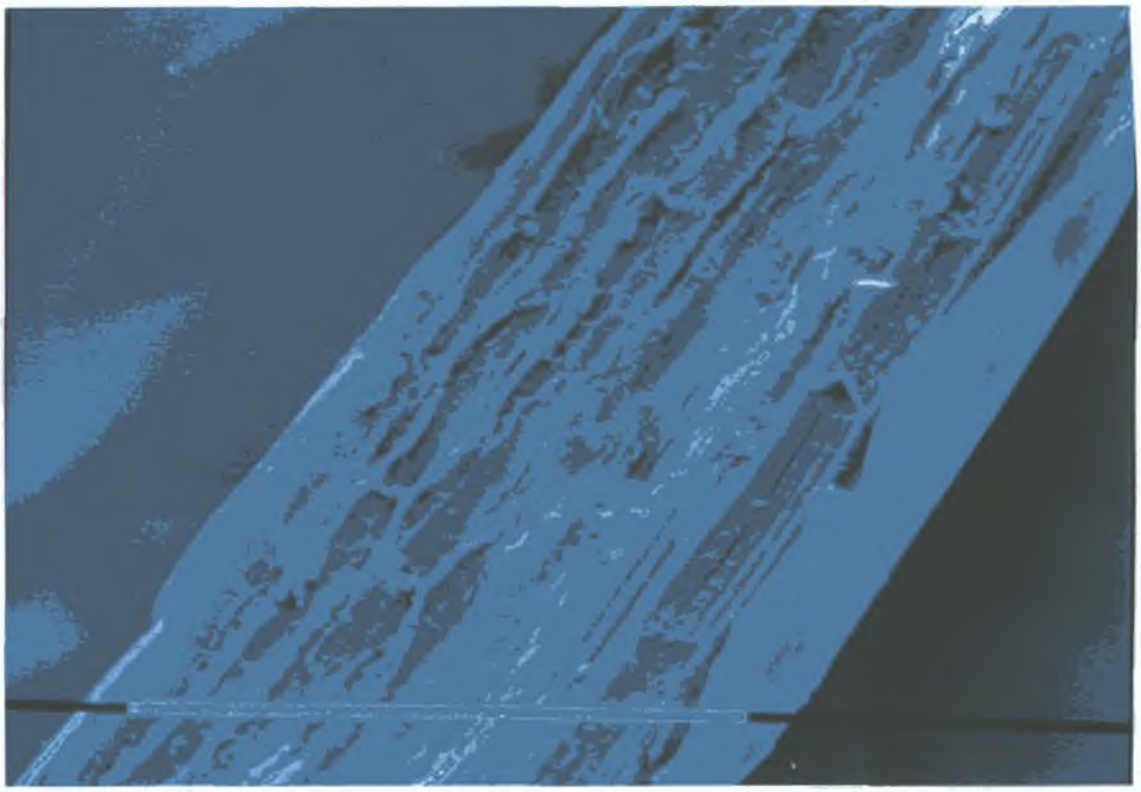

(a)

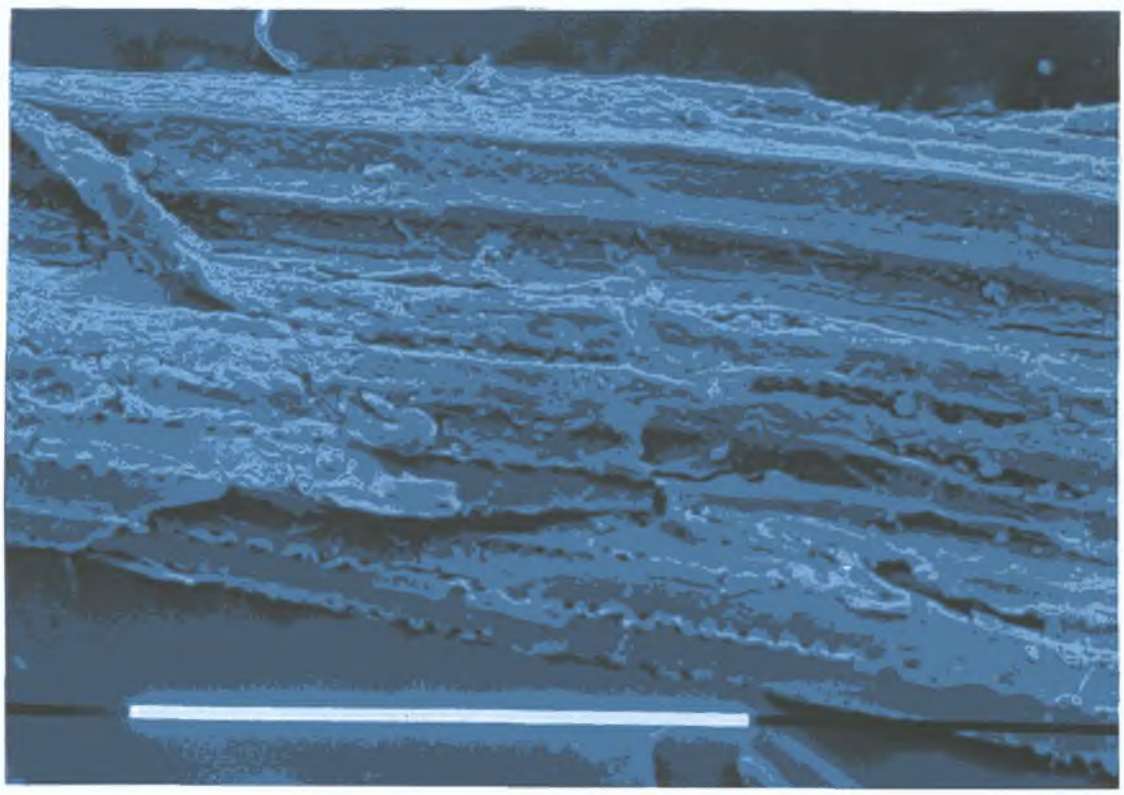

(b)

Figure 2.22 Micrographs of PF Samples

Note: Scale bar (a) 100 μm; (b) 100 μm.

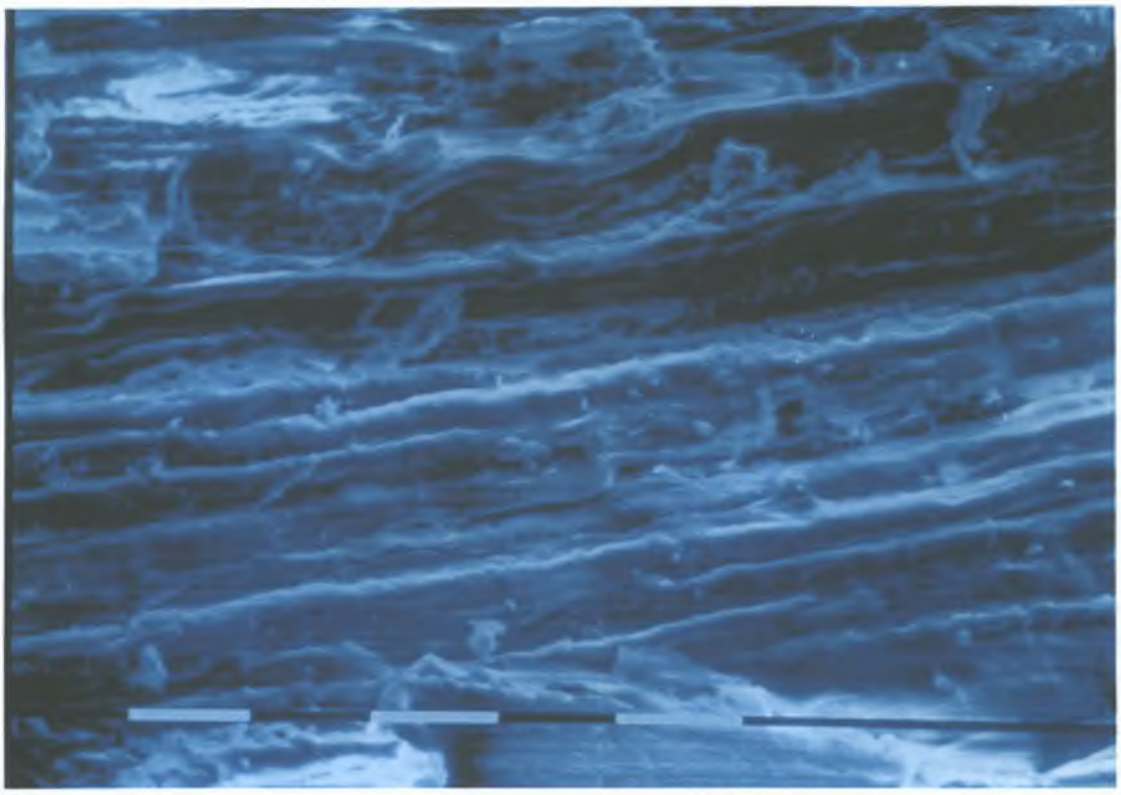

(c)

Figure 2.22 Micrographs of PF Samples (continued)

Note: Scale bar (c)10 μm.

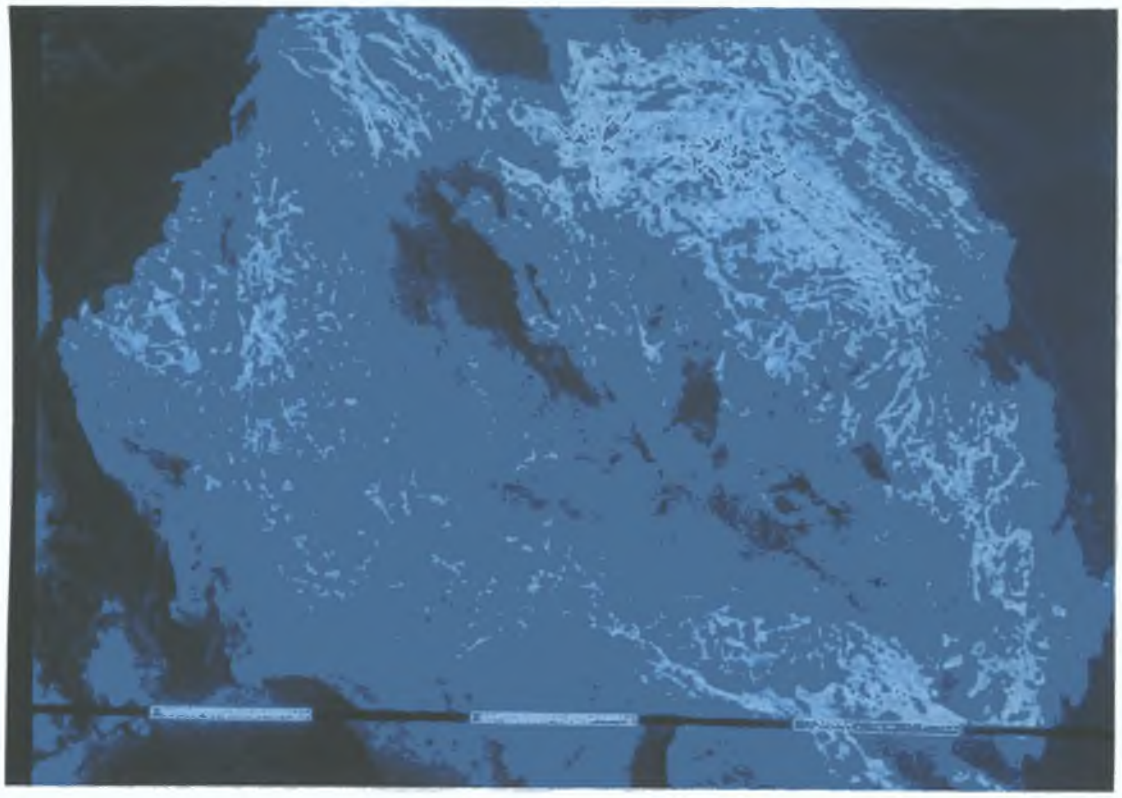

(a)

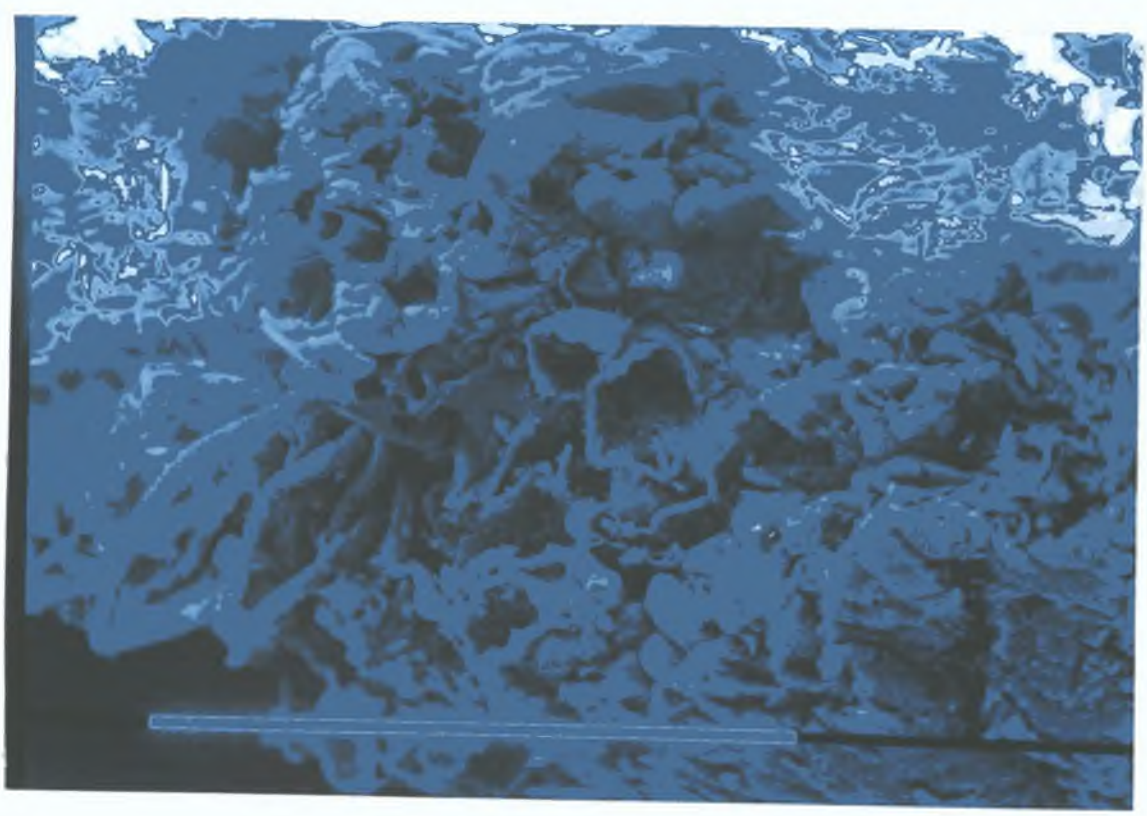

(b)

Figure 2.23 Micrographs of PM Samples

Note: Scale bar (a) 100 μm; (b) 100 μm.

(c) Point of Zero Charge of PF

The determination of the point of zero charge of PF was carried out by acid-base titration. The purpose of this study was to attempt to determine the sign of the surface charge of the PF in aqueous solution. This had important implications for two of the methods used for the determination of the surface area of the PF, namely the adsorption of methylene blue and the negative adsorption of chloride ions, both of which are discussed in Chapter 3.

It will be recalled from Chapter 1 that for the clay minerals there exists two types of charge, a permanent charge which is due to isomorphic substitution, and a pH-dependent charge. For the inorganic constituents of soil the most abundant and reactive surface functional group is the hydroxyl (OH) group. Similarly, for soil organic matter carboxylic acid (COOH) and phenolic-OH are the most abundant functional groups present. For this reason, the two most important potential determining ions for soil constituents are H^+ and OH^- (16). Thus, the sign and the magnitude of the surface charge will be pH-dependent in such instances.

The results from the determination of the point of zero charge of PF are presented in Table 2.17. The table shows the amount of acid (H^+) or base (OH^-) in milli-moles adsorbed per 100g (dry weight) of PF and the equilibrium pH of the solution in the background electrolyte (NaCl at 1.0, 0.1 and 0.01 M). A graph illustrating the results given in Table 2.17 is shown in Figure 2.24. It can be seen from Figure 2.24 that the slopes of the titration curves were smooth and had no sharp inflection points. Within the pH range examined (pH 1 to 7) the three titration curves remained roughly parallel to each other with some divergence of the curves with increasing pH of the solution. There was some indication of convergence of the curves between pH 2.5 to 3.0, but at no point over the pH range did the curves intersect. Thus, it may be concluded that within the pH range studied the PF does not appear to have a point of zero electrical charge, or more precisely a point of zero salt effect. However, the near convergence of the titration curves between pH 2.5 and 3.0 may indicate that within this pH range the surface charge of the peat is at its minimum value, i.e. that the net surface charge is at its closest to zero.

It is difficult to comment on the result presented in this work since there is little available data in the literature for comparison. This in itself may indicate that there is a general difficulty in determining a point of zero charge for peat materials. Chang and Choi (18) reported that the point of zero charge for two peat soils (organic matter contents of 53.7 and 43.3 %) occurred at about pH 4.0. However, the authors noted that the point of zero charge was dependent on the overall

Table 2.17 **Results for the Determination of the Point of Zero Charge of PF**

(a) 1 0 M NaCl

Adsorbed H^+/ OH^- (milli-moles 100 g^{-1})	pH
67 20	5 55
54 20	5 16
40 60	4 43
27 10	3 88
13 50	3 21
0 00	2 49
- 8 00	1 78
- 17 40	1 46
- 16 28	1 21
- 19 47	1 10
- 26 00	1 03
- 31 73	0 95
- 34 80	0 92

(b) 0 1 M NaCl

Adsorbed H+/ OH- (milli-moles 100 g^{-1})	pH
67 20	6 28
54 20	5 83
40 60	5 76
27 10	4 50
13 50	3 81
0 00	2 57
- 9 87	2 25
- 13 00	1 79
- 16 27	1 61
- 23 92	1 51
- 18 27	1 35
- 31 73	1 28
- 48 20	1 28

Table 2 17 **Results for the Determination of the Point of Zero Charge of PF (Continued)**

(c) 0 01 M NaCl

Adsorbed H+/ OH- (milli-moles 100 g^{-1})	pH
67 20	6 98
54 20	6 73
40 60	5 72
27 10	5 47
13 50	4 48
0 00	3 37
- 11 2	2 40
- 17 87	1 95
- 22 93	1 77
- 20 53	1 61
- 36 67	1 60
- 40 40	1 50

Note The sign of the H^+/OH^- values are positive for the adsorption of H^+ and negative for the adsorption of OH^- Adsorbed H^+/OH^- values are ± 0 68 milli-moles 100 g^{-1}, pH values are ± 0 13 pH units

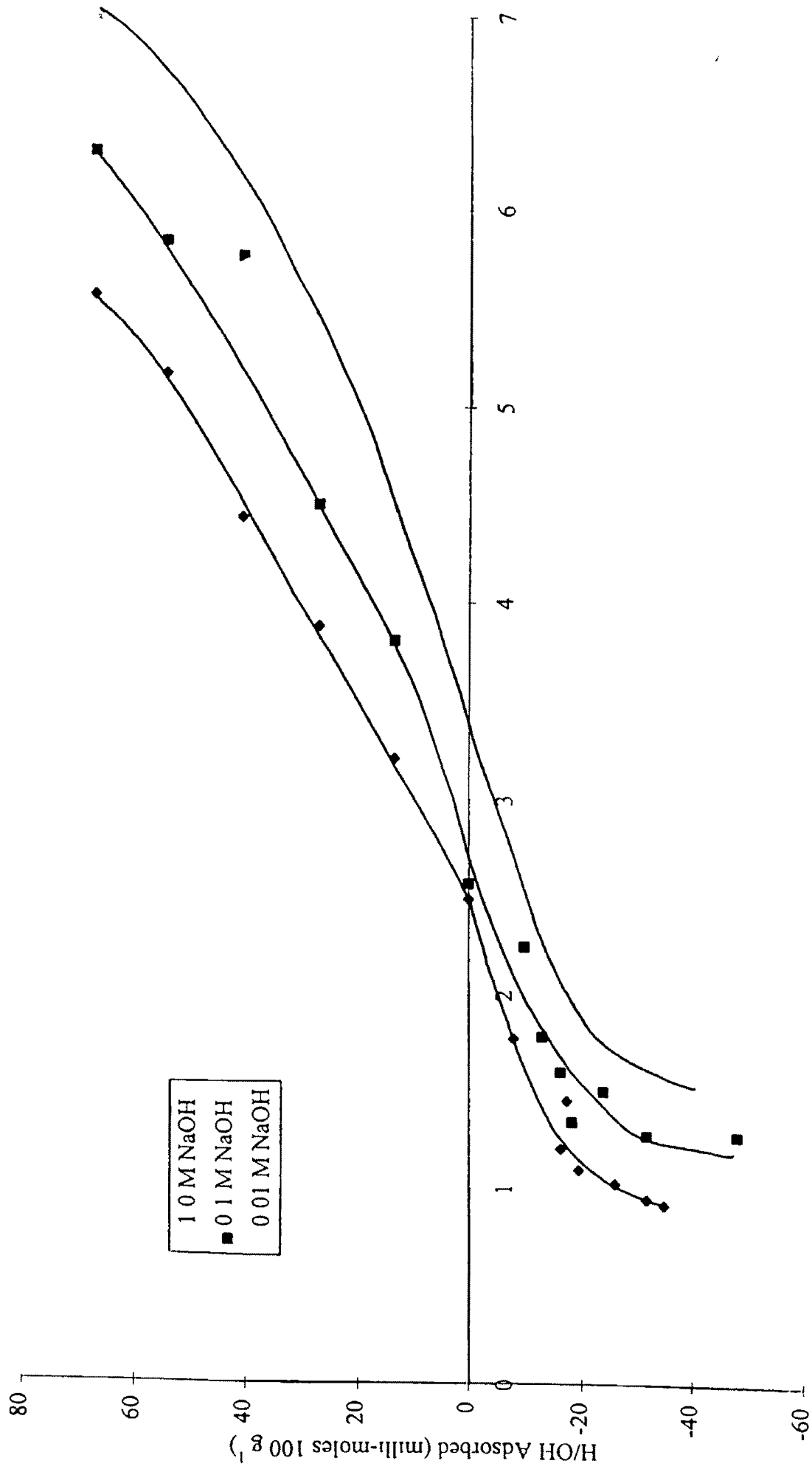

Figure 2.24 Acid-Base Titration Curves for PF

organic and inorganic composition of the soil It has already been stated in Section 1 4 1 that the point of zero charge of a mineral soil is influenced by its organic matter content Specifically, that the point of zero charge of a mineral soil is found to decrease with increasing organic matter content This is due to the abundance of acidic functional groups in the organic matter (16, 19) This would imply that the point of zero charge of soil organic matter (assuming that they have one) is in the low acidic pH

Concerning the sign of the surface charge of the PF, it can be concluded that it must be negative This conclusion can be arrived at from the observation that the large number of oxygen containing functional groups present in PF, particularly the carboxyl and phenolic-OH groups, on dissociation will give rise to a negative charge (5) Also, if it is assumed that a point of zero charge exists for PF, then a negatively charged surface can be deduced from a comparison of the titration curves shown in Figure 2 24 with the results of Chang and Choi (18) shown in Figure 1 19 Above the point of zero charge the order of the titration cures was 1 0 M > 0 1 M > 0 01 M, while below the point of zero charge the order of the titration curves was reversed, 0 01 M > 0 1 M > 1 0 M (This trend in the order of titration curves is also evident for mineral soils [16]) Comparing the results presented in this work with those of Chang and Choi (18) it can be seen that the relative order of the titration curves was 1 0 M > 0 1 M > 0 01 M which would suggest that the PF is above its point of zero charge

(d) <u>Thermal Analysis of Peat Samples</u>

The results from TGA runs for the PM, PMA and PMG samples (all 500 to 180 μm size fraction) are shown in Table 2 18 and typical TGA traces for the three materials are shown in Figures 2 25 The TGA results for the various size fractions of PF are shown in Table 2 19 and typical TGA curves are shown in Figure 2 26

The results for all four materials studied can be divided into four stages of weight loss which were as follows

(i) Stage 1 which occurred from 20°C to 87°-104°C was due to the evaporation of absorbed water from the samples Weight losses of between 9 to 14 % were recorded in this region of the TGA curves,

Table 2.18 TGA Results for PM, PMA and PMG

Material	Stage 1		Stage 2		Stage 3		Stage 4		Ash
	Temp range (°C)	Loss (%)	Temp range (°C)	Loss (%)	Temp range (°C)	Loss (%)	Temp range (°C)	Loss (%)	remaining (%)
PM	25 - 87	10	87 - 192	3	192 - 350	36	350 - 1000	43	8
PMG	25 - 103	13	103 - 202	3	202 - 374	28	374 - 1000	51	5
PMA	25 - 104	9	104 - 201	3	201 - 342	41	342 - 1000	40	7

Note Temperature values are ± 13°C, percentage weight losses are ± 4 %

Table 2.19 TGA Results for PF

Size fraction (μm)	Stage 1		Stage 2		Stage 3		Stage 4		Ash
	Temp range (°C)	Loss (%)	Temp range (°C)	Loss (%)	Temp range (°C)	Loss (%)	Temp range (°C)	Loss (%)	remaining (%)
710-500	25 - 85	10	85 - 220	3	220 - 388	38	388 - 1000	39	10
500-180	25 - 85	14	85 - 207	2	207 - 385	36	385 - 1000	35	13
180-90	25 - 95	10	95 - 200	2	200 - 357	36	357 - 1000	36	16

Note Temperature values are ± 13°C, percentage weight losses are ± 4 %

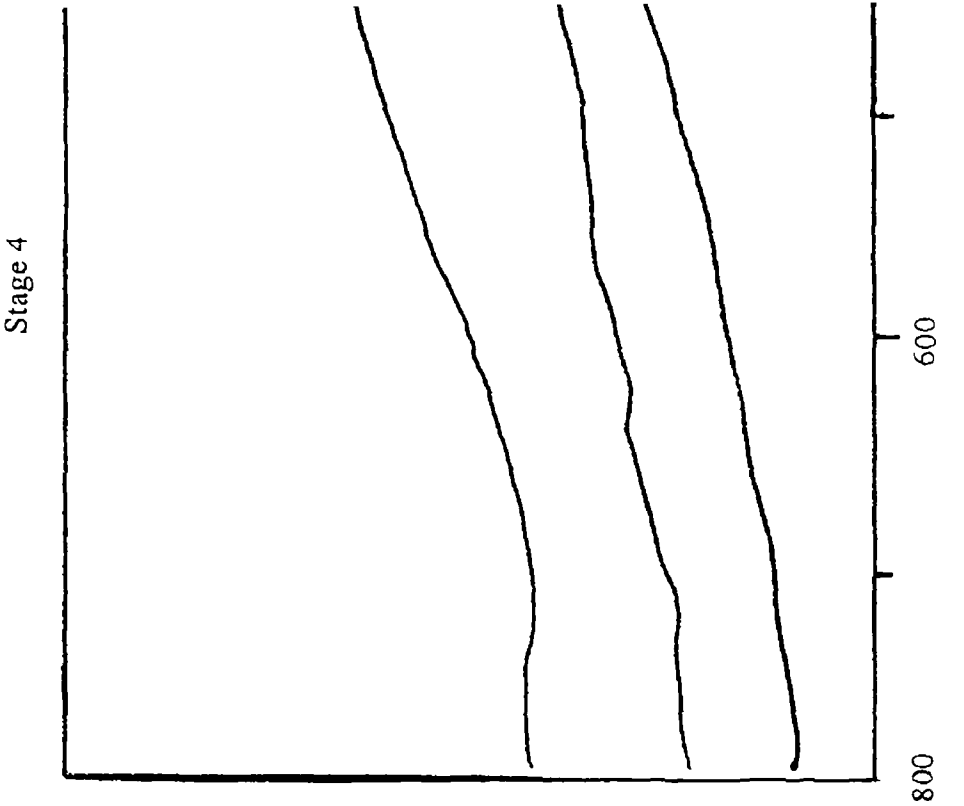

Figure 2 25 TGA Curves for PM, PMG and PMA

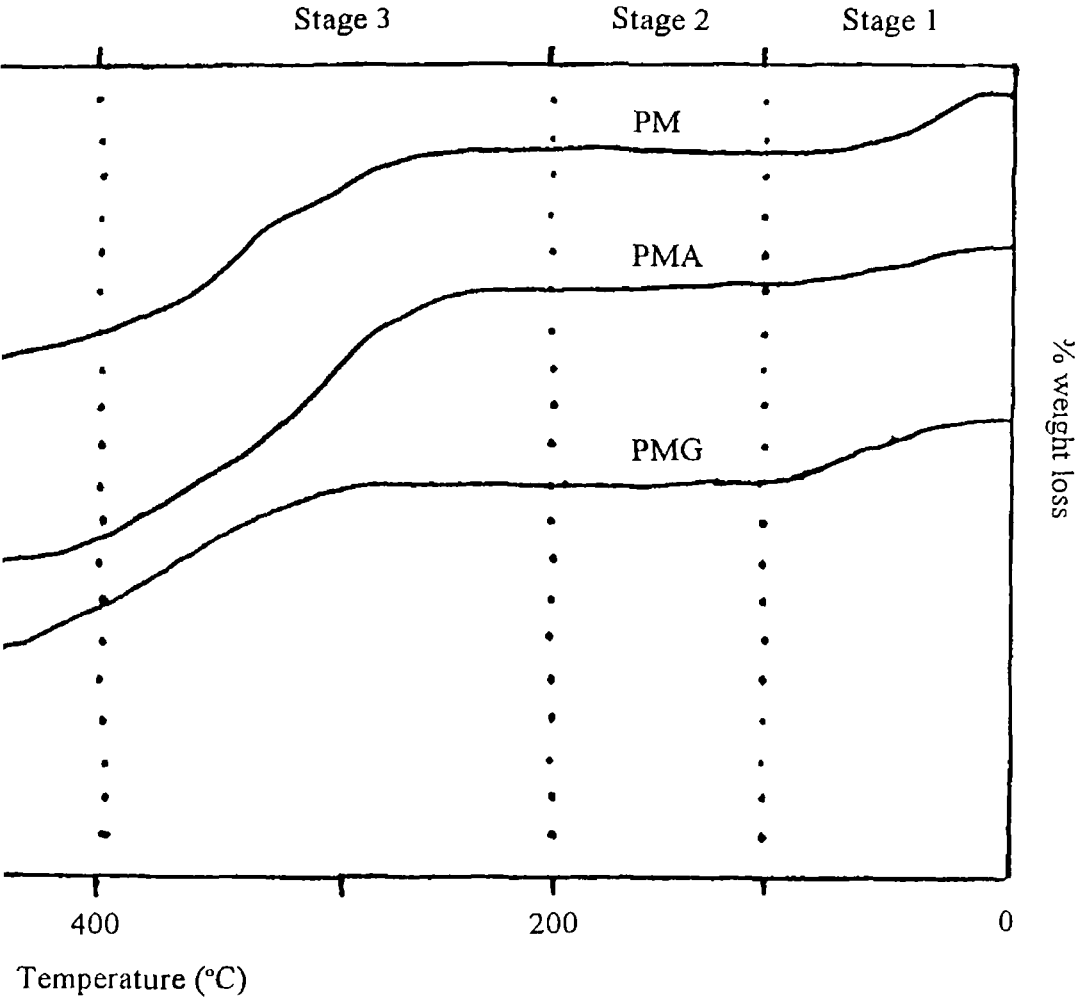
Stage 3
Stage 2
Stage 1
PM
PMA
PMG
% weight loss
400
200
0
Temperature (°C)

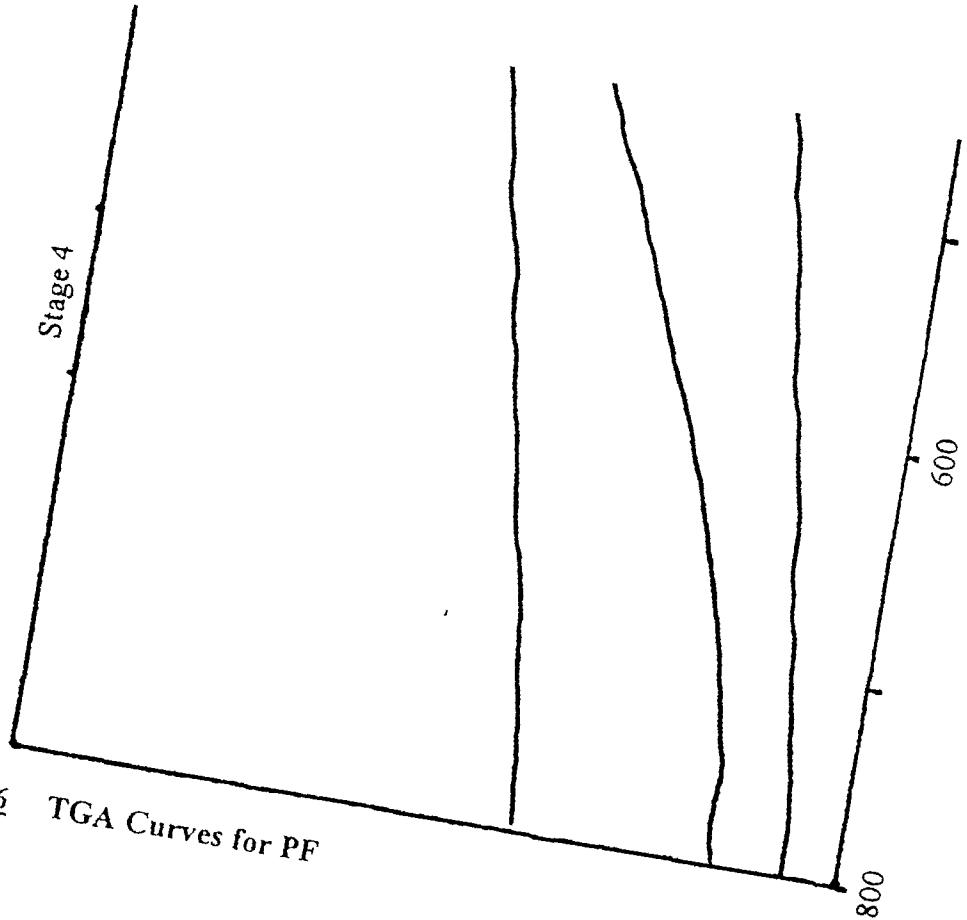

Figure 2.26 TGA Curves for PF

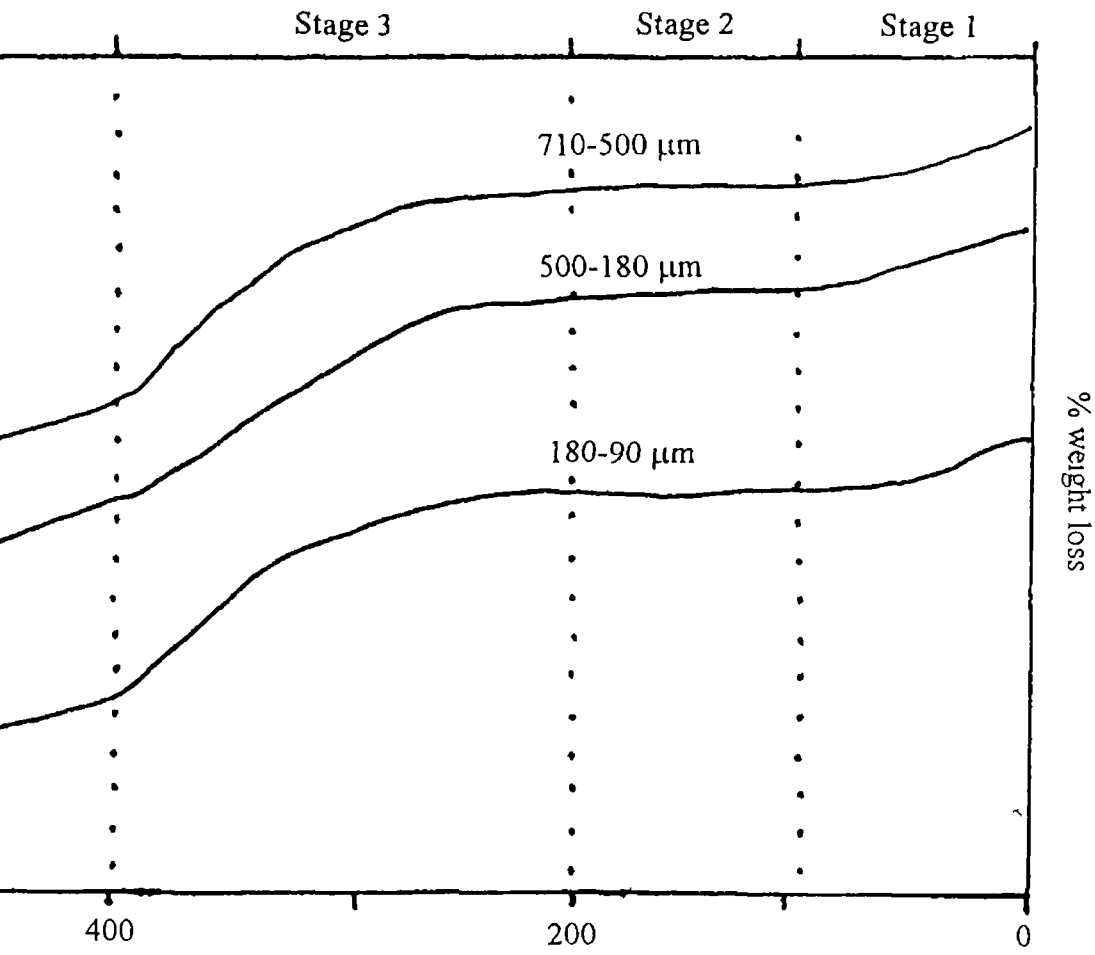
Stage 3
Stage 2
Stage 1
710-500 μm
500-180 μm
180-90 μm
% weight loss
400
200
0
Temperature (°C)

(ii) Stage 2 was a region of small weight loss of between 2 to 3 % Stage 2 extended from about 100°C to 200°C for the PM, PMA and PMG samples For the PF samples the upper temperature of stage 2 was found to shift to lower temperatures (from 220° to 200°C) with decreasing size of the PF particles used,

(iii) Stage 3 marked the start of thermal decomposition of the peat material For the PM, PMA and PMG samples this stage of weight loss began between 192° and 202°C For the PF samples (Table 2 19) it can be seen that the temperature at which this region of weight loss began shifted to lower temperatures with decreasing size fraction (from 220° to 200°C) of the peat Except for the PMG which had a weight loss of about 28 % in this temperature region, the other three peat materials recorded weight losses of between 36 to 41 % The decreasing size of the PF samples did not appear to greatly affect the percentage weight loss to the sample,

(iv) Stage 4 was a region of variable weight loss to the peat samples Weight losses of between 35 to 51 % were recorded for the four peat materials The size of the weight loss to the PF samples did not appear to be influenced by the size fraction (35 to 39 %)

(v) The amount of ash remaining after heating of the peat samples was found to be higher than the ash contents measured for the peat samples heated in the muffle furnace (see Tables 2 16, 2 18 and 2 19) It was found that the PM, PMA and PMG had ash contents of between 5 % and 8 % while the ash content of the PM samples increased from 10 % to 16 % with decreasing size fraction The lower ash content values in Table 2 16 are due to prolonged heating of the peat samples at 1000°C It is likely that prolonged heating of the peat samples in the TGA apparatus would result in similarly low ash contents as those in Table 2 16

The results from DSC runs for PM, PMG and PMA are presented in Table 2 20 and typical traces for the three peat materials are shown in Figure 2 27

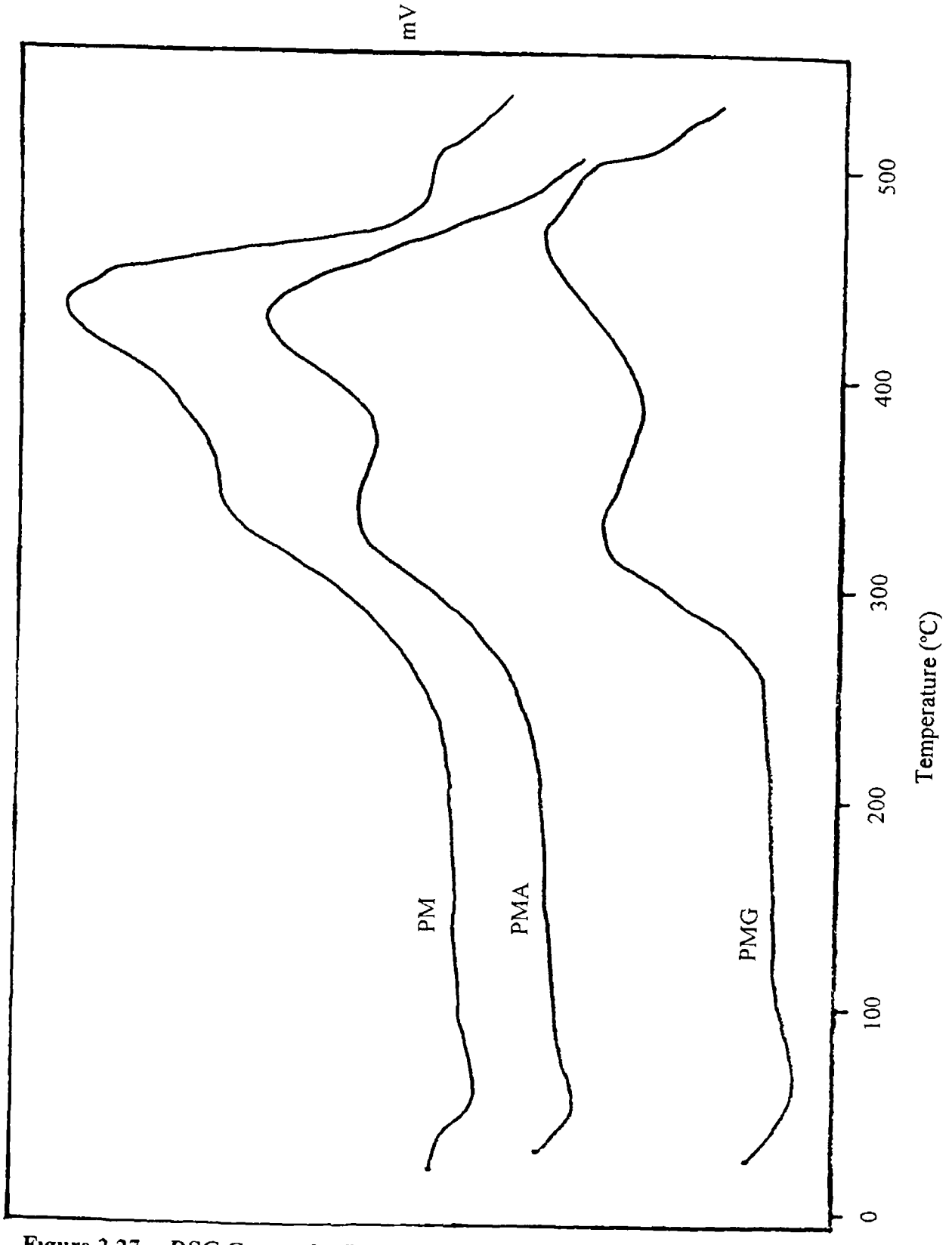

Figure 2.27 DSC Curves for PM, PMG and PMA

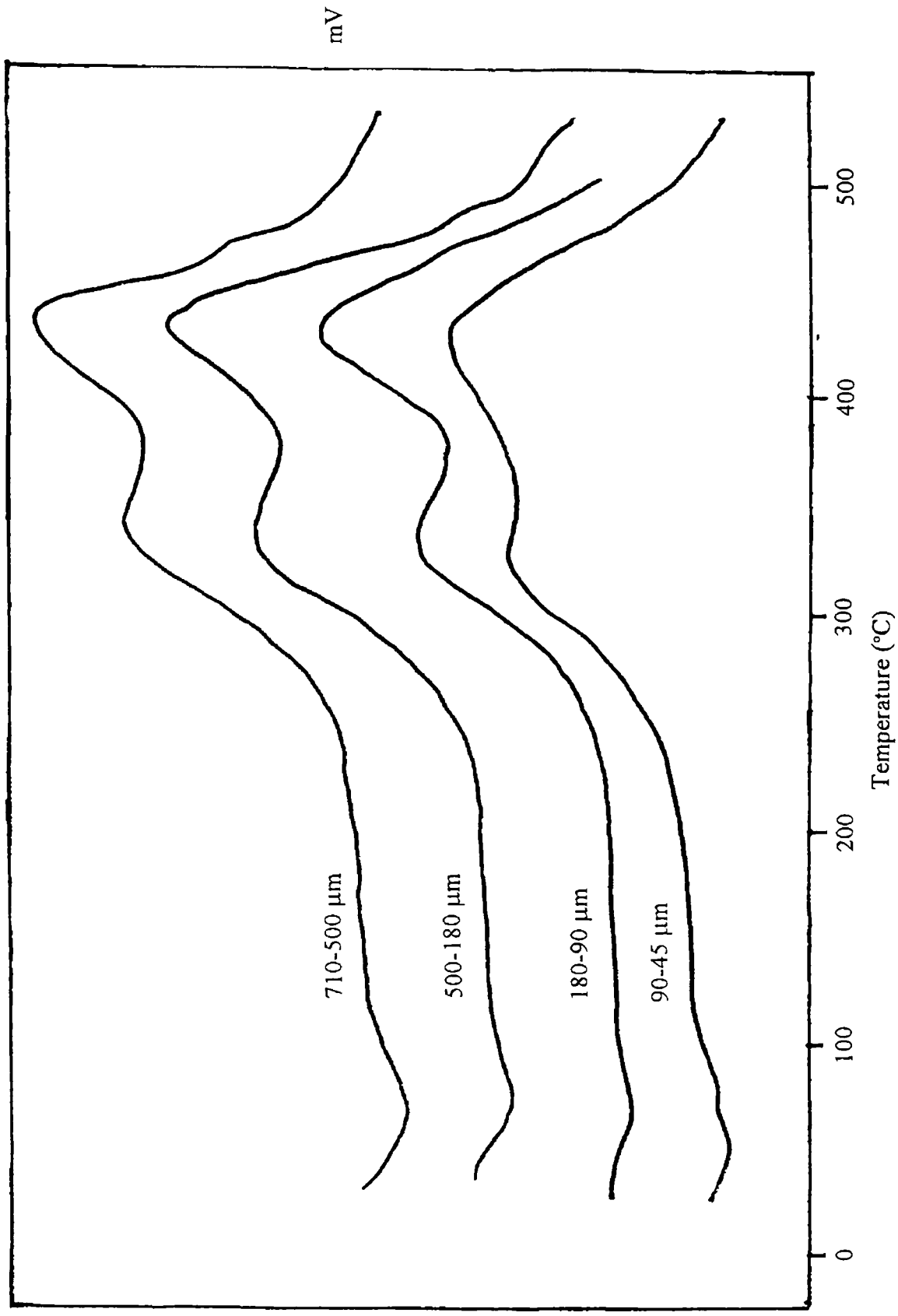

Figure 2 28 DSC Curves for PF

Table 2.20 DSC Results for PM, PMG and PMA

Material	Endothermic peak maximum (°C)	Ignition point (°C)	Exothermic peak maxima (°C)		
			I	II	III
PM	49	197	333	435	459
PMG	60	198	326	474	508
PMA	50	202	338	422	446

Note Values are ± 7°C

The results from DSC analysis of the PF are shown in Table 2 21 and typical DSC traces for the peat shown in Figure 2 28

Table 2.21 DSC Results For PF

Size fraction (μm)	Endothermic peak maximum (°C)	Ignition point (°C)	Exothermic peak maxima (°C)		
			I	II	III
710-500	68	245	342	454	-
500-180	53	202	337	435	471
180-90	62	199	331	415	495
90-45	59	209	323	417	495

Note Values are ± 7°C

The DSC results for all four peat materials were divided into several regions of thermal activity, which were as follows,

(i) an endothermic peak was initially recorded for all four peat samples The peak maxima varied from 49° to 62°C, and corresponded to the evaporation of water from the samples,

(ii) a region of little to no thermal activity was recorded between the endothermic peak and the 'ignition point' temperature The ignition point temperature was defined as the beginning of exothermic activity in the sample The ignition point was similar for all samples, between 197° and 202°C, see Table 2 20 The

ignition point was observed to shift to lower temperatures with decreasing size fraction of the PF samples (from 245° to 209°C),

(iii) the first exothermic peak (indicated as exothermic peak I in Tables 2 20 and 2 21) for the peat samples occurred between 323° and 342°C However, for the PF samples the position of the peak maximum was observed to decrease from 342° to 323°C with decreasing size of the PF particles,

(iv) exothermic peak II occurred at 435° and 422°C for PM and PMA samples respectively, while it was considerably higher at 474°C for the PMG For the PF samples the maximum of peak II shifted downwards from 454° to 415°C with decreasing size of the PF particles,

(iv) exothermic peak III was the final peak to be detected from the peat samples in the temperature range studied The position of peak III was found to be much more variable for the PM, PMG and PMA samples, see Table 2 20 For the PF it can be seen that peak III was not detectable for the 710-500 μm size fraction, but became apparent from the 500-180 μm size fraction downwards The peak maximum was observed to shift to higher temperatures (from 471° to 495°C) with decreasing size fraction of the PF

Comparing the TGA and DSC results it can be seen that there is a large degree of similarity between their respective events It can be seen that the weight loss recorded in Stage 1 of the TGA results co-incides with the endothermic peak recorded on the DSC traces Both peaks correspond to water evaporation from the peat samples, which is supported from several studies on the thermal decomposition of peat materials (9-13) The weight loss of 9 to 14 % recorded was in good agreement with the humidity value of 12 to 17 % measured for the physical properties of the peat samples shown in Table 2 16

Stage 2 of the TGA results corresponded to the region of little to no thermal activity from the DSC traces Of particular interest is the upper limit of this region (referred to as the ignition point in the DSC results) as it marks the start of thermal decomposition of the peat samples From the TGA and DSC results it can be seen that the upper temperature was in the region of 200°C Ranta *et al* (12) reported an ignition temperature of 228°C for a Finnish peat (see Table 2 14) which is about 28°C higher than the value quoted in this study However, it should be noted that the Finnish peat had a humification value of H 7 Thus, the Finnish peat would have a lower cellulose content and higher lignin, bitumen and humic acid content than the

peat materials studied in this work (see next paragraph) As a result the ignition temperature of the Finnish peat was shifted to a higher value Indeed, from Table 2 14 it can be seen that the ignition point of the cellulose materials (which is grouped under 'the readily hydrolyzable and water soluble components') was 194°C, which is only 6°C lower than the value quoted in this work

The temperature range of Stage 3 corresponding to weight losses of between 35 to 45 % co-incided approximately with exothermic peak maxima I recorded from DSC traces which occurred at about 333°C for all four peat materials From the literature sources it is evident that this region of the TGA and DSC traces correspond to the decomposition of cellulose and other easily decomposed plant carbohydrates This is supported from the results of several studies which report peak maxima corresponding to cellulose decomposition at similar temperatures, DTG maxima situated at 280°C (10) and 300°C (11), DTA maxima at c 330°C (11) and 296°C (12)

Stage 4 of TGA traces which was the variable region of weight loss to the peat samples overlapped with exothermic peaks II and III from the DSC results This region of the TGA and DSC traces in general correspond to the decomposition of the lignin, bitumen and humic material fractions of peat reported by other workers

- exothermic peak II which occurred at about 438°C for the peat materials studied in this work may be due to the decomposition of bitumens and/or humic substances, since the decomposition of both materials have peak maxima in this temperature range Levesque and Dinel (11) reported an exothermic peak maximum between 418° to 432°C which was associated with the decomposition of humic substances, while Ranta *et al* (12) reported that the decomposition of bitumens and humic substances both gave exothermic peak maxima near 425°C
- exothermic peak III which occurred at about 479°C for the four peat materials co-incides with the decomposition of lignin which according to Ranta *et al* (12) occurs with an exothermic peak maximum at 470°C

Since DSC traces did not go above 500°C no higher exothermic peaks were recorded, though it can be seen from the TGA traces that there is still peat material undergoing thermal decomposition above this temperature, which would include the bitumens, lignin and humic substances (12)

(e) **FT-IR Spectroscopy of PF**

The FT-IR spectroscopy was carried out on unheated and heated (from 150° to 1000°C inclusive) PF samples The IR spectra obtained are shown in Figure 2 29 From an examination of the results the IR spectra were divided into two broad groups

(i) the first group of spectra consisted of the PF from the unheated sample to the sample heated at 420°C inclusive This group of spectra was characterised by a large number of absorption peaks in the 1700 to 1000 cm^{-1} range The position of these peaks did not change that much with an increase in temperature up to 420°C,

(ii) the second group of spectra consists of PF samples heated from 430° to 1000°C inclusive This group of spectra showed a number of characteristic absorption peaks which distinguished them from the first group of spectra In particular these spectra were dominated by two strong absorption peaks, the first at about 1435 to 1445 cm^{-1}, and the second double peak at c 1120 cm^{-1} and 1150 cm^{-1}, and several sharp peaks below 1000 cm^{-1}

A comparison of the IR spectra with the results from the thermal analysis of the PF indicated that the above division of the spectra did follow a recognisable trend The IR spectra up to 420°C followed the loss of cellulose and other easily decomposed materials from the PF While the spectra above 420°C were due to the presence of lignin, bitumens, humic substances, etc , materials which only begin to decompose above this temperature At the higher temperatures (600° and 1000°C) the IR spectra were due to the inorganic materials present in the PF sample

Given the complex chemical composition of the PF it was difficult to assign all of the adsorption bands to specific functional groups However, the most notable absorption bands were as follows

(i) a broad absorption band centred at 3351 cm^{-1} for the unheated peat sample which was due to O-H bond absorption (20-23) The broadness of this absorption band indicated the presence of a wide variety of OH containing groups such as alcoholic OH, phenolic OH, hydrogen bonded OH, chelated OH and carboxylic acid OH (20, 21) Heating of the peat had two effects on this absorption band

- the intensity of the peak was observed to decrease with heating of the peat sample, reaching a minimum at 420°C Above this temperature the intensity of the peak increased slightly, but thereafter did not change from

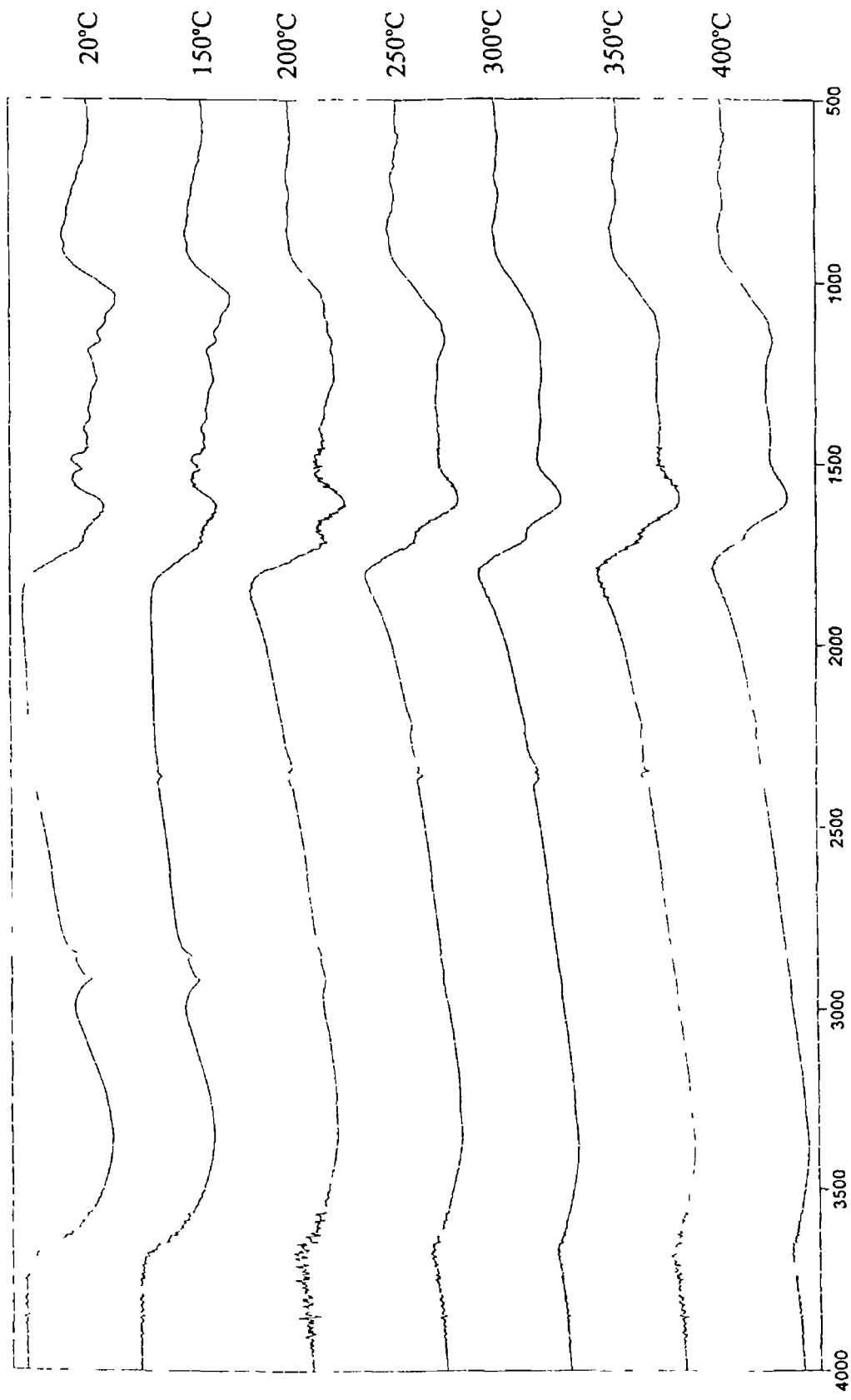

Figure 2 29 **IR Spectra of PF Samples**

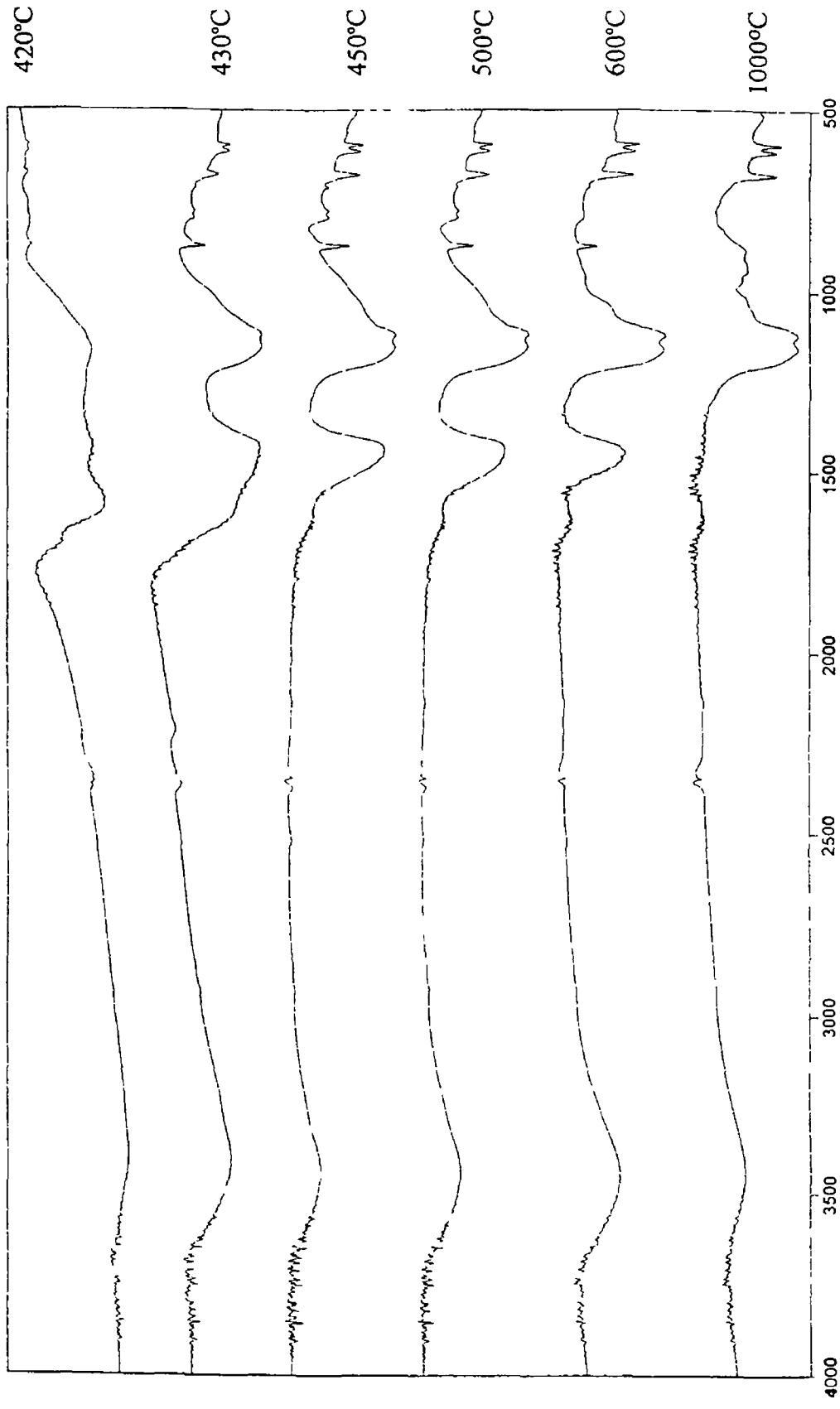

Figure 2 29 **IR Spectra of PF Samples (Continued)**

430° to 1000°C The presence of this peak at such high temperatures may have been due to the re-absorption of water moisture from the atmosphere during handling of the KBr discs Schnitzer and Hoffman (17) reported a similar decrease in the intensity of the OH absorbency band as the heating temperature of the SOM material was increased The decrease in intensity of the absorption band was attributed by the authors to the loss of phenolic OH groups which was completed between 400° to 450°C

- the relative position of this absorption peak was observed to increase with increasing temperature of the PF sample, the peak shifted from 3351 cm^{-1} for the unheated sample to 3454 cm^{-1} for the sample heated to 1000°C,

(ii) the absorption peak at c 2920 cm^{-1} and a second peak at c 2850 cm^{-1} were attributed to aliphatic C-H bond absorption (17-23) These two peaks were evident in IR spectra up to 250°C, but their intensity was observed to decrease in size with increasing temperature, above 250°C they were no longer visible A similar decrease was noted by Schnitzer and Hoffman (17) with the heating of SOM samples, they reported that the prominence of these peaks dropped rapidly in IR spectra from 400°C onwards,

(iii) a shoulder peak, detectable at 1707 cm^{-1} for the unheated peat sample, was attributed to C=O bond absorption from carboxylic acid and ester linkages (17) The relative position of this peak was observed to decrease slightly with increasing temperature, by 420°C it had decreased to 1699 cm^{-1} Above 420°C this absorption band was no longer detectable It has been suggested that the downward shifting of this peak and the peak at 1625 cm^{-1} are due to an increase in the aromatic content of the samples with heating (17) This is certainly in keeping with the results of the thermal analysis of the peat,

(iv) the prominent peak at 1625 cm^{-1} for the unheated PF sample was of uncertain origin This peak may be due to aromatic C=C bonds (17, 20, 22), to hydrogen bonded C=O of quinone or to COO^- (17-23) The position of this peak was observed to decrease with increasing temperature of the sample, by 430°C it was barely visible as a shoulder peak at 1603 cm^{-1} Above 430°C it was no longer visible in the IR spectra of the peat samples,

(v) a series of absorption peaks between 1600 cm^{-1} and 1000 cm^{-1} for the unheated peat sample The identification of these peaks was difficult, but most of them can be attributed to oxygen containing functional groups (17-23) The main absorption maxima were as follows, 1515 cm^{-1} which may be due to aromatic C=C (21, 22), the peak positioned at 1269 cm^{-1} may indicate the presence of the ether C-O-C structures (22), the peak at 1159 cm^{-1} may be due to alcoholic OH

(23), and the absorption peak at 1035 cm^{-1} is possibly due to C-O stretching of primary alcohols or to Si-O (20, 22) from the inorganic material present in the sample The presence of these peaks were observed to decrease in prominence with increasing temperature of the peat sample and they were no longer visible in the IR spectra above 420°C,

(vi) a peak at 1464 cm^{-1} which appeared in the spectra from 430°C onwards The position of this peak remained at about the same position up to 550°C, but it had disappeared from the IR spectrum of the peat sample heated to 1000°C No possible identity can be suggested for this peak,

(vii) a broad, double peak with maxima positioned at 1150 and 1119 cm^{-1} was clearly visible in the IR spectra from 430°C onwards The peak was observed to increase in prominence with increasing charring temperature of the sample The identity of this absorption peak is unknown, but given that this double peak was present at 1000°C it is more than likely associated with the residual inorganic material of the sample (17),

(viii) a series of small, sharp peaks below 1000 cm^{-1} became prominent from 450°C onwards The peak maxima were situated at 876, 800, 679, 613 and 595 cm^{-1} respectfully Schnitzer and Hoffman (17) noted three absorption bands located at 875, 825 and 750 cm^{-1} which were evident in IR spectra above 400°C, these were associated with aromatic C-H absorption However, given the fact that the absorption bands (except for 876 cm^{-1}) in Figure 2 29 were still visible in the sample heated to 1000°C it is most likely that they are associated with inorganic material

2.5.3 Conclusion

The experimental work carried out in this chapter examined the physicochemical properties of four peat materials, namely PM, PF and two processed forms of PM, PMA and PMG The peat materials differed greatly in physical appearance, ranging from the fragment and fibrous remains of plant materials in the PF and PM samples to the compacted, granulated forms of the PMA and PMG materials However, the samples were found to have similar physicochemical properties They were all acidic in nature having pH values between pH 3 0 to 4 3, they had moisture contents of between 12 to 17 %, and ash contents of 1 to 2 % (which indicated the relative low state of decomposition of the peat materials) The largest difference between the peats was in their densities, PF and PM had densities which were considerably lower than the PMA and PMG samples The high densities

of the latter two materials was due to compression of the original PM materials into hard granulated forms

An attempt to determine the zero point of charge of PF proved to be inconclusive There was some indication of convergence of the titration curves between pH 2 5 and 3 0, but at no point over the pH range examined did the curves intersect The near convergence of the curves between pH 2 5 and 3 0 may suggest that the net surface charge of the peat is at a minimum in this pH region, i e at its closest to zero surface charge However, if it is assumed that the PF does in fact possess a point of zero charge, then it must lie beyond the pH range examined Further work is required in this area, possibly the use of other techniques for determining the point of zero charge, such as electrophoretic mobility, may give better results

Thermal analysis of the peat materials by DSC and TGA indicated that there were several stages of decomposition of the samples From DSC traces it was found that the ignition point for the peats occurred at about 200°C Above this temperature there were three recorded exothermic peaks indicating the decomposition of specific components of the peat material These peaks were as follows, peak I which had its peak maximum at c 333°C, this peak was due to the decomposition of cellulose, peak II, at c 438°C, was due to the decomposition of bitumens and/or humic substances, and peak III, at c 479°C, resulted from the decomposition of lignin

IR spectra of PF showed that there was a variety of chemical functional groups present (mainly oxygen containing) Given the complex chemical composition of the peat it was difficult to assign specific functional groups to particular peaks A gradual change in the spectra of the peat was observed as the samples were heated reflecting the gradual thermal decomposition of the samples There was a clear transition temperature among the IR spectra which allowed the spectra to be divided into two broad groups Those samples heated at temperatures up to 420°C were characterised by a large number of absorption band originating from cellulose and other peat materials It has been found from thermal analysis that these materials undergo thermal decomposition below 420°C PF samples heated at temperatures above 420°C gave IR spectra resulting from the enriched presence of lignin, bitumen and humic substances which decompose above 400°C In particular, the spectra above 420°C were dominated by a double band position at about 1150 and 1119 cm^{-1} which proved to be unidentifiable but which must have been due to inorganic materials since it was still present in IR spectra for PF samples heated to 1000°C It will be seen in Section 3 5 2 1 that the variation in the surface area of the peat fibre which is observed as the heating temperature of the sample is increased is due to the thermal decomposition of the peat

2 6 References

(1) Hassett, J J and Banwart, W L , Soils and their Environment, Prentice-Hall, (1992)

(2) Fuchsman, C H, Peat, Industrial Chemistry and Technology, Academic Press, (1980)

(3) Spedding, P J , Fuel, 67, 883-900 (1988)

(4) Boron, D J , Evans, E W and Peterson, J M , Int J Coal Geology, 8, 1-31 (1987)

(5) Puustjarvi, V and Robertson, R A , Appl Bot, 3, 23-38 (1975)

(6) Paul, E A , Soil Microbiology and Biochemistry, 91-114, Academic Press, (1989)

(7) Sposito, G , The Surface Chemistry of Soils, Oxford University Press, (1984)

(8) Puustjarvi, V , Peat and Plant Yearbook 1981-1982, 33-47 (1982)

(9) Schnitzer, M and Hoffman, I , Soil Sci Soc Amer Proc , 30, 63-66 (1966)

(10) Schnitzer, M and Hoffman, I , Soil Sci Soc Amer Proc , 31, 708-709 (1967)

(11) Levesque, M and Dinel, H , Geoderma, 20, 201-213 (1978)

(12) Ranta, J , Ekman, E and Asplund, D , Proceedings of the 6th International Peat Congress, 6, 670-675 (1980)

(13) Atanasov, O and Rustschev, D , Thermochimica Acta, 90, 373-377 (1985)

(14) Puustjarvi, V , Peat and Plant Yearbook 1973-1975, 5-10 (1976)

(15) Furusawa, N , Togashi, I , Hirai, M , Shoda, M and Kubota, H , J Ferment Technol , 62(6), 589-594 (1984)

(16) van Raij, G and Peech M , Soil Sci Soc Amer Proc , 36, 587-593 (1972)

(17) Schnitzer, M and Hoffman, I , Soil Sci Soc Amer Proc , 28, 520-525 (1964)

(18) Chang, S M and Choi, J , J Korean Agricultural Chemical Society, 30(1), 1-8 (1987)

(19) Morais, F I , Page, A L and Lund, L J , Soil Sci Soc Amer J, 40, 521-527 (1976)

(20) Schnitzer, M , "Humic Substances, Chemistry and Reactions", in Soil Organic Matter, eds Schnitzer, M and Khan, S U , (1978)

(21) Socrates, G , Infrared Characteristics Group Frequencies, Wiley, (1980)

(22) Eltantawy, I M and Baverez, M , Soil Sci Soc Am J , 42, 903-905 (1978)

(23) Sipos S , Sipos, E and Sefer, I , Acta Phys Chem , 27, 135-140 (1981)

(24) Hammond, R F , Proceedings of the 7th International Peat Congress, 7(1), 168-187 (1984)

(25) Association of Official Analytical Chemists, Official Methods of Analysis, 15th edition, AOAC, (1990)

Chapter 3

The Sorption of Organic Compounds by Soil Organic Matter

3 Introduction

Over the last 40 years interest has grown on the fate of organic compounds in subsurface soils (1, 2) This interest has increased in significance since the early 1970s when it was realised that many of the widely used organic compounds, particularly those applied directly to the soil such as pesticides, herbicides etc , could persist in the soil for years with long term consequences for the environment (1, 2) In general the fate of many organic compounds within the soil is poorly understood It is known that most of these compounds are rapidly degraded by a combination of physical, chemical and biological processes, and as a result, they pose no long term hazards to the environment However, many organic compounds are known to persist for very long periods in the soil For example in one extreme case of the persistence of the pesticide DDT it was found that 40 to 45 % of an initially high loading of the pesticide was still present in a soil sample after 14 years (3) (See Appendix A for a list of the common names and chemical names of the organic compounds cited) Thus, the recalcitrant nature of many of the organic compounds applied to the soil can have potentially harmful consequences for plant, animal and ultimately human life due to their build up in the environment over time

The sorption of organic compounds by soil is one of the most important factors determining their long term fate in the environment particularly in relation to their movement and bioavailability Most studies on the uptake and retention of organic compounds by soil have concentrated on the fate of the organic compounds within the vadose zone (The vadose zone refers to the layer of soil which is not completely water saturated between the water table and ground level) The classes of compounds studied include the most frequently used pesticides, herbicides, organic solvents, etc , which are used in agriculture and industry

This chapter discusses the various sorption mechanisms and environmental factors which influence the sorption and retention of non-ionic organic compounds by soil organic matter (SOM) It also reviews the contentious issues concerning the surface area of SOM which is interrelated with the sorption mechanism of SOM, particularly for the non-ionic class of organic compounds

3 1 Sorption Phenomena

Since the following text will discuss the mechanistic roles of SOM and to some extent the role of minerals in the uptake of organic compounds some terminology is used frequently in referring to the mechanisms involved The term sorption is

preferentially used throughout this text to describe the uptake of organic compounds by soil and its constituents, as it avoids reference to any specific mechanism In particular sorption is used when discussing the uptake of non-ionic organic compounds by SOM The term adsorption is used to describe the condensation of a vapour or solute onto the surface or interior pores of a solid The term partition (also referred to as absorption) is used to describe the dissolution of the sorbed material into the soil organic phase (i e the SOM) by dispersive forces (van der Waals forces) This is analogous to the extraction of a solute from the aqueous phase and into a liquid organic phase When the organic phase is a solid, partitioning is distinguished from adsorption by the implication that there is a homogeneous distribution of the sorbed material throughout the entire volume of the solid phase, whereas in adsorption the sorbate is confined exclusively to the surface of the solid

In general the sorption of a particular compound by soil is not a straight forward process Depending on the nature of the sorbate and the general physicochemical properties of the soil several different sorption mechanisms may be acting simultaneously For example the uptake of 4-chloroaniline by soil may involve any of several different sorption mechanisms, including van der Waals forces, chemisorption, adsorption, ion-ion interactions, and partitioning (4), see Figure 3 1

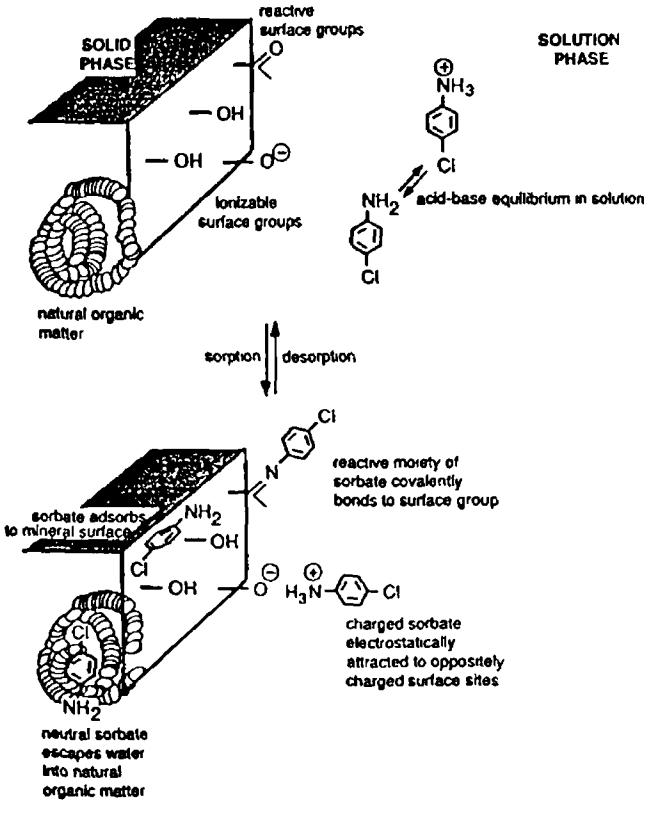

Figure 3 1 **Some Sorbent-Sorbent Interactions Possibly Controlling the Association of a Sorbate (4-Chloroaniline) with Soil Constituents (4)**

This chapter is concerned with the sorption of organic compounds, specifically compounds of the non-ionic class, by SOM and to some extent their uptake by the soil mineral fraction However, the other sorption mechanisms particularly adsorption cannot be ignored and are also discussed in the following sections

3 1.1 Adsorption

When a gas (or solute) is brought into contact with a surface some of it will be adsorbed onto that surface As is explained later the forces involved in such a process may be non-specific or specific Strictly there are two forms of adsorption (5-8)

(i) positive adsorption which arises from attractive forces between the adsorbent and the adsorbate It results in the concentration of the adsorbate at the surface of the adsorbent In this text positive adsorption will be referred to simply as adsorption,

(ii) negative adsorption is less familiar and is due to the repulsion of the adsorbate from the surface of the adsorbent As a result the concentration of the adsorbate is greater in bulk solution than near or at the surface of the adsorbate The phenomenon of negative adsorption is returned to later in this Chapter when it is discussed in relation to its use as a method for the determination of surface area of soil constituents

In addition to the two forms of adsorption there are two types of (positive) adsorption, namely physisorption and chemisorption which are compared in Table 3 1 The main differences between physisorption and chemisorption are

(i) physisorption is the result of non-specific, weak molecular forces of attraction between molecules, such as those involving van der Waals or hydrophobic interactions (see below) The heats of adsorption are characteristically low physisorption is significant at low temperatures 'but its importance rapidly decreases with increasing temperature of the system,

(ii) chemisorption involves a chemical modification to the surface of the adsorbent due to the formation of a chemical bond between the adsorbate and the adsorbent The two distinguishing features of chemisorption are

- that it can take place at extremely low adsorbate concentrations (typically less than 0 01 of saturation vapour pressure (7) and still produce adsorbent site saturation,

Table 3 1 Comparison of Physisorption and Chemisorption (8)

Physisorption	Chemisorption
Attraction between the adsorbent and the adsorbate usually involves weak van der Waals forces	Attraction between the adsorbent and the adsorbate involves the formation of a chemical bond
Low heats of adsorption ranging from 20 to 40 kJ mol^{-1}	Relatively high heats of adsorption ranging from 40 to 400 kJ mol^{-1}
Low activation energies	Relatively high activation energies
Occurs at low temperatures, decreasing with increasing temperature	Occurs at relatively higher temperatures
Completely reversible	Generally irreversible
The extent of adsorption is approximately related to the ease of liquefication of the gas	No such correlation as physisorption
Not normally specific	Often highly specific
Multilayer adsorption	Monolayer adsorption

- it can take place at elevated temperatures where physical adsorption is much less apparent

Chemisorption is an exothermic process and is characterised by large heats of adsorption typically in the range 40 to 400 kJ mol^{-1} Frequently, chemisorption may require an activation energy

The distinction between these two types of adsorption in not always clear and adsorption of a particular compound onto the surface of a material may fall between either classification

3 1 2 The Forces of Adsorption

There are a number of different intermolecular forces of attraction which give rise to adsorption (5), see Table 3 2 These forces (except for chemisorption which has already been discussed) are as follows

(i) the van der Waals forces of attraction, this type of molecular interaction arises from the random fluctuations in the distribution of the electrons as they circulate in their molecular orbitals As a consequence of the fluctuations electron-rich and electron-poor regions develop momentarily within and between

Table 3.2 **Types of Molecular Interaction Resulting in Adsorption and the Forces Involved (5)**

Type of interaction	Forces involved
van der Waals	Electrostatic
Hydrophobic	Entropy generation
Charge transfer and hydrogen bonding	Electrostatic
Direct and induced ion-dipole and dipole-dipole interaction	Electrostatic
Ligand exchange	Electrostatic
Ion exchange	Electrostatic
Magnetic	Magnetic
Chemisorption	Electrostatic

molecules. Over short time periods the creation of such dipoles within molecules gives rise to intermolecular attraction over short distances between molecules, namely the van der Waals forces. These forces are weak, as reflected by their specific heats of adsorption, typically 4 to 8 kJ mol^{-1} (5). However, they are additive and in general their magnitude is found to increase with increasing size of the adsorbate molecules. Under certain conditions, such as the adsorption of hydrocarbons from aqueous solution, van der Waals forces can be augmented by the disruption of the local liquid-water structure due to the phenomenon of hydrophobic bonding which is discussed next;

(ii) hydrophobic interactions; the importance of hydrophobic interactions in soils arise from the unusual properties of liquid-water particularly in relation to its structure. These properties influence the interactions of molecules that contain sizeable hydrophobic moieties. Liquid-water is considered to be composed of two types of structural arrangements of H_2O molecules, namely ice-berg and void structures (4, 5). The ice-berg regions of water consist of an ice-like framework of H_2O molecules within which one H_2O molecule is tetrahedrally co-ordinated to four other H_2O molecules by hydrogen bonding, whereas the void regions contain H_2O molecule which have melted out of the ice-like framework. The H_2O molecules in the void regions are orientationally disordered and consequently are packed much more tightly together than in the ice-berg regions.

The solublisation of a non-polar molecule, for example a hydrocarbon, by liquid-water is an energetically favourable process since heat is released. This means that hydrocarbon-water interactions are more favourable than hydrocarbon-hydrocarbon interactions (5). However, the solubilisation of the hydrocarbon has a

restructuring effect on the void H_2O molecules that are adjacent to the hydrocarbon These H_2O molecules form a partial cage of ice-like hydrogen-bonded clusters that surround the hydrocarbon As a result, the entropy of the aqueous system is reduced, which is thermodynamically unfavourable Therefore, processes which remove the hydrophobic molecule from solution and consequently keep the entropy of the system at a maximum are favoured It is important to realise that the hydrophobic bonding does not result from a direct attraction between non-polar groups, since the van der Waals forces of attraction are too weak to explain the observed effects Since many organic compounds contain significant hydrophobic moieties, adsorption through a combination of hydrophobic interactions and van der Waals forces has been suggested to be an important mechanism in soils (5)

It may be concluded that hydrophobic interactions are predominantly entropy driven at low temperatures In addition it is interesting to note that hydrophobic interactions become stronger at higher temperatures This is due to the breakdown of the ice-like structures in water and an increasing sensitivity to entropy changes in the system The energy and entropy changes which accompany the transfer of hydrophobic compounds at higher temperatures are increasingly positive, thus, their solubilisation becomes increasing unfavourable

(iii) hydrogen-bonding which is considered here under a separate heading to charge transfer due to its special importance in soil adsorption phenomena Hydrogen-bonding systems can be generally expressed as XH $\cdots$ Y, where X represents an electronegative atom (typically O or N) covalently bounded to H Due to the electonegativity of X, the electrons of the X-H bond are drawn towards the X atom which becomes slightly negatively charged (δ -) as a result, and consequently the H gains a slight positive charge (δ +) The H is capable of attracting an electron-rich centre, Y, and results in the formation of a hydrogen bond, this is indicated by the dotted line as follows

$$\begin{array}{cccc} -O-H & \cdots & X- \\ \delta- & \delta+ & & \delta- \end{array}$$

Hydrogen-bonding usually occurs through unpaired electrons, or more unusually through the sharing of π-molecular orbitals Typical heats for hydrogen bonding range from 2 kJ mol^{-1} for weak hydrogen bonding to upward of 63 kJ mol^{-1} for cases of very strong bonding (5) The most typical examples of hydrogen-bonding include O-H O and O-H N The ability of an adsorbent to adsorb a solute from solution through hydrogen-bonding will depend on the relative

strength of the solute-hydrogen bond to that of the solvent (water)-hydrogen bond. Adsorption of the solute from solution will occur where the strength of the solute-hydrogen bond is greater than that of the solvent-hydrogen bond.

(iv) charge transfer; the formation of a charge transfer complex arises from the interaction between an electron-donor molecule and an electron-acceptor molecule (5). This is due to the partial overlap of their molecular orbitals and a partial exchange of electron densities. Such complexes are formed between structures containing π-bonds or lone pair electrons. Electron donors can be divided into:

- those which contain electron-rich π-electron clouds, e.g. aliphatic and aromatic hydrocarbons;
- molecules which have lone pair donors, such as alcohols, thiols, ethers, thioethers.

Similarly, electron acceptors can be divided into compounds with:

- electron deficient π-electron clouds, such as s-trinitrobenzene;
- the weakly acidic hydrogens, such as 2,4-D.

The heats of adsorption for charge transfer range from 0 to 63 kJ mol^{-1}, and the energy of complexation will vary with solvent conditions (5). Charge transfer mechanisms have been suggested to be involved in the binding of many organic compounds to the aromatic cores present in SOM particularly in the humic materials (5).

(v) ligand exchange which involves the replacement of one or more ligands by the adsorbate molecule (5). For ligand exchange to occur the adsorbate must be a stronger chelating agent than that which the ligand will replace. Bonding may proceed through direct bonding or through indirect bonding by means of a water bridge. This mechanism has been suggested for the bonding of s-triazines to the residual transition metals of humic acids as shown in Figure 3.2 (5).

(vi) direct and induced ion-dipole and dipole-dipole interactions; ion-dipole and dipole-dipole interactions may contribute to the adsorption of polar and ionic organic compounds (5).

(vii) ion exchange refers to the adsorption of ionic compounds. Ion exchange consists of the adsorption of positively (negatively) charged species to negatively (positively) charged surface functional groups. This consists of the transfer of ions between the surface of the adsorbent and the solution. Ion exchange is affected by

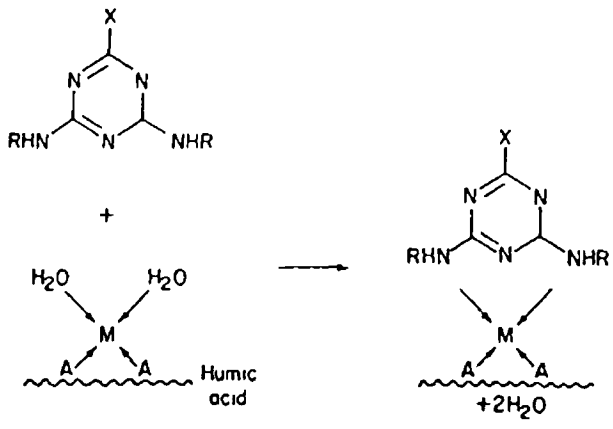

Figure 3.2 **Ligand Exchange (5)**

the nature of the adsorbate and adsorbent, and particularly by the pH of the solution

(viii) magnetic interactions between molecules are generally insignificant when compared to the electrostatic forces of attraction However, they may occur between molecules which contain conjugate double bonds and the conjugated double bonds of humic substances (5)

3 1 3 Absorption (Partitioning)

The significance of partitioning as a sorption mechanism has been increasingly recognised over the last decade (4) Its importance becomes apparent in soils which contain a significant level of organic matter, particularly in relation to the sorption of organic compounds that have a sizeable hydrophobic moiety As previously described the presence of such hydrophobic structures results in a tendency for these molecules to be 'forced' out of aqueous solution due to entropic considerations As a consequence, hydrophobic molecules have a greater tendency to be removed from solution by sorption to soil constituents (4)

However, the adsorption of hydrophobic compounds by the mineral fraction of the soil is hampered by the polar nature of most mineral surfaces (which is due to the presence of hydroxyl and other oxygen containing moieties) As a result of their polar nature, mineral surfaces have a stronger tendency to favour interactions with polar molecules such as water than with hydrophobic molecules (4) Thus, for adsorption of a hydrophobic compound to occur under moist soil conditions it has first to displace water at the mineral surface, which is an energetically unfavourable process

In contrast, in soils which have a significant organic matter content, hydrophobic molecules can escape readily from solution by partitioning into the organic matter The organic matter fraction of soil may be viewed as consisting largely of macromolecules which exist as chain-like structures of material coiled into globular units that occur as isolated patches coating the mineral surface of the soil, see Figure 3 3 (4) The coiling of the organic matter is brought about because it minimises the hydrophobic surface area which it exposes to the aqueous solution As a result, SOM can be pictured as being composed of a flexible material which is loosely held together and highly 'porous' in nature Into this material organic solutes can easily penetrate and thus dissolve into the organic phase of the soil Partitioning of the organic solutes does not require the displacement of adsorbed H_2O molecules Also, SOM is not as polar as the mineral fraction, it can only form hydrogen bonds at limited points along its structure, for instance where carboxyl and phenol-OH functional groups occur Partitioning occurs partially because of the chemical similarity between the SOM and the sorbed organic molecules which dissolve into SOM through dispersive forces such as van der Waals interactions, but also because of the existence of hydrophobic pockets in the SOM which allow hydrophobic molecules to 'escape' from the aqueous solution

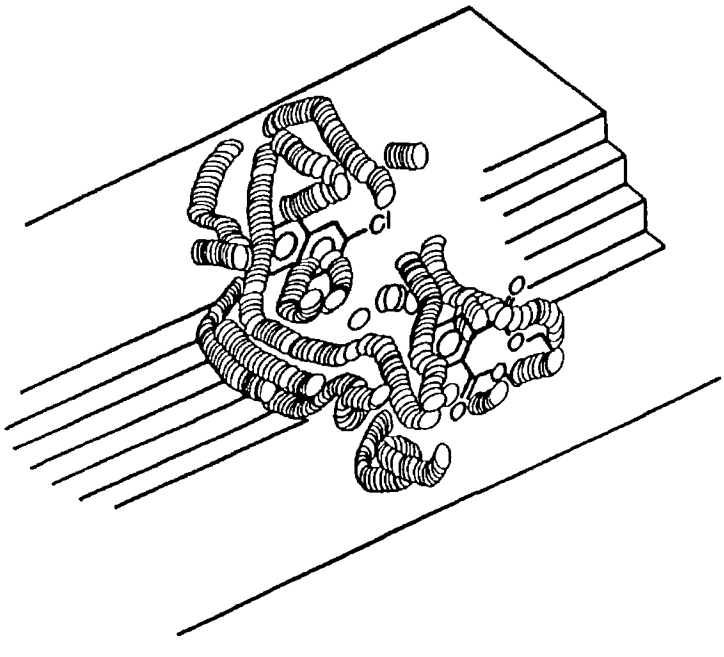

Figure 3 3 Conceptualisation of the Partitioning of Organic Sorbates with SOM (4) Note The figure shows the sorption of non-ionic organic compounds (here represented by 2-chloronapthalene and diethylphthatate) by small pockets of organic material coating the mineral surfaces of the soil

Thus, it may be concluded that partitioning of hydrophobic organic compounds into SOM occurs through a combination of hydrophobic interactions and dissolution into the organic matter phase

3.1 4 Classification of the Sorption Isotherms

(a) Adsorption Isotherms

The sorption process is generally studied using the sorption isotherm For adsorption from the vapour phase Brunauer divided the various isotherms into the five classic isotherm types (I to V), which are shown schematically in Figure 3 4 (7) The figure shows the amount of adsorbate taken up by the solid versus P/P_0, the relative pressure of the adsorbing vapour, where P is the partial pressure of the vapour and P_0 is its saturation pressure

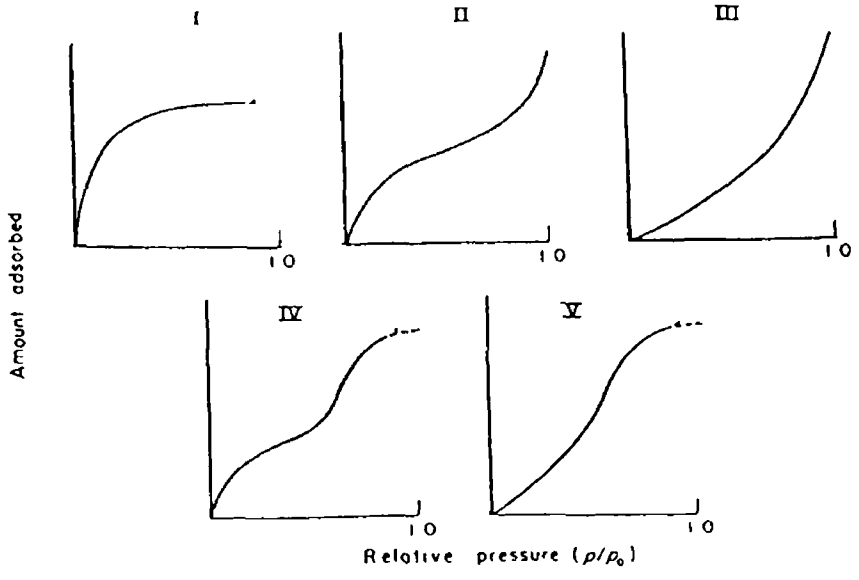

Figure 3 4 **Classification of Isotherms for Adsorption from the Vapour Phase According to Brunauer (7)**

The type I isotherm is the familiar Langmuir adsorption isotherm The curve of such an isotherm is observed to approach a limiting value (the plateau region) which is presumed to correspond to monolayer coverage of the adsorbent surface The type I isotherm is generally observed for adsorption on microporous solids (i e pores < 20 Å)

such as charcoal, silica and molecular sieves such as Linde 13X (7) The type I isotherm is also found in the cases of chemisorption

The type II isotherm is the most commonly encountered isotherm and is sometimes referred to as the BET isotherm It is observed for the adsorption of vapours onto non-porous solids At low relative pressures the curve is characterised by the (usual) presence of the inflection point B, which is generally accepted to correspond to monolayer coverage of the surface Monolayer coverage of the adsorbent usually occurs for P/P_0 values approaching 0 3 (7) Above the inflection point there is a further rise to the curve which represents the adsorption of further layers onto the surface, i e multi-layer formation

The type III isotherm is characterised by a curve which remains convex to the P/P_0 axis This isotherm is relatively rare and is thought to occur in cases where the heat of adsorption is equal to or less than the heat of liquefaction of the adsorbate (7) In such instances adsorption is co-operative in nature due to the fact that the adsorbate-adsorbent forces of attraction are much weaker than the adsorbate-adsorbate interactions In other words, the more molecules that are already adsorbed onto the surface of the solid, the easier it is for further molecules to become adsorbed The adsorption of cyclohexane on calcium carbonate and the adsorption of benzene on dehydrated silica gel have been given as examples of type III isotherms (7) As with the type II isotherm, the type III isotherm is generally encountered for non-porous solids (7)

The type IV is similar to the type II isotherm except that at P/P_0 values approaching saturation of the gas phase the isotherm is observed to level off to form a second plateau region The formation of the second plateau is thought to reflect capillary condensation of the adsorbate in the pores of the solid (7) Thus, the type IV adsorption isotherm is observed for the adsorption of vapours onto porous solids (as is the Type V isotherm below)

The type V isotherm is similar to the type III, but again it is observed to level off to form a plateau at P/P_0 values approaching vapour saturation of the gas phase for the same reasons as the type IV

A similar classification for adsorption from the liquid phase has been devised by Giles and co-workers (9) The various isotherms were discussed in terms of the adsorbent-adsorbate, adsorbate-adsorbate and adsorbent-solvent interactions and also of the orientation of adsorbed molecules on the surface of the solid This system divides the various isotherms into four classes, namely S, L, H and C, according to

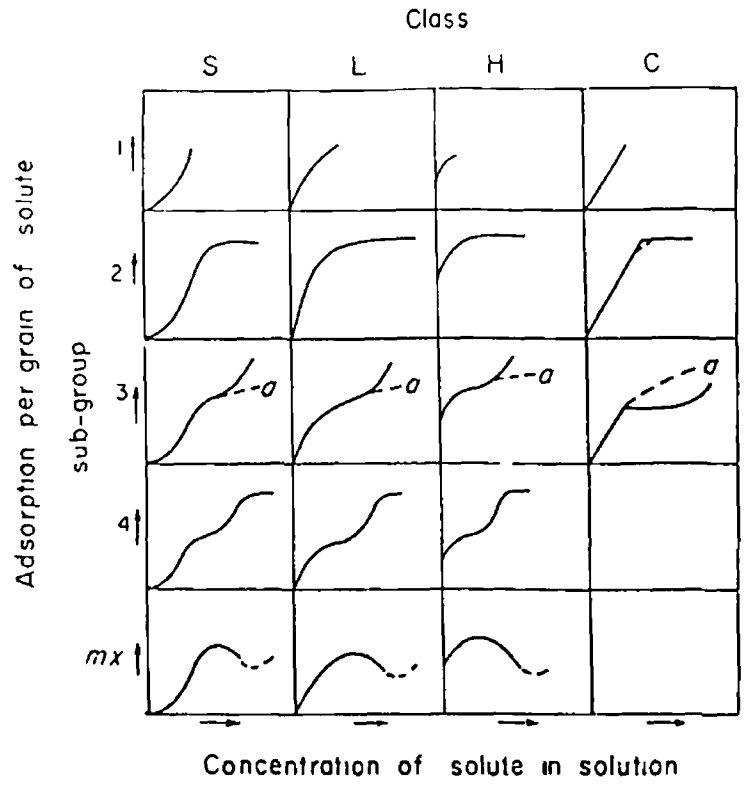

Figure 3 5 Classification of Isotherms for Adsorption from Solution According to Giles and Co-workers (9) Note According to this classification Brunauer's five types of vapour phase adsorption isotherms are defined as, H 2 (type I), L 3 (type II), S 1 (type III), L 4 (type IV), S 2 (type V)

the nature of the initial slope of the isotherm and subsequently into subgroups, as shown schematically in Figure 3 5

The S-adsorption isotherm has an initial slope which rises in a convex manner to the solute (adsorbate) concentration axis, which suggests that adsorption of the solute becomes easier as the concentration rises The shape of the isotherm indicates that the forces of attraction between the adsorbent and the solute at low concentration is less than the affinity of the solution for the solute (9) Thus, the S-type isotherm is equivalent to the type III isotherm for adsorption from the gas phase In the case of organic solutes this indicates co-operative adsorption of the adsorbate to the surface of the solid Initially the organic adsorbate becomes stabilised on the surface of the solid and in turn there is an enhanced affinity of the surface for further adsorbate molecules to be adsorbed

The initial slope of the L-isotherm is observed not to increase with an increase in the solute concentration This arises from the high relative affinity of the adsorbent for the solute at low concentrations coupled with the decrease in the

amount of surface area available for adsorption as the solute concentration increases The L-isotherm, particularly the L2, is the most commonly observed isotherm for adsorption studies by soil systems (10)

The H-isotherm is an extreme case of the L-isotherm It is characterised by a large initial slope due to a large relative force of attraction between the solute and the adsorbent This large affinity usually arises from either a highly specific interaction occurring between the adsorbate and the adsorbent, or by a significant contribution by van der Waals forces to the adsorption process

The C-isotherm is characterised by an initial slope which remains linear and independent of the concentration of the solute until the maximum possible adsorption has been reached The C-isotherm can be produced by either a constant 'partitioning' of the solute between the surface of the solid and the external solution or due to a proportional increase in the area available for adsorption as the amount of adsorbate taken up increases (9)

(b) Partition Isotherm

The C1-isotherm of Figure 3 5 can also be interpreted as the absorption or constant partitioning of the vapour or solute between the bulk material of the solid and the exterior gas or liquid phases As a result the partition isotherm is invariably linear to high concentrations of the vapour or solute Any curvature to the slope of the isotherm (C2 of Figure 3 5) is only observed at relatively high concentrations of the vapour or solute The linear isotherms that have been observed for the sorption of non-ionic compounds by SOM (4) have been interpreted as being due to the partitioning of the organic sorbate between the SOM phase and the gas or liquid phases (see further on)

3 1 5 Mathematical Description of the Sorption Isotherms

The variously observed isotherms discussed in the preceding section can be described by mathematical equations which are discussed below

(a) **Adsorption**

The three commonly used equations which are used to describe adsorption of vapours or solutes by a solid are the Freundhch, Langmuir, and the Brunauer-Emmett-Teller (BET) equations (5-8, 10, 11)

The Freundlich equation is purely empirical, but its use is still retained in the literature The equation can be expressed as follows

$$\frac{x}{m} = k\ C^n \qquad \text{Equation 3 1}$$

where x/m is the amount of adsorbate adsorbed per unit mass of adsorbent, C is the solution concentration of the adsorbate at equilibrium, and k and n are terms which may be related to binding energy The major short coming of the Freundlich equation is that there is no upper limit to the amount that can be adsorbed by the adsorbent (5) However, the equation has been found to work adequately well for intermediate concentrations and has been frequently used to compare the adsorptivity of a wide number of adsorbent materials including soil

The Langmuir equation has a more sound conceptual basis than the Freundlich equation It was initially developed for the adsorption of gases onto solids (the type I adsorption isotherm of Figure 3 4), but it has also been applied to adsorption from solution (the L-isotherms of Figure 3 5) In deriving the equation a number of general assumptions were made about the adsorption process, which were as follows (5)

- the energy of adsorption is constant and independent of the surface coverage,
- the adsorption sites are discreet and there is no interaction between adsorbed molecules,
- the maximum adsorption possible is that of a complete monolayer coverage of the surface

The equation describes the adsorption of an adsorbate onto the surface of a solid material which is approaching a limiting value It is assumed that the plateau region of the curve corresponds to monolayer coverage of the surface For adsorption from the vapour phase the Langmuir equation has the form

$$q = \frac{bp}{1+bp} \qquad \text{Equation 3 2}$$

where q is the fraction of the surface covered by the gas, p is the equilibrium pressure of the gas, and b is a constant related to the rates of adsorption/desorption The Langmuir equation is more commonly used for sorption from aqueous solutions, thus Equation 3 2 can be rewritten in terms of concentration and in a linear form as follows

$$\frac{C}{x/m} = \frac{1}{k\,Q_m} + \frac{C}{Q_m} \qquad \text{Equation 3 3}$$

where C is the equilibrium concentration of the solute in solution, x/m is the amount of solute adsorbed per unit mass of adsorbent, Q_m the adsorption maximum (i e monolayer capacity) and k a term related to the binding energy

It should be noted that in general the Langmuir equation is not as successful in describing adsorption from the liquid phase as it is from the vapour phase This is due to the idealised assumptions which were made in its derivation In particular the assumption that all adsorption sites are equivalent is a gross approximation particularly when considering adsorption by soil (5, 7) Soil is a heterogeneous material, thus all adsorption sites cannot be expected to be equal A second inaccurate assumption is that all adsorption sites are discreet and adsorbed molecules do not interact, there will be some interaction between adsorbed molecules In addition, in many instances adsorption does not stop once monolayer coverage of the adsorbate surface has been achieved and therefore subsequent layers are also adsorbed (i e multi-layer formation)

The BET equation was also developed for the adsorption of gases, but unlike the Langmuir equation it takes into account multi-layer formation on the surface of the adsorbent (see type II isotherm of Figure 3 4) (6, 7) For adsorption from the vapour phase the equation has the following form

$$\frac{P/P_o}{V(1-P/P_o)} = \frac{1}{V_m C} + \frac{(C-1)}{V_m C}\,\frac{P}{P_o} \qquad \text{Equation 3 4}$$

where P is the equilibrium pressure of the adsorbate, P_o the saturation vapour pressure of the adsorbate which is the vapour pressure of the liquefied gas at the adsorbing temperature, V the volume of gas adsorbed (at STP), V_m the volume of gas adsorbed (at STP) for monolayer coverage, C a term related to the energy of adsorption The BET equation is found to reduce to the Langmuir equation at low relative pressures (7)

One of the assumptions of the BET equation is that the probabilities of evaporation and condensation of the adsorbate from each layer formed, as well as the energies associated with each of these properties, is independent of the amount adsorbed (V) This assumption is found to be approximately true in the P/P_0 range 0 05 to 0 3 (7) A second short coming of the BET equation is that it assumes that the number of layers adsorbed becomes infinite when the saturation pressure is reached In fact it is often the case that the number of layers reaches only a fimte number at saturation pressures

(b) Partitioning

The partitioning of a non-ionic organic compound in the soil is considered to occur between two immisible phases, namely the organic matter fraction of the soil (i e the SOM) and the aqueous phase (or in the case of dry soils with the vapour phase) For partitioning between SOM and the aqueous solution the partition coefficient, K_{om}, which is the ratio of the amount (usually in terms of concentration) of the organic compound in each phase, is defined as follows

$$K_{om} = \frac{C_{om}}{C_w} \qquad \text{Equation 3 5}$$

where C_{om} and C_w are the concentrations of the organic compound in the SOM and aqueous phases respectively (4)

Since the partitioning of the organic compound is considered to be due to its dissolution into the SOM phase, the partition process may be viewed as occurring between two immisible solutions, thus Equation 3 5 can be rewritten as follows

$$K_{om} = \frac{x_{om} V_{om} \rho_{om}^{-1}}{x_w V_w^{-1}} \qquad \text{Equation 3 6}$$

where x_{om} and x_w are the mole fraction concentrations of the sorbate in the SOM and aqueous solutions respectively, V_{om} and V_w are the molar volumes of the two phases, and ρ_{om} is the density of the organic matter (4) Choosing the pure liquid of the sorbate to serve as the reference state, and using the relationship $x = \gamma$ **Error! Reference source not found.**$^{-1}$, Equation 3 6 can be rewritten as follows

$$K_{om} = \frac{\gamma_w V_w}{\gamma_{om} V_{om} \rho_{om}} \qquad \text{Equation 3 7}$$

where γ_w and γ_{om} are the activity coefficients of the sorbate in the aqueous and SOM phases respectively (4) The term γ_{om} reflects the incompatibility of the sorbate dissolved in the SOM as compared to its solubility in a liquid of itself For a given organic compound (of limited water solubility) and a particular soil all the terms on the right-hand side of Equation 3 7 are virtually constant for all concentrations of the organic compound in the aqueous phase (4) The value of γ_w is practically independent of C_w for non-ionic organic compounds, and since V_w, V_{om} and ρ_{om} are properties of the solution and the organic matter phase which are generally unaffected by the presence of very small (typically submilhmolar) levels of the organic compound these values remain virtually constant In addition the value of γ_{om} in the SOM may not be too much above 1 if this material is as 'accommodating' to the organic sorbate as a more ideal organic solvent such as n-octanol Thus, the value of K_{om} would be expected to remain constant for a particular sorbate-sorbent system This is seen in the sorption isotherms for the partition of organic compounds between soil and aqueous phases which remain linear up to relatively high concentrations of the organic compound in the liquid phase

3 2 The Determination of Surface Area

The surface area of solids can be measured by positive and negative adsorption methods (10) which are discussed below

(a) Positive Adsorption Methods

The measurement of surface area by positive adsorption methods require the satisfaction of the three following criteria (10)

(i) there must be a pronounced accumulation of the adsorbate molecule (referred to as the probe) from either the gas or liquid phases onto the surface of the solid, i e positive adsorption,

(ii) the cross-sectional area occupied by the probe, A_m, in the monolayer must be known,

(iii) the amount of probe adsorbed per unit mass, Q_m, corresponding to monolayer coverage of the solid must be determined

Adsorption of a vapour phase molecule is the commonly used method for surface area determination (7) The most frequently used probe is N_2, but numerous other probes including Ar, Kr, Xe, ethane and benzene have also been used (7) These probes have the advantage of being non-specifically adsorbed by the surface of the solid and are generally small enough (in the case of the fixed gases) to pass through pores into the interior of the solid The cross-sectional area (A_m) of the probe is often a quantity that is difficult to establish because of the lack of knowledge as to the exact mode of packing of the adsorbed molecules in the monolayer The A_m value is usually calculated from the density of the adsorbate in the ordinary liquid or solid form It is assumed in calculating A_m that the arrangement of the molecules on the surface is the same as it would be on a plane surface if placed within the bulk liquid (or solid) without disturbing the pre-existing arrangement of the liquid The formula used to determine A_m is as follows (7),

$$A_m = f\left(\frac{M}{rN}\right)^{2/3} \qquad \text{Equation 3 8}$$

where M is the molecular weight of the adsorbate, r its liquid density, f the packing factor a value which depends on the number of nearest neighbour, and N Avogadro's number The value of f is usually taken to be 1 091 which arises from the commonly encountered arrangement of twelve nearest neighbours in the bulk liquid and six on the plane For the adsorption of N_2 at liquid nitrogen temperatures (-196°C), Equation 3 8 yields a value of 16 x 10^{-20} m^2 per adsorbed N_2 molecule

The surface area of a solid material can only be measured for probe-adsorbent systems which give the type I, type II or type IV isotherms (7) In such instances there is usually a clearly defined inflection point B, which corresponds to the monolayer capacity of the solid, Q_m Thus, Q_m can be determined from direct inspection of the curve to find point B, or more commonly by applying the BET equation to the data points For the BET equation a plot of $(P/P_o)/V(1-P/P_o)$ versus P/P_o will give a straight line of slope $(C-1)/V_mC$ and intercept $1/V_mC$ The Langmuir equation can also be applied to the results, for adsorption from the liquid phase a plot of C/(x/m) versus C will give a straight line with slope $1/Q_m$ and intercept $1/k\ Q_m$ Once the value of Q_m (or V_m) and A_m have been determined, the surface area, S, of a solid material can be calculated from the following simple equation (7),

$$S = \frac{Q_m A_m N}{M} \qquad \text{Equation 3 9}$$

where N is Avogadro's number and M the molecular weight of the adsorbate

It should be noted that for adsorption from the liquid phase it is considerably more difficult to determine surface area (7) This is because in general the probe molecules used are often large and complicated in shape, thus, calculation of a suitable A_m value is difficult Secondly, the competitive adsorption of the solvent introduces complications, in relation to the calculation of Q_m It has been found that the plateau region does not necessarily correspond to monolayer coverage of the solid, and there is usually a considerable amount of solvent molecules adsorbed to the surface with the probe

(b) Negative Adsorption Methods

It has been previously described in Chapter 1 that in general most solids bear a surface charge in aqueous solution (10) Negative adsorption of ionic species will occur from the solid due to their repulsion from the surface This occurs because the charge of the ionic species has the same sign as the charge on the solid surface Consider as an example the case of a negatively charge surface in an aqueous solution containing Na^+ and Cl^- ions At the interfacial region between the surface and the solution there will be a higher concentration of Na^+ ions than in the bulk solution This is due to the attraction of the cations to the negatively charged surface, hence the formation of the electric double layer Conversely, this region immediately adjacent to the surface is greatly depleted in Cl^- ions due to their repulsion from the negatively charged surface Thus, the concentration of Cl^- ions in the bulk solution will increase relative to the concentration of Cl^- ions immediately adjacent to the surface The region immediately adjacent to the surface of the solid is referred to as the exclusion volume, and it has been found to be proportional to the surface area of the solid (10) Therefore, its measurement can be used to determine the specific surface area of the solid (The specific surface area measured by the exclusion volume method is referred to as the exclusion area in this work)

Sposito (10) described an experiment which takes advantage of the phenomenon of negative adsorption to determine the specific surface area of a solid material The experiment consists of two identical chambers separated by a water permeable membrane To both chambers is added an aqueous solution containing a chosen ion i The initial concentration of ion i in both chambers is C_{oi} (mol dm^{-3}) The moles of charge contributed by ion i to the solution is $| Z_i | C_{oi} V$, where Z_i is the valence of the ion i, C_{oi} is the initial concentration of the ion i, and V the volume of the solution To one of the chambers was added an amount, m_s (kg), of solid, and assuming that repulsion of ion i has occurred from the surface of the solid, there will be a movement of ions from the chamber containing the suspended solid to the

chamber containing only solution At equilibrium the concentration of ion i in the chamber which does not contain suspended solid will have increased to a value C_i Thus, the increase in the concentration of ion i can be related to the simultaneous decrease in its concentration in the chamber containing the suspended solid as follows

$$|Z_i| C_i V_{ex} = \frac{|Z_i| C_i V - |Z_i| C_{oi} V}{m_s} \qquad \text{Equation 3 10}$$

where V_{ex} is the exclusion volume (dm^3 kg^{-1}) (i e the volume of solution immediately adjacent to the solid surface from which ion i is excluded) The exclusion volume represents the volume (per unit mass of suspended solid) which is depleted of ion i in the chamber containing the suspension The expression which relates the exclusion volume in a 1 1 electrolyte solution to the surface area of a solid (which is derived in Appendix B) has the final form

$$V_{ex} = 2S_E/(\beta c)^{1/2} - \delta S_E \qquad \text{Equation 3 11}$$

where the constant $\beta = 1\ 084 \times 10^{16}$ m mol^{-1} at 298 15 K, S_E is the exclusion volume determined surface area of the solid (m^2 kg^{-1}), and δ is the distance between the two planes of the electric double layer Equation 3 11 predicts that a plot of V_{ex} versus $c^{-1/2}$ will be a straight line with the slope proportional to the exclusion surface area, S_E Thus, knowing the slope of the line, S_E can be calculated from the following equation

$$S_E = (\beta)^{1/2} (\text{slope}/2) \qquad \text{Equation 3 12}$$

3 2.1 The Surface Area of Soil Constituents

It will be recalled from Chapter 1 that the highly decomposed organic matter (i e the humic substances) which is the dominant fraction of SOM is an amorphous, polymeric material of poorly defined structure In addition, the forces of interaction between the organic molecules and particles which comprise SOM are complex and quite variable As a result, the question of what constitutes the surface area of SOM is not only problematic but it is also a contentious issue Until recently (about 1980) it was generally accepted that the surface area of SOM was of the order of 560 to 800 m^2 g^{-1} as determined from the sorption of ethylene glycol (12), a value which was subsequently propagated in the general literature on the subject (1, 5, 13) However, more recent measurements of the surface area of peat and other SOM materials have indicated that it has a considerably smaller value, ranging from 1 to 2 m^2 g^{-1} (14) to c 27 m^2 g^{-1} (15) from N_2 adsorption

The size of the surface area of SOM has important implications for its sorption mechanism, particularly in relation to its uptake of the non-ionic class of organic compounds A large surface area for SOM would support adsorption as the dominant mechanism for retention of this class of organic compounds On the other hand, a small surface area would suggest that partitioning into the SOM contributes significantly to the retention of such organic compounds However, it is difficult to say what exactly constitutes the surface area of SOM, and the problem is not helped by the very large differences in the surface area values which have been reported

However, before discussing the surface area of SOM it is necessary to briefly examine the methods used to measure the surface area of the mineral fraction of the soil, particularly the clays This is relevant to the discussion on the surface area of SOM since the methods used to measure the mineral surfaces, and the interpretation of these results, have been carried over to the measurement of SOM

3.2 1.1 The Surface Area of Soil Minerals

It has long been recognised that for the clay minerals there exists two distinct surfaces which can be measured (10) The first is the small external surface of the clay and the second is the very large internal (interlayer) surfaces which exist between the sheet structure of the clay It has already been discussed in Chapter 1 that the sheet layers of the 1 1 non-expandable clays are held tightly together by hydrogen-bonding and as a consequence adsorbing molecules are excluded from the interlayer regions of the clay structure Thus, the (measurable) surface area of the non-expandable clays consists almost exclusively of the external surface regions which are relatively small in size In contrast, the sheet structure of the 2 1 expandable clays are held together by much weaker forces of attraction (such as van der Waals forces) As a result, the attractive forces can be overcome by intercalating polar molecules, such as water, which force the sheets apart, exposing the internal surfaces of these clays which are substantially greater in size than their external surfaces In the aqueous environment these internal surfaces may be exposed due to the penetration of water molecules into the interlayer regions Consequently, these surfaces are available for adsorption of organic solutes in the soil environment

(a) Positive Adsorption Methods

The standard method for measuring the surface area of clay minerals is by determination of the amount of adsorbate (referred to as the probe) required for monolayer coverage of the surface of the material This monolayer value is usually

calculated by application of the BET equation to the sorption data (10) The choice of probe is important for surface area determination, as it demonstrates the operationally defined nature of surface area, i e the magnitude of the surface area measured is dependent on the experimental conditions under which the measurement in carried out and the nature of the probe used (10) With respect to clays two classes of probes are distinguishable

(i) the weakly interacting probes which are non-selectively adsorbed onto the surface of materials The most widely used probe of this class is N_2, but other probes such as Ar and Kr have also been used (10) This class of probe is used to measure the external surfaces of the non-expanding and expanding clays,

(ii) the second class of probe consists of the polar molecules, these include ethylene glycol (EG) (12), ethylene glycol monoethyl ether (EGME) (16-18), H_2O and N-cetylpyridinium bromide (PCB) (10) Such polar molecules can penetrate into the interlayer regions of the expandable clays which contain inner-sphere complexes between metal cations and the clay surface (see Section 1 2) This is assuming that these complexes are intrinsically less stable than the outer-sphere complexes involving the solvated metal cations The solvation of the complexed metal cations by the probe is favoured when the metals have a large charge to ionic radius ratio (10) Therefore, cations such as Li^+, Na^+, Mg^{2+} and Ca^{2+}, are associated with mterlayer solvation, whereas, K^+, Rb^+, and Cs^+ tend not to be (10)

The total surface area of expandable clays is usually measured using a combination of a weakly interacting probe and a polar probe, typically N_2 and H_2O respectively (10) In the case of H_2O adsorption by expandable clays, it has been found from X-ray diffraction studies that the intercalated H_2O molecules are present as a monolayer between the sheets (10) This means that the adsorption of water vapour onto expandable minerals consists of monolayer coverage of the external surface and only one-half of the accessible internal surfaces The total surface area of an expandable clay (S_M) can be calculated from the following simple equation (10)

$$S_M = 2\,S_W - S_N \qquad \text{Equation 3 13}$$

where S_W is the surface area measured by water vapour (internal and external surfaces), and S_N is the surface area measured by N_2 adsorption (external surface)

Typical results for the determination of the surface area of various clay minerals are presented in Table 3 3 (10) The surface areas were measured by a

combination of N_2 and H_2O or N_2 and CPB adsorption From Table 3 3 it can be clearly seen that the surface area of kaolinite is relatively small (c 15 to 19 m^2 g^{-1}) and is independent of the probe used since all adsorbed molecules are confined to the external surface of the clay In contrast large differences in the surface area values exist for the Na-montmorillonite samples, N_2-adsorption gives surface area values of 14 to 33 m^2 g^{-1} ,whereas the polar probes yield values of c 800 to 850 m^2 g^{-1} due to their ability to penetrate into the internal regions of the clay

Table 3 3 The Surface Area of Various Phyllosilicates as Determined by N_2, H_2O or N-Cetylpyridinium Bromide Adsorption (10)

Clay mineral	Surface area (m^2 g^{-1})		
	N_2	H_2O	N_2 and CPB
Kaolinite (Na-form, Peerless)	18 6	18 8	-
Kaolinite (Bath, South Carolina)	18 0	-	15 0
Illitic mica (Na-form, Illinois)	-	102 0	-
Illitic mica (Na-form, Fithian, Illinois)	93 0	-	96 0
Vermiculite (Mg-form, Ilano, Texas)	3 1	712 0	-
Vermiculite (Kenya)	<1 0	-	726 0
Montmorillonite (Na-form,Wyoming)	33 0	847 0	-
Montmorillomte (Na-form,Wyoming)	14 0	-	800 0

Note Parentheses refer to the form of the mineral where known, and the geographical source of the sample CPB = N-cetylpyridmium bromide

A single point technique based on the adsorption of either EG or EGME has also been used to measure the surface area of clay minerals (12, 16-18) The basic assumption of this technique is that only monolayer coverage of the clay occurs for the adsorption of EG or EGME However, the validity of this method has been questioned, particularly in relation to its use for the measurement of the surface area of SOM (14, 19) This is discussed in the following sections

(b) Negative Adsorption Methods

The advantage of the exclusion volume method is that it requires an aqueous solution to be in contact with the solid material As a result, the specific surface area

measured should reflect the structure of the solid material in its natural state in the soil This is in contrast to the gas phase methods, such as N_2 adsorption, which require that the sample is dry before the surface area can be measured Drying of the soil sample may result in its shrinkage and lead to blockage of pores etc , which would prevent the gas from gaining access to the internal surfaces of the sample This is clearly the situation for the expandable clays which have small specific surface areas when measured by N_2 adsorption and very large surface areas when measured by H_2O adsorption This is clearly illustrated in the results of Edwards *et al* (20-22) who compared the surface area of non-expanding and expanding clay samples by the exclusion volume and BET (N_2) methods (see further on)

Application of the exclusion volume method for the measurement of surface area have been reported by Schofield (23) Using the results reported by Mattson (24) for the negative adsorption of Cl^-, NO_3^-, SO_4^{2-} and CN^- ions by a bentonite sample, Schofield (23) calculated the specific surface area of the bentonite to be 470 $m^2 g^{-1}$ Van den Hul and Lyklema (25) successfully applied the exclusion volume method to determine the surface area of an AgI suspension to be between 1 to 5 $m^2 g^{-1}$ which closely agreed with the surface area measured by other methods Schofield and Samson (26) measured the exclusion surface area of several kaolinite samples They determined that negative adsorption of Cl^- ions occurred for suspensions of the kaolmite samples in 0 005 M NaCl at pH values above pH 6 5 The exclusion surface areas measured for several of the kaolmite samples are shown in Table 3 4 From this table it can be seen that the exclusion surface areas were in good agreement with the corresponding BET (N_2) determined specific surface areas

Table 3 4 Specific Surface Area of Kaolinite Samples Measured by Exclusion Volume and BET (N_2) Methods (26)

Kaolinite Sample	Mineralogy[a]	Surface area ($m^2 g^{-1}$)	
		BET(N_2)	Exclusion area
F	K, Ms (trace)	-	15
C	K, Ms	6	8
M	K (pure)	10	9
G	K, Mt, Mc	16	18
S	K, Fe	39	25

Note [a] K = kaolmite, Mc = mica, Mt = montmorillomte, Ms = muscovite, Fe = hydrated iron oxide

Quirk (27) explained that the generally lower exclusion areas reported by Schofield and Samson (26) was due to positive adsorption of Cl^- ions which was still occurring at alkaline conditions as high as pH 10 It was reported that when allowances were made for this positive adsorption the correct value (i e the BET (N_2) value) was obtained for the surface area

A detailed examination of the exclusion volume method was made by Edwards *et al* (20, 21) to determine the specific surface areas of monoionic illite and montmorillonite clays (Monoionic refers to the presence of a single exchangeable cationic species adsorbed to the clay, e g Na^+-montmorillonite contains Na^+ as the monoionic species) The method used consisted of adding known amounts of chloride solution to suspensions of the clay samples and allowing the solutions to come to equilibrium The solution and the solid material were subsequently separated by centrifugation and the concentration of the chloride ions in the supernatant and in the sediment samples was measured The results were plotted as a graph of Vex versus $q/(z\beta c)^{1/2}$ which gave a straight line with slope equal to the surface area of the clay in $cm^2\ g^{-1}$, see Figure 3 6

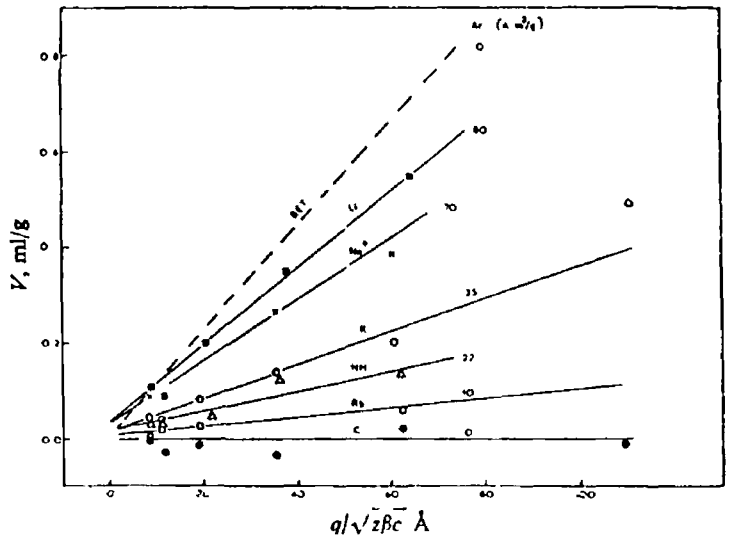

Figure 3 6 Chloride Exclusion by Monoionic Illite Clays (20)

Note Vex (ml g^{-1}), q constant (= 2, for 1 1 electrolyte), z charge of ion (= 1, for 1 1 electrolyte), β= 1 06 x 10^{15} cm mequiv $^{-1}$ at 25 °C, and c bulk concentration (mequiv cm^{-3})

The slopes of the graphs were then used to calculate the specific surface area of the clays The exclusion surface areas which are presented in Table 3 5 were compared to the corresponding BET (N_2) surface area values of the clay samples For the illite samples it can be seen from Table 3 5 that the BET (N_2) surface areas remained at a similar value, varying from 105 $m^2\ g^{-1}$ for the Rb^+-illite to 118 $m^2\ g^{-1}$ for the NH_4^+-

illite However, the size of the exclusion surface areas were found in all cases to be less than the corresponding BET (N_2) values In addition the exclusion surface areas varied considerably in magnitude, ranging from 80 m^2 g^{-1} for the Li^+-illite to 0 m^2 g^{-1} for the Cs^+-illite It was observed that the exclusion areas decreased in the order $Li^+ > Na^+ > K^+ > Rb^+ > Cs^+$ which corresponded to the order of increasing ionic radius of the exchangeable cation

Table 3.5 Comparison of the Surface Areas of Illite and Montmorillonite Clays Determined by N_2 Adsorption and Chloride Exclusion (20, 21)

Exchangeable cation	Surface area (m^2 g^{-1})			
	Illite		Montmorillonite	
	BET(N_2)	Exclusion area	BET(N_2)	Exclusion area
Li^+	116	80	66	650
Na^+	109	70	46	560
K^+	113	35	64	436
NH_4^+	118	22	59	256
Rb^+	105	10	-	-
Cs^+	112	0	146	156

Note BET (N_2) is N_2 measured specific surface area

The inverse relationship between the exclusion surface area and the ionic radius of the exchangeable cation follows the general observation that the larger the cation the greater its tendency to form inner-sphere complexes (10) Thus, it was concluded that the reduction in the exclusion surface area was due to the greater tendency of the exchangeable cations to form inner-sphere complexes with the surface of the illite clay as the ionic radius of the cation increased The creation of such inner-sphere coinplexes resulted in the formation of electrically neutral surfaces which in turn no longer repelled Cl^- ions As a result, the exclusion surface area was always less than the corresponding area probed by N_2 molecules, and it decreased with increasing inner-sphere complex formation between the exchangeable cation and the clay

A similar decrease in the exclusion surface area with increasing size of the exchangeable cation was found for the montmorillonite samples, see Table 3 5 However, the exclusion surface areas were all greater than the corresponding BET (N_2) surface areas which was in keeping with the expandable nature of this clay

group As can be seen from Table 3 5 the BET (N_2) surface area remained at a similar level from 46 m^2 g^{-1} for Na^+-montmorillonite to 66 m^2 g^{-1} for Li^+-montmorillonite, the only exception being Cs^+-montmorillonite which had a surface area of 146 m^2 g^{-1} The exclusion surface areas were found to vary from 650 m^2 g^{-1} for Li^+-montmorillonite to 156 m^2 g^{-1} for Cs^+-montmorillomte This was due to the expansion of the montmorillomte samples in solution which exposed their interfacial surfaces Thus, there was a greater surface area available from which the Cl^- ions were repelled from

The influence of exchangeable cations was further examined by Edwards *et al* (22) for several di-valent (Mg^{2+}, Ca^{2+}, Sr^{2+}, Ba^{2+}) and one tri-valent (Al^{3+}) cation forms of illite and montmorillonite clays It was found that for the illite samples there was no significant negative adsorption of Cl^- ions from the Ba^{2+}- and Sr^{2+}-illites This indicated that there was an absence of an electric double layer on the surface of these illites There was some negative adsorption measured for the Ca^{2+}-illite sample corresponding to an exclusion area of 16 m^2 g^{-1}, this compared to a BET(N_2) area of 102 m^2 g^{-1} For the Mg^{2+}-illite sample, positive adsorption of Cl^- ions occurred which was concluded to mask any negative adsorption which may have been occurring

It was found for the Mg^{2+}-, Ca^{2+}- and Ba^{2+}- forms of the montmorillonite sample that the exclusion areas decreased in the order $Ca^{2+} > Mg^{2+} > Ba^{2+}$, see Table 3 6 The difference between the exclusion areas for the Ca^{2+}- and Ba^{2+}-montmorillonite samples was thought to be due to the greater tendency of the less hydrated Ba^{2+} to bind with the clay surface to give uncharged sites The Mg^{2+} had a tendency to hydrolyse and adsorb Cl^- ions, thus giving low negative adsorption values The results for the Al^{3+}-illite and montmorillonite samples indicated that positive and negative adsorption of Cl^- ions was occurring (this was also occurring for the Mg^{2+} forms of these clays), but that negative adsorption only became apparent as it approached a maximum value

Table 3 6 **Comparison of the Specific Surface Areas of Divalent Montmorillonite Measured by Chloride Exclusion (22)**

Exchangeable cation	Surface are (m^2 g^{-1})	
	BET(N_2)	Exclusion area
Mg^{2+}	59	74
Ca^{2+}	40	110
Ba^{2+}	47	64

3 2 1 2 The Surface Area of Soil Organic Matter

(a) Positive Adsorption Methods

The earliest reported measurement of the surface area of SOM was made by Bower and Gschwend (12) in 1952 using the single point ethylene glycol (EG) retention method In this method the liquid EG was mixed with a soil sample, the excess liquid was then removed by placing the sample under vacuum and evaporating it off The amount of EG remaining, which was measured by the weight increase to the sample, was assumed to be adsorbed as a monolayer on the surface In the study of Bower and Gschwend (12) the surface area of SOM was calculated, from the sorption of EG, to be between 558 to 803 $m^2\ g^{-1}$ However, it should be noted that this value was in fact based on the decrease in the surface area of soil samples once they had been treated with H_2O_2 to remove the organic matter Thus, the reported value was not a direct measurement of the surface area of the organic matter of the soils studied This large surface area for SOM was subsequently accepted and propagated in the general literature

As an example of this entrenchment Jurinak and Volman (28) estimated the surface area of several mineral soil samples using ethylene dibromide (EDB) as the probe The surface areas measured were compared to the internal and external surface areas measured using EG, see Table 3 7 (It was not stated how it was possible to use EG to measure both the internal and external surfaces of the soils)

Table 3.7 Comparison of Surface Areas Measured by EDB and EG Retention (28)

Soil	BET(EDB) area ($m^2\ g^{-1}$)	EG retention ($m^2\ g^{-1}$)	
		External area	Total area
Yolo silt clay[a]	35 9	47	200
Yolo loam[a]	18 7	21	97
Salmas clay[a]	23 9	35	145
Meloland clay loam[a]	26 3	28	103
Hanford sandy loam[b]	3 69	5 2	22
Aiken clay loam[c]	26 9	46	93
Staten peat muck[c]	11 7	20	264

Note ([a]) montmorillonite predominates ([b]) illite ([c]) kaolin

Jurinak and Volman (28) concluded from Table 3 7 that EDB was restricted to adsorption onto the external surface of the clay soils since it gave small surface area values However, for the Staten peak muck (35 % organic matter) it was assumed that the low surface area was due to the inability of EDB to gain access to the large internal surfaces of the organic matter This was due to the large size of the EDB molecule which prevented it from gaining access to the smaller capillaries This last statement clearly demonstrates the bias in favour for an external/internal surface area model for SOM which existed in the literature at the time

However, in 1979 Poost and McKay (15) reported measurement of the surface area of peat moss and wood materials using several different techniques The methods employed were mercury porosimetry, N_2-adsorption using the BET equation, and the adsorption of the dyes Telon blue and Methylene blue from dilute aqueous solutions using the Langmuir equation to calculate monolayer converge of the peat surface The surface areas determined by each of these methods are given in Table 3 8

Table 3 8 The Surface Area of Peat Moss by Various Techniques (15)

Particle size (μm)	Surface area (m^2 g^{-1})			
	Mercury porosimeter	Methylene blue	Telon blue	N_2
150-250	2 62	122 2	11 8	27 3
250-355	2 52	113 6	8 7	26 6
355-500	2 47	104 0	7 8	26 6
500-710	2 40	88 9	6 7	26 5
710-1000	2 33	77 5	5 2	26 5

The areas measured by mercury porosimetry were found to be about ten times smaller than the values measured by N_2-adsorption It was suggested that this discrepancy was due to either (i) the immobility of the adsorbed mercury atoms on the surface of the peat and/ or (ii) the larger atomic diameter of mercury compared to the diameter of the N_2 molecule which restricted the mercury atoms from penetrating the microporous structure of the peat

For adsorption of the dyes it was found that telon blue gave smaller surface area values compared to N_2 adsorption This was thought to be due to the repulsion of the negatively charged dye molecule by the negatively charged peat surface Conversely, the very large surface areas measured from methylene blue adsorption

was due to a strong chemical interaction between the positively charged dye molecule and the negatively charged peat surface

Poost and McKay (15) concluded that the use of N_2 gave the most realistic measurement of the surface area available for physical adsorption by the peat The large apparent surface areas obtained from methylene blue adsorption were considered to be due to a combination of chemisorption and stacking of the dye molecules on the surface of the peat

Chiou and co-workers (14) determined the surface area of four organic soils by N_2-adsorption using the BET method The organic soils used were a Florida peat, a Houghton muck, a purified soil humic acid in the freeze-dried form, and an oven-dried humic acid which was extracted from an alkaline solution of the freeze-dried humic acid The results of the measurement of the organic soils are given in Table 3 9

Table 3.9 Surface Areas of Various Organic Soils (14)

Organic soil[a]	OM (%)[b]	Surface area (m^2 g^{-1})
Florida peat	86 4	0 61
Houghton muck	91 9	0 73
Freeze-dried humic acid	98 9	18 0
Oven-dried humic acid	98 9	0 71

Note ([a]) All organic soil materials were out-gassed under vacuum at 105°C for 6 h, before N_2-adsorption ([b]) OM organic matter content

Chiou *et al* (14) noted that all the values were below 1 m^2 g^{-1}, except for the freeze-dried sample The relatively large value of 18 m^2 g^{-1} for the freeze-dried sample was considered to be an artefact of the drying process Chiou *et al* (14) concluded that the discrepancy between the surface areas measured by N_2-adsorption and the EG method was due to confusion between what they termed the 'free surface area' of SOM and its 'apparent surface area'

(i) the free surface area as defined by Chiou *et al* (14) consists of the solid-vacuum interfacial area of a solid This surface area existed before adsorption occurred and its measurement does not involve any structural changes to the adsorbent The free surface area can only be determined by the use of a weakly interacting probe such as N_2 and its measurement is based on the following assumptions

- only physical adsorption is involved,
- the surface area is not changed by the adsorption of the probe,
- it does not involve the dissolution of the adsorbate into the solid

(ii) on the other hand, the apparent surface area (which according to Chiou and co-workers does not in fact exist for SOM, since it is based on the erroneous assumption that the probe used is confined to the surface of the material) is the area measured by the uptake of an 'adsorbate' which either changes the structure of the solid, or dissolves into it, or both Probes which alter the adsorbent structure include such polar molecules as EG and H_2O Under this definition of apparent surface area are the surfaces measured for the expandable clays, which Chiou *et al* (14) argue are the result of alterations to the clay structure due to the adsorption of the polar molecules which swell the structures Whereas, the weakly interacting N_2 molecule does not cause swelling of the expandable clays, and thus gives a measure of the true surface area Chiou *et al* (14) considered that if such internal surfaces did exist for soil constituents then it would be logical that they would be accessible to small molecules such as N_2 Therefore, they conclude that the apparent surface area is not a well defined quantity, because it does not refer to the surface area of the SOM before the measurement is carried out

Pennell and Rao (13) have criticised Chiou and co-worker's (14) method of determining the surface area of SOM and their conclusions They insist that SOM does contain internal surfaces and that the measurement of these surfaces is an operationally defined process, i e it is dependent on both the experimental conditions used and the nature of the probe Pennell and Rao (13) argue that it is not possible to directly compare the surface area of SOM measured for organic soils by the N_2/BET method used by Chiou *et al* (14) to the values derived from soils with relatively low organic matter contents using EG/H_2O_2 (i e the method used by Bower and Gschwend (12) They suggest that H_2O_2 treatment may alter the composition of soil components and they doubt the equivalence of EG molecular coverage on SOM compared to its coverage on mineral surfaces They quote the example of Whittlesey Black Fen soil (see Table 3 10) which when it was treated in the same manner as described by Bower and Gschwend (12) indicated that SOM has a surface area of 92 m^2 g^{-1} However, treatment of Whittlesey Black Fen with H_2O_2 caused a reduction in EG calculated surface area (99 0 m^2 g^{-1} before treatment, 71 0 m^2 g^{-1} after treatment) but an increase in the N_2/BET measured surface area (12 7 m^2 g^{-1}

Table 3.10 **Comparison of the Surface Area of Various Soils and Clay Minerals Determined by the BET And EG Retention (13)**

Soil	OM[a] (%)	BET surface area ($m^2 g^{-1}$)			EG surface area ($m^2 g^{-1}$)
		N_2	EDB[b]	H_2O	
Whittlesey Black Fen	16 43	12 7	17 5	126 0	99 0
Whittlesey Black Fen/H_2O_2[c]	0 29	71 0	50 5	80 0	71 0
Ashurst Garden	4 55	6 3	4 6	29 6	45 8
Ashurst Field	2 41	1 9	3 3	18 9	25 8
Boston silt	2 66	28 6	23 2	46 6	46 0
Wyoming bentonite	nd	65 0	61 0	382 0	372 0

Note [a] Organic matter [b] Ethylene dibromide [c] treated with H_2O_2 to remove organic matter from the soil

before, 71 0 $m^2 g^{-1}$ after treatment) Thus, they conclude that mineral surfaces have a greater capacity than SOM to adsorb non-polar N_2 molecules

Pennell and Rao (13) argued that there is a considerable body of evidence to indicate that non-polar organic vapours adsorb onto the surface of anhydrous SOM in much the same manner as N_2, and that the organic vapours do not partition into the SOM as suggested by Chiou and co-workers (14) They present data which demonstrates that the surface areas measured from the retention of non-polar organic vapours (ethylene dibromide, p-xylene, toluene) on soil samples give similar values to those calculated from the adsorption of N_2, see Table 3 10 and Table 3 11, whereas, the more polar molecules (H_2O, EG and EGME) yield larger surface area values because of their ability to penetrate into the interior of SOM and minerals Pennell and Rao (13) were of the opinion that it is not necessarily the size of the adsorbate, but the magnitude of the adsorbate-adsorbent interactions (which are strongly correlated with adsorbate polarity) that dictates the degree to which an adsorbate explores the internal surfaces of a dry adsorbent

In conclusion Pennell and Rao (13) proposed that SOM consists of a "three-dimensional system, in which a multi-polymer phase exists in a semi-structured framework", which contains hydrophobic moieties and polar functional groups The organic material is kept together by a number of weak intermolecular forces such as hydrogen-bonding, hydrophobic interactions and π-bonding According to their model, under anhydrous conditions the polar functional groups are oriented to the

Table 3.11 **Comparison of the Surface Area of Soils and Clay Minerals Determined by the BET and EGME Retention Methods (13)**

Soil	OC[a] (%)	BET surface area ($m^2 g^{-1}$)				EGME surface area ($m^2 g^{-1}$)
		N_2	p-xylene	toluene	H_2O	
Webster soil	3 02	4 2	-	5	69	101 0
Oldsmar soil	1 09	0 2	-	-	8	3 8
Bentonite	0 48	14 4	17	16	-	690 0
Kaolinite	0 07	13 6	10	9	15	30 9
Lula aquafier	0 01	7 7	4	-	10	10 5

Note [a] Organic carbon content

interior of the SOM and as a result its surface becomes hydrophobic As a result, weakly interacting adsorbates such as N_2 and non-polar organic vapours are restricted to condensing onto the external surface of the SOM Thus, the use of such probes will only give measurement of the external surface area of SOM They argue that the surface area of 18 $m^2 g^{-1}$ for the freeze-dried organic matter sample measured by Chiou *et al* (14) is the most likely value for the external surface since they consider freeze-drying of the humic acid materials to maintain the intricate structural network In contrast, polar molecules are able to interact with the SOM and gain access to the internal surfaces and consequently these molecules measure the total surface area Under water saturated conditions the multi-polymer phase behaves as a conventional partitioning medium for non-ionic organic compounds

In answer to Pennell and Rao's criticism (13), Chiou *et al* (29) have reaffirmed their model of SOM as a partitioning medium for organic sorbates They argue that their definition of what constitutes the surface area of a material (i e the free surface area) is the only valid definition The surface area measurements given by Pennell and Rao (13) in Tables 3 10 and 3 11 are dismissed by Chiou *et al* (29), since they argue that the organic matter content of the soils studied was small and that the mineral fraction of the soil dominated the sorption process Chiou *et al* (29) point out that there would be little difference between the surface areas measured by N_2 or the organic vapours of low polarity for soils of low organic matter content

More recently Chiou *et al* (19) have reported on the sorption of N_2 and EGME vapour on several soils and soil components using the BET method The objective was to examine if EGME was an appropriate probe for the determination of the surface areas of soil components It was expected that both probes would yield

similar surfaces areas on samples that did not exhibit bulk penetration by EGME, and, that for soils which contained a significant organic matter content or for expanding/solvating minerals, there should exist a significant difference between the N_2 and EGME derived measurements

The results, which are presented in Table 3 12, consisted of $Q_m(N_2)$ the amount of N_2 required for monolayer coverage of the sorbent from which the surface area of the materials was calculated, Q_m(EGME)eq the equivalent amount of EGME required for monolayer coverage of the sorbent which was calculated from the $Q_m(N_2)$ value, and the experimentally derived Q_m(EGME)ap value which is the apparent amount of EGME giving monolayer coverage of the sorbents This latter value was referred to as the apparent monolayer coverage value because bulk penetration or site specific interactions with the EGME were considered to be occurring for some of the sorbent materials studied

The results presented in Table 3 12 for the surface area measurements could be divided into two broad groups

(i) those sorbates which were relatively free of organic matter and swelling /solvating minerals, the Ottawa sand, hematite, aluminium oxide, kaolinite, and synthetic hydrous iron oxide The surface areas measured by BET(N_2) varied from 0 11 $m^2\ g^{-1}$ for sand to 186 $m^2\ g^{-1}$ for the synthetic hydrous iron oxide As expected there was a close agreement between the surface areas measured by $Q_m(N_2)$ and those obtained by Q_m(EGME)ap, since the ratio of (EGME)ap/(EGME)eq for these materials (Table 3 12) were all approximately equal to 1 The similarity of the results was due to the fact that EGME did not exhibit bulk penetration in these materials

(ii) the remaining materials, Woodburn soil, natural hydrous iron oxide, illite, Ca-montmorillonite and peat, the $Q_m(N_2)$ surface areas of which varied from 1 26 $m^2\ g^{-1}$ for peat to 75 9 $m^2\ g^{-1}$ for Ca-montmorillonite For these samples the Qm(EGME)ap value for EGME monolayer coverage was found to over estimate the Q_m(EGME)eq value The (EGME)ap/(EGME)eq values were found to range from 1 85 for the natural hydrous iron oxide to 7 6 for the Ca-montmorillonite sample The discrepancy between the two EGME values was considered to be a result of the structural swelling (or due to partitioning in the case of the peat sample) which occurred in these materials due to solvation of cations by EGME As a consequence Chiou *et al* (19) considered that it was incorrect to use the Q_m(EGME)ap value to estimate the surface area of these materials

Table 3.12

A Comparison of the Q_m (N_2) Monolayer Capacities, BET (N_2) Surface Areas, Q_m (EGME)eq Equivalent Monolayer Capacities, and Q_m (EGME)ap Apparent Monolayer Capacities of Various Soils and Minerals (19)

Bulk penetration	Adsorbent	Q_m (N_2) (mg g^{-1})	BET N_2 area (m^2 g^{-1})	Q_m(EGME)eq (mg g^{-1})	Q_m(EGME)ap (mg g^{-1})	Q_m(EGME)ap/ Q_m(EGME)eq
absent	Ottawa sand	0 032	0 11	0 042	0 035	0 83
	Hematite	0 14	0 50	0 18	0 18	1 00
	Aluminium oxide	0 87	3 03	1 13	1 02	0 90
	Kaolinite	6 03	21 0	7 84	7 90	1 01
	Synthetic anhydrous iron oxide	53 4	186	69 4	61 2	0 88
present	Peat	0 36	1 26	0 47	-	-
	Woodburn soil	3 22	11 2	4 19	13 4	3 20
	Natural hydrous iron oxide	3 31	11 5	4 30	7 98	1 86
	Illite	19 3	67 2	25 1	38 0	1 51
	Ca-montmorillonite	21 8	75 9	28 3	215	7 60

The $Q_m(N_2)$ values are from N_2 adsorption isotherms and the BET equation, $Q_m(N_2)$ values are used to determine the surface areas of samples, Q_m(EGME)eq are values equivalent to $Q_m(N_2)$ for the same surface areas of samples, Q_m(EGME)ap values are from the EGME sorption isotherms and the BET equation, assuming that no penetration or specific interaction occurs The ratio of Q_m (EGME)ap to Q_m (EGME)eq, when significantly greater than 1, expresses the extent of EGME penetration or specific interaction

Concerning the peat sample, the N_2 isotherm was observed to correspond to the Brunauer Type II adsorption isotherm (see Figure 3 7), while the EGME isotherm was found to be linear, suggesting that partition was occurring in this case The limiting capacity (i e the maximum solubility) of EGME was determined by extrapolation of the linear isotherm to $P/P_0 = 1$ The limiting sorption capacity was calculated to be 190 mg g^{-1} (normalised for the organic content of the peat), which was similar to the value of 150 to 250 mg g^{-1} for EG retention by SOM reported by Bower and Gschwend (12) However, since the EGME isotherm was linear for the peat, Chiou *et al* (19) concluded that the BET equation could not be applied and that there was no theoretical basis for calculating Q_m(EGME)ap In addition, they calculated the extent to which the organic matter content in a soil sample would introduce errors into the determination of the surface areas by EGME retention For a sample containing 1 % SOM the error would be 5 m^2 g^{-1} if the measurement is taken near the saturation pressure, and reduces to 0 3 to 0 5 m^2 g^{-1} for $P/P_0 = 0$ 05 to 0 1 It is concluded that the error in surface area measurement introduced due to SOM content would be much greater than that caused by expanding clay content because of the difference in shape between the two EGME isotherms for the two materials

Concerning the solvation of EGME by solvating clays, minerals and organic matter, Chiou *et al* (19) suggest that a useful analytical procedure which should be carried out is as follows,

- determination of sorption isotherms for EGME and N_2 on the sample,
- determination of the ash and organic matter content of the sample,
- subtraction from the total EGME isotherm the portion of the EGME isotherm corresponding to surface coverage This is obtained by multiplying $Q_m(N_2)$ by the factor 1 3, which accounts for the difference in the molecular weight and areas of the EGME and N_2 molecules, assuming there is equal surface coverage,
- subtracting from the resultant curve the linear isotherm calculated for the organic content of the sample (based on EGME solubility in peat) if it is significant

The results should be an isotherm that reflects the effect of cation solvation by EGME on the sample These calculations have been carried out for Woodburn soil in Figure 3 8 Chiou *et al* (19) concluded that the sorption of neutral and relatively non-polar organic vapours do not exhibit significant penetration into expanding clay or partition into SOM, and they present a selection of results to prove their statement However, similar agreements would not be expected for soils containing a high-organic matter content because there would be significant partitioning of the organic sorbents into the organic matter The continued use of

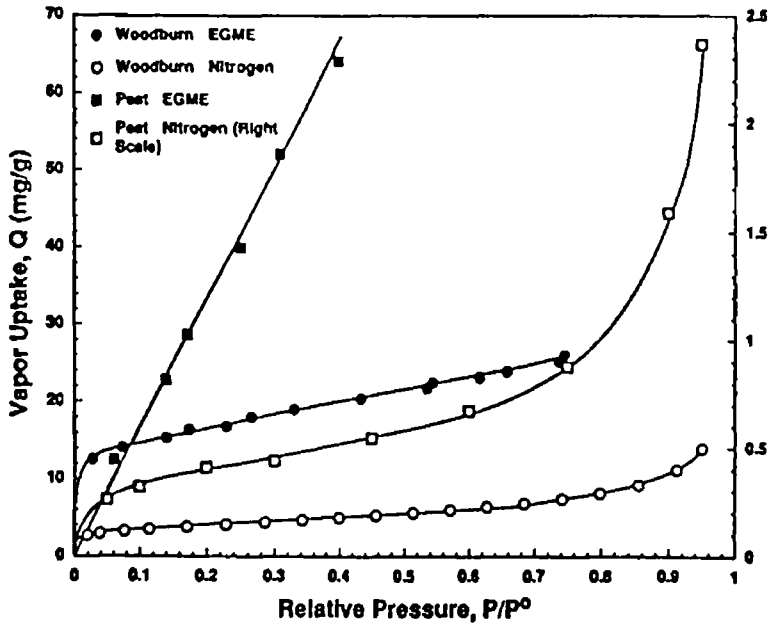

Figure 3 7 Isotherms for EGME and N_2 Sorption on Peat and Woodburn Soils (19)

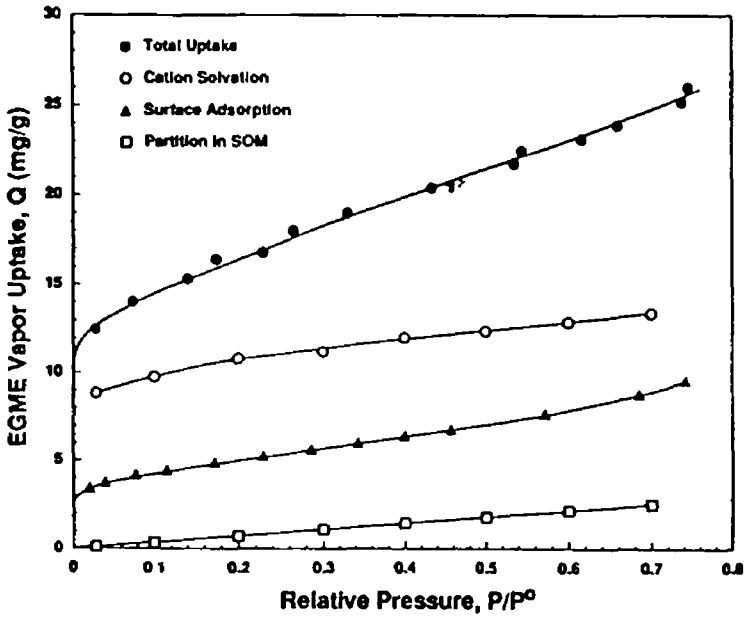

Figure 3 8 Isotherms for the Uptake of EGME on Woodburn Soil by Cation Solvation, Surface Adsorption and Partition into SOM (19)

polar molecules, such as EGME, for surface area determination of soil constituents is strongly criticised by Chiou *et al* (19)

This is particularly so when expandable clays and/or SOM are present From the results which they present, they consider that it is clearly evident that excess EGME sorption by SOM was due to dissolution of EGME into the organic matter Also, that excess EGME sorption by clays is related to cation solvation and is affected by the type of cation and solvent

(b) Negative Adsorption Methods

There is no reported application of the exclusion volume method for the measurement of the surface area of soil organic matter However, interestingly enough Schofield (23) measured the exclusion surface area of jute fibre which is an organic fibrous material of plant origin The surface area of jute fibre was reported to be about 160 $m^2 g^{-1}$, a value which was reported to be about a thousand times the external surface area of the jute (a value for the external surface area was not given nor was the surface area measured by any other method) It is unfortunate that Schofield (23) did not give further information on the jute fibre measurements since the reference to internal and external surfaces is of immediate relevance to the preceding discussion on surface area of soil organic matter

3 3 Sorption of Non-Ionic Organic Compounds by Soil

The sorption of the non-ionic class of organic compounds is reviewed in this section Sections 3 3 1 and 3 3 2 are concerned with the sorption of organic compounds from the aqueous and non-aqueous phases respectively, while Section 3 3 3 deals with the sorption of the organic compounds from the vapour phase and the influence of the soil's humidity on the sorption process The emphasis of this review is on the role of soil organic matter in the sorption process However, reference is also made to sorption by the mineral fraction of soil since early investigators generally considered soil to be a single sorbent material which had a single sorption (adsorption) mechanism

3.3.1 Sorption from the Aqueous Phase

Most of the early investigative work on the sorption process dealt with sorption from the aqueous phase As has been previously mentioned, research

concentrated on the fate of pesticides in the soil One of the most important observations made by early investigators was that the amount of organic solute taken up by the soil was found to generally increase with increasing organic matter content of the soil (30-35) However, these early studies on the sorption of organic compounds by SOM assumed that adsorption onto the SOM surface was the principal mechanism of uptake This assumption was based principally on the large surface area of c 560 to 800 m^2 g^{-1} for SOM that was reported by Bower and Gschwend (12) Thus, it was postulated that SOM acted as a high surface area adsorbent, in other words in much the same manner as the mineral fraction of the soil However, recently Chiou and co-workers (36-38) have argued that soil should not be viewed as a single, uniform sorbent material, but rather as a dual sorbent material, in which the mineral fraction acts as a conventional high surface area adsorbent, and the SOM fraction acts as a partitioning medium for sorbed organic compounds (i e the organic compounds dissolve into the soil organic phase) The following observations made from the work of early investigators and from their own investigations (which are discussed in the following text) have been cited by Chiou and co-workers as evidence which supports a partition model for the retention of non-ionic organic compounds in SOM,

(i) the observed sorption isotherms for the retention of organic compounds by SOM are linear to high relative concentrations of the organic compounds in the liquid and vapours phases,

(ii) the low values for the heats of sorption which have been measured for the sorption of organic compounds from the liquid and vapour phases are incompatible with an adsorption only mechanism,

(iii) the lack of competitive effects for the uptake of binary solutes by SOM from aqueous solution This is unlike adsorption where a finite surface area is available for the uptake of organic compounds In such a situation, competition between organic solutes would be expected to occur if adsorption was the principal mechanism of sorption,

(iv) the sorption capacity of SOM for organic compounds shows a marginal decrease with increasing humidity This is in sharp contrast to the case for mineral surfaces which show a very large decrease (> 90 % in most cases) in their sorption capacity for organic compounds with increasing humidity,

(v) the compatibility of the sorption data for SOM with a model for solute solubility in organic (amorphous) polymers,

(vi) the small surface areas of SOM as determined by the BET (N_2) method (see Section 3 2 1 2) The amount of organic compounds retained by SOM are too large if adsorption is assumed to be the mechanism of sorption since there is not enough surface area available to accommodate the sorbate

In 1979 Chiou and co-workers (36) initially suggested that the sorption of non-ionic organic compounds from aqueous solution is due primarily to solute partitioning into SOM They presented results for the sorption of a series of organic compounds (tetrachloroethene, 1,2-dichlorobenzene, 1,1,1-trichloroethane, 1,1,2,2-tetrachloroethane, 1,2-dibromoethane, 1,2-dichloropropane and 1,2-dichloroethane) by Willamette silt loam (1 6 % organic matter, 26 % clay, 3 3 % sand, 69 % silt) which they claimed supported their model The results of their study are presented in Figure 3 9

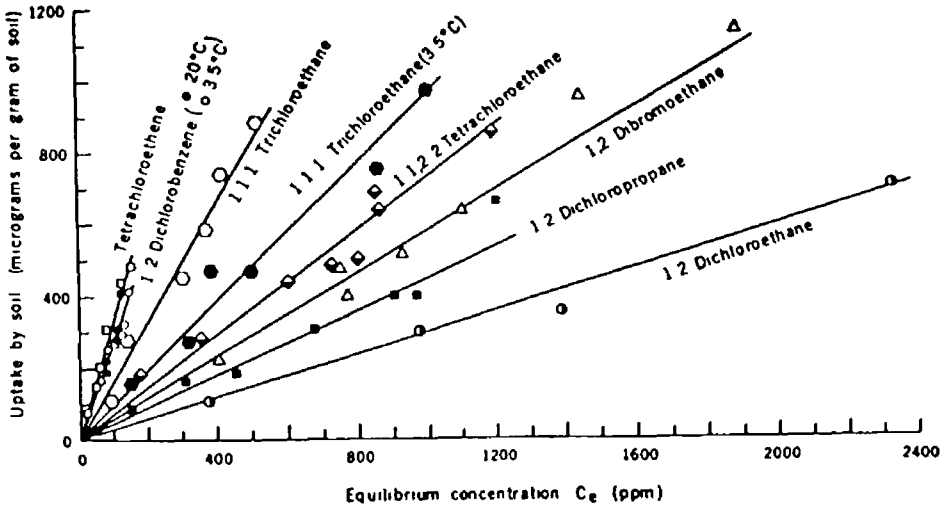

Figure 3 9 Sorption Isotherms for Various Organic Compounds by Willamette Silt Loam (36) Note the figure shows the amount of organic solute retained by the soil versus the equilibrium concentration of the organic solute in aqueous solution at 20°C

From their results, Chiou *et al* (36) made the following observations which they claimed supported the model of SOM as a partitioning medium

(i) the sorption isotherms were found to be linear with no indication of curvature even at concentrations which approached solute saturation of the aqueous solution This was particularly apparent in the case of tetrachloroethene and

1,2-dichlorobenzene which were examined at concentrations approaching 75 to 95 % of their maximum solubility values in water, see Figure 3 9,

(ii) that the K values, the calculated soil-water partition coefficient (termed G in the study) for the organic compounds, as determined from the slope of the isotherms (see Table 3 13), were found to be inversely proportional to their water solubilities (S) This inverse relationship can be more clearly seen in Figure 3 10 which shows a linear relationship between log K versus log S for the organic compounds studied by Chiou *et al* (36) (also included are values taken from other studies, these are referenced in [36])

(iii) the observed low enthalpies for solute uptake Chiou *et al* (36) note that the molar heat of transfer (ΔH) of an organic solute from the aqueous phase to the organic phase by partitioning is related by the following equation

$$\Delta H = \Delta H_o - \Delta H_w \qquad \text{Equation 3 14}$$

where ΔH_o and ΔH_w are the molar heats of solution in the organic phase (in this case SOM) and water phase respectively, both of which are usually positive Since Chiou *et al* (36) note that ΔH_w is usually large for compounds of low water solubility, the corresponding ΔH_o should be much smaller because of the greater solubility of the organics in the SOM phase According to Equation 3 14 the heat of partition of an organic solute should be relatively small and less exothermic than its heat of adsorption from the aqueous phase Thus, Chiou *et al* (36) stated that for 1,2-dichlorobenzene the ΔH value was practically zero and for 1,1,1-trichloroethane it was found to be positive (values not given) Such low values for the sorption of the organic compounds were in keeping with a partition mechanism

Chiou and co-workers (38) developed the partition model further by viewing SOM as composed mainly of amorphous polymeric structures (see Chapter 1) From this assumption the relationship between the partition coefficient, K, and the water solubility for a slightly water-soluble organic solute in an organic solvent-water mixture (in which the solvent has a small solubility in the water phase) could be described by the following equation,

$$\log K = - \log S - \log V_o^* - \log \gamma_o^* + \log (\gamma_w^* / \gamma_w) \qquad \text{Equation 3 15}$$

where K is the solute partition coefficient (i e the ratio of the solute concentration in the organic phase to that in water), S is the molar water solubility of the solute at the

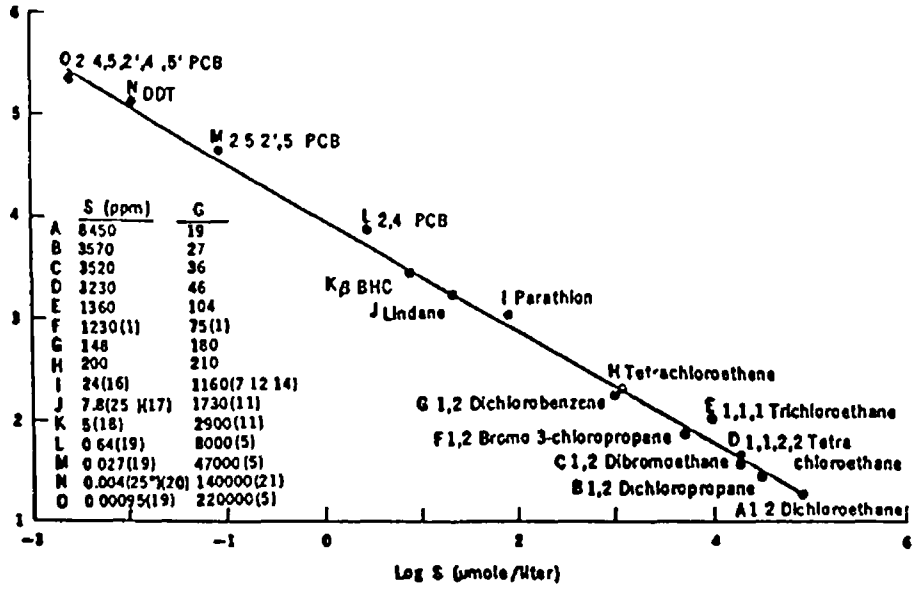

Figure 3.10 **Soil-Water Partition Coefficients (K) of Various Organic Compounds Versus Their Water Solubilities (S) (36)**

Table 3.13 **The Soil-Water Partition Coefficient (K) and the Water Solubility of Various Organic Compounds (36)**

Sorbate	Water solubility, S (ppm)	Partition coefficient, K (-)
1,2-Dichloroethane	8450	19
1,2-Dichloropropane	3570	27
1,2-Dibromoethane	3520	36
1,1,2,2-Tetrachloroethane	3230	46
1,1,1-Tetrachloroethane	11360	104
1,2-Bromo-3-chloropropane[a]	1230	75
1,2-Dichlorobenzene	148	180
Tetrachloroethene	200	210
Parathion[a]	24	1160
Lindane[a]	7 8	1730
β-BHC[a]	5	2900
2,4'-PCB[a]	0 64	8000
2,5,2',5'-PCB[a]	0 027	47000
DDT[a]	0 004	140000
2,4,5,2',4',5'-PCB[a]	0 00095	220000

Note [a] The values for these compounds are taken from the literature, these are referenced in Chiou *et al* (36), PCB = polychlorinated biphenyl

system temperature (mol dm^{-3}), V_o^* is the molar volume of water-saturated organic phase (dm^{-3} mol^{-1}), γ_o^* is the solute activity coefficient in water-saturated solvent phase, γ_w is the solute activity coefficient in water, and γ_w^* is the solute activity coefficient in solvent-saturated water From Equation 3 15 an 'ideal line' for the partitioning of a solute between an organic solvent (such as octanol) and water has the form,

$$\log K^o = - \log S - \log V_o^* \qquad \text{Equation 3 16}$$

where K^o represents the partition coefficient when the solute forms an ideal solution in the water-saturated solvent phase, and where the organic solute's solubility in water is not affected by the solvent dissolved in the aqueous phase However, Equation 3 15 must be corrected to take into account the effects of the size disparity which exists between the solute and the solvent for the partitioning of the solute into a macro-molecular organic phase (i e the SOM) The corrected equation which was developed by Chiou *et al* (38) has the form

$$\log K_{om} = - \log SV - \log \rho - (1 + \chi)/2\ 303 \qquad \text{Equation 3 17}$$

where K_{om} is the solute partition coefficient between SOM and water, V is the molar volume of the solute (dm^3 mol^{-1}) The density of the organic phase, ρ, was introduced to express the concentration of the solute in the organic phase on a mass-to-mass basis (because the volume of the amorphous material is often more difficult to determine) The interaction parameter, χ (dimensionless), is the sum of the excess enthalpic (χ_h) and entropic (χ_s) contributions to the incompatibility of the solute in the macromolecular organic phase From Equation 3 17 the hypothetical 'ideal line' can be derived, which assumes that there is negligible heats of interaction (i e $\chi = \chi_s$),

$$\log K^o_{om} = - \log SV - \log \rho - (1 + \chi_s)/2\ 303 \qquad \text{Equation 3 18}$$

where the o superscript of K^o_{om} indicates that the equation assumes that $\chi = \chi_s$, where χ_s is assigned a value of 0 25 for high molecular weight polymers, and ρ is taken to have a value of 1 2 (which is derived from comparison with values for similar polymeric materials) It follows from the use of Equation 3 18 as the 'ideal line' for the partition of an organic solute into SOM and the experimentally derived data of log K^o_{om}, that the incompatibility of the solute with the (water saturated) SOM can be determined by the following relationship

$$(\chi - \chi_s)/2\ 303 = \log (K^o_{om}/ K_{om}) \qquad \text{Equation 3 19}$$

Thus, if $(\chi - \chi_s)/2.303$ is small (i.e. solute incompatibility with the SOM is low) when compared to log SV for a group of organic solutes then the relationship between log K_{om} and log SV should be linear.

Using the above relationships, Chiou *et al* (38) proceeded to study the sorption of 12 aromatic compounds (benzene, chlorinated benzene derivatives and polychlorinated biphenyls [PCBs]) on a Woodburn soil. The aim was to examine the factors effecting K_{om} for the sorption of the organic compounds partitioning into SOM. The relationships of log K_{om} versus log SV, log K_{om} versus log S (the relationship of K_{om} to water solubility of the solute) and log K_{om} versus log K_{ow} (the relationship between K_{om} and the n-octanol-water partition coefficient) were examined. The Kom values shown in Table 3.14 were obtained from the slopes of the sorption isotherms for the uptake of the organic solutes divided by the organic matter content of the soil (i.e. the om subscript indicates that the partition coefficient has been normalised for organic matter content).

Table 3.14 Log K_{om} Values for the Partition of 12 Organic Compounds in Woodburn Soil (38)

Sorbate	K_{om}[a]	Sorbate	K_{om}[a]
Benzene	39.8	1,4-Dichlorobenzene	158.5
Anisole	19.9	1,2,4-Trichlorobenzene	501.2
Chlorobenzene	47.9	2-PCB	1698.2
Ethylbenzene	95.5	2,2'-PCB	4786.3
1,2-Dichlorobenzene	186.2	2,4'-PCB	7762.5
1,3-Dichlorobenzene	169.8	2,4,4'-PCB	23988.3

Note: [a] The K_{om} values are converted from the log K_{om} values given by Chiou *et al* (37).

It was found that a plot of log K_{om} versus log SV gave a straight line which was below the 'ideal line' indicating that SOM is an inferior partitioning medium when compared to organic solvents such as n-octanol, see Figure 3.11. This finding was considered to be reasonable since in general SOM is more polar (due to the presence of oxygen) than organic solvents such as n-octanol. The results of the study indicated that the extent of water insolubility is the primary factor effecting K_{om}. The effect of solute incompatibility with SOM is significant but a secondary factor.

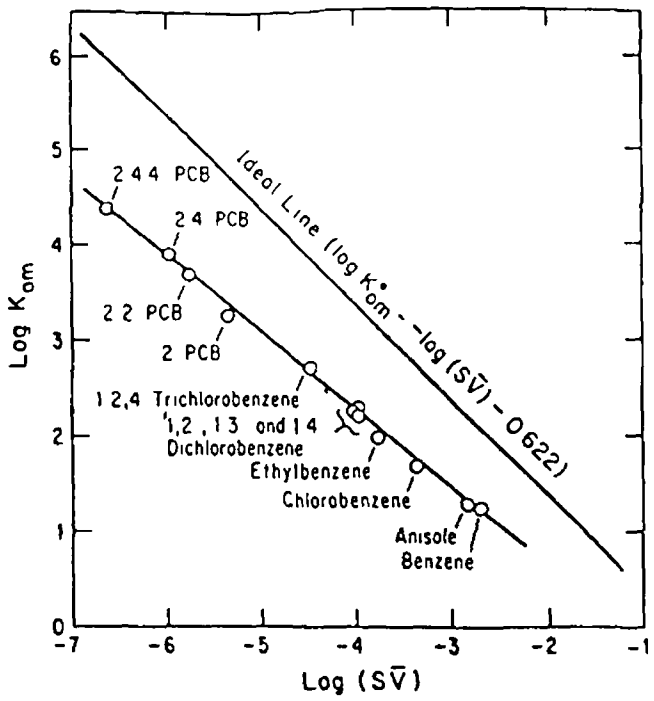

Figure 3.11 **Plot of Experimentally Derived Log K_{om} Values Versus Log SV Values For Various Organic Compound In Comparison with the Ideal Line for SOM-Water System (38)** Note The 'ideal line' log K_{om} = -log SV - 0 622 which is shown in the figure is derived from allowing χ_S = 0 25 and ρ = 1 2

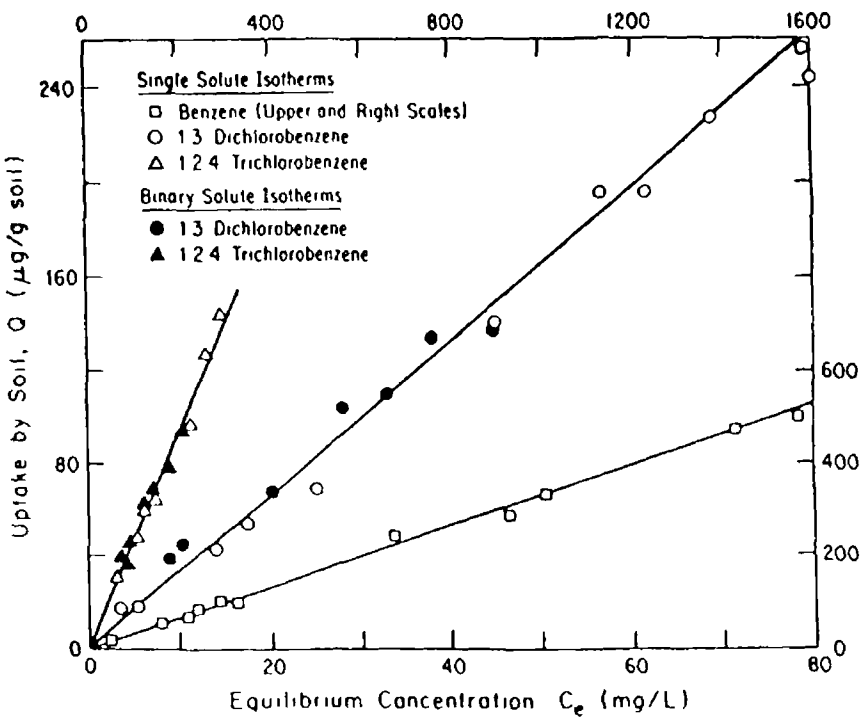

Figure 3 12 **Sorption Isotherms for the Uptake of Single-Solute and Binary-Solutes by Woodburn Soil (38)**

Chiou *et al* (38) also examined the effects of competitive sorption by soil Sorption isotherms for the uptake of single and binary solute mixtures of 1,3-dichlorobenzene and 1,2,4-trichlorobenzene were examined The results which are shown in Figure 3 12 clearly show that the uptake of the single and binary solute systems gave near identical isotherms This indicated that direct competition between organic compounds for sorption sites was minimal, i e uptake of the organic solutes was largely by partitioning Chiou *et al* (38) argued that such a lack of competition between organic compounds strongly supported the partition mechanism In the case of adsorption direct competition between binary mixtures of organic compounds should have been observed, since there is only a finite number of sites available for adsorbing molecules

Rutherford *et al* (39) examined the influence of SOM polarity on the partition coefficient (K_{om}) for the sorption of organic solutes They studied the sorption of benzene and carbon tetrachloride on three organic soils, namely a muck (81 5 % organic matter content), a peat (86 4 %) and a peat extract (85 %), and on cellulose (100 %) These organic materials were chosen for the variation in their polarity (as expressed by the ratio of O + N to C) which was about 1 1 for cellulose (the most polar), 0 8 for muck, 0 7 for peat and 0 5 for extracted peat (the least polar) It was initially observed that the sorption isotherms for the two organic solutes were linear on all materials examined which was in keeping with the partition model for SOM, see Figure 3 13

From the results shown in Figure 3 13 it was noted that K_{om} and the limiting (i e maximum) partition capacity (Q^o_{om}) for benzene and carbon tetrachloride increased with decreasing polarity of the four organic materials, see Table 3 15 (The superscript o indicates that the Q^o_{om} values were calculated by extrapolation of the sorption isotherm to the saturation point, i e where $P/P_o = 1$ for gas phase or $C_e/C_w = 1$ for liquid phase) It can be seen that the sorption capacity of the four sorbents decreased in the order extracted peat > peat > muck > cellulose, which correlated with increasing polarity of the organic materials This indicated a strong dependence of Kom on the polarity of the organic matter sample Overall it was found that there was an increase in the Kom value of both organic solutes by a factor of c 40 on going from the highly polar cellulose to the relatively non-polar extracted peat sample

(a)

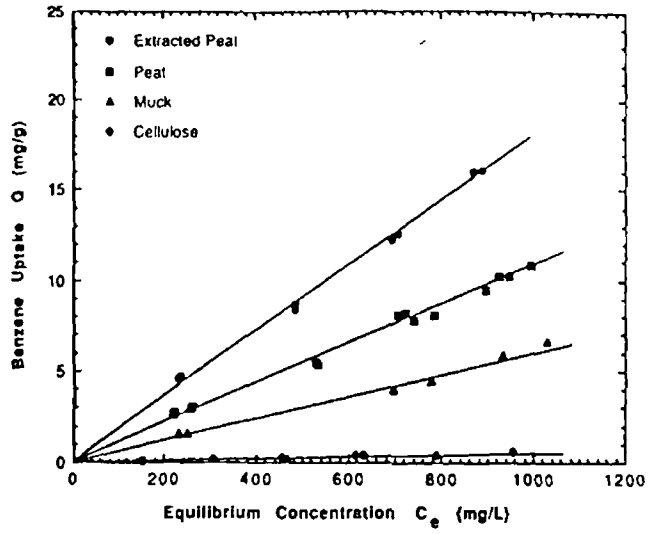

(b)

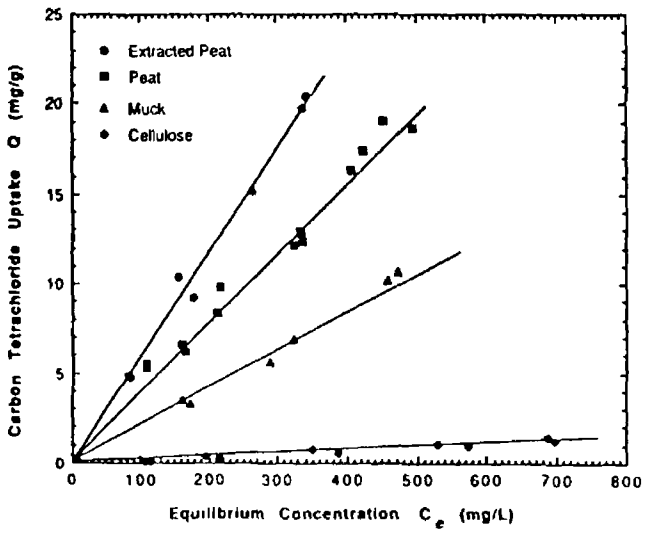

Figure 3 13 **Sorption Isotherms for the Uptake of (a) Benzene and (b) Carbon Tetrachloride on Various Organic Matter Materials (39)**

Table 3 15 **Sorption coefficient (K_{om}) and Limiting Sorption Capacity (Q^o_{om}) of Benzene and Carbon Tetrachloride for Various Sorbents (39)**

Sorbent material	Benzene			Carbon tetrachloride		
	K_{om} (-)	Q^o_{om} (mg g^{-1})	Q^o_{om} (cm^3 Kg^{-1})	K_{om} (-)	Q^o_{om} (mg g^{-1})	Q^o_{om} (cm^3 Kg^{-1})
Extracted peat	20 8	37 1	42 2	73 5	58 8	36 9
Peat	12 5	22 0	25 1	44 6	35 6	22 3
Muck	7 67	13 7	15 5	27 8	22 2	13 9
Cellulose	0 56	1 00	1 13	1 75	1 40	0 88

The influence of the polarity of the organic matter on K_{om} can be more clearly seen in Figure 3 14 which shows K_{om} versus the polarity of the organic matter (as expressed by the O + N to C ratio) It can be seen that the value of K_{om} increases rapidly with decreasing polarity of the sorbent material In other words, as the sorbent decreases in polarity it becomes increasingly better as a non-polar environment for organic compounds of limited water solubility to escape into The results of Figure 3 14 provide a useful basis for assessing the variation in K_{om} values which have been recorded for the same organic compound in different SOM materials In particular the K_{om} values observed for cellulose appear to be the lower limit for a given solute partitioning into SOM because of its high polar content

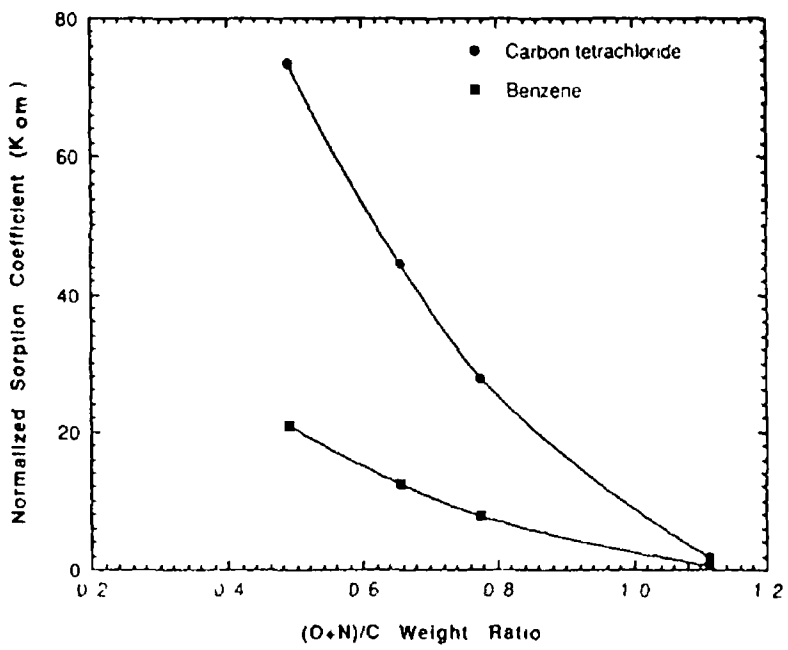

Figure 3 14 **Variation of the Partition Coefficient (K_{om}) with the O + N to C Ratio of the Sorbent Materials (39)**

Rutherford and Chiou (40) reported on the effects of water saturation on the sorption of low polarity solutes by organic soils The soils examined were a peat (86 4 % organic matter content, calculated from data given) and a muck (81 5 % organic matter) It was reported that the sorption of carbon tetrachloride, trichloroethylene and benzene from the aqueous phase by the organic soils gave linear sorption isotherms, see Figure 3 15

Under water saturated conditions the limiting sorption capacity (Q^{o}_{om}) of the peat and muck samples for the uptake of water was reported to be c 370 mg g^{-1} and 390 mg g^{-1} respectively These Q^{o}_{om} values are high when it is considered that the values correspond to water saturation of SOM of about 38 % by weight (dry weight basis) Again, this indicated that absorption of the water molecules was occurring, since such large amounts of water could not possibly be accommodated on the surface of these materials The partition coefficients (K_{om}) for the organic compounds were calculated from the sorption isotherms shown in Figure 3 15 and are given in Table 3 16 It was found that the K_{om} values for the sorption of the organic solutes were higher in the peat than in the muck This difference was thought to be due to the difference in the polarity of the two SOM materials (From the data given the polarities of the peat and muck samples, expressed as the O + N to C ratio were calculated to be 0 66 and 0 78 respectively) The sorption of the hydrophobic solutes was higher in the peat than in the muck because of the lower polarity of the peat as previously discussed by Rutherford *et al* (39)

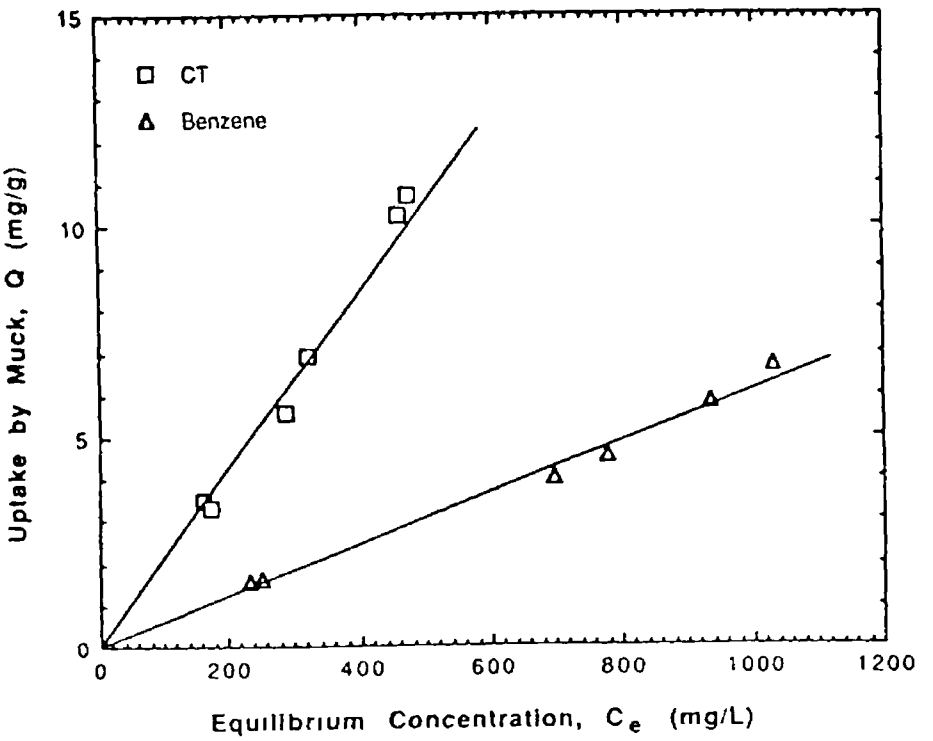

Figure 3 15 **Sorption Isotherms for Organic Solutes on Muck (40)**

Table 3.16 **K_{om} Values for the Sorption of Three Organic Compounds by Peat and Muck (40)**

Sorbate	K_{om}	
	Peat	Muck
Benzene	12.5	7.67
Trichloroethylene	33.1	nd[a]
Carbon tetrachloride	44.6	27.8

Note [a] nd, not determined

A comparison of the sorption of the three organic compounds from the vapour and aqueous phases indicated that water saturation of the SOM reduced the amount of organic solute retained by the organic matter by an average value of about 42 %, see Figure 3.16. This value is relatively small when compared to water saturation of mineral surfaces which can reduce their uptake of organic compounds by > 90 %. In this case the suppression of solute uptake is due to the successful competition of water molecules for adsorption sites on the mineral surfaces, this is discussed in Section 3.3.3.

It was found that water saturation of the peat reduced uptake (on a dry weight basis) by 44 % for benzene, 55 % for trichloroethylene and 46 % for carbon tetrachloride, see Table 3.17. For the muck sample the reduction was observed to be slightly less, 41 % for benzene and 28 % for carbon tetrachloride (trichloroethylene data not given). The relatively smaller effect of water saturation on the amount of organic solute taken up by the muck was thought to be due to the higher polar group content of the muck compared to the peat. It was postulated that penetration of the muck matrix by water molecules did not significantly increase its polarity, whereas, water saturation of the peat greatly increased its polarity when compared to the dry peat.

Table 3.17 **Q^{o}_{om} Values for the Uptake of Organic Compounds on Peat and Muck Samples (40)**

Sorbate	SOM	Q^{o}_{om} (mg g^{-1})	
		Aqueous phase	Vapour phase
Benzene	peat	22.0	38.9
Trichloroethylene	peat	36.4	80.0
Carbon tetrachloride	peat	35.6	65.9
Benzene	muck	13.7	23.4
Carbon tetrachloride	muck	22.2	30.7

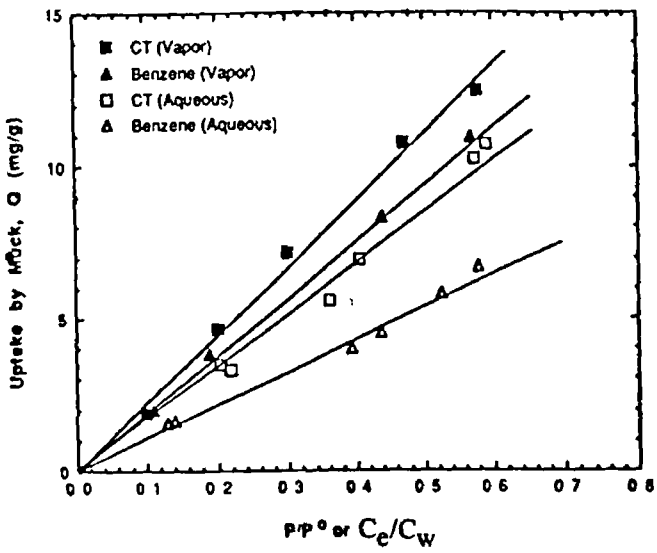

(a)

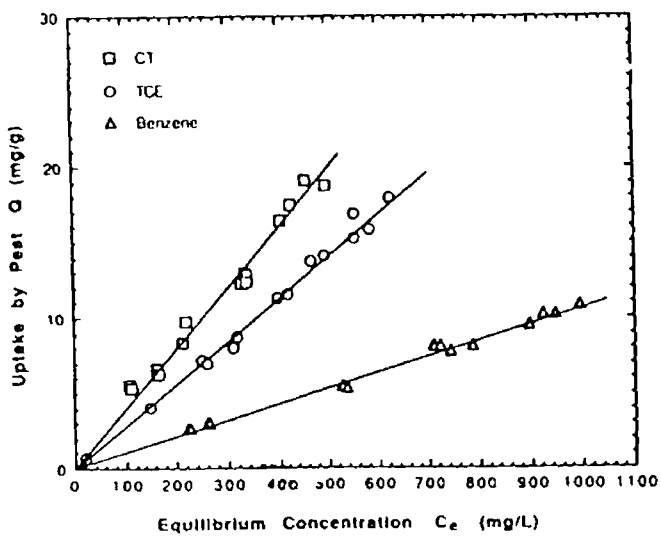

(b)

Figure 3.16 **Comparison of the Sorption of Carbon Tetrachloride, Trichloroethylene and Benzene from the Vapour and Aqueous Phases on (a) Muck and (b) Peat Soils (40)** Note C_e/C_w is the relative aqueous phase concentration of the organic solutes where C_e is the equilibrium concentration of the solute in the aqueous phase and C_w is its water saturation value

Rutherford and Chiou (40) considered that the effects of water saturation on solute partition into organic matter could be qualitatively described by comparing the effects of water saturation of the organic matter and the effect of water saturation of the organic solvent on the forces of interaction between the solvent and the solute molecules This may be expressed by the equation developed by Flory which describes the solubility of a liquid solute in a (amorphous) polymer in which the molar volume of the liquid is negligibly small compared to that of the polymer This equation is

$$\ln \phi^o + \phi_p + \chi\phi^2_p = 0 \qquad \text{Equation 3 20}$$

where ϕ^o is the volume fraction solubility of the liquid, ϕ_p is the volume fraction of the polymer ($\phi_p = 1 - \phi^o$), and χ is the Flory-interaction parameter which expresses the extent of molecular interaction between solute and polymer as previously described by Chiou *et al* (38) Since it has been shown that for relatively non-polar solutes in polar SOM the contribution of χ_s to χ is small relative to χ_h, then χ_h can be reasonably correlated by the equation

$$\chi_h = (V_1/RT)(\delta_1-\delta_p)^2 \qquad \text{Equation 3 21}$$

where V_1 is the molar volume of the solute, R the ideal gas constant, T the absolute temperature , and δ_1 and δ_p are the solubility parameters of the solute and polymer respectively From Equations 3 20 and 3 21 the solubility of a solute in a polymer is seen to decrease with increasing χ_h or with increasing $(\delta_1-\delta_p)^2$ Because δ of a substance usually increases with increasing polarity, the δ_1 for non-polar molecules are typically small For example δ_1 for benzene, trichloroethylene and carbon tetrachloride were calculated to be 9 2, 9 2 and 8 6 $(cal/cm^3)^{0\,5}$ respectively This compared to a δ_p value of c 13 0 $(cal/cm^3)^{0\,5}$ for water-saturated SOM The fact that these organic compounds are taken up to a greater extent in dry SOM compared to wet SOM suggested that δ_p for SOM increases with saturation Thus, it was calculated that δ_p for dry peat and wet peat were 12 5 and 13 0 $(cal/cm^3)^{0\,5}$ respectively, while dry muck and wet muck were 12 9 and 13 3 $(cal/cm^3)^{0\,5}$ respectively The greater δ_p for water saturated SOM and hence the reduction in solute solubility in saturated SOM can be attributed to an increased polarity of SOM by water

3 3 2 Sorption from Non-Aqueous Phases

There are few reported studies on the sorption of organic compounds by soil from non-aqueous solutions (i e organic solvents) However, those which have been reported do support a dual sorption mechanism for soil In particular, these studies have demonstrated the importance of relative humidity (see Section 3 3 3) on the adsorption of organic solutes by mineral surfaces It can be postulated that the mineral and organic matter fractions of soil should differ significantly in their uptake of non-ionic organic compounds from non-aqueous solvents The uptake of organic solutes by the organic matter fraction should be minimally effected, since sorption is principally through the dissolution of the solute into the organic phase of the soil (see Sections 3 3 1 and 3 3 3) The uptake of the solute by the mineral fraction will be dictated by the effectiveness of the solute's ability to compete with the solvent for adsorption sites Significant adsorption of the solute will occur if it can displace successfully adsorbed solvent molecules, this effect increases with increasing polarity of the solute

Hance (31) examined the sorption of diuron from aqueous and from petroleum solutions by an organic matter extract (76% organic matter) and on an oxidised form of the organic matter fraction (organic matter content not stated) It was reported that the sorption of diuron by the oxidised organic matter was greater from the petroleum solution than from the aqueous solution, while the sorption of the diuron from the aqueous solution was greatest on the organic matter and least on the oxidised organic matter Hance (31) concluded that there was competition occurring between the water and diuron molecules for adsorption sites, and that in general the uptake of diuron from aqueous solutions was higher with organic matter than with minerals

Mills and Biggar (32) reported on the sorption of lindane (γ–BHC) by a Staten peaty muck (22 % organic matter) and a Venado clay (50 % montmorillonite, 0 6 % organic matter) from aqueous and hexane solutions It was found that the uptake of lindane from aqueous solution was higher with the peaty muck than with the Venado clay However, the sorption capacity of the clay for lindane was observed to increase for the clay-hexane system, and to be slightly higher than the sorption capacity of the peaty muck It was concluded that polar lindane molecule competes successfully with the non-polar hexane for adsorption sites on the mineral surfaces

Yaron and Saltzman (41) reported on the sorption of parathion from aqueous and hexane solutions on dry and hydrated (15, 32, 50, 98 % RH) mineral soils The

sorption of parathion from hexane on dry soils was compared to the sorption of the parathion from wet soils It was found that the slightly polar parathion molecules compete efficiently with the non-polar hexane molecules for adsorption sites As the relative humidity of the soil was increased it was observed that the uptake of parathion decreased This was due to the gradual decrease in the amount of water free surface until at saturation of the soil no parathion was adsorbed This result is comparative to the decreased sorption of organic vapours as the relative humidity of the soil is increased (see below)

3 3.3 Sorption from the Vapour Phase and the Effect of Humidity

The results from the investigation of the sorption of organic vapours by soils showed that dry mineral soils, particularly the clays, were powerful adsorbents for organic compounds Also, that the sorption capacity of the clays greatly exceeded the sorption capacity of the organic matter fraction for organic vapours

Hanson and Nex (42) observed the influence of soil moisture on the amount of organic vapour retained by mineral soil samples They reported that at moisture levels below the wilting point of the soil (c 5 to 7 % moisture content) ethylene dibromide (1,2-dibromoethane) vapour was strongly retained, see Figure 3 17 (The wilting point is the water level below which wilting of plants growing in that soil occurs) However, its sorption decreased sharply to a minimum near the wilting point A small, linear increase in the sorption of ethylene dibromide was observed to occur above the wilting point which was due to the absorption into the aqueous phase surrounding the soil particles

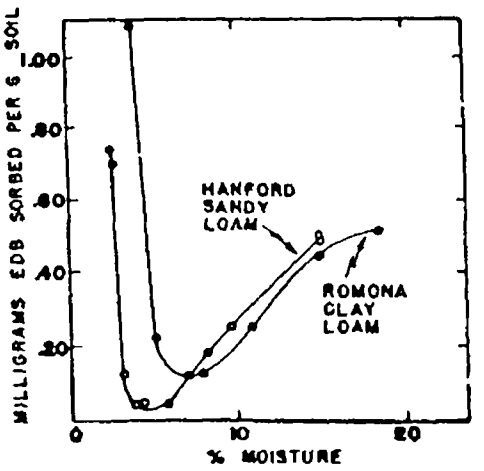

Figure 3 17 Sorption of Ethylene Dibromide in Two Soils with Varying Moisture Contents (42)

Jurinak (43) and Jurinak and Volman (28) reported that the sorption capacity of mineral soils for ethylene dibromide was dependent on the clay type and the exchangeable (solvating) cation present The sorption isotherms on dry soil samples were observed to be non-linear, and to fit the BET equation (28), see Section 3 2 1 2 Jurmak (43) reported that adsorption of ethylene dibromide on Ca-montmorillomte, -illite and -kaolinite indicated that adsorption was more restricted on the Ca-montmorillomte than on the Ca-kaolinite, with the Ca-illite being intermediate The dimensions of the capillaries associated with the clay minerals was considered to be the limiting factor in the adsorption of the organic vapour The influence of solvating cation for clay samples was found to be in the order Mg > Ca > Na (43)

Call (44) examined the sorption of ethylene dibromide on moist soils He found that as the humidity of the soil increased, the amount of ethylene dibromide retained by the soil decreased This was considered to be due to competition between the water and organic vapour for adsorption sites on the mineral surfaces The H_2O molecules were considered to be able to displace the adsorbed ethylene dibromide molecules An interesting discrepancy was found with Ca-montmorillonite soils, i e higher sorption values of ethylene dibromide at relative humidities of 5 to 20 % than at 0 % due to interlamellar swelling

Leistra (33) reported on the sorption of cis- and trans-1,3-dichloropropene vapours on three soils (a 'humerous sand', a 'peaty' sand and a peat with organic matter contents of 5 5, 18 and 95 % respectively) at 2°, 11° and 20°C The sorption isotherms were observed to be linear in the concentration range studied (0 to 40 mg cm^{-3}), see Figure 3 18

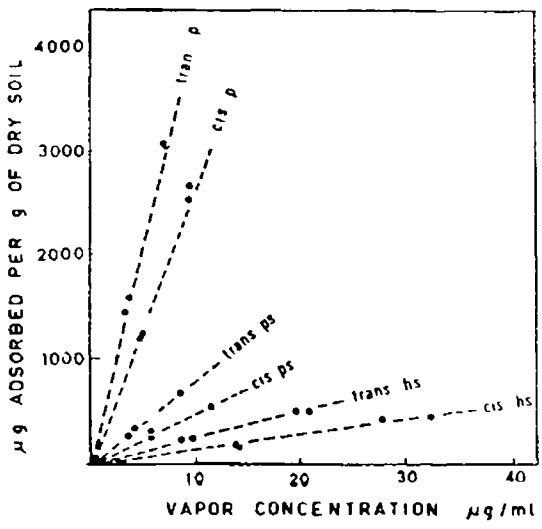

Figure 3 18 Sorption Isotherms for cis- and trans-1,3-Dichloropropene at 20°C (33) Note hs = humerous sand, ps = peaty sand, p = peat

The results of Leistra (33) which are presented in Table 3 18 show that the adsorption coefficient K(s/v) (which was the amount of organic vapour adsorbed per gram of dry soil divided by the equilibrium concentration of the vapour in the gas phase) for the trans-isomer was greater than the K(s/v) value for the cis-isomer Thus, the trans-isomer was retained by the soil samples in greater amounts It was observed that the amount of organic vapour retained by the soil increased with

(i) decreasing temperature, the amount of vapour sorbed at 2°C was about three times higher than the amount sorbed at 20°C,

(ii) increasing organic matter content of the soil, from Table 3 18 it can be seen that the sorption capacities increased in the order humerous sand < peaty sand < peat

Table 3 18 Sorption Coefficient K(s/v) for cis- and trans-1,3-Dichloropropene (33)

Soil	OM (%)	Temperature °C	Adsorption coefficient K(s/v)	
			cis-isomer	trans-isomer
Humus sand	5 5	2	38	68
		11	22	40
		20	14	24
Peaty sand	18	2	130	220
		11	78	130
		20	47	77
Peat	95	2	680	1250
		11	430	720
		20	260	410

Chiou and Shoup (45) reported on the sorption of water vapour and several organic vapours on Woodburn soil (consisting of 1 5 % organic matter, 9 % sand, 68 % silt, and 21 % clay [mainly kaohnite and mica]) The sorption of water, benzene, chlorobenzene, p-dichlorobenzene, m-dichlorobenzene, 1,2,4-trichlorobenzene was examined on dry soil samples The sorption isotherms were found to be non-linear and their shape corresponded to the Brunauer Type II sorption isotherm, see Figure 3 19 The sorption capacity of the Woodburn soil for the various organic vapours was found to be dependent on the polarity of the sorbate It was observed that the sorption capacities were lower for those organic compounds

that were not strong wetting agents on the polar mineral surface This was evident from the relative order of sorption seen in Figure 3 19, which at low P/P_0 values had the order, 1,2,4-trichlorobenzene (the most polar) > m-dichlorobenzene ~ p-dichlorobenzene ~ chlorobenzene > benzene (the least polar)

The fact that the adsorption of the organic vapours by the mineral surface was enhanced by the polarity of the sorbate was seen by Chiou and Shoup (45) to indicate that water must be a strong competitor for adsorption sites on the mineral surface As an example it was reported that the maximum capacity of dry Woodburn soil for the uptake of m-dichlorobenzene was c 45 mg g^{-1}, which is about 100 times the limiting uptake of the compound by the same soil from water Such a difference indicates the powerful suppression by water on the adsorption of organic vapour by soil minerals This is clearly seen from the results for the sorption of benzene, m-dichlorobenzene, and 1,2,4-trichlorobenzene by the Woodburn soil as a function of relative humidity

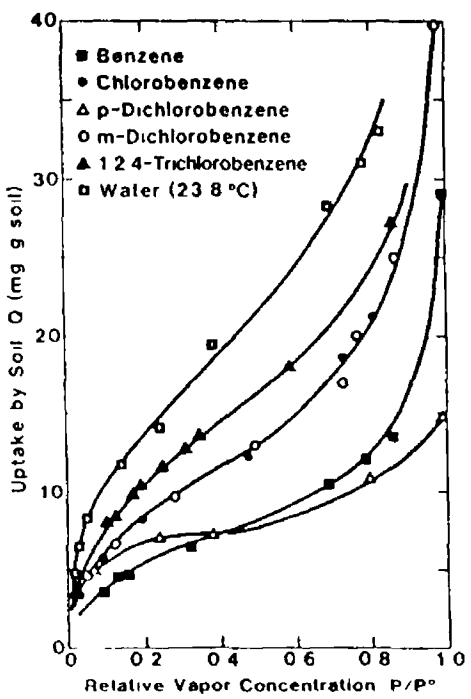

Figure 3 19 **The Uptake of Organic Vapours and Water by a Dry Woodburn Soil (45)**

The presence of water was found to sharply suppress the sorption capacity of the soil for the organic vapours, as an example the uptake of 1,2,4-trichlorobenzene is shown in Figure 3 20 In general it was found that with increasing relative humidity of the soil the shape of the isotherm became increasingly linear, and by 90 % RH the amount of organic vapour retained by the soil was comparable with their sorption from the aqueous phase The linearity of the isotherm at high relative humidity was considered to be due to the suppressive effects of water which was much better at

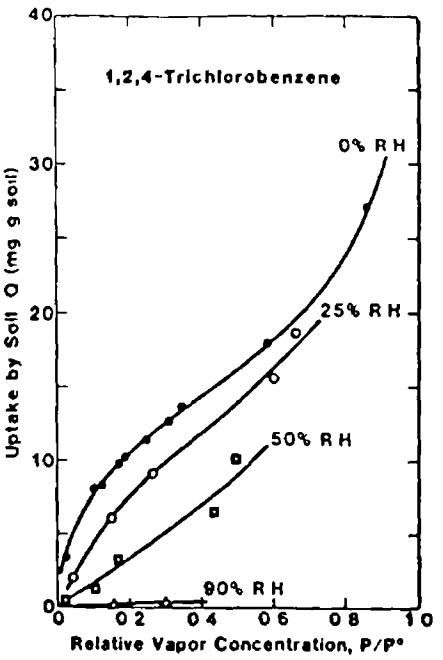

Figure 3 20 The Uptake of an Organic Vapour (1,2,4-Trichlorobenzene) by Woodburn Soil as a Function of Relative Humidity (45)

competing for adsorption sites than the less polar organic vapours The minimal level of sorption that was observed at high relative humidities was due to partitioning of the organic compounds into the SOM fraction of the soil samples

The amount of vapour required for monolayer coverage (Q_m) of the Woodburn soil was calculated using the BET equation, see Table 3 19 (45) These monolayer capacities were established at relatively low P/P_o values (<0 18) except for benzene which occurred at $P/P_o \sim 0\ 23$ The observed capacities at higher P/P_o values were reported to greatly exceed the monolayer values It is interesting to note that the Q_m values in Table 3 19 increase with increasing polarity of the molecule

Table 3 19 BET Monolayer Capacities (Q_m) on Dry Woodburn Soil (45)

Sorbate	Q_m (mg/g)
Benzene	5 57
Chlorobenzene	7 53
m-Dichlorobenzene	7 42
p-Dichlorobenzene	5 54
1,2,4-Trichlorobenzene	9 53
Water	11 7

Chiou *et al* (46) subsequently examined the sorption of water and organic vapours on a dry soil of high organic matter content (Sanhedron soil humic acid with an ash content of 1 19 %) The organic sorbates used were ethanol, benzene, hexane, carbon tetrachloride, 1,1,1-trichloroethane, trichloroethylene, tetrachloroethylene, and 1,2-dibromoethane The sorption isotherms for water and the organic vapours were found to be linear up to high P/P_0 values, see Figure 3 21 This result was considered to be consistent with Chiou and co-worker's model of SOM as a partitioning medium for organic compounds The small curvature of the slope noted at low P/P_0 values was attributed to specific adsorption interactions occurring between the sorbates and surface functional groups present in the SOM Similarly the curvature at high P/P_0 values was considered to be due to simultaneous adsorption to the exterior surfaces of the humic acid

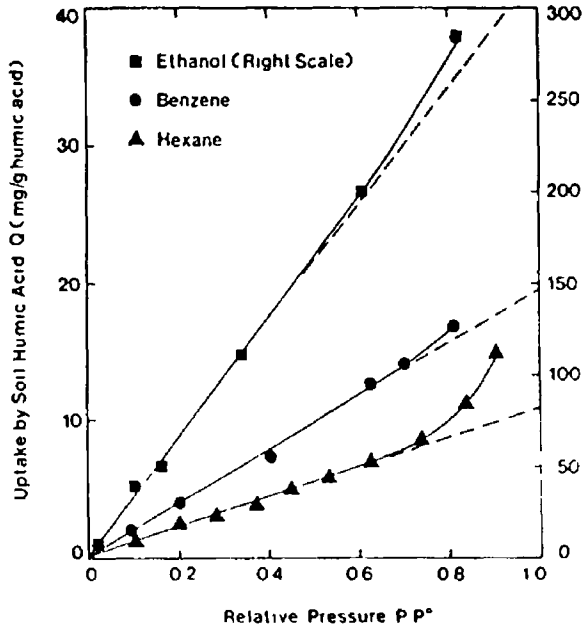

Figure 3 21 The Sorption of Organic Vapours by Sanhedron Soil (46)

From extrapolation of the linear isotherms to $P/P_0 = 1$ the limiting sorption value, Q_{ha}, of the humic acid was determined, see Table 3 20 The larger Q_{ha} values for water and ethanol compared to the other sorbates were considered to be consistent with the polar nature of the humic acid as a partitioning medium On a weight basis it can be seen that the Q_{ha} value ranged from 11 0 for hexane to 37 0 mg g^{-1} for 1,2-dibromoethane, which is a difference of a factor of c 3 4 However, on a volume basis, Q_{ha} values are seen to be similar, assuming the density of the sorbed liquids to be the same as their bulk-liquid densities Thus, it can be seen that the difference of the limiting sorption capacities in the humic acid on the weigh basis is due primarily to differences in the density of the organic liquid

Table 3.20 **Limiting Sorption (Partition) Capacity (Q_{ha}) of Various Organic Compounds and Water on Sanhedron Soil Humic Acid (46)**

Sorbate	Limiting sorption capacity of humic acid	
	mg g^{-1}	cm^{-3} g^{-1}
Water	245	0 245
Ethanol	345	0 440
Hexane	11 0	0 0167
Benzene	20 2	0 0231
1,1,1-trichloroethane	24 8	0 0185
Tetrachloroethylene	25 5	0 0157
Carbon tetrachloride	26 3	0 0165
Trichloroethylene	27 4	0 0188
1,2-dibromoethane	37 0	0 0170

Chiou *et al* (46) conclude that SOM is a better sorbent for non-polar compounds than humic acid, suggesting that the overall polarity of SOM is lower than that of humic acid Since humin constitutes a significant fraction of SOM the lower polarity of SOM can be attributed to this fraction of the humic substances

Rutherford and Chiou (40) reported on the sorption of water, benzene, trichloroethylene, and carbon tetrachloride vapours on a peat (86 4 % organic matter) and a muck (81 5 % organic matter) The shape of the sorption isotherms were found to be linear in the relative pressure range studied (P/P_o = 0 to c 0 6), see Figure 3 22 The linearity of the isotherms suggested to the authors that only one type of intermolecular force was responsible for the partitioning of the organic sorbates into the organic matter In view of the low polarity of the sorbates used the van der Waals forces were considered to be the most likely forces involved The large amount taken up could not be accounted for given the small surface area of the organic soils (as measured by the BET(N_2) method)

(a)

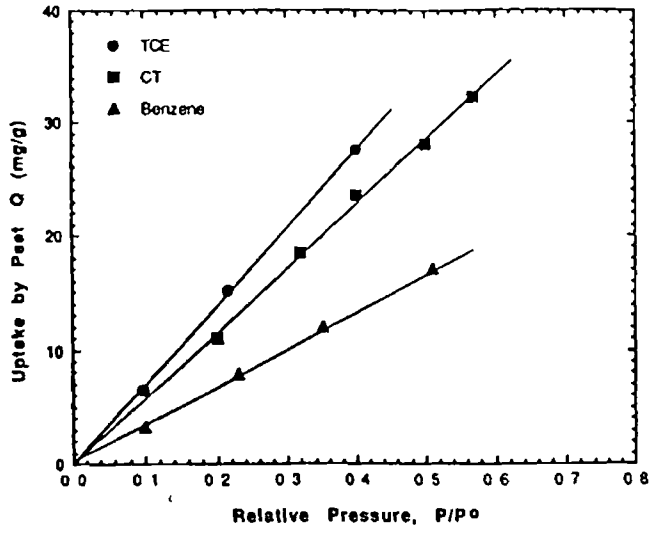

(b)

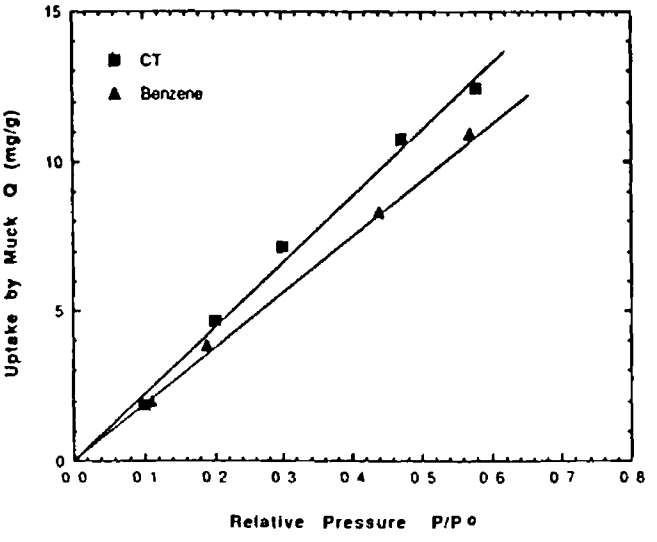

Figure 3 22 Sorption of Organic Vapours by (a) Peat and (b) Muck Samples (40) Note Sorption was under anhydrous conditions

Chiou and Kile (47) reported on the effects of polar and non-polar groups on the sorption of organic compounds by SOM They studied the sorption of n-hexane, 1,4-dioxane, nitroethane, acetone, acetonitrile, 1-propanol, ethanol and methanol on a dry peat soil (86 4 % organic matter) The isotherms for all organic vapours examined were found to be linear in the relative pressure range studied (P/P_0 = 0 to 0 45), see Figure 3 23 Extrapolation of the linear isotherms to P/P_0 = 1 enabled the limiting capacities, Q^0_{om}, of the organic sorbates in peat to be determined, see Table 3 21 It was found that the sorption capacity of the peat decreased from 620 mg g^{-1} for methanol to c 29 mg g^{-1} for n-hexane, and that the trend decreased with decreasing polarity of the molecules The greater sorption capacity of the peat for the polar molecules was attributed to the stronger interaction between the polar vapours and the polar peat than between the peat and the non-polar compounds

(a)

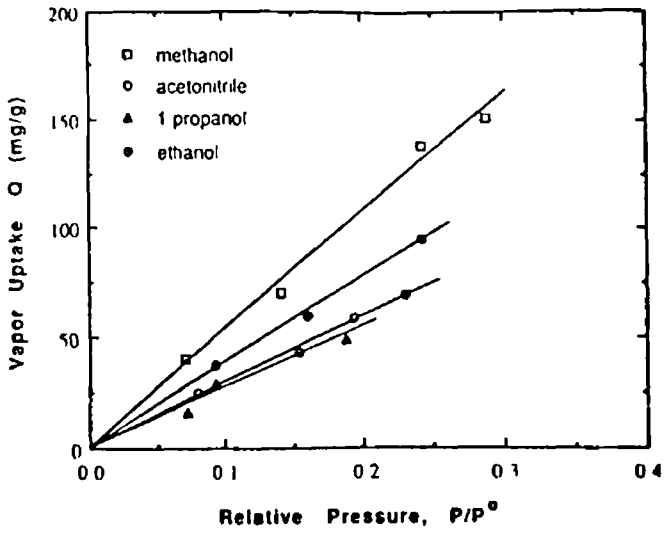

(b)

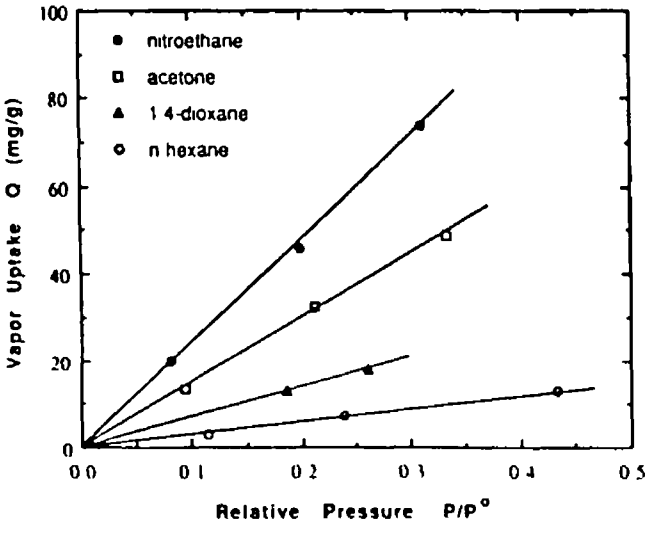

Figure 3 23 **Sorption of Various Polar Organic Vapours on Peat (47)**

Table 3 21 **Partition Capacities (Q^{o}_{om}) for Various Organic Sorbates in Peat Organic Matter (47)**

Sorbate	Q^{o}_{om} (mg g^{-1})
n-Hexane	28 2
1,4-Dioxane	80 2
Acetone	171
Nitroethane	272
Acetonitrile	344
n-Propanol	313
Ethanol	396
Methanol	620

3 4 Summary

The long term fate of organic compounds in the soil is influenced by its organic matter content It has been found that the higher the organic matter content of the soil the greater is its retention capacity for organic compounds Originally, soil was viewed as a single sorption material, and that the mineral and organic matter fractions acted as high surface area adsorbing materials However, more recently a dual sorption model for soil has emerged which views the soil mineral fraction as a conventional high surface area adsorbent while the organic matter is considered to be a partitioning medium

In relation to the sorption mechanism, one of the more important properties of soil is the size of the surface area of its constituents For the mineral fraction there is a distinction between the small external surface area of the non-expandable clays and the very large internal surface areas of the expandable clays External surface areas can be measured using weakly interacting probes such as N_2, but polar molecules such as water, EG or EGME must be used to measure the internal surfaces However, the situation is more difficult for SOM because of the uncertainty associated with its structure The surface area of SOM varies from about 1 0 $m^2\ g^{-1}$ by N_2 adsorption to values upwards of 800 $m^2\ g^{-1}$ by EG measurements The conventional interpretation of these results based on the clay model would suggest that the external and internal surface areas of SOM are being measured However, Chiou and co-workers have argued that the surface area of SOM can only be measured with weakly interacting probes The polar probes are not adsorbed onto the SOM surfaces, but are absorbed (i e dissolve) into the organic matter Therefore, the use of polar probes will give erroneously high surface area values

Concerning the sorption mechanism of SOM for non-ionic organic compounds it is now widely accepted that SOM acts as a partitioning medium for the uptake of such compounds Evidence, which has been cited supporting the partition model, includes the linear shape of the sorption isotherms for the uptake of organic compounds from the liquid and vapour phases, the low heats of sorption, the lack of competition between binary solute mixtures, and the fact that humidity does not inhibit the uptake of organic compounds to the extent that it does for mineral surfaces

3 5 Experimental Work

The aims of the experimental work presented in this chapter were two fold, firstly to measure the surface area of the peat materials which were previously characterised in Chapter 2 The surface areas of the peat samples were measured by the commonly used method of N_2 adsorption at liquid N_2 temperatures (-195°C) using the BET equation In addition the surface area of the peat fibre (PF) was also measured by the adsorption of the dye methylene blue from aqueous solution, and from the exclusion volume method which was based on the negative adsorption of Cl^- ions

Secondly, this work studied the sorption mechanism of uptake of a series of alcohols (ethanol to 1-hexanol) from the vapour and aqueous phases by PF Specifically, it was hoped to be able to determine whether the dominant sorption mechanism was by adsorption or absorption (partitioning) of the alcohols by the PF

3 5 1 Experimental Details

The peat samples studied were peat fibre (PF), peat moss (PM), and the two processed forms of peat material, PMA and PMG The description of these materials and their physicochemical properties have already been discussed in Section 2 5 1 The initial pre-treatment carried out on the peat samples consisted of air drying at 20°C followed by size fractionation as previously described in Section 2 5 1

(a) Surface Area Determination

Three methods were used to determine the surface area of the peat materials

Nitrogen Adsorption using the BET Method

The adsorption of N_2 by the peat samples was carried out using the Micromeritics Pulse-Chemisorb 2700 instrument Surface areas were measured as follows about 0 3 g of sample was added to a pre-weighed sample holder, and the holder attached to the instrument The peat sample was then outgassed, in a He/N_2 gas stream, by heating to remove water vapour and other contaminants before the surface area was measured The standard outgassing conditions used involved heating the peat at 110°C for 30 minutes followed by heating at 150°C for a further 3 hours under a gas flow of 20 cm^3 min^{-1} These temperatures were chosen from an

examination of the TGA results (see Section 2 4 2) which indicated that thermal decomposition of peat samples did not occur below these temperatures

The surface area of the sample was then measured using the single point BET method (see Appendix C) (48) This consisted of measuring the amount of N_2 gas adsorbed by the sample at liquid nitrogen temperature (-196°C) from a gas stream containing an N_2 He gas ratio of 30 70 Desorption was determined by heating the sample to room temperature (20°C) and measuring the amount of N_2 evolved from the sample Each sample underwent three adsorption/desorption cycles, the amount of N_2 adsorbed/desorbed by the sample was detected by a thermal conductivity detector (TCD) The sample was re-weighed to obtain the final dry weight, and the surface area of the peat expressed as the number of square meters per gram (dry weight) of the sample (m^2 g^{-1}) The surface area values were usually the mean of triplicate sample measurements The instrument contained an in-built integrator which converted the amount of N_2 adsorbed/desorbed by the sample to an area value (in m^2) The instrument was first calibrated by the injection of 1 cm^3 of N_2 gas at room temperature and corrected to STP It was found that the difference in surface area values between adsorption/desorption values and between cycles was usually within 5 %, while sample variation for the sample peat material was typically within 10 %

The effects of temperature on the surface area of the PF was also studied About 30 g of PF was heated from 150° to 900°C in 50°C steps in a muffle furnace, the sample being held for 2 hours at each temperature After the allotted time period of heating about 1 g of the heated sample was removed and cooled to room temperature in a desiccator The heated sample was then outgassed and its surface area measured as previously described

Methylene Blue

The method of adsorption of methylene blue from aqueous solution by the PF was adapted from the method of Poost and McKay (15) which was as follows

(i) about 50 mg of oven dried PF (500-180 μm size fraction) was weighed into 250 cm^3 volumetric flasks To this was added, in duplicate sets, 100 cm^3 of methylene blue solution of concentrations ranging from 10 to 500 mg-dye cm^{-3} A blank consisting of 50 mg PF and 100 cm^3 water was also included The flasks were tightly stoppered and the samples shaken for 2 days at 20° (± 2°) C

(ii) the peat was then removed by filtering the solution using Whatman no 1 filter paper and the final concentration of the dye solution determined colorimetrically using a Shimadsu UV-240 spectrophotometer set at 665 nm

(iii) the amount of dye remaining in solution was determined by reference to a calibration curve of methylene blue absorbance versus dye concentration (5 to 500 mg-dye cm^{-3}) The methylene blue standard solutions were filtered in the same manner as the peat sample solutions prior to absorbancy measurements The control absorbance was subtracted from each of the sample solutions The difference between the initial dye concentration and its final concentration in solution was taken to be the amount of dye adsorbed by the PF

Exclusion Volume

The exclusion volume method used was adapted from that described by Edwards *et al* (20)

(i) initially, about 10 g of PF (500-180 μm size fraction) was washed with 200 cm^3 x 5 aliquots of deionised water to remove chloride salts The peat was dried at 110°C overnight, and allowed to cool to room temperature in a dessicator

(ii) about 0 5 g of the washed PF was measured into sample bottles, in triplicate sets, 20 cm^3 of NaCl solution (concentrations from 1 to 500 mg-Cl^- cm^{-3}) was added to each sample The samples bottles were tightly stoppered and shaken for 2 days at 20° (± 2°) C

(iii) the sample bottles were then centrifuged at 5,000 rpm for 15 minutes to separate the PF from the aqueous solution The final concentration of the Cl^- ions in the PF sediment and the supernatant (bulk aqueous solution) were measured using an Orion Cl^- ion selective probe (model 94-17B) The Cl^- ion concentration was determined from a calibration curve of Cl^- concentration between 1 to 500 mg-Cl^- cm^{-3} versus mV The measurements were carried out as described in the instructions manual of the Cl^- probe (49)

(b) Sorption of Alcohols from the Vapour Phases

Gas phase sorption studies for the uptake of alcohol vapours by the PF were carried out using the sorption apparatus illustrated in Figure 3 24 (45) The operation of the apparatus was as follows, air initially entered the system by passing through a

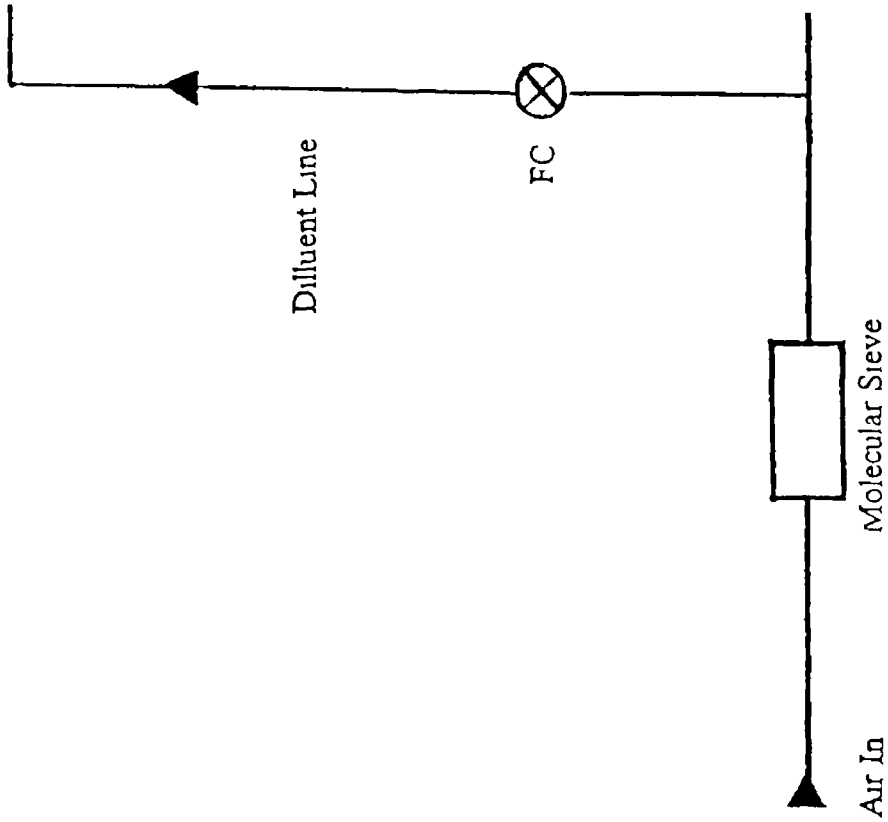

Figure 3.24 Sorption Apparatus Used for the Sorption of Alcohol Vapours by PF

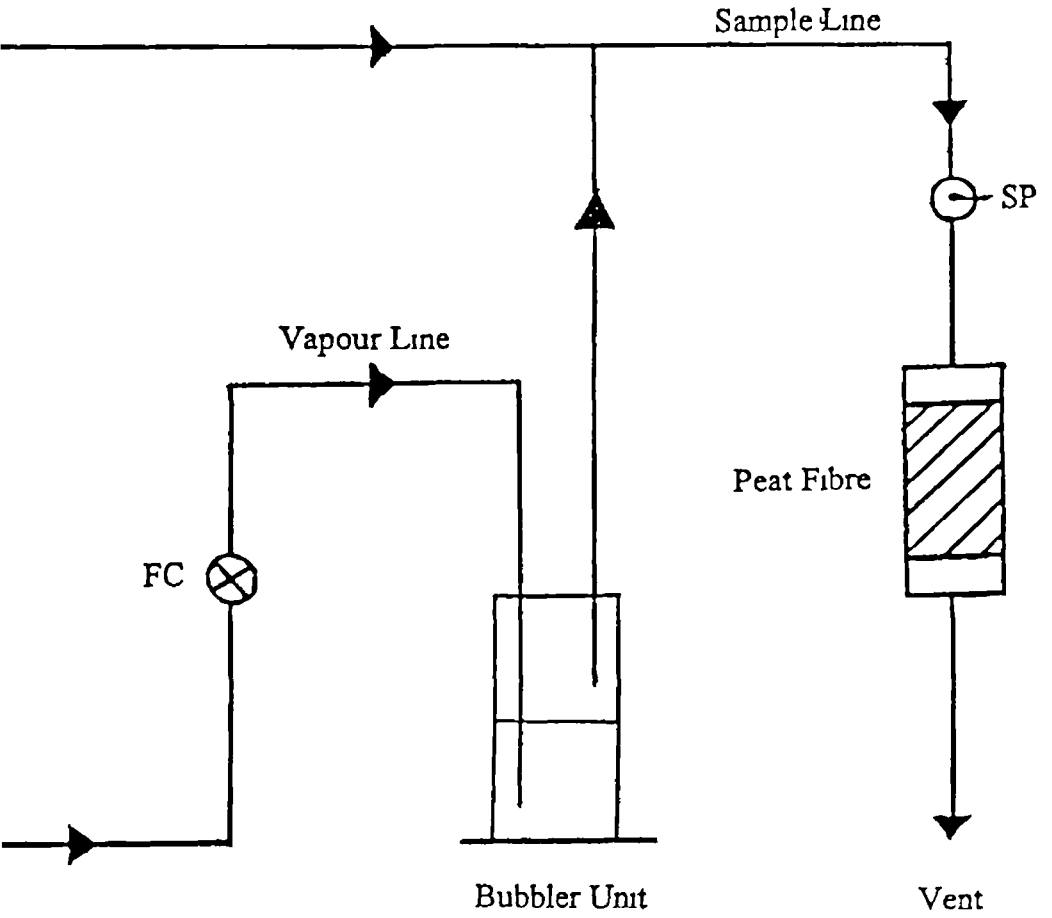
Sample Line
SP
Vapour Line
Peat Fibre
FC
Bubbler Unit
Vent

drying column containing 5 Å molecular sieve to remove water moisture and other contaminants from the gas stream The gas line then split into a diluent and a vapour line respectively, the rate of air flow through each line was controlled by a flow controller (labelled FC in Figure 3 24) The air passing through the vapour line became saturated in alcohol vapour once it had been bubbled through the liquid alcohol contained in the bubbler unit The vapour line then re-joined the dilluent line to form the sample line, and the alcohol vapour passed over the PF sample in the sample holder before going to the vent

Gas samples were taken through the rubber septum of the gas sampling port (SP) situated along the sample line The gas samples were taken using a gas-tight syringe and the vapour concentration of the alcohol measured by gas chromatography (see below) The overall vapour concentration was controlled by adjusting the air flow through the dilluent and vapour lines while maintaining the overall flow rate at 40 (± 1) cm^3 min^{-1} over the sample The sample holders used in the experiments consisted of polypropylene tube with an internal diameter of 1 cm and a length of 3 cm Teflon tubing and swage lock fittings were used through out the apparatus, except for the stainless steal fittings used for the sample holder

The sorption experiments basically consisted of measuring the amount of alcohol sorbed by the PF at different vapour concentrations of the alcohol The sorption studies were carried out as follows, initially, the vapour concentration of the alcohol was adjusted to the desired concentration and the system allowed to equilibrate overnight About 3 g of oven dried PF (500-180 μm size fraction) was accurately measured into a clean, pre-weighed sample holder, which was then attached to the sample line and the system thereafter allowed to run continuously The weight increase to the sample holder plus PF was taken to be equal to the amount of alcohol sorbed by the PF once the weight increase due to the adsorption of vapour to the sample holder wall had been corrected for This correction consisted of subtracting the weight gain to a empty sample holder which was also connected to the sample line The weight increase in the peat sample and the vapour concentration at the sample were measured every 2 to 4 days Equilibrium between the vapour concentration of the alcohol and the amount of alcohol sorbed by the PF was considered to be reached once weight increase to the sample had stopped This usually took between 3 to 4 weeks in the case of the ethanol and propanol experiments, but reduced to 2 weeks for the higher alcohols Temperature variation over this time period was 20° (± 2°) C The amount of alcohol sorbed by the PF was expressed in mg g^{-1} The results were the average of duplicate sample measurements

(c) Sorption of Alcohol from the Aqueous Phase

For aqueous phase sorption studies glass vials of about 12 cm^3 internal volume, sealed with teflon-lined rubber septa and aluminium crimp caps were used About 0 35 g of oven dried peat (500-180 μm size fraction) was weighed into each vial and the remaining volume of the vial filled with water to remove any head space Care was taken to remove trapped air bubbles before the vials were sealed To prevent biological activity, the water used contained 1 0 mM $HgCl_2$ The volume of water added to each vial was determined by weight measurement which assumed that the density of the aqueous solution to be 1 g cm^{-3} Using a precision microliter syringe the required amount of alcohol was added to each vial through the septum once the vial had been sealed Samples were shaken for 5 to 7 days at 20° (± 2°) C, and the final concentration of the alcohol in solution measured by gas chromatography The amount of alcohol sorbed by the PF was taken to be the difference between the initial and final concentration of the alcohol in solution The amount of alcohol sorbed by the PF was expressed in mg g^{-1} The results were the results of triplicate sample measurements

A Perkin-Elmer GC F11 incorporating an FID was used to measure the vapour and aqueous phase concentrations of the alcohols The GC column used was 5 % DC-710 liquid stationary phase on Chromosorb W AW The GC conditions used for the measurement of the alcohol concentrations are shown in Table 3 22 The peaks were measured using a Packard-Hewitt integrator The concentration of the alcohol in the vapour and aqueous phases was determined by reference to a standard calibration curve of alcohol vapour phase (or aqueous phase) concentration versus peak area Correlation coefficients for the calibration curves were usually greater than 0 99 To prepare the calibration curves for the vapour phase alcohols a known volume of the liquid alcohol was evaporated in a gas sampling bottle of known internal volume

Table 3 22 GC Conditions Used For the Measurement Of Alcohol

Alcohol	Gas flow rate (cm^3 min^{-1})	Block temp	Attenuation		Oven temp (°C)
			vapour	aqueous	
Ethanol	40	3½	5×10^2	50×10^1	100
2-Propanol	40	3½	2×10^2	50×10^1	100
1-Butanol	40	3½	1×10^2	50×10^1	140
1-Pentanol	40	3½	1×10^2	50×10^1	160
1-Hexanol	40	3½	50×10^1	50×10^1	180

Note vapour = vapour phase measurements, aqueous = aqueous phase measurements

3 5 2 Results and Discussion

The results for the measurement of the surface area of the peat materials are presented in Section 3 5 2 1 The sorption of a series of alcohols from the vapour and aqueous phase by the PF is presented and the mechanisms involved are discussed in Section 3 5 2 2

3 5 2 1 Surface Area Determination

(a) Nitrogen Adsorption Using the BET Method

The surface areas for the peat samples were calculated using the single point BET method In calculating the surface area of the peat materials the cross-sectional area (A_m) occupied by one molecule of N_2 at -195°C was taken to be 16 2 x10^{-20} m^2 (48) The surface area measured for PF, PM, PMA and PMG samples (500-180 μm size fraction) are presented in Table 3 23, while Table 3 24 shows the surface area of PF as a function of its particle size For both sets of results standard outgassing conditions were used Examining the results presented in Table 3 23 it can be seen that the peat moss and PMG samples had similar surface areas of about 2 0 m^2 g^{-1} while the surface area of the PMA sample was higher at about 2 5 m^2 g^{-1} The surface area of the PF size fractions were found to increase slightly with decreasing size fraction of the peat, from 2 13 m^2 g^{-1} (1000-710 μm) to 2 53 m^2 g^{-1} (90-45 μm)

Table 3 23 Surface Area of PF, PM, PMA and PMG Determined from N_2 Adsorption

Peat Sample[a]	Surface area (m^2 g^{-1})
PF	2 38
PM	2 04
PMA	2 41
PMG	1 94

Note ([a]) size fraction 500-180 μm Surface area values for all materials were typically ± 10 %

Table 3.24 **Surface Area of PF Determined from N_2 Adsorption as a Function of Size Fraction**

Size fraction (μm)	Surface area ($m^2 g^{-1}$)
1000-710	2 13
710-500	2 33
500-180	2 38
180-90	2 47
90-45	2 53

Note Surface area values ± 10 %

The influence of heating temperature and time of heating on the surface area of PF was also examined The surface areas measured are shown in Table 3 25, and the results shown graphically in Figure 3 25

Table 3 25 **Surface Area of PF as a Function of Pre-treatment Time and Temperature Determined from N_2 Adsorption**

Pre-treatment temperature (°C)	Surface area ($m^2 g^{-1}$)		
	Pre-treatment time (hours)		
	3	4 to 7	20 to 24
20	-	-	2 39
60	2 32	2 49	2 12
80	2 44	2 42	-
110	2 28	2 33	2 26
150	2 38	2 25	2 71
170	4 30	-	3 56
200	1 63	-	-
300	8 72	-	-
350	30 61	-	-
400	44 02	-	-
500	22 39	-	-
900	8 90	-	-

Note Surface area values are typically ± 10 %

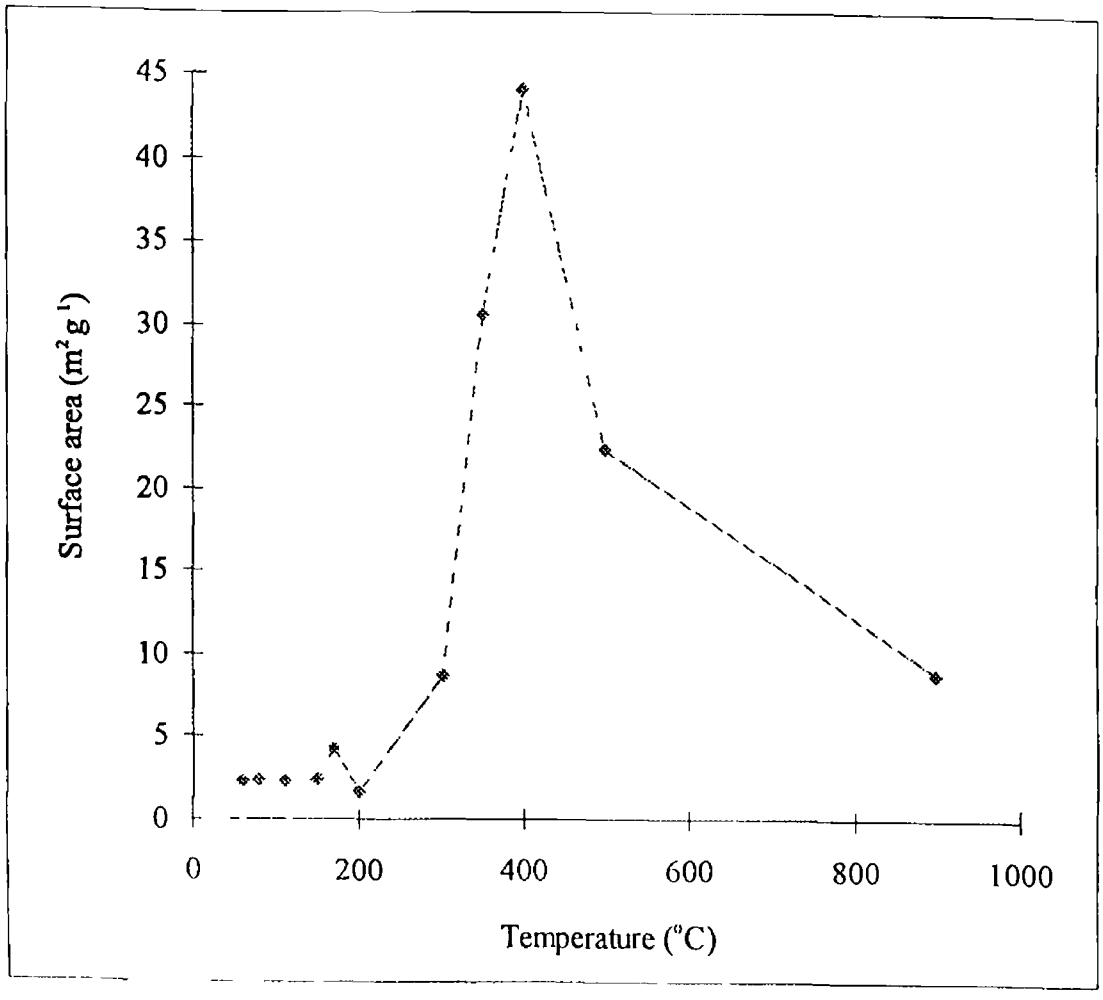

Figure 3.25 **Variation in the Surface Area of PF with Heating Temperature**
Note 3 hours pretreatment time

It can be seen from Table 3 25 that there was no significant variation in the surface area of the PF samples heated at temperatures up to and including 150°C Over this temperature range the area values varied from about 2 1 to 2 7 m^2 g^{-1} It can be seen that prolonged heating of the peat at temperatures up to 110°C did cause a slight decrease in the surface area of samples The only exception to this trend were the samples heated at 150°C for 20 to 24 hours which were found to have slightly increased surface areas of about 2 7 m^2 g^{-1} This may indicate that prolonged heating of the PF at 150°C did cause some thermal decomposition of the samples to occur It was found that there was a doubling in the surface area to about 4 3 m^2 g^{-1} on heating the peat from 150° to 170°C Heating above 200°C caused further increases to the surface area of the heated samples, which reached a maximum value of about 44 m^2 g^{-1} for samples heated at 400°C The surface area was observed to decrease above 400°C until it reached a value of about 9 m^2 g^{-1} by for peat samples heated at 900°C

The increase in the surface area of peat samples up to a maximum area at a pre-treatment temperature of 400°C may be explained from a comparison with the thermal analysis results for peat samples discussed in Section 2 4 3 It will be remembered that there was a 36 to 38 % decrease in the weight of peat samples in the temperature range 200° to 390°C corresponding to the exothermic maximum I of the DSC results This temperature range was considered to correspond to the decomposition of the easily decomposed peat materials, but in particular to the decomposition of the cellulose fraction of the peat (50) In contrast, the lignin fraction of the peat was more resistant to thermal decomposition and began to decompose at temperatures above 400°C (51) Thus, the increase in surface area of the peat samples in the 170° to 400°C temperature range can be readily seen to occur in the same temperature range as the decomposition of the cellulose fraction It can be envisaged that as the cellulose decomposes, escaping gases create channels in the peat, thus increasing the overall porosity while leaving the lignin skeleton of the charred samples virtually intact The decomposition of the cellulose can be seen to expose new surfaces in the peat material as the temperature increases, the surface area reaching its maximum value at about 400°C Above this temperature the surface area decreases due to the gradual degradation of the lignin skeleton of the peat, reaching a value of 9 m^2 g^{-1} by 900°C

The BET (N_2) values presented for the surface areas of the peat materials in Tables 3 23 and 3 24 agree well with the BET (N_2) areas reported by Chiou and co-workers who reported that the surface area of SOM materials are typically 0 5 to 1 5 m^2 g^{-1} (14, 19, 29) A higher BET (N_2) value of 25 m^2 g^{-1} was reported by Poost and McKay (15) for a peat moss sample This value is about ten times the value

reported here and in view of the area quoted by others is quite high The nearest value which approaches it is the surface area of 18 m^2 g^{-1} reported by Chiou *et al* (14) for a freeze-dried humic acid sample However, the authors suggested that in this instance the large surface area was an artefact of the freeze-drying procedure Since the pre-treatment temperature used by Poost and McKay (15) was similar to the pre-treatment temperatures used by Chiou *et al* (14, 19) and in this work, it can be concluded that in all likelihood it is due to natural sample variability Further comment on the use of N_2-adsorption for the measurement of the surface areas of SOM is discussed later

(b) Methylene Blue Dye Adsorption

The second method used to measure the surface area of the PF was the adsorption of methylene blue from aqueous solution The results for the adsorption of methylene blue by the peat are presented in Table 3 26 The table shows x/m, the amount of dye adsorbed (in mg) per gram of PF (dry weight), and Caq, the equilibrium concentration of the dye in solution (mg cm^{-3})

Table 3 26 Results for the Adsorption of Methylene Blue by PF

Caq (mg cm^{-3})	x/m (mg g^{-1})
0 001	20 0
0 009	81 9
0 019	62 6
0 051	97 4
0 151	98 6
0 239	121 3
0 401	198 0

Note Caq values are ± 0 004 mg cm^{-3}, x/m values are ± 2 1 mg g^{-1}

The adsorption isotherm of x/m versus Caq is shown in Figure 3 26 A comparison of Figure 3 26 with the isotherm classification system of Giles *et al* (9) (Figure 3 5, see Section 3 1 4) suggested that the isotherm was of the H-type This was indicated by the fact that at low concentrations of the dye the slope of the isotherm was observed to rise sharply, this is characteristic of strong adsorbate-adsorbent interaction, i e most of the dye was being adsorbed from solution by the peat at these concentrations It can be seen from Figure 3 26 that there was a plateau-like region between Caq values of 0 02 mg cm^{-3} to 0 25 mg cm^{-3} Above the Caq

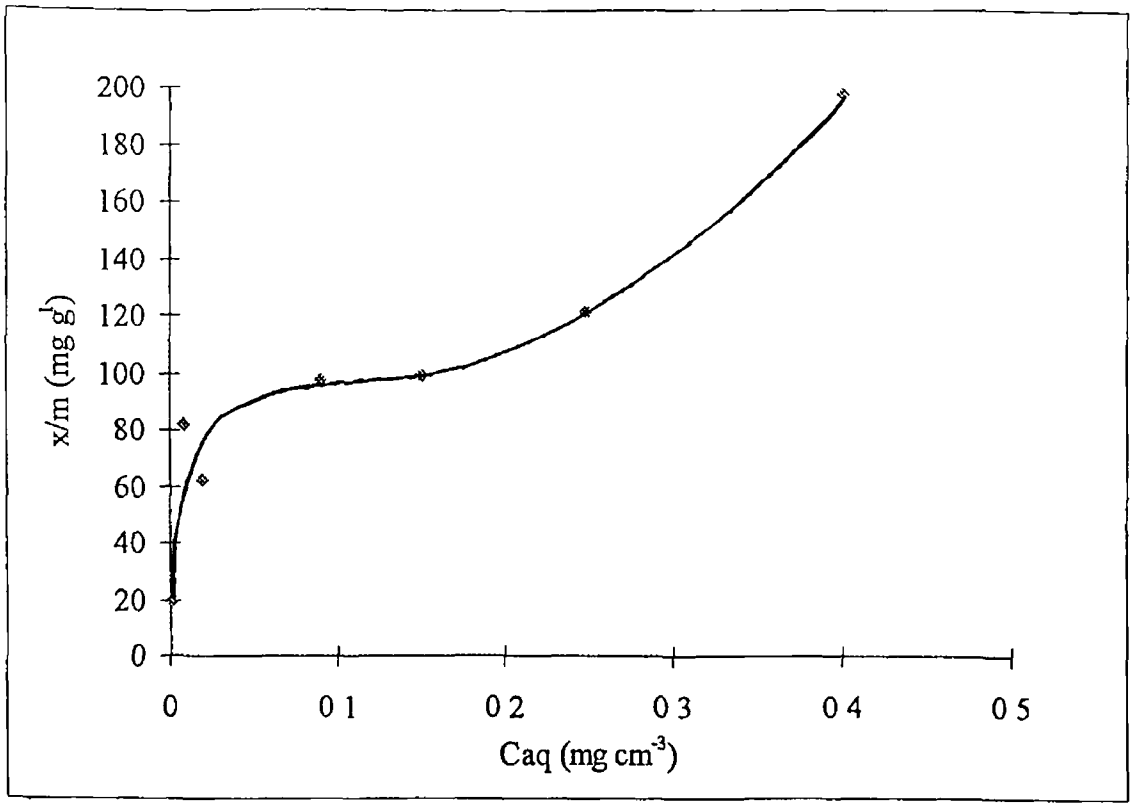

Figure 3 26 **Adsorption Isotherm for the Uptake of Methylene Blue on PF**

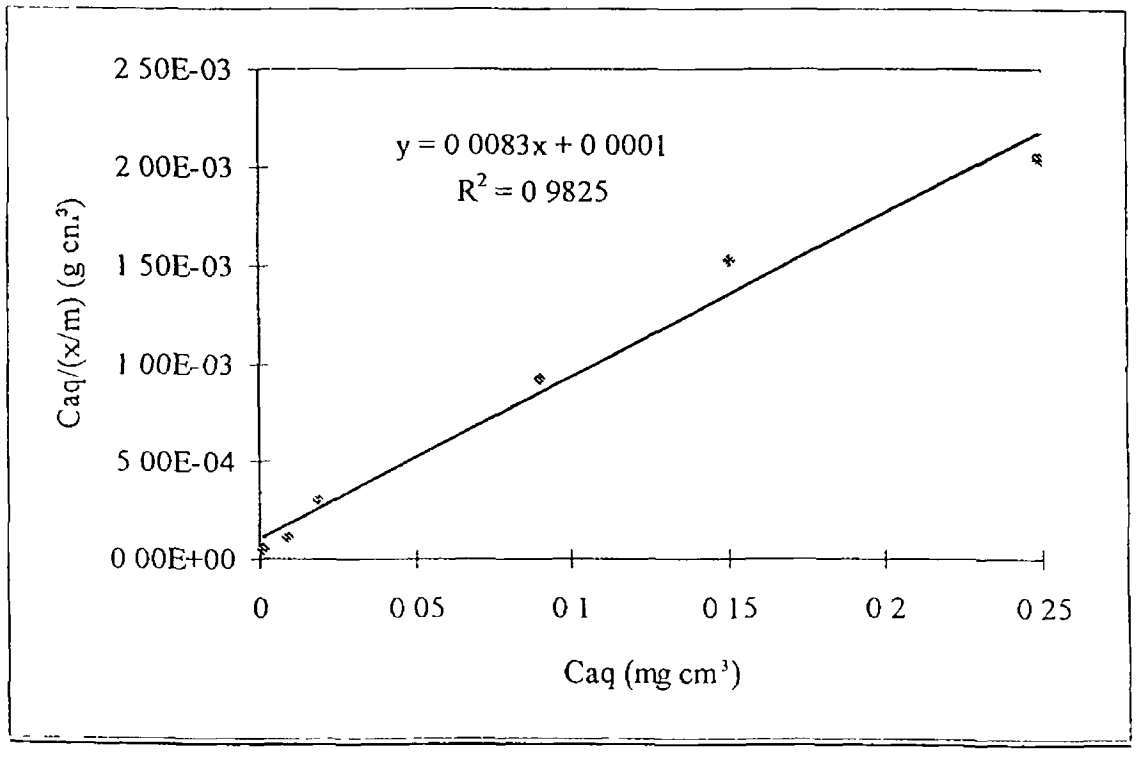

Figure 3 27 **Plot of Caq/(x/m) versus Caq**

value of 0 25 mg cm^{-3} there was a further increase in the amount of dye adsorbed by the peat which is generally assumed in the literature to indicate multi-layer formation (7)

The linear form of the Langmuir equation (Equation 3 3) was subsequently applied to the results shown in Table 3 26 The results were plotted as a graph of Caq/(x/m) versus Caq which gave a straight line of slope 0 0083 g mg^{-1}, an intercept of 0 0001 g cm^{-3} and a linear correlation of 0 983, see Figure 3 27 From Section 3 1 5 it will be recalled that the monolayer capacity of a solid, Q_m, and the slope of the line are inversely related, i e slope = $1/Q_m$ Thus, the monolayer value for the adsorption of methylene blue by PF was calculated to be 120 48 (± 2 10) mg g^{-1}

The surface area of the PF was calculated using Equation 3 9, taking the molecular weight of the dye molecule as 284 and the A_m value for the dye to be 120 x 10^{-20} m^2 (15), a value which assumes that the dye is adsorbed flat on the surface (see later) The surface area of the PF was calculated to be 307 0 (± 5 0) m^2 g^{-1} Poost and McKay (15) also used methylene blue adsorption to measure the surface area of peat moss, they reported an area of 100 m^2 g^{-1} for peat moss by this method This value is about 30 % of the surface area value reported in this work

The surface area of 307 0 m^2 g^{-1} is significantly greater than the BET(N_2) value of 2 3 m^2 g^{-1} reported in this work In accounting for the large increase in the surface area of the peat moss when compared to the BET(N_2) area, Poost and McKay (15) noted that the uptake of the dye was in fact most likely due to a combination of chemisorption and adsorption of colloidal micelles of the dye Chemisorption of the dye by the peat sample was occurring due to the fact that methylene blue is positively charged in solution and as a result there was strong ionic interaction between the positively charged dye molecules and the negatively charged peat surface (due to the presence of ionised surface hydroxyl and carboxyl groups) This observation is supported from the classification of the isotherm as H-type which is an indication of strong adsorbate-adsorbent interactions as in chemisorption The most likely reason for the increased surface area comes from the observation that dye molecules tended to form colloidal micelles in solution which can be adsorbed onto the surface of solid material As a result the Q_m value calculated does not correspond to monolayer coverage of the surface (see below)

It was thought that repeating the adsorption of the dye at the point of zero charge of the peat and at low concentrations of the dye may have given more reliable results But, it will be recalled from Section 2 5 2 that it was not possible to determine the zero point of charge of the PF Thus, it was not possible to see if such

an experiment would have produced any significant difference to the monolayer capacity and thus the surface area of the PF

It is possible that the large surface area increase in aqueous solution is due to the swelling of the PF in solution which results in an 'opening up' of the material and the exposure of new surfaces which are capable of adsorbing solute molecules However, it is much more reasonable to assume that the large bulky nature of the dye molecule would cause it to be excluded from small pores, thus, reducing the surface area available for adsorption of the probe

Gregg and Sing (7) were of the opinion that the use of dyestuffs to determine the surface area of solids should be regarded as a secondary method at best since there are many problems associated with their use The two principal problems are

(i) the uncertainty associated with evaluating a value for Q_m It has been found that the plateau region of adsorption isotherms do not necessarily correspond to monolayer coverage of the surface of the solid In many instances there can be appreciable amounts of solvent molecules adsorbed on the surface along with the probe In addition, adsorption isotherms can reach a plateau region which is considerably lower than the calculated monolayer capacity of the solid for the probe

(ii) the difficulty in arriving at a suitable value of A_m for the dye molecule The range in A_m values for a particular dye can be considerable, for instance A_m values for methylene blue have been quoted as 102×10^{-20} and 108×10^{-20} m^2 per molecule from adsorption studies on Spheron and Graphon (both forms of graphite with well defined surface areas) respectively from aqueous solution (7) However, these A_m values were considered to be too small if the adsorbed molecules were lying flat on the surface, which would require the A_m to be 135×10^{-20} m^2 per molecule, but the A_m values were too high if the molecules were oriented perpendicular to the surface, which would require an A_m of only 75×10^{-20} m^2 per molecule It has been suggested that the molecules are adsorbed in a vertical orientation, but that there is mutual repulsion occurring between the dye molecules Other workers have quoted A_m values of 78×10^{-20} m^2 per molecule from the adsorption of methylene blue on graphitised carbon black and 130×10^{-20} m^2 per molecule on nongraphitised carbon black (7)

Therefore, even in situations where the monolayer capacity of the dye can be determined with reasonable accuracy there is still considerable uncertainty as to the value of A_m for the dye

The large differences in A_m values arise from the lack of knowledge concerning the orientation of the adsorbed dye molecules which may be adsorbed in a vertical or horizontal position with respect to the surface of the solid In addition to molecular orientation, it is well known that most dyestuffs tend to from colloidal micelles at high concentrations in aqueous solution Thus, it is possible that such micelles are adsorbed onto the solid, which would not correspond to monolayer coverage of the solid surface Gregg and Sing (7) state that the following factors should be taken into account when the use of a dyestuff is being considered to determine the surface area of a solid,

(i) the size and shape of the molecule should be known,

(ii) the orientation of the adsorbed dye molecule on the surface of the solid should be known,

(iii) the number of adsorbed layers must be known Dyestuffs are particularly prone to the formation of colloidal micelles in solution, thus, it must be known whether the molecules are adsorbed as single molecules, dimers or as micelles,

(iv) the dye molecule should be of sufficient solubility to enable the flat portion of the isotherm to be reached experimentally

In the light of the discussion of Gregg and Sing (7) the surface area calculated for PF from the adsorption of methylene blue must be accepted with caution It is more than likely that the Q_m value of 120 5 mg g^{-1} does not correspond to monolayer coverage of the surface of the peat, but to multilayer adsorption or to the adsorption of colloidal micelles In addition, there is no way of determining that the dye was adsorbed flat and that the area occupied by one dye molecule is 120 $x10^{-20}$ m^2 Thus, the surface area value measured from methylene blue adsorption is doubtful and in all probability greatly overestimates the surface area (if it is assumed that the dye molecule is not excluded from internal pores which may be present in the material)

(c) Negative Adsorption of Chloride Ions

In view of the difficulty associated with the measurement of the surface area of PF, an additional method was used to compare with the surface area values measured by the positive adsorption methods The exclusion volume method which is based on the negative adsorption (i e repulsion) of Cl^- ions from the surface of the

PF was used (see Section 3 2 1 1 and 3 2 1 2) The exclusion volume method had several advantages over the positive adsorption methods which were as follows (10)

(i) the method relies solely on the repulsion of Cl^- ions from the negatively charged peat surface It does not require positive adsorption of probe molecules, thus the ambiguity over adsorption versus absorption by the peat is avoided,

(ii) it does not require that values for either the monolayer coverage of the peat surface (Q_m) or the cross-sectional area of the probe (A_m) be known The problems associated with measurement of Q_m and A_m particularly in relation to methylene blue adsorption have already been discussed

(iii) apart from swelling of the PF due to its immersion in the aqueous solution, structural changes due to the sorption of the probe are avoided The newly exposed surfaces due to swelling are presumably available for the repulsion of Cl^- ions Thus, the surface area of swollen PF should be measurable by this method

The results for the negative adsorption of Cl^- ions by PF are presented in Table 3 27 The table shows, Cpf and Caq, which are the concentration of Cl^- ions in the PF and in the bulk aqueous solution respectively, and Vex, the corresponding exclusion volume from which Cl^- ions were repelled from the surface of PF The values of V_{ex} were calculated from Equation 3 10

$$|Z_1| C_1 V_{ex} = \frac{|Z_1| Caq\, V - |Z_1| Cpf\, V}{m_S} \qquad \text{Equation 3 10}$$

To measure the surface area of the PF a graph of Vex versus $Caq^{-1/2}$ was plotted, see Figure 3 28 The best straight line through the data points had a slope of 3×10^{-5} $mol^{-1/2}$ $dm^{3/2}$ kg^{-1}, an intercept of 0 0005 dm^3 kg^{-1} and a correlation of 0 6602 The surface area of the PF was calculated from the results using Equation 3 12

$$S_E = (\beta)^{1/2} (slope/2) \qquad \text{Equation 3 12}$$

which directly relates the slope of the line of Vex versus $Caq^{-1/2}$ to the surface area of the PF Inserting the value of the slope into Equation 3 12 the surface area of the PF which repelled Cl^- ions was calculated to be 0 05 m^2 g^{-1} under the conditions of the experiment

Table 3 27 **The Results for Exclusion Volume Experiment on PF**

Caq (mM dm^{-3})	Cpf (mM dm^{-3})	Vex (x 10^{-3} dm^3 kg^{-1})
0 149	0 139	2 67
0 330	0 317	1 57
0 479	0 453	2 15
0 641	0 625	0 99
0 641	0 623	1 15
0 948	0 899	2 05
0 944	0 913	1 32
2 946	2 856	1 08
4 147	4 109	3 85
10 587	10 370	0 78
13 085	12 846	0 91

Note values are ± 5 %

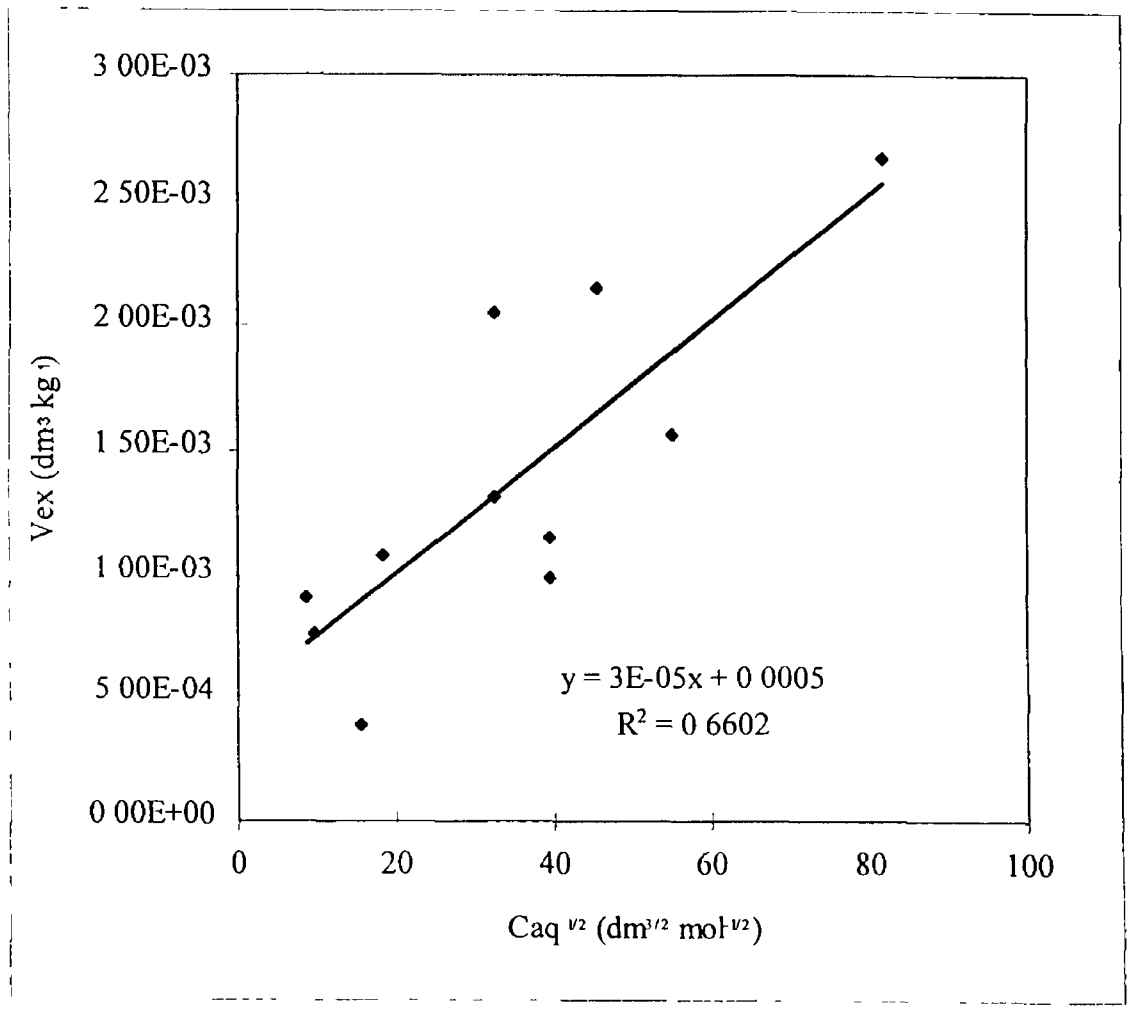

Figure 3 28 **Plot of Exclusion Volume (Vex) versus $Caq^{-1/2}$**

It has been previously discussed that the exclusion volume method has been successfully used to measure the surface area of several materials including kaolinite (26) and illite and montmorillonite samples (20-22) In particular the method appears to confirm the swell model for the expandable clays There is no reference in the literature to its application for the measurement of the surface area of SOM materials, though it has been reported by Schofield (23) that the surface area of jute fibre was about 160 m^2 g^{-1} from Cl^- exclusion experiments Thus, extension of the exclusion volume method for surface area determination to organic matter samples may be possible The exclusion surface area value of 0 05 m^2 g^{-1} is considerably closer to the BET (N_2) value than the methylene blue determined area In addition, the size of the exclusion area conforms to the generally observed trend that the exclusion area is less than the BET (N_2) area This trend is thought to be due to the formation of complexes between surface charged groups and exchangeable cations which produce an electrically neutral surface at that point (10)

However, the main difficulty encountered with this method was that with increasing concentrations of NaCl, the solution became increasingly dark in colour which indicated the increased solubilization of peat materials As a consequence the physical state of the surface of the peat was being altered as the experiment proceeded which was an undesirable phenomenon Thus, the validity of the result is doubtful and must be accepted with caution

Considering the various values obtained for the surface areas of PF it should be noted that a direct comparison of the values obtained by the vapour phase and the aqueous phase methods must be done with caution, since a distinct division must be made between the two sets of results The vapour phase measurements require the sample to be dry, thus shrinkage of the peat will have occurred This reduces the surface area which would be normally present under naturally occurring soil conditions Whereas, the aqueous based methods, would result in some swelling of the PF in solution, which may lead to increased surfaces available for adsorption

It is clear from a comparison of the results that the surface areas measured by the methods differ greatly in value, see Table 3 28 It can be seen from Table 3 28 that the surface area measured by the BET (N_2) method is over 130 times smaller than the surface area determined by methylene blue adsorption In contrast the exclusion surface area was found to be about 50 times smaller than the BET (N_2) value However, the surface areas reported in the literature for peat and other SOM materials also differ significantly in value, ranging from less than 1 m^2 g^{-1} by BET (N_2) estimation (14, 19, 29), to 100 m^2 g^{-1} (15) from methylene blue adsorption, and

Table 3.28 Comparison of Methods of Surface Areas Determination and the Measured Surface Area Values for PF

Method of Determination	Surface area ($m^2 g^{-1}$)
BET (N_2)	2 3
Methylene blue adsorption	307
Exclusion volume	0 05

areas in excess of 800 $m^2 g^{-1}$ from ethylene glycol retention (12) Such differences for the surface area of SOM arise from the methods used to measure the area of the sample and the interpretation of the results obtained

It has already been discussed why the surface area values obtained by the methylene blue and exclusion volume methods should be accepted with caution This is particularly so in the case of the methylene blue method which in all likelihood over estimates the surface area of the PF, since the determined Q_m value of 120 48 $m^2 g^{-1}$ does not correspond to monolayer coverage of the peat surface Therefore, surface area determination by weakly interacting probes such as N_2 or interacting probes such as the vaporous alcohols remain to be considered

It will be recalled that Pennell and Rao (13) argued for a large surface area for SOM They considered that N_2 and non-polar organic vapours are adsorbed onto the external surface of SOM which are small and are of the order of 1 to 2 $m^2 g^{-1}$ In contrast polar molecules such as EG can interact with the SOM, and penetrate into the internal regions of the material, and as a result explore the total surface area of the SOM which is done in a similar manner to the model proposed for clays However, Chiou *et al* (29) pointed out that the low organic matter contents of the soils discussed by Pennell and Rao (13) support their argument and would give similar surface area results for both for the interactive and non-interactive probes This was supported by later work by Rutherford and Chiou (40) which showed that sorption of neutral organic vapours on organic soils gave linear isotherms (and much larger surface areas than BET(N_2) values

Chiou *et al* (14) distinguished between two kinds of surfaces present in SOM and other soil solids, namely the 'free surface' and the 'apparent surface' The 'free surface' of a material consisted of the solid-vacuum interfacial area of the solid It existed before the surface area was measured and the act of measuring it does not physically or chemically alter the solid material in any way, nor does it involve the probe penetrating into the solid matrix itself to reach internal surfaces The 'free

surface' area can only be measured using non-interacting probes such as N_2 On the other hand the 'apparent surface' was the surface which was measured by the use of interacting probes such as water or organic vapours in the case of SOM which either chemically or physically alter the material being examined Included under the 'apparent surface' definition were the internal surfaces measured by the use of polar probe molecules on expandable clays and SOM As a consequence the 'apparent surface' area is not a well defined quantity, since it is dependent on the strength of interaction of the probe molecule used, and it does not in fact refer to a specific surface area which existed prior to the measurement

However, the extension by Chiou *et al* (14) of the definition of apparent surface area to include the expandable surface area of clays leads to the erroneous conclusion that the internal surface areas measured for expandable clays is incorrect The argument of Chiou *et al* (14) that the internal surfaces of these clays does not exist before the measurement and that the surface area measured depends on the exchangeable cation present are valid observations and should be taken into account when surface area is being measured, but the authors fail to make evident that such phenomena as swelling is a well established phenomena It does occur under field conditions and water and other polar molecules do in fact swell these clays, giving them substantial increases in surface area Thus, the definition of Chiou *et al* (14) for surface area is a valid working definition of what constitutes a material's surface in the case of a well defined, rigid material, however, it fails to take into account well established swelling phenomena of the expandable clays

It is difficult if not impossible to deduce whether probes are being adsorbed onto the surface of the organic material or being absorbed into the material (see following section) All researchers agree that non-interacting probes such as N_2 are adsorbed onto the external surface of the material, and that their adsorption does not in any way alter the physical or chemical properties of the material Thus, it is valid to state that the surface area measured by N_2 adsorption is the surface area 'seen by the molecule' Similarly, it can be argued that the surface area measured by an interacting probe is the area 'seen' by such a molecule In other words surface area is an operationally defined property of the material in question, that is assuming that the probe is adsorbed and not absorbed into the matrix of the material Therefore, the surface area of the peat is directly dependent on the sorption mechanism of the probe which is discussed later

These results do emphasise the need to understand the material being studied and the possible interactions (either chemical or physical) which may be occurring It is evident that the distinction between adsorption and absorption of the probe is not

as clear as would be desired for investigative purposes Therefore, a method of surface area determination which does not lend itself to ambiguity in relation to its mechanism of operation, and which measures the area of the peat in an aqueous environment to take into account swelling of the material, is required The best candidate would appear to be the exclusion volume method for reasons which have already been discussed The method is based on the repulsion of ions from the surface of the material, thus structural changes which may be brought about by the sorption of the probe are avoided The measured area of about 0 05 m^2 g^{-1} is surprisingly close to the BET (N_2) value and would strongly support a small surface area for PF However, as has been stated, the use of the exclusion volume method is not without its problems The results reported here are questionable since it was noticed that at higher concentrations of NaCl the solution became increasingly darker in colour indicating organic material was being released into solution, which would have consequently altered the nature of the material being studied

In conclusion, the case for a small surface area for the PF and other peat materials examined in this study is favoured The surface areas measured by the BET (N_2) method were low and was supported by the exclusion volume measurement Though there is not firm evidence to support this conclusion, it is based partially on the fact that the peat materials studied had undergone relatively little decomposition As such, they consist of a mixture of several large organic polymers, particularly cellulose and lignin, which give the peat materials a rigid, well defined structure This is unlike the situation for the well decomposed SOM material which have been studied by other researchers Highly decomposed SOM is more ambiguous in structure and intermolecular interactions because of its higher state of humification As a result the presence of (extensive) internal surfaces for PF is unlikely since it can undergo little expansion, this would be particularly the case for the claim that the internal surfaces can only be explored by interacting probes The question of surface area is returned to briefly in the following section where the sorption of alcohol vapours are used to measure the surface area of PF (see Table 3 30)

3 5 2 2 Sorption of Alcohols from the Vapour and Aqueous Phases

(a) Sorption from the Vapour Phase

The results for the sorption of the vapour phase alcohols by the PF under 0 % humidity conditions are shown in Table 3 29 The table shows the amount of alcohol retained per gram of PF (x/m) versus the relative vapour phase concentration (C/C_o)

Table 3 29 **The Results for the Sorption of Vapour Phase Alcohol By Peat Fibre Under 0 % Relative Humidity**

(a) Ethanol Sorption

Vapour Concentration (C/C_o)	x/m (mg g^{-1})
0 09	11 30
0 12	13 00
0 17	27 86
0 32	34 04
0 51	101 65

(b) 2-Propanol Sorption

Vapour Concentration (C/C_o)	x/m (mg g-1)
0 03	3 81
0 08	5 46
0 14	6 63
0 27	11 10
0 33	25 89

(c) 1-Butanol Sorption

Vapour Concentration (C/C_o)	x/m (mg g^{-1})
0 02	2 59
0 09	3 36
0 17	4 40
0 22	4 81
0 40	15 47

(d) 1-Pentanol Sorption

Vapour Concentration (C/C_o)	x/m (mg g^{-1})
0 13	2 31
0 28	2 89
0 36	4 98
0 41	5 82

Note for C_o values see Appendix D, x/m values are ± 10 %

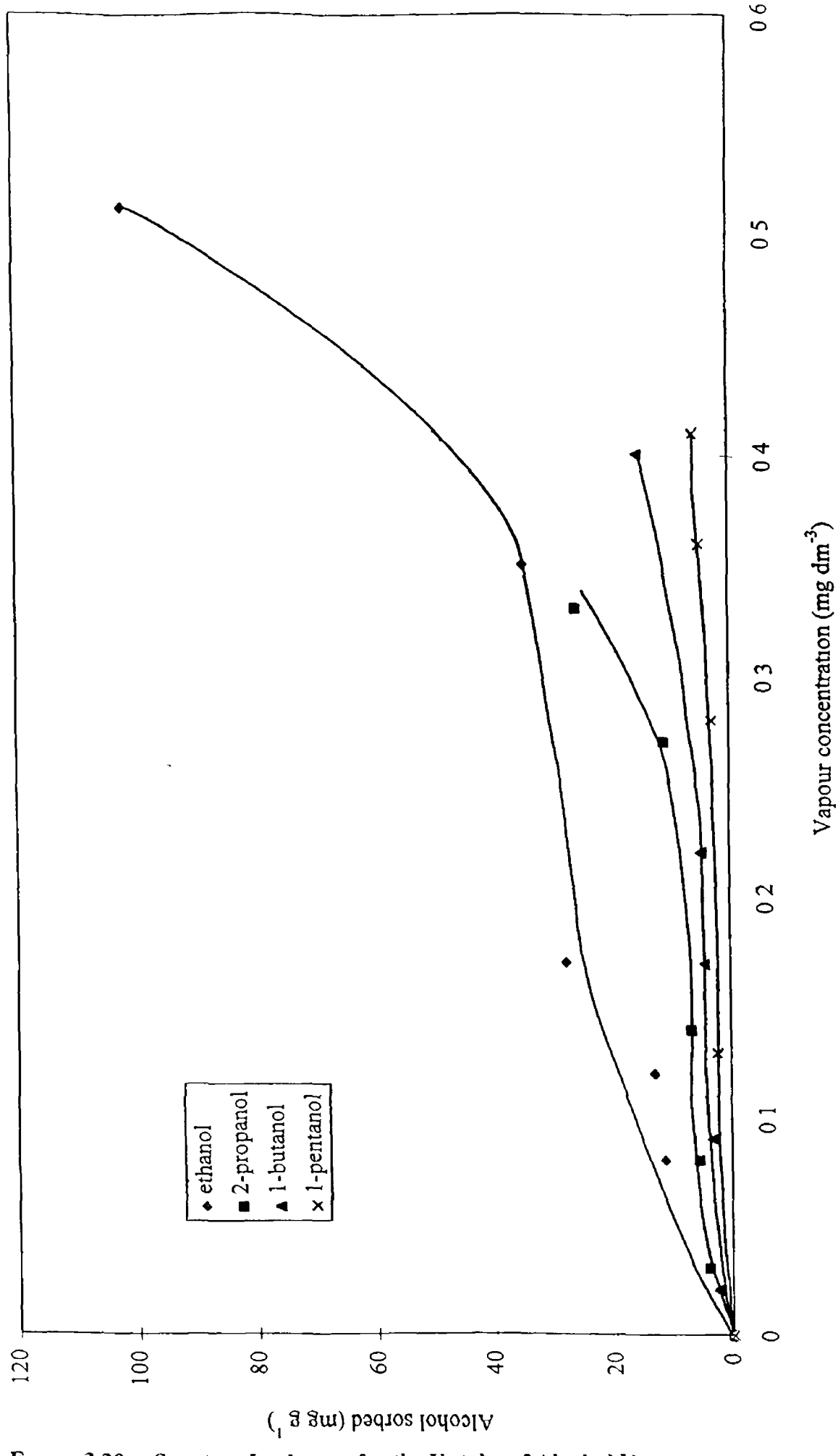

Figure 3.29 Sorption Isotherms for the Uptake of Alcohol Vapours by Peat Fibre at 0 % Relative Humidity

of the alcohol vapour (the relative pressure (P/P_0) was not measured), where C and C_0 (mg dm^{-3}) are the concentration of the alcohol vapour in the gas phase and its saturation value in the gas phase respectively The C_0 values for the alcohols were calculated from the vapour pressure data from the CRC Handbook of Chemical and Physical Data (52) to the ideal gas equation,

$$PV = nRT \qquad \text{Equation 3 20}$$

where the symbols have there usual meaning The calculation of the C_0 values for the alcohols are shown in Appendix D

The sorption isotherms are illustrated in Figure 3 29, this figure shows the amount of alcohol sorbed by the PF (mg/g) versus the relative concentration (C/C_0) of the alcohol vapours at 20°C From an examination of Figure 3 29 it can be seen that the isotherms appear to conform to the Brunauer type II isotherm, this is the typical isotherm type encountered for non-porous solids (7) (see next paragraph) This is evident from the slope of the isotherms at low relative concentrations which were observed to be concave to the x-axis As the relative vapour concentration was increased the isotherms approached a plateau region, which corresponds to monolayer coverage of the solid surface (7), at higher relative concentrations the isotherms were observed to increase further in a convex fashion to the x-axis The plateau region of the isotherm was found to be small in the case of ethanol but to increase in broadness and flatness as the alcohol series was ascended (i e from ethanol to 1-pentanol)

It should be noted that the isotherms are incomplete and do not extend beyond $C/C_0 > 0\ 5$ Thus, the classification of the isotherms as type II is by no means definite It is possible that if the relative concentrations were increased to near saturation levels of the vapour phase the isotherms would in fact have reached a second plateau region, which would indicate that they were of type IV Such isotherms are encountered for porous solid materials, the second plateau corresponding to saturation of the pores (7) The inability to reach C/C_0 values greater than 0 5 was due to the low vapour pressures of the higher alcohols which made it difficult to obtain high vapour concentrations of the alcohols In addition, it was found that at high concentrations ($C/C_0 > 0\ 5$) of the lower alcohols there was significant condensation of the alcohols onto the walls of the tubing, this invariably lead to dripping of the alcohol liquid onto the peat samples, resulting in erroneously high weight readings

From Figure 3.29 it can be seen that the amount of alcohol sorbed by the peat decreased in the order ethanol > 2-propanol > 1-butanol > 1-pentanol. The trend follows the increasing size of the molecules and their decreasing polarity. The non-linear shape of the isotherms would suggest that the principal mechanism of alcohol uptake by the PF was by adsorption. This conclusion contradicts the results of Chiou *et al* (19, 40, 46, 47) who found that the sorption isotherms of organic vapours from the gas phase on peat and other SOM materials were invariably liner to high relative pressures of the vapour. The linear shape of the isotherms was considered to be due to absorption of the vapours by the SOM. However, in some instances it was noted that there was a slight curvature to the isotherms at low and high P/P_0 (46). At low P/P_0 levels the curvature was considered to be due to specific adsorption of organic vapours by surface functional groups. Similarly, the curvature of the otherwise linear isotherms at high P/P_0 values approaching saturation of the gas phase were considered to be due to condensation of the vapour onto the surface of the SOM.

The contradiction between the results presented in this work and those reported by Chiou and co-workers is most probably due to the large particle size of the PF used (500-180 μm), and to its rigid structure of the peat which would have significantly hindered absorption of the alcohols into the peat interior. However, it was evident from the length of time required for equilibrium to be reached for the lower alcohols that there was some absorption occurring. It was found that the time required for the weight increase in PF to reach equilibrium took up to 21 days in the case of the ethanol and 2-propanol studies . This time peroid reduced to less than 14 days for the 1-pentanol studies.

As to the nature of the adsorption forces, it has been noted by Gregg and Sing (7) that the van der Waals forces of attraction are the dominant forces of adsorption for non-polar molecules. Whereas, for polar molecules, such as alcohols, van der Waals forces become secondary and the principal mechanism of adsorption is due to polar interactions. Thus, the dominant mechanism for the sorption of the alcohol vapours by PF would appear to be dependent on the polarity of the alcohol. It can be readily seen that the sorption trend decreases with decreasing polarity of the alcohols. This observation is supported by the findings of Chiou and Shoup (45) who noted that the relative order of sorption of benzene and chlorinated benzene derivatives on soil samples was dependent on their polarity. The order of sorption was found to decrease with decreasing polarity of the molecules. In addition, it was reported that SOM had higher sorption capacities for polar molecules such as water and ethanol than for non-polar molecules such as carbon tetrachloride etc.

(b) Sorption from the Aqueous Phase

The results for the sorption of the alcohols from aqueous solution by the PF are shown in Table 3 30 The table shows x/m, the amount of alcohol retained per gram of dry PF, versus Caq, the equilibrium concentration of the alcohol in solution, which was in the concentration range 0 to 120 mg dm^{-3} Figure 3 30, which illustrates the results graphically, shows that the amount of alcohol retained by the PF ranged from 0 to 1 6 mg g^{-1} It can be seen that the sorption of the alcohols from aqueous solution increased in the order ethanol < 2-propanol < 1-butanol < 1-pentanol < 1-hexanol, which was the reverse of the vapour phase results This trend was in keeping with the observation that the amount of organic solute taken up from aqueous solution by SOM is inversely related to the solubility of the solute in water (36-38) In this instance the solubility of the alcohols decreased in the order ethanol ~ 2-propanol (both miscible) > 1-butanol > 1-pentanol > 1-hexanol The partition model proposes that SOM acts as a partitioning medium for organic solutes in very much the same manner as an organic liquid phase Hydrophobic molecules which have low water solubilities can escape from the polar water environment into the interior of the less polar SOM phase Thus, sorption is a consequence of van der Waals forces and hydrophobic interactions

A direct comparison of the results with sorption data reported elsewhere for the uptake of organic solutes by SOM is difficult, but in general the amount of alcohol retained by PF is less than the values reported elsewhere for SOM (36, 38-40) This may reflect the greater water solubility of the alcohols compared to other organic solutes and the nature (i e polarity) of the SOM materials being used The sorption of benzene and carbon tetrachloride on various organic materials including peat, muck and cellulose was reported to range from 0 to 20 mg g^{-1}, in the solute concentration range 0 to 1000 mg dm^{-3} (39) The lowest sorption capacity was found to be on cellulose (< 1 mg g^{-1}) due to its high relative polar nature compared to the other materials The low sorption capacity of the PF may be due to its high cellulose content, which accounts for about 30 % of its dry weight from TGA results, see Section 2 5 2

It has been argued by Chiou and co-workers that sorption of organic solutes from the aqueous phase by SOM is by partition (i e absorption) The evidence which they cited to support the partition model included the linearity of the isotherms to high relative concentrations of organic compounds from the vapour and liquid phases (36-38) Concerning the shape of the isotherms, it can be seen from Figure

Table 3.30 **Results for the Sorption of Alcohols from Aqueous Solution by PF**

(a) Ethanol Sorption

Solute concentration ($mg\ dm^{-3}$)	x/m ($mg\ g^{-1}$)
17 89	0 09
40 15	0 10
60 35	0 05
78 61	0 08
86 75	0 10
111 52	0 11

(b) 2-Propanol Sorption

Solute concentration ($mg\ dm^{-3}$)	x/m ($mg\ g^{-1}$)
23 85	0 05
43 5	0 20
55 30	0 19
74 48	0 14
117 03	0 32

(c) 1-Butanol Sorption

Solute concentration ($mg\ dm^{-3}$)	x/m ($mg\ g^{-1}$)
17 54	0 12
27 80	0 24
45 25	0 38
72 01	0 42
93 15	0 44
113 13	0 77

Table 3.30 **Results for the Sorption of Alcohols from Aqueous Solution by PF (Continued)**

(d) 1-Pentanol Sorption

Solute concentration ($mg\ dm^{-3}$)	x/m ($mg\ g^{-1}$)
23 51	0 40
42 38	0 40
68 42	0 47
91 75	0 49
119 45	0 68

(e) 1-Hexanol Sorption

Solute concentration ($mg\ dm^{-3}$)	x/m ($mg\ g^{-1}$)
18 75	0 22
36 75	0 51
52 05	0 82
66 25	1 05
88 15	1 18
115 62	1 49

Note solute concentration and x/m values are ±10 %

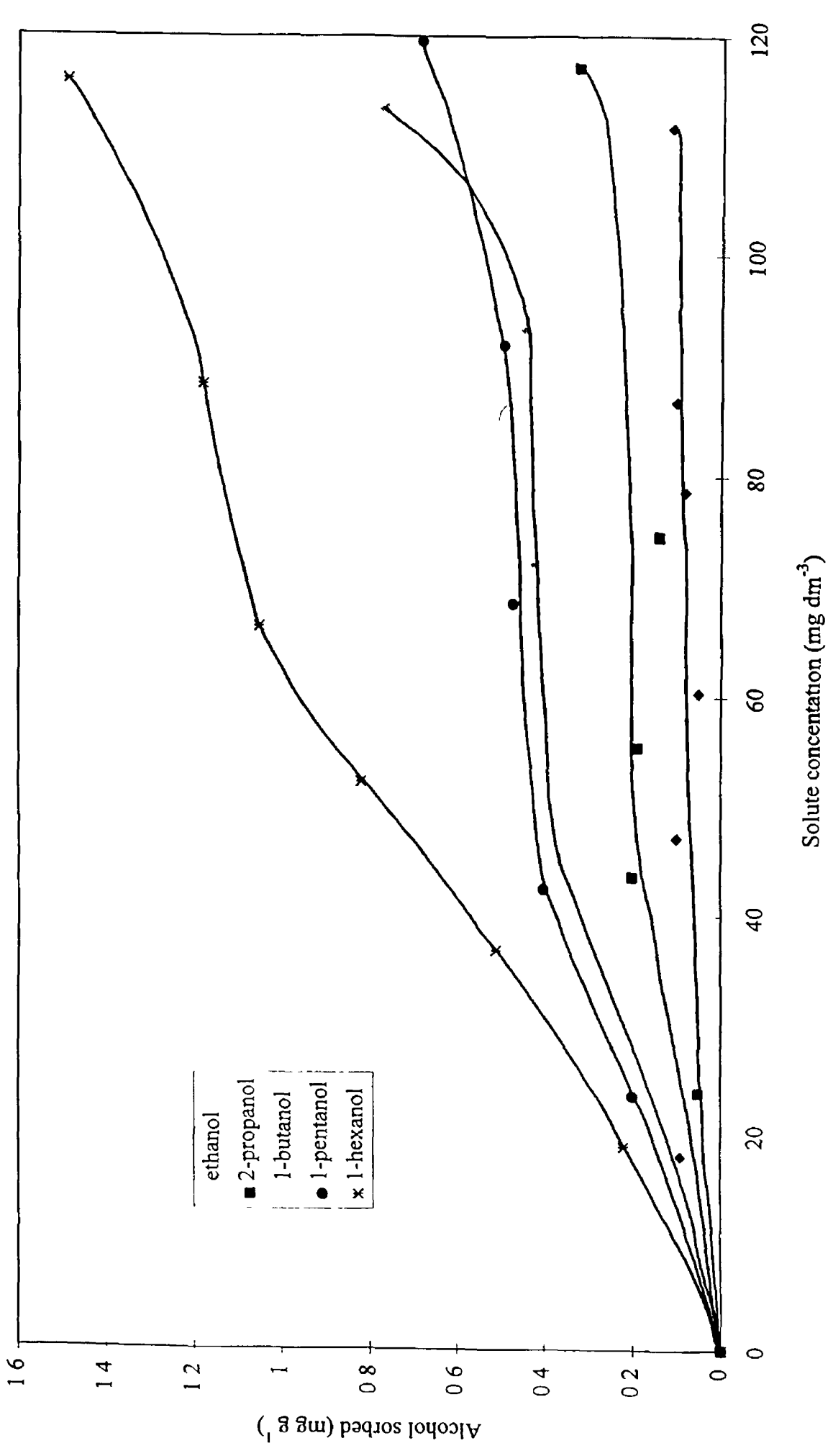

Figure 3.30 Sorption of Alcohol Series from Aqueous Solution by PF

3 30 that the sorption isotherms are non-linear in the concentration range studied The ethanol to 1-pentanol isotherms are similar to the L 3 category of isotherms, while the convex shape of the 1-hexanol isotherm at low concentrations would suggest it belongs to the S 3 category, refer to Figure 3 5 (9) For the 1-hexanol isotherm this would suggest that adsorption of 1-hexanol molecules is poor at low solute concentrations, but as the amount of alcohol adsorbed to the surface increases, the affinity of the surface to adsorb more molecules increases

The non-linear shape of the isotherms would suggest that adsorption of the alcohols was occurring and not partitioning, which contradicts the results of Chiou and co-workers (36-38) The explanation for the non-linearity of the isotherms is again to do with the size fraction used and the rigidity of the peat structure, as previously discussed for the vapour phase results

(c) Sorption from the Aqueous Phase, Binary Mixtures

An additional observation noted by Chiou and co-workers to support the partition model for SOM is the lack of solute competition in binary solute systems (38) It has been found that the amount of solute retained by SOM does not significantly diminish due to competition for adsorption sites Thus, to determine if adsorption or absorption of the alcohols was occurring, binary sorption isotherms of the alcohols were determined This consisted of comparing the sorption of 1-hexanol (the alcohol with the highest uptake capacity on PF) with the uptake of ethanol, 2-propanol, 1-butanol and 1-pentanol The results of this study are shown in Table 3 31 and illustrated graphically in Figure 3 31 (a) to (d) As can be seen the sorption isotherms for the single and binary sorption isotherms are virtually identical There is a slight decrease in the amount of alcohols sorbed by the PF in the binary system, but it was very small and was considered to be negligible This suggests that at low solute concentrations there is little direct competition between solute molecules for adsorption sites This may be a result of low coverage of the PF surface at low solute concentrations which would allow for the simultaneous uptake of binary solutes without direct competition occurring However, further study of the binary solute systems to higher solute concentrations would be required to support this assumption

Table 3.31 **Results for the Sorption of the Binary Alcohol Solutions by PF**

(a) Ethanol versus 1-hexanol

Ethanol		1-Hexanol	
concentration ($mg\ dm^{-3}$)	x/m ($mg\ g^{-1}$)	concentration ($mg\ dm^{-3}$)	x/m ($mg\ g^{-1}$)
30 70	0 05	24 80	0 33
64 40	0 03	52 10	0 60
94 30	0 04	79 70	0 91
126 40	0 03	111 40	1 20

(b) 2-Propanol versus 1-Hexanol

2-Propanol		1-Hexanol	
concentration ($mg\ dm^{-3}$)	x/m ($mg\ g^{-1}$)	concentration ($mg\ dm^{-3}$)	x/m ($mg\ g^{-1}$)
18 36	0 13	15 1	0 25
59 63	0 16	37 3	0 71
87 85	0 19	57 55	0 90
109 26	0 17	85 95	1 10
122 26	0 19	-	-
140 44	0 28	-	-

(c) 1-Butanol versus 1-Hexanol

1-Butanol		1-Hexanol	
concentration ($mg\ dm^{-3}$)	x/m ($mg\ g^{-1}$)	concentration ($mg\ dm^{-3}$)	x/m ($mg\ g^{-1}$)
25 1	0 04	19 75	0 36
35 0	0 26	36 7	0 65
49 05	0 23	60 1	0 77
76 6	0 27	76 43	1 03
93 6	0 20	-	-
101 5	0 19	-	-

(d) 1-Pentanol versus 1-Hexanol

1-Pentanol		1-Hexanol	
concentration ($mg\ dm^{-3}$)	x/m ($mg\ g^{-1}$)	concentration ($mg\ dm^{-3}$)	x/m ($mg\ g^{-1}$)
24 44	0 37	24 35	0 30
43 84	0 35	47 40	0 72
55 14	0 43	61 78	0 75
66 63	0 53	83 50	0 94
101 52	0 42	102 58	1 20
122 38	0 39	-	-

Note solute concentration and x/m values are ± 10 %

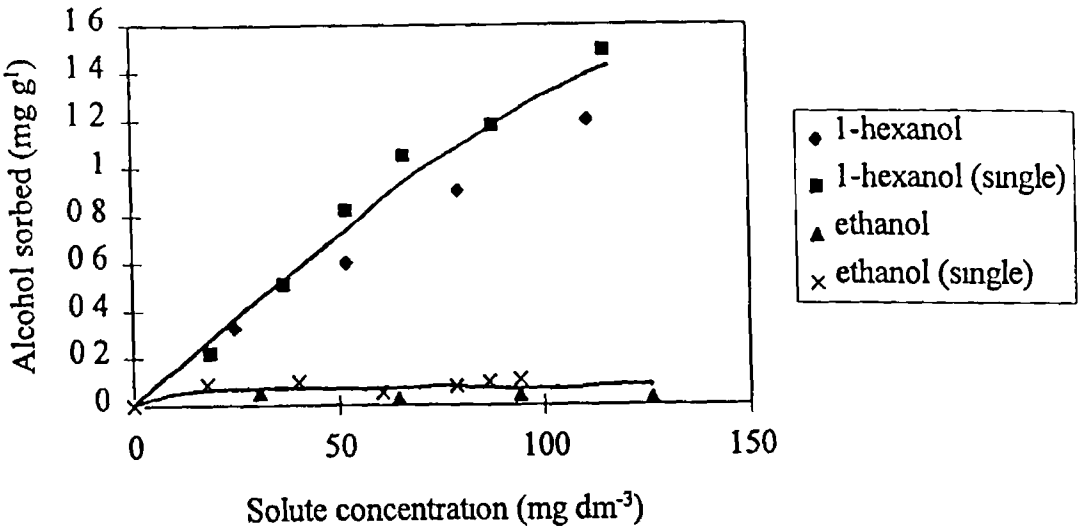

(a) 1-Ethanol versus Hexanol

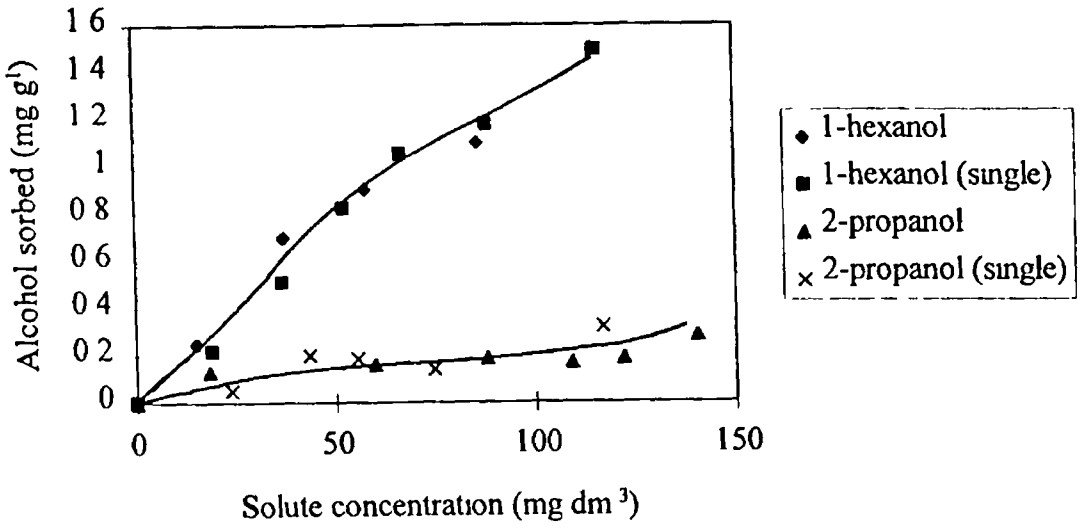

(b) 1-Propanol versus Hexanol

Figure 3 31 Binary Sorption Isotherms for Alcohols on PF

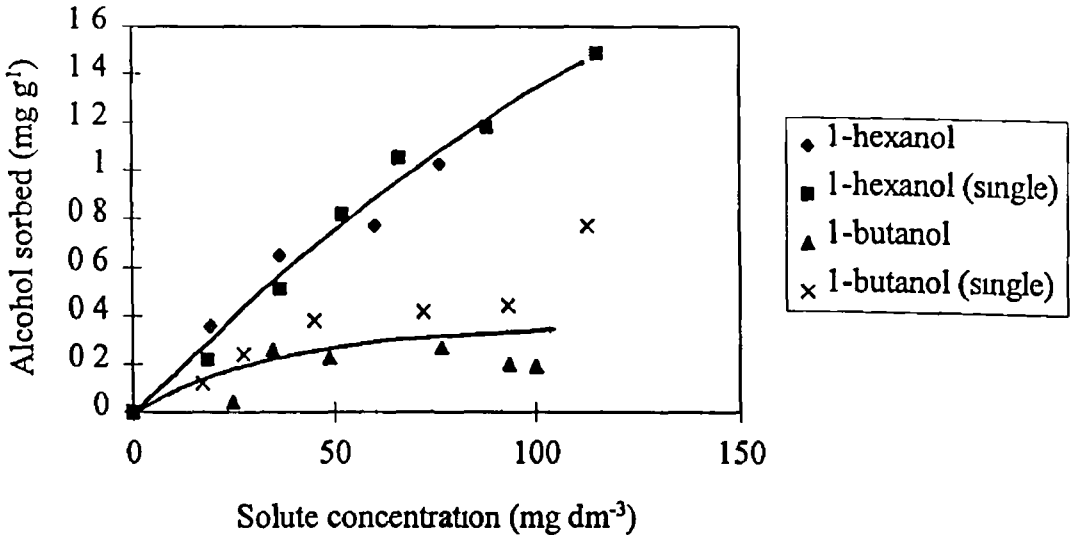

(c) 1-Butanol versus Hexanol

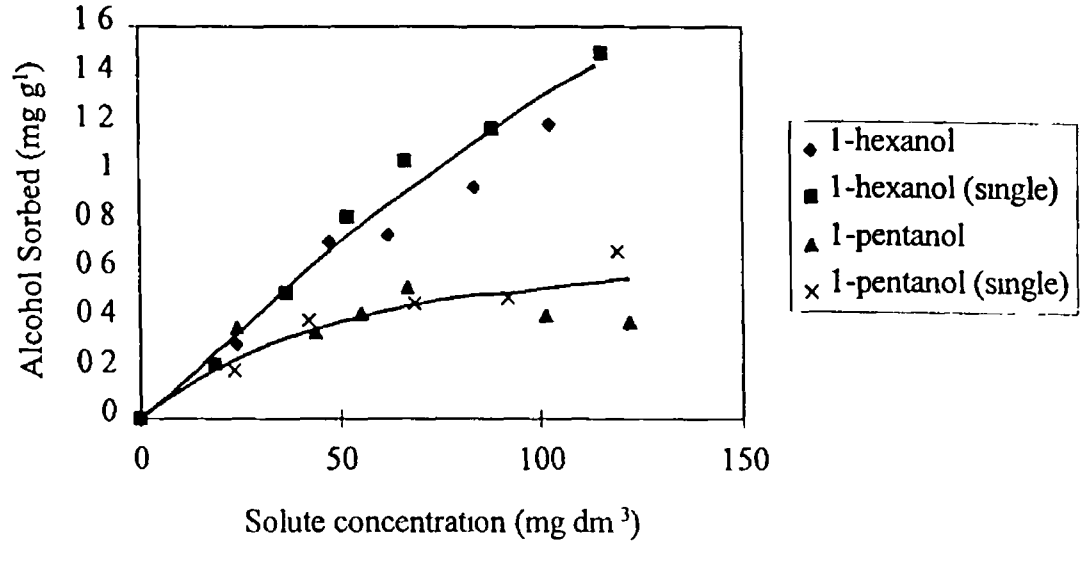

(d) 1-Pentanol versus Hexanol

Figure 3 31 Binary Sorption Isotherms for Alcohols on PF (Continued)

The results from vapour and aqueous phase sorption results were also used to calculate the surface area of the PF (see Section 3 5 2 1), see Table 3 32

Table 3 32 Calculated A_m, Q_m and Surface Area Values Using Alcohols

Alcohol	A_m ($x10^{-20}$ m^2 mol^{-1})	Vapour phase		Aqueous phase	
		Q_m (mg g^{-1})	area (m^2 g^{-1})	Q_m (mg g^{-1})	area (m^2 g^{-1})
Ethanol	23 0	34 3	103 0	0 11	0 33
2-Propanol	27 5	9 5	26 0	0 17	0 45
1-Butanol	31 1	4 0	10 2	0 39	1 04
1-Pentanol	34 7	3 7	8 8	0 45	1 16

The A_m values (the cross-sectional area of the alcohol molecules) were calculated by applying Equation 3 8 to the molecular weight and density data for the alcohols given in the CRC Handbook (52) The amount of alcohol required for monolayer coverage, Q_m, of the PF was calculated by applying the linear form of the Langmuir and BET equations (Equation 3 3 and 3 4) to the aqueous and vapour phase results respectively (in the case of the aqueous phase sorption data the 1-hexanol results were not used since this isotherm did not belong to the Langmuir classification) The data points which gave the best straight line, were used to calculate Q_m, the correlation for the straight lines (R^2) were > 0 93 in all cases

It can be seen from Table 3 32 that the calculated surface area of the PF using the data in Table 3 29 decreased as the size of the alcohol increased The measured surface area decreased from about 100 m^2 g^{-1} in the case of ethanol to about 9 m^2 g^{-1} for 1-pentanol Thus, the surface area values from the vapour phase results can be seen to support the conclusion that absorption of the lower alcohols was also occurring, since the trend can be attributed to the increasing difficulty of the alcohol molecules to penetrate into the interior of the peat as their size becomes bigger As a result, the alcohol molecules become increasingly confined to the surface of the PF and approach the BET(N_2) value of 2 3 m^2 g^{-1} Conversely the aqueous phase results show the opposite trend in surface areas as they increase from 0 33 m^2 g^{-1} for ethanol adsorption to 1 16 m^2 g^{-1} for 1-pentanol adsorption The small surface areas measured for the aqueous phase give additional support for a small surface area for PF

3 6 4 Conclusion

The three different methods used to measure the surface area of the PF gave three different surface area values ranging from 0 05 m^2 g^{-1} for the exclusion volume method to 307 m^2 g^{-1} from methylene blue adsorption studies In the case of the methylene blue results it has been reported elsewhere (15) that multilayer formation and not monolayer coverage of the peat was occurring Thus, the large value was considered to be an over estimate the true surface area With the exclusion volume results it was noted that there was increasing solubility of peat materials at the higher NaCl concentrations which would have effected the surface area measured Although, the small surface area measured by this method did agree well with the BET (N_2) value of 2 3 m^2 g^{-1} The closeness of the BET (N_2) and exclusion volume values was considered to support the opinion that the surface area of the PF samples was small

From the results it is evident that there is considerable ambiguity over the surface area of the PF The results from the surface area measurements can be interpreted to fit either surface area model The underlying problem is of course the sorption mechanism of the probe, i e whether adsorption or absorption is occurring, and if the probe's interaction with SOM does in any way alter the material It is clear that what constitutes the surface area of SOM cannot be resolved until an acceptable method which is unambiguous in its mechanism is found

Of the three methods used to determine the surface area of the peat fibre, the negative adsorption method is the most promising, since it does not require a knowledge of the cross-sectional area of the probe or the monolayer capacity to be determined Thus, this method should be investigated further, particularly in comparative studies with other surface area methods Future work should examine if any correlation exists between the methods, particularly between the BET(N_2) and the negative adsorption method, and should include the examination of several different forms of soil organic matter

Sorption studies examined the uptake of a series of alcohols from the vapour and aqueous phases It was observed that the sorption of the alcohol vapours gave Brunauer type II isotherms on the peat, and that the non-linear shape of the isotherm indicated that adsorption was occurring There was some evidence to suggest that absorption was also occurring, particularly in the case of the lower alcohols The order of uptake of the alcohols was ethanol > 2-propanol > 1-butanol > 1-pentanol which followed the decreasing polarity of the molecules This observation was in keeping with the results of other studies which reported that sorption of organic vapours from the vapour phase onto SOM materials was dependent on the polarity of

the molecules But, the results differed in that the dominant sorption mechanism was by adsorption and not partitioning into the peat

Further work should include the continuation of the sorption isotherms to higher relative concentrations of the alcohol vapours This is to examine whether the sorption isotherms can be classified as being either type II or type IV It has been discussed in Section 3 1 4 that the type II isotherm is characterised by a continuous increase in its slope with increasing vapour concentration, while the type IV isotherm is characterised by the formation of a plateau at high vapour concentrations (7) In addition, the effects of water suppression on the uptake of the alcohol vapours by the peat fibre could also be examined by repeating the sorption studies at different relative humidities It will be recalled that the presence of water vapour significantly reduces the amount of organic vapour retained by soil samples when adsorption is the principal sorption mechanism (45), but its effects are less pronounced when partitioning dominates the sorption process (40)

It was found that sorption from the aqueous phase gave non-linear isotherms, indicating that adsorption was occurring, and that the order of uptake was the reverse of the vapour phase studies, namely 1-hexanol > 1-pentanol > 1-butanol > 2-propanol > ethanol The order of uptake was inversely related to the water solubility of the alcohols which was in agreement with observations reported elsewhere The dominant forces of sorption from the aqueous phase were considered to be due to a combination of van der Waals and hydrophobic interactions However, additional work is required to fully understand the sorption processes This would include extending the sorption isotherms to higher solute concentrations This is to examine if the non-linearity of the curves extends to higher solute concentration, since it is possible that the observed shape of the isotherms is due to specific solute-surface interactions at low concentrations (46), and that partitioning of the alcohols dominates at higher solute concentrations once all the surface sites have become saturated

The results from the binary sorption studies suggested that competition between the alcohols for sorption sites on the peat surface was minimal in the concentration range studied However, if adsorption is accepted as the dominant sorption mechanism then it would be expected that competition between the solutes should occur It may be that at low solute concentration surface coverage is so low as to be able to accommodate competing solute molecules without noticeable competition occurring between them Therefore, extension of the binary isotherms to higher solute concentrations is recommended to examine if competition becomes more noticeable at higher concentrations

3 7 References

(1) Bailey, G W and White, J L , J. Agri. Food Chem., 12, 324-332 (1964)

(2) Spencer, W F and Cliath M M , J. Agri. Food Chem., 20(3), 645-649 (1972)

(3) Nash, R G and Woolson, E A , Science, 157, 924-927 (1967)

(4) Schwarzenbach, R P , Gschwend, P M and Imboden, D M , Environmental Organic Chemistry, Wiley Interscience (1993)

(5) Hamaker, J W and Thompson, J M , in Organic Chemicals in the Soil Environment, eds Goring, C A I and Hamaker, J W , Volume 1, 49-143, Marcel Dekker Inc (1972)

(6) Adamson, A W , Physical Chemistry of Surfaces, Wiley Interscience (1990)

(7) Gregg, S J and Sing, K S W , in Adsorption, Surface Area and Porosity, Academic Press (1967)

(8) Gross, J M and Wiseall, B , Principles of Physical Chemistry, McDonald and Evans Hand Book Series, McDonald and Evans Ltd , Plymouth (1979)

(9) Giles, C H , MacEwan, T H , Nakhwa, S N and Smith, D , J. Chem. Soc., 786, 3973-3993 (1960)

(10) Sposito, G , The Surface Chemistry of Soils, Oxford University Press (1984)

(11) Huang, P M , "Adsorption Processes in the Soil", In Handbook of Environmental Chemistry, Hutzinger, O (ed), Part 2 (A), 47-59 Academic press (1982)

(12) Bower, C A and Gschwend, F B , Soil Sci. Proc., 16, 342-345 (1952)

(13) Pennell, K D and Rao, P S C , Environ Sci. Technol , 26, 402-404 (1992)

(14) Chiou, C T , Lee, J-F and Boyd, S A , Environ. Sci Technol., 24, 1164-1166 (1990)

(15) Poost, V J P and McKay, G , J. Appl. Poly. Sci., 23, 1117-1129 (1979)

(16) Carter, D L , Heilman, M D and Gonzalez, C L , Soil Sci , 100, 356-360 (1965)

(17) Ratner-Zohar, Y , Banin, A and Chen, Y , Soil Sci Soc Am J , 47, 1056-1058 (1983)

(18) Rao P S C , Ogwada, R A and Rhue, R D , Chemosphere, 18(11/12), 2177-2191 (1989)

(19) Chiou, C T , Rutherford, D W and Manes, M , Environ. Sci. Technol , 27, 1587-1594 (1993)

(20) Edwards, D G , Posner, A M and Quirk, J P , Transact Faraday Soc., 61, 2808-2815 (1965)

(21) Edwards, D G , Posner, A M and Quirk, J P , Transact. Faraday Soc., 61, 2816-2819 (1965)

(22) Edwards, D G , Posner, A M and Quirk, J P , Transact. Faraday Soc., 61, 2820-2823 (1965)
(23) Schofield, R K , Nature, 160, 408-410 (1947)
(24) Mattson, S , Soil Sci , 28, 179 (1929), *op cit* Schofield, R K , Nature, 160, 408-410 (1947)
(25) van den Hul, H J and Lyklema, J , J. Colloid Inter. Sci., 23, 500 (1967)
(26) Schofield, R K and Samson, H R , Discuss. Faraday Soc., 18, 135-1145 (1954)
(27) Quirk, J P, Nature, 188, 253-254 (1960)
(28) Jurinak, J J and Volman, D H , Soil Sci., 83, 487-496 (1957)
(29) Chiou, C T , Lee, J-F and Boyd, S A , Environ. Sci. Technol., 26, 404-406 (1992)
(30) Bowman, M C , Schechter, M S , and Carter, R C , J. Agri. Food Chem., 13(4), 360-365 (1965)
(31) Hance, R J , Weed Res., 5, 108-114 (1965)
(32) Mills, A C and Biggar, J W , Soil Sci. Soc. Amer. Proc., 33, 210-216 (1969)
(33) Leistra M , J. Agri. Food Chem., 18(6), 1124-1126 (1970)
(34) Shin, Y -O , Chodan, J J and Wolcott, A R , J. Agri. Food Chem., 18(6), 1129-1133 (1970)
(35) Saltzman, Kliger and Yaron, J. Agri Food Chem., 20(6), 1224-1226 (1972)
(36) Chiou, C T , Peters, L J and Freed, V H , Science, 206, 831-832 (1979)
(37) Chiou, C T , Peters, L J and Freed, V H , Science, 213, 683-684 (1981)
(38) Chiou, C T, Porter, P E and Schmedding, D W , Environ. Sci. Technol , 17, 227-231 (1983)
(39) Rutherford, D W , Chiou, C T and Kile, D E , Environ Sci Technol , 26, 336-340 (1992)
(40) Rutherford, D W and Chiou, C T , Environ Sci. Technol , 26, 965-970 (1992)
(41) Yaron, B and Saltzman, S , Soil Sci. Soc Amer Proc , 36, 583-586 (1972)
(42) Hanson, W J and Nex, R W , Soil Sci , 76, 209-214 (1953)
(43) Jurinak, J J , Soil Sci Soc. Am Proc , 21, 599-602 (1957)
(44) Call, F , J Sci Food Agric , 8, 630-639 (1957)
(45) Chiou, C T and Shoup, T D , Environ. Sci. Technol , 19, 1196-1200 (1985)
(46) Chiou, C T , Kile, D E and Malcolm, R L , Environ. Sci. Technol , 22, 298-303 (1988)
(47) Chiou, C T and Kile, D E , Environ Sci Technol., 28, 1139-1144 (1994)
(48) Instruction Manual for PulseChemisorb 2700, Micrometrics Corporation, USA (1986)
(49) Instruction Manual for the 94-17B Chloride Ion Selective Probe, Orion Corporation, USA (1994)

(50) Schnitzer, M and Hoffman, I , Soil Sci. Soc. Amer. Proc., 31, 708-709 (1967)

(51) Ranta, J , Ekman, E and Asplund, D , Proc. 6th Int. Peat Congrs., 6, 670-675 (1980)

(52) Lide, D R (ed), CRC Handbook of Chemistry and Physics, 75th edition (1995)

Chapter 4

Elimination of Contaminants from Waste Gases by Biofiltration

4 Introduction

Biofiltration may be defined as the use of a biologically active filter material for the elimination of gaseous contaminants from a waste gas stream which is passing through the filter-bed Within the filter-bed the contaminants are retained by the filter material and are subsequently degraded by the micro-organisms which inhabit the filtering material Since the early 1980s, biofiltration has been used increasingly for the treatment of waste gases emanating from industrial and agricultural sources (1) As with other gas treatment systems, the aim of biofiltration is to substantially reduce (or completely eliminate) the levels of gaseous contaminants present in the waste gas stream The elimination is achieved due to the presence of micro-organisms in the filter-bed which, under oxygen rich conditions, oxidise the contaminants to end products such as CO_2 and H_2O

There are few examples to be found in the literature concerning the use of biofiltration prior to the early 1980s Several early applications of biofioltration have been described elsewhere (2, 3) These refer to the use of soil beds to eliminate odours emanating from water treatment plants and agricultural sources However, there was little interest in the mechanism of the elimination process other than the microbial action responsible for the degradation of the contaminants In North America, biofiltration remained confined to a few locations, because biological methods in general were considered to be too inefficient when compared to other methods such as combustion which were available at that time However, more recently the' growing restrictions on the emission levels of gaseous pollutants has resulted in an increased interest in biofiltration in North America In Europe, notably in Germany and the Netherlands, and in Japan there has been a longer tradition, and more wide spread use of biofiltration for the reduction of odours prior to the 1980s (4-6)

A reduction in the levels of gaseous contaminants being released into the atmosphere is desirable for two reasons

(i) to remove the unpleasant odour that can be associated with waste gases from particular sources Many malodorous compounds are detectable to the human sense of smell at very low concentrations, for example sulphur containing compounds such as hydrogen sulphide (H_2S), or methanethiol (CH_3SH) can be detected at ppm levels The presence of such unpleasant odours are the most noticeable form of air pollution At their most trivial, malodours can be a nuisance, restricting out-door activities, but they can result in feelings of nausea

and can in some instances pose a serious health risk to local populations The growing problem of malodorous gases is partially due to their increasing production, but mainly to the spread of urban areas to sites close to industrial and agricultural zones (7) Traditionally, local populations had no choice but to put up with unpleasant odours, but increasingly local residents see no reason why they should have to suffer their presence

(ii) to reduce the levels of hazardous materials being released into the environment Many of the released compounds can pose serious health risks to local human populations, and also have detrimental effects on the environment Apart from the well-known examples of sulphur dioxide (SO_2) and nitrous oxides (NOx), increasing amounts of organic compounds are being released into the atmosphere The eventual fate of many of the organic compounds in the environment is unknown The results of these gaseous contaminants include acid rain, deforestation, corrosion to buildings, reduction of crop yields, depletion of the ozone layer, and the formation of smog over large cities

Government legislation and international agreements are setting maximum emission levels for atmospheric contaminants, and thereby applying pressure on industry to reduce the discharge levels of these compounds Most European countries have national laws relating to air pollution, the strongest being in the heavily industrial countries such as Germany, the United Kingdom and the Netherlands, and there are several European Union directives on air pollution (8) These directives relate particularly to NOx, SO_2, CO, and CO_2 levels from automobile exhausts and industrial sources, but there is growing awareness for the need to limit the emissions of volatile organic compounds as well International agreements such as the Geneva Convention of 1979 and its subsequent protocols commit the signing countries to substantial reductions in the emissions of NO_x, SO_2 and volatile organic compounds (8)

The gaseous contaminants present in waste gases can be divided into two general classes

(i) volatile inorganic compounds (VICs), such as ammonia (NH_3) and H_2S, which are two of the principal malodorous compounds present in waste gases Other VICs include SO_2, HCl, and NO_x

(ii) volatile organic compounds (VOCs), which include a wide range of organic compounds, but in particular aliphatic, aromatic and chlorinated hydrocarbons and other oxygen, nitrogen and sulphur containing organic compounds

This chapter discusses the application of biofiltration for the treatment of waste gases, particularly in relation to reducing the emissions of odorous compounds It begins with a brief outline of the various methods available for the treatment of waste gases before proceeding to a detailed discussion of biofiltration It describes the various operating conditions required for the operation of a biofilter The development of biofiltration and the literature concerned with the elimination of both the VOC and VIC classes of compounds are also discussed The results from a lab-scale biofilter for the elimination of vapour phase ethanol are presented in Section 4 7 of this chapter

4 1 Methods of Waste Gas Treatment

The methods that are presently available for the treatment of waste gases can be divided into four categories, namely physical, thermal, chemical, and biological methods

(i) Physical methods The physical methods of waste gas treatment are adsorption, absorption and condensation It should be noted that all physical methods merely eliminate the contaminants from the gas stream, they do not degrade the compounds This can be advantageous where the contaminants are valuable, and they can be reused in the industrial process However, in most instances the contaminants are unwanted and in this case a further processing of the waste is necessary The physical methods of waste gas treatment are as follows

- Adsorption As the waste gas flows through an adsorbent material, the contaminant molecules can condense onto the surface of the adsorbant and are held there by the van der Waals forces of molecular attraction The adsorbants used include activated carbon, silica gel, and zeolites These materials have very large surface areas, typically in the range of 300 to 1000 $m^2 g^{-1}$ Once the adsorbant has become saturated it can be regenerated by heating it, or by passing steam or hot air over it to remove the adsorbed contaminants
- Absorption This method is also referred to as wet scrubbing The contaminated gas is forced to rise up through a packed bed over which downward moving water flows The more readily water soluble compounds are rapidly absorbed into the aqueous phase The removal of VICs by this method is generally better than that of VOCs, due to the usually low water solubility of most VOC compounds However, the addition of oxidising agents such as permanganate or hypochlorite to degrade the absorbed contaminants can increase the overall rate of both VIC and VOC removal from the gas stream

- Condensation With condensation, the waste gas is cooled to sub-zero temperatures which liquefies the contaminants, thus, removing them from the gas stream Typically, temperatures of about -40° C are required to condense moderately volatile VOCs and even lower temperatures are needed for the removal of the more volatile compounds

(ii) Thermal Methods The thermal methods of waste gas treatment involves the degradation of the contaminants by oxidation at high temperatures, typically in the range of 700° to 1200° C Thermal treatment of waste gases require that there is good mixing of the waste gas with the oxidant, that the temperature is sufficiently high to ensure complete combustion of the contaminants, and that the gas has a residence time of at least 0 5 to 1 second in the furnace Failure to completely oxidise the contaminants can result in the release of harmful by-products and of NO_x into the atmosphere Catalytic combustion can considerably reduce the temperatures required for elimination to below 500° C However, the use of such catalysts can be expensive as they have to be frequently replaced due to ageing, and because of the build up of poisoning agents which reduce the activity of the catalyst

(iii) Chemical Methods Strong oxidising agents such as ozone or chlorine can be used to break down the contaminant molecules This is not a favoured method of treatment because of the expense of these agents, and the difficulty involved in handling these compounds due to their toxic and corrosive natures

(iv) Biological Methods The biological methods involve the uses of micro-organisms to degrade the contaminant molecules By far the largest group of micro-organisms used are the bacteria, but filamentous fungi and yeasts are also employed to some extent The micro-organisms use the contaminant molecules as a carbon source and/or energy source, depending on the nature of the molecule, and convert it to new cell biomass, and ultimately under aerobic conditions, to CO_2 and H_2O Thus, with biological systems, the contaminants are removed from the gas stream and eliminated in one step There is no accumulation of waste or harmful by-products which have to be dealt with further on in the treatment process

The three biological methods of waste gas treatment are, bioscrubbers, trickle beds, and biofilters These are distinguished by

- the mobility of the aqueous phase, which is either moving or stationary,
- the micro-flora (micro-organisms), which are either freely dispersed in the aqueous phase or are immobilised on a support material, see Table 4 1

Table 4.1 **Distinction of the Biological Waste Gas Treatment Systems (9)**

Micro-flora	Aqueous phase	
	Mobile	Stationary
Dispersed	Bioscrubber	-
Immobilised	Trickle bed	Biofilter

(a) Bioscrubbers

The bioscrubber consists of two units, a scrubber compartment and a regeneration tank (see Figure 4 1) In the scrubber compartment, incoming waste gas rises up through a tower and comes into contact with downward falling water droplets As a result, oxygen and the contaminant molecules are absorbed into the liquid phase The liquid then passes to the regeneration tank where the contaminant molecules are degraded by the freely suspended micro-organisms, which are kept agitated to prevent their settling Under high concentrations of contaminants extra oxygen is added to the tank to ensure complete elimination of the molecules The microbial activity is kept at its optimum level by careful control of the physical and chemical parameters of the aqueous phase, such as temperature, pH and the addition of nutrients

Because of the low water solubility of the majority of VOCs, diffusion between the waste gas and aqueous phase is the principal limitation in the bioscrubber and in the other two biological techniques Diffusion can be improved by allowing the micro-organisms to circulate in the scrubber compartment, so that the contaminant molecules are degraded as they are absorbed Another solution is to add an organic solvent to the bioscrubber, which readily absorbs the VOCs, and in turn transfers it to the aqueous phase (10, 11) The solvent must fulfil a number of criteria, namely it must be non-toxic to the micro-organisms, non-degradable, have a low water solubility and have a low partial pressure to prevent loss through evaporation Solvents which have been suggested include silicones and phthalates

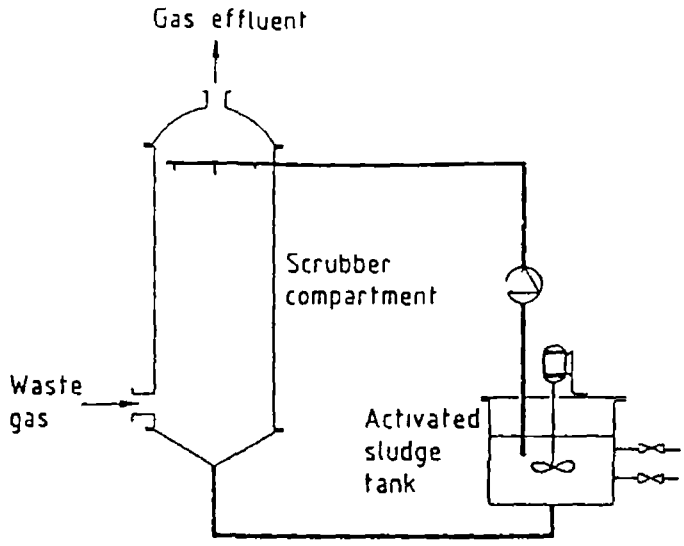

Figure 4 1 **Schematic Diagram of a Bioscrubber (9)**

(b) Trickle Beds

A typical trickle bed consists of a large tower filled with an inert packing material which acts as a support for the development of a biofilm (see Figure 4 2) The trickle bed is similar in construction to the biofilter (see below) except that there is a constant flow of water down over the biofilm The waste gas flows up through the bed and oxygen and the contaminant molecules are absorbed into the aqueous phase They are subsequently transferred to the biofilm where they are degraded by the micro-organisms

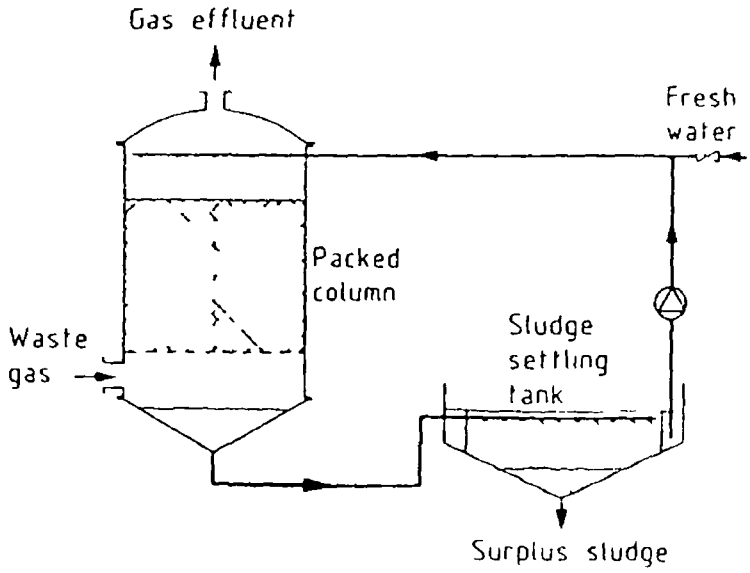

Figure 4 2 **Schematic Diagram of a Trickle Filter (9)**

The packing materials used include ceramics, activated carbon, glass, etc These materials have moderate surface areas to allow for biofilm development Typically the contact areas of these materials is about 100 to 300 m^2 m^{-3} in the trickle filter column In addition, use of these materials creates large void spaces in the column, which prevents clogging of the bed by excess growth of the biofilm Again, nutrient and pH levels are controlled to optimise biological activity within the bed

(c) Biofilters

The biofilter consists of a bed of biologically active material, such as peat, compost or wood chippings (2, 12), with other materials such as tree bark, heather, polyethylene beads, etc , added to give bulk to the filter-bed A typical biofilter is shown schematically in Figure 4 3 The filter material is usually stacked to a bed height of 1 to 2 m, higher beds tend to compact with age which leads to increase in the back pressure of the system As the waste gas flows through the bed, oxygen and contaminant molecules diffuse into the liquid phase and in turn are transferred into the biolayer where degradation takes place To prevent the biofilter from drying out, the gas is passed through a humidifier unit before entering the biofilter, and a sprinkling system periodically wets the bed The size of the biofilter can vary considerably, from tens to hundreds of square metres for single bed systems, depending on the volume of gas to be treated and the area available for the filter-bed Where space is limited multi-stage biofilters consisting of stacked beds have been constructed (2) Multi-stage biofilters have the added advantage of improving the elimination of mixed compounds from waste gases

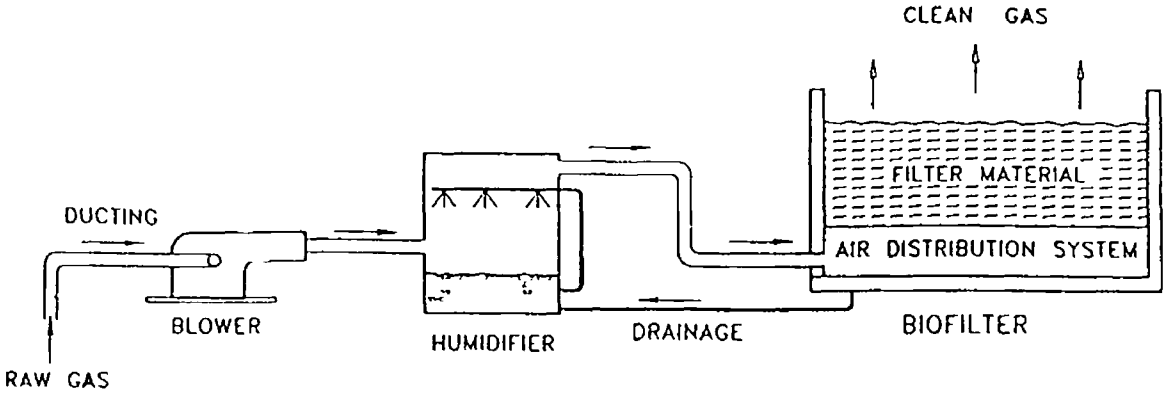

Figure 4 3 Schematic Diagram of a Typical Biofilter (2)

Comparisons between the biological systems (i e bioscrubbers, trickle beds, and biofilters) are difficult due to their different operating conditions Parameters, such as temperature, pH, nutrient supply, etc , are much easier to control for the bioscrubber and the trickle bed As a result, the optimal growth conditions (thus, maximum removal efficiencies) for the microbial species are much easier to maintain in these systems However, higher cell densities occur in the trickle bed and the biofilter than in the bioscrubber

The first three elimination methods which have been discussed (physical, thermal, and chemical) are highly efficient and can remove over 99 % of the contaminants present, when chosen correctly and operated under their optimal conditions But, their main disadvantage is the cost involved in the building and running of these systems, which can be very expensive This is particularly the case in the treatment of gases which contain contaminants in the low ppm concentration range The treatment of such low levels of contaminants can be very uneconomical As a result of this, industries are increasingly turning their attention to the advantages of biological treatment methods, because of their relative cheapness when compared to the other methods From Tables 4 2 and 4 3, which compare the cost of various elimination methods to biofiltration, it can be seen that biological methods (here represented by biofiltration) are usually the cheapest treatment systems presently available However, there are a number of disadvantages associated with biological systems, one of the most important is their relative slowness when compared to the other methods The other problems associated with the operation of biofilters are discussed in the following sections

Table 4 2 Comparison of the Cost of Various Pollution Control Technologies (1)

Elimination method	Total cost in US$[a] (per 10^6 ft^3 air)
Incineration	130
Chlorine	60
Ozone	60
Activated carbon (with regeneration)	20
Biofiltration	8

Note ([a]) US$ 1992 values

Table 4.3 **Operational Costs of Various Pollution Control Systems (1)**

System	Fuel/Energy consumption (US$[a] per cfm)	Power (W per cfm)
Incineration	15	negligible
Wet scrubbing	up to 8	1
Soil beds	0	0 6

Note [a] US$ 1992 values

4 2 Operational Parameters of a Biofilter

There are several basic parameters which must be considered for the running of a biofilter Most of these parameters essentially optimise the conditions within the bed to maximise the biological activity, which in turn is responsible for the elimination capacity of the biofilter These parameters are discussed in the following sections

(a) The Filter Material

The choice of filter material is important in the operation of a biofilter Bulky materials which resist compacting and contain large void spaces, to keep back pressures low and prevent clogging, are favoured From the biological view point, the material must be capable of supporting the development of an adequate biofilm Various filter materials such as ceramics, glass, activated carbon, and plastics can be used, but materials with a high content of organic matter are favoured and include wood (13, 14), compost (15), heather and fibrous peat (12,16-18) These natural materials have a number of advantages over the inert materials

(i) they are very cheap and quite plentiful,

(ii) they have high water retention capacity, which prevents rapid drying out of the bed, for example peat can hold up to 20 times its dry weight in water,

(iii) being 'natural' materials they act as better supports for the development of the biofilm, buffering the micro-organisms against adverse conditions and can supply additional nutrients to the microbes which they may require,

(iv) they are an excellent source of micro-organisms, thus, it is not always necessary to isolate microbial strains capable of degrading the targeted contaminant

The choice of filter material has been reported to influence the back pressure and the performance of the biofilter

(i) the pressure drop across the filter-bed can vary considerably depending on the filter material used, its age and the bed's humidity Zeisig (19) compared the pressure drop across four different materials (garbage compost, soil humus, bark compost and fibrous peat) and found that the peat gave the lowest pressure drop, due to its fibrous nature which resisted compacting, see Figure 4 4 In contrast, the use of garbage compost gave a pressure drop which was 8 to 10 times higher than that of fibrous peat Van Langenhove *et al* (13) compared the back pressure across beds composed of either wood bark or fibrous peat at different humidities It was observed that the wood bark gave the lowest back pressure values, and that the back pressure increased with humidity, see Figure 4 5 Ageing of the bed will eventually lead to compacting of the material and an increase in the back pressure To prevent this happening, 'bulking materials' such as polystyrene beads (16), or wood bark (20) are often mixed in with the organic material This also has the advantage of reducing the energy required to force the waste gas through the bed Don (20) reported that the addition of wood bark as a bulking agent to compost resulted in a 50 % reduction in the cost of the elimination process

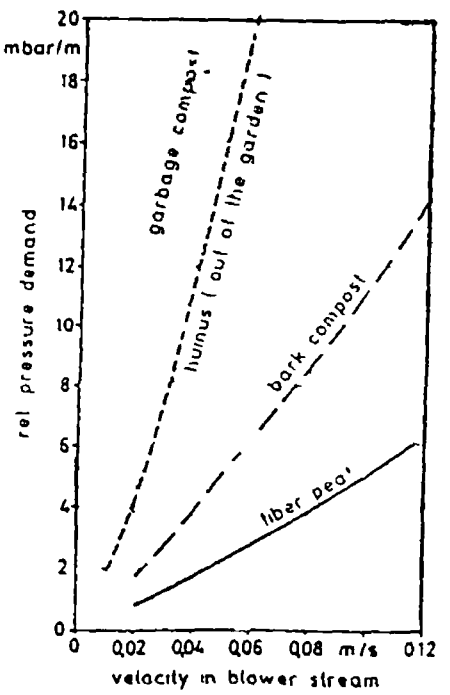

Figure 4 4 **Variation of Back Pressure with Filter Material (19)** Note Relative humidity 20 %

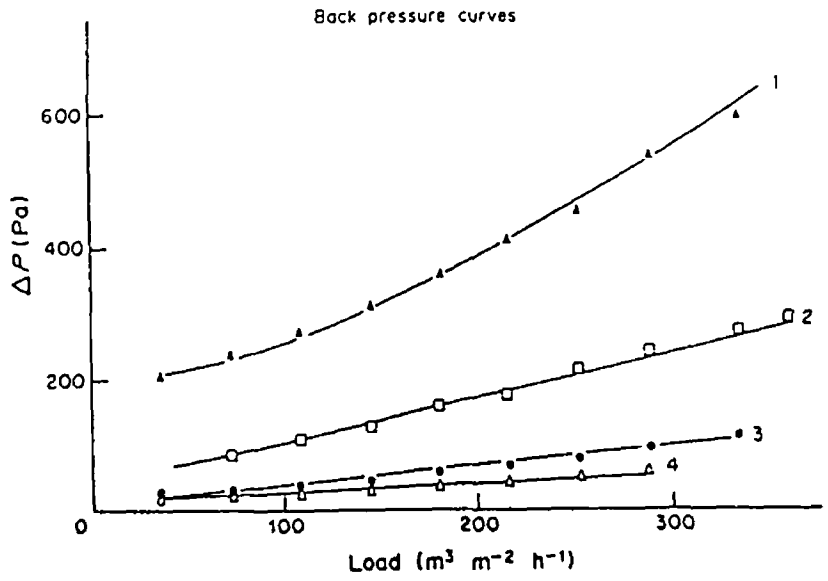

Figure 4.5 A Comparison of the Back Pressure for Fibrous Peat and Wood Bark as a Function of the Bed's Humidity (13) Note Curve 1 - peat fibre (68 % moisture), curve 2 - peat fibre (28 % moisture), curve 3- wood bark (68 % moisture), curve 4- wood bark (28 % moisture)

(ii) the removal efficiency of the biofilter has also been found to be influenced by the choice of filter material A study by Lehtomaki *et al* (14) compared peat, wood bark, and compost as filter materials for the treatment of a waste gas containing phenolic compounds, ammonia and formaldehyde From Table 4 4 it can be seen that the removal efficiency was found to decrease in the order compost > peat > wood bark for the compounds studied For overall odour removal, wood bark and compost were more efficient than peat However, it is unclear from Lehtomaki *et al*'s report whether this trend was due to the packing material itself, or due to the activity of different microbial populations in the different materials

A similar variation in removal efficiency was reported by Don (20) who found that a biofilter containing a bark/compost mix had a higher elimination efficiency for NH_3 removal than a biofilter containing a peat/heather mix, see Figure 4 6 Again, Don does not explain the reason for the variation in removal efficiencies with filter material used

Table 4.4 **The Influence of Filter Material on the Elimination Efficiency of the Biofilter (14)**

Compound eliminated	Filter material		
	Peat	Wood bark	Compost
Phenolic compounds and formaldehyde	85	80	89
Ammonia	84	60	>95
Overall odour	75	84	83

Note the values refer to the percentage elimination efficiency of the biofilter Organic compounds concentration 11 to 110 mg m^{-3} (as propane), the loading of the exhaust gas was 66 to 200 m^3 m^{-2} h^{-1}, temperature 27-34° C

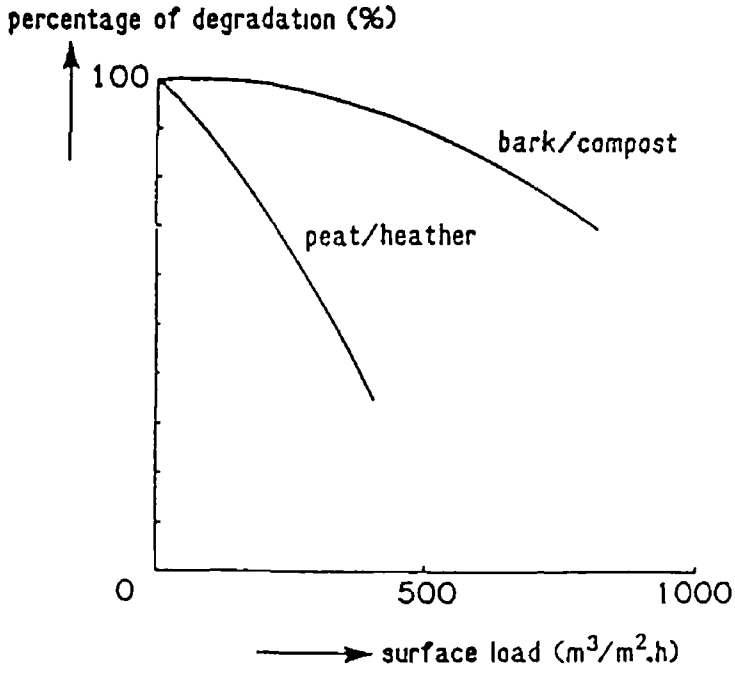

Figure 4 6 **The Influence of Filter Material on the Removal Efficiency (%) of NH_3 (20)**

A clearer example of the influence of filter material on the biofilter's performance was reported by Cox *et al* (21) who compared the removal of styrene by activated carbon (six types), polyurethane, and perlite beds The highest removal rates were found to occur with the polyurethane and perlite materials, which favoured the growth of styrene-degrading fungi, see Table 4 5 In contrast, the activated carbon beds favoured bacterial growth and were found to be poorer at degrading the styrene (no correlation could be found between

any of the activated carbon properties [surface area, buffering capacity, etc] and the elimination capacity of the filter bed for styrene) It was suggested that the difference in removal efficiencies was due to the large variation in the pH of the beds The activated carbon beds (pH 5 6 to 5 8) were considered to be better at adsorbing the acidic by-products of styrene degradation which allowed for the selection of bacteria over fungi Whereas, the lower pH of the polyurethane and perlite beds (pH 2 6 to 2 7), prevented the adsorption of acidic by-products and favoured the growth of acid tolerant, styrene degrading-fungi

Table 4.5 **Influence of Packing Material on the Elimination of Styrene (21)**

Packing material	Influent 290 mg m^{-3}	Influent 675 mg m^{-3}
	Effluent (mg m^{-3})	Effluent (mg m^{-3})
Carbon RB 1	110	392
Carbon RB 2	7	186
Carbon RB 3	14	130
Carbon RB 1-3	39	200
Carbon RBAA 1	94	105
Carbon RO 3	20	283
Polyurethane	0	35
Perlite	0	6

(b) Humidity

A relative humidity of between 30 to 60 % (w/w) is generally required to maintain adequate biological activity within the biofilter (2, 12) However, due to the large gas flow rates, water evaporation from the bed is a problem The waste gas entering the biofilter can be dry, and can result in the evaporation of moisture from the bed which will eventually lead to drying out of the bed Water loss from the bed can be reduced by pre-humidifying the waste gas before it enters the biofilter But, eventual drying out of the bed will still occur due to the heat generated by biological activity, which can raise the bed temperature high enough for water loss to be significant (2) Periodic sprinkling can solve this problem, although over wetting of the bed will lead to an increase in back pressure and the development of anaerobic areas Cycles of over wetting/drying will also lead to eventual shrinkage and compacting of the bed, and can result in reduced elimination capacity of the biofilter, therefore, it is important that the humidity be closely monitored (2, 12, 22)

The humidity must be high enough to provide an adequate environment for biological activity, and not too high to cause back pressure problems, or lead to the formation of anaerobic areas Weckhuysen *et al* (23) determined that an optimum humidity level of 57 % was required for butanal elimination in a wood bark biofilter Similarly, van Langenhove *et al* (13) reported an optimum humidity of 65 % for the elimination of H_2S, using a wood bark biofilter

(c) Temperature

The temperature of the waste gas entering the bed can significantly influence the performance of the biofilter Biological activity (and as a result the elimination capacity) within the biofilter has been found to increase with temperature up to about 40°C Ottengraf and Disks (24) noted that a rise of 7°C doubled the biofilter's elimination capacity for styrene, see Table 4 6 However, in general the increased elimination capacity at higher temperatures can be offset by a reduction in the water solubility of the gaseous contaminants

It is not unusual for the waste gas entering the biofilter to be hot, i e from a biological view point at 40°C or higher, in such instances it is recommended to cool the inlet gas before it enters the biofilter to between 20° and 40°C (2, 12) This temperature range favours the growth of mesophilic species (micro-organisms which prefer moderate growth temperatures, i e up to 40°C), and thus avoiding the selection of thermophilic species (micro-organisms adapted to growing at high temperatures) within the filter-bed, which can be a disadvantage when the bed is only in periodic use Thermophilic micro-organisms will die off at low temperatures, which will result in a longer starting up period

Table 4 6 The Influence of Temperature on the Elimination Capacity of a Styrene Eliminating Biofilter (24)

Gas flow rate ($m\ h^{-1}$)	Temperature (°C)	Elimination capacity ($g\ m^{-3}\ h^{-1}$)
50	20	46
50	27	82
100	20	42
100	27	80

Note the gas inlet concentrations not stated

Since the majority of biofilters are open bed systems, seasonal variation in temperature can significantly affect the removal efficiency of the biofilter Winter temperatures can drop well below 10°C, which may severely reduce the elimination capacity of the bed In such instances over-sizing of the biofilter should be considered to take seasonal variations into account However, Lehtomaki *et al* (14) reported that the operation of the biofilter is not significantly affected at low temperatures provided that the temperature of the inlet gas is high enough Removal efficiencies of 80 to 90 % were regained within 24 hours after short periods of shut down at temperatures between 1° and 4°C Freezing at -10°C for a week led to a 69 % drop in the biological activity of the peat filter, a 29 % drop in the bark filter, but only a 3 % drop in the compost filter (14) In contrast, with closed systems the seasonal variation in temperatures is not a problem as the temperature of the biofilter can be more easily controlled

(d) pH of the Bed

Control of the bed's pH is required to optimise the biological activity A particular microbial species will have its optimum pH range (usually between pH 4 to 8) where its degradative activity is at its maximum However, usually a heterogeneous population of micro-organisms is responsible for the elimination of the gaseous contaminants Therefore, most biofilters are operated at a compromise value of about pH 7 (2)

In addition, the nature of the contaminants that are being eliminated, and their break-down products can alter the pH of the filter-bed The presence of organic acids will tend to reduce the bed's pH, similarly basic compounds such as NH_3 can shift the bed to higher pH's, or due to the formation of nitrates and nitrites make the bed acidic (25) Also, the formation of H_2SO_4, from sulphur containing compounds (26), or HCl, from chlorinated compounds (17), can dramatically reduce the activity of the bed if they are not neutralised

The pH of the bed is usually adjusted by mixing a buffering material such as $CaCO_3$ or $Ca(OH)_2$ with the support material, and/or by adding a buffering material to the water sprayed onto the bed (2, 17)

(e) Waste Gas Loading

The volumes of waste gas passing through a biofilter are wide ranging from 1,000 to upwards of 100,000 $m^3\ h^{-1}$ This is contrasted to the low concentrations of

contaminants in the gas, typically in the low ppm range The loading of the waste gas to the biofilter is usually expressed as one of the following (12)

(i) the filter volume load, which is the volume of waste gas passing through a unit volume of filter material per unit time, expressed in units of $m^3\ m^{-3}\ h^{-1}$ This is also referred to as the gas velocity or space velocity (SV), the number of times the volume of the filter-bed is completely aerated per hour Typical SV values range from 50 to 200 $m^3\ m^{-3}\ h^{-1}$,

(ii) the filter area load, which is the volume of waste gas flowing through a unit cross sectional area of the filter material (i e the area perpendicular to the direction of flow) per unit time, expressed in units of $m^3\ m^{-2}\ h^{-1}$,

(iii) the specific filter load, which is the mass of gaseous contaminants (in the waste gas) passing through a unit volume of the filter material per unit time, expressed in units of $g\ m^{-3}\ h^{-1}$ The last expression is the only one of the three which contains the amount of contaminants entering the bed, with the first two definitions the concentration of the contaminants must be included separately

Care must be taken not to overload the biofilter otherwise it can lead to killing of the micro-organisms It is usual to begin operation at a low loading to allow the microbes to adapt, before increasing to the maximum loading capacity of the bed, which will vary depending on the system For instance, Togashi *et al* (18) determined that for NH_3 elimination with a peat biofilter, the load should not exceed 70 % of the nitrification capacity of the bed Loadings m excess of this value lead to an irreversible decline in the bed's elimination capacity The periodic variation in loading to the bed can also reduce the performance of the biofilter Ottengraf *et al* (17, 27) described a biofiltration system which had an activated carbon adsorption unit upstream of the biofilter This unit ensured that a steady loading was delivered to the biofilter At high loading times the unit adsorbed contaminants from the waste gas and slowly desorbed them at the low loading times

The presence of toxic compounds in the waste gas stream has also been found to hinder the biofilter's operation van Langenhove *et al* (28) reported that the presence of the toxic gas SO_2 seriously hindered the elimination of aldehydes in a tree bark biofilter At an SO_2 concentration of 100 ppm the elimination of aldehydes was found to be irreversibly inhibited The removal rate was reduced by 60 % at a SO_2 concentration of 40 ppm, and at 10 ppm or less there was no detectable reduction in the biofilters performance for the removal of the aldehydes

A similar reduction in the elimination capacity for a particular compound can occur when there is more than one compound present in the waste gas In such instances preferential degradation of compounds can be occurring, i e di-auxic phenomena (17, 24) Di-auxism occurs when there is more than one energy source (i e gaseous contaminant) available for the micro-organisms to utilise The more rapidly metabolised compounds are degraded first while compounds which are more difficult to metabolise are only slowly attacked by the micro-organisms For example in the elimination of methanol from a waste gas stream it was reported that high concentrations of isobutanol led to the inhibition of methanol degradation (22) To overcome di-auxism Ottengraf *et al* (17) have suggested the use of multi-stage biofilters for the treatment of complex gases In such biofilters, each stage is designed to eliminate a specific compound from the gas stream

(f) Addition of Nutrients

The supply of inorganic nutrients has been reported to influence the performance of a biofilter Hartmans *et al* (15) reported that the elimination of styrene in a compost biofilter gradually decreased due to the eventual exhaustion of the available nutrient in the bed Weckhuysen *et al* (23) observed that the addition of nutrients to a butanal degrading biofilter increased the removal efficiency by 11 % compared to a biofilter without a nutrient supply Similarly, Don (20) reported that the elimination of styrene increased with the addition of inorganic nutrients to the biofilter Thus, the addition of nutrients to the biofilter does improve its elimination capacity However, the nutrients supplied will depend to some extent on the gaseous contaminants being eliminated For VOCs the frequent addition of inorganic sources of nitrogen and phosphorous, at a ratio of carbon to nitrogen to phosphorous of 200 10 1 is recommended (12)

(g) Microflora

For the successful operation of the biofilter the presence of a microbial species capable of degrading the target contaminant is obviously one of the most important parameters For easily degraded compounds such as the alcohols, ketones, esters, etc , isolation of a species capable of degrading them is generally not necessary The filter material, in particular the organic materials such as peat and compost, usually contain a wide variety of micro-organisms which can readily degrade the compound in question However, many other compounds, such as the hydrocarbons and halogenated hydrocarbons, are not as readily degraded by microbial action As a result, the elimination of these compounds by biological

methods can be difficult Table 4 7 lists the major classes of VICs and VOCs according to their biodegradability Most of the compounds in the slowly and very slowly degraded groupings in Table 4 7 are termed xenobiotic compounds ("strange to life") They are of man-made origin and do not occur naturally in nature

Table 4.7 Classification of VOCs and VICs by Their Biodegradabihty (1)

Rapidly degraded VOC	Rapidly degraded VICs	Slowly degraded VOC	Very slowly degraded VOC
Alcohols	H_2S	Hydrocarbons[a]	Halogenated
Aldehydes	NOx (not N_2O)	Phenols	hydrocarbons[b]
Amines	SO_2	Methylene	Polyaromatic
Ethers	NH_3	chloride	hydrocarbons
Ketones	HCl		CS_2
Organic acids	PH_3		
Other O, N and S containing compounds	SiH_4 HF		

Note ([a]) aliphatics degrade faster than aromatics such as xylene, toluene and benzene ([b]) e g trichloroethylene, trichloroethane, tetrachloromethane and pentachlorophenol

Xenobiotic compounds contain structural features which cannot be degraded by the vast majority of organisms (29) As a result, xenobiotics are at best only slowly degraded over a long period by micro-organisms in nature In extreme cases where the molecule is also resistant to chemical and physical attack it can persist indefinitely, in such instances the compound is referred to as recalcitrant The reason for this is that the micro-organisms lack the range of enzyme specificity required for the utilisation of the compound in question Some compounds can be partially degraded through a process referred to as co-metabolism (or co-oxidation) This can only occur in the presence of a second substrate which the micro-organism can use as a nutrient source The micro-organism cannot grow on the co-metabolite alone The partial degradation of the xenobiotic compound is due to its structural similarity with a compound which can be degraded by the micro-organism However, the total degradation of the xenobiotic compound to inorganic end products cannot occur, this may be due to a number of different reasons (29), which include the following

(i) the production of a dead end product, which cannot be degraded further

(ii) the production of a compound which is toxic to the micro-organism,

(iii) the inactivation of an enzyme in the degradative pathway due to an irreversible reaction occurring with a breakdown product

The best sources of novel microbial species are from sites located near chemical industries, from activated sludge or waste water treatment plants, and from previously conditioned biofilter-beds, bioscrubbers, etc The usual method of isolation is to grow the microbial samples under conditions where the sole carbon source for the microbes is the compound of interest (17) Micro-organisms which can survive and grow under such conditions, are isolated and further tested to confirm if they do in fact degrade the compound Once a xenobiotic degrading micro-organism has been isolated, it can be inoculated onto a filter-bed to improve the elimination of the targeted compound A number of reports in the literature on biofiltration are concerned with the isolation, identification and the improvement of microbial strains for the elimination of specific compounds A list of some of these compounds and the microbial species which were found to degrade them or give improved degradation rates in biofilters is shown in Table 4 8

Table 4 8 **Microbial Species which show Improved Rates of Degradation for the Listed Compounds**

Microbial species	Compound	Reference
Xanthobacter autotrophicus	1,2-dichloroethane	17
Nocardia sp	xylene	17
Nocardia sp	styrene	17
Hyphomicrobium sp	dichloromethane	17
Methylomonas fodinarum	methane	30
Exophiala jeamelmei	styrene	31
Pseudomonas putida	phenol	32
Thiobacillus sp	carbon disulphide	33
Pseudomonas acidovorans	methyl disulphide	34
Hyphomicrobium sp	dimethyl disulphide	35

(h) Maintenance and Monitoring of the Biofilter's Performance

As has already been mentioned, one of the main advantages of biofiltration is the minimum amount of maintenance which the system requires Daily monitoring of the gas' humidity, its temperature, and the back pressure of the bed, is recommended, and occasional sampling of the bed's humidity and its pH is also suggested (12) The lifetime of a biofilter is quite long, periods of up to 5 to 7 years have been reported (2), only occasional turning of the filter-bed was required to prevent settling

The efficiency of the biofilter can be measured by monitoring the inlet and outlet gas concentrations of the total organic content (TOC) of the waste gas or of a specific contaminant, or by the overall reduction in the odour of the waste gas The elimination capacity of the bed is usually expressed as the percentage reduction in the concentration of compound(s) or odour content of the outlet gas compared to the inlet levels It is also expressed as the amount of compound (or carbon) eliminated per unit volume of the filter-bed per hour

4 3 Kinetics of the Biofiltration Process

Ottengraf *et al* (16, 17, 24, 36) has examined the kinetics of the elimination process in detail, using experimental and pilot scale biofilters From their results they have divided the kinetics of the elimination process into

(i) the macro-kinetics of the system which can be described as the absorption of the gaseous contaminant into the aqueous layer surrounding the filter material particles, its transfer to the biolayer and its simultaneous biodegradation by the micro-organisms inhabiting the filter bed The macro-kinetics consist of several physiochemical parameters, such as the mass diffusion of substrate (i e gaseous contaminant), oxygen and other nutrients, the aqueous solubility of the compound, residence times in the filter-bed, etc ,

(ii) the micro-kinetics, which are the metabolic processes of the microbes, such as the rate of substrate (i e the contaminant) oxidation, substrate/product inhibition, di-auxic phenomena, etc

An assumption made by Ottengraf *et al* (16, 17, 24, 36) is that the micro-kinetics conforms to the Monod relationship for substrate degradation, this equation is as follows

$$R = \frac{K_{max} C X}{(C + K_{max})} \qquad \text{Equation 4 1}$$

where R is the rate of contaminant degradation, K_{max} is the maximum rate constant, C the contaminant concentration in the aqueous layer, and X the active biomass concentration This equation describes the rate of contaminant utilisation by a pure culture degrading a single limiting carbon source The actual equation which would have to be derived for a true situation in a biofilter is much more complex, due to the heterogeneous mix of microflora and the presence of several different substrates in the gas stream

The degradation of all the compounds that have been examined by Ottengraf *et al* (16, 17, 24, 36) are reported to conform to zero-order kinetics down to very low substrate concentrations, indicating that the rate of substrate degradation is independent of its concentration This implies that 100 % elimination of the contaminants can be achieved given a long enough residence time in the biofilter The elimination capacity (the removal rate) of the biofilter is defined in the following equation

$$EC = \omega/H (C_i - Co) \qquad \text{Equation 4 2}$$

where, EC is the elimination capacity (g m^{-3} h^{-1}), ω is the filter area load, referred to as the superficial gas flow rate (m h^{-1}) by Ottengraf *et al*, H is the bed height (m), and C_i and Co are the gas inlet and outlet concentrations (g m^{-3}) respectively The elimination capacity is usually expressed as the number of grams of compound which are eliminated by the biofilter, however, some authors use the number of grams of carbon (C-g) eliminated

The elimination of the contaminant can also be expressed as the percentage elimination capacity (%EC) of the biofilter, which is also referred to as the removal efficiency (13)

$$\%EC = (1 - Co/C_i) * 100\ \% \qquad \text{Equation 4 3}$$

where the symbols have the same meaning as above in Equation 4 2

Three distinct elimination regimes can be distinguished in the operation of a biofilter, see Figure 4 7

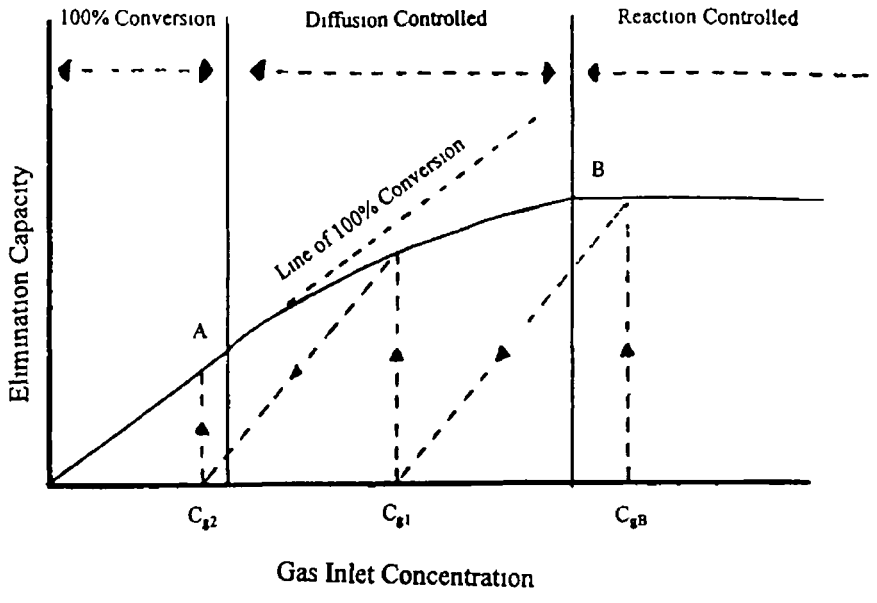

Figure 4 7 **The Operational Regimes of a Biofilter as a Function of its Gas Inlet Concentration (24)**

(i) the complete conversion regime, this occurs when the loading to the biofilter, defined as (ω/H)*Ci, is very low enabling complete removal of the contaminant to occur (below point A),

(ii) the diffusion controlled regime (occurring between points A and B), where the transport of substrate is the limiting factor governing the elimination process,

(iii) the reaction controlled regime, the loading to the biofilter is so high that it is operating at its maximum elimination capacity This regime is divided from the diffusion controlled regime at a vapour concentration known as the critical gas concentration (point B) In the reaction controlled regime the rate of removal is limited by the rate of biological degradation of the contaminant A further increase in the elimination capacity can only occur by the addition of nutrients which may be limiting the microbial activity, or by seeding the bed with a microbial strain which has a much higher elimination capacity for the contaminant in question

Ottengraf and Disks (24) conclude that in a multi-stage biofilter, each stage having a bed height H, the outlet concentration of the contaminants in the gas may be found by the construction of a graph similar to the one depicted in Figure 4 7 Thus, at an inlet concentration of C_{go}, the gas concentration at the exit of the first stage will be C_{g1} In turn C_{g1} will be the inlet concentration of the second stage, which will have an outlet concentration of C_{g2}, etc Therefore, the total number of stages (i e total height of filter-bed) required can be calculated to achieve a desired elimination efficiency of the contaminants

4 4 Biofiltration of non-Nitrogen and non-Sulphur Containing VOCs

The VOCs in this section have been classified into three categories, namely rapidly degraded (Section 4 4 1), slowly degraded (Section 4 4 2), and very slowly degraded compounds (Section 4 4 3) according to their biodegradability (see Table 4 7)

4 4.1 Rapidly Degraded VOCs

The rapidly degraded VOCs contain structural units recognised by the vast majority of microbial species, and include alcohols, ketones, aldehydes As a result, it is usually not necessary to seed the biofilter with specifically selected degrading microbial strains In general, conditioning of the bed will select for those strains which can tolerate the presence of the particular compound, and that are capable of using the compound as a nutrient source

Ottengraf *et al* (16, 17, 27) reported several studies on the elimination of rapidly degraded VOCs, using peat or compost biofilters For the elimination of a mixture of toluene, ethyl acetate, butyl acetate and butanol in a five-stage biofilter, Ottengraf *et al* (16) reported that all the VOCs were being simultaneously degraded in the first stage at an overall elimination rate of about 20 to 40 g m^{-2} h^{-1} (see Figure 4 8) Nearly all of the butanol and ethyl acetate were reported to be eliminated in the first stage whereas toluene was still being eliminated in the higher stages, see Figure 4 8 The critical gas phase concentrations (see Section 4 3) were determined from inspection of a graph of the elimination capacity of the biofilter for each of the compounds as a function of the compound's inlet gas concentration (Figure 4 8) The critical gas phase concentrations were reported to be 1 13 g m^{-3} for toluene, 0 47 g m^{-3} for ethyl acetate, 0 29 g m^{-3} for butyl acetate, and 0 14 g m^{-3} for butanol The slower degraded compounds, particularly toluene were still being degraded up to the fifth stage

Similar results were reported with a three stage biofilter for the elimination of a mixture of acetone, ethanol, 1-propanol and dichloromethane (17) It was observed that the elimination of acetone was mainly in the first stage, whereas ethanol and 1-propanol were eliminated in the second stage (see Table 4 9) Degradation of dichloromethane was not recorded at all during the initial part of the experimental run Dichloromethane was only degraded after the addition of a culture of *Hyphomicrobium* sp to the third stage of the filter bed A second study reported by Ottengraf et al (17) reported on the elimination of a lacquer solvent containing

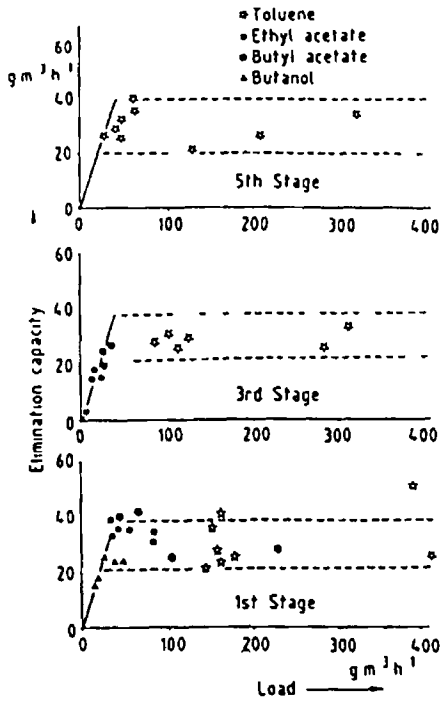

Figure 4 8 **Elimination of Solvent Mixture in a Five-Stage Biofilter (16)**

Table 4 9 **A Summary of Ottengraf et al's Results for the Biofiltration of Rapidly Degraded VOCs**

Compound eliminated	Load $m^3\ m^{-2}\ h^{-1}$	Gas inlet concentration $g\ m^{-3}$	Elimination capacity		Ref
			%	$g\ m^{-3}\ h^{-1}$	
toluene	30 (535)[a]	5 606 (0 308)[a]	N S	21	16
butyl acetate		1 527 (0 050)		27	
ethyl acetate		1 377 (0 064)		32	
butanol		0 692 (0)		32	
1-propanol	245	0 4 total	N S	58 (78)[a]	17
ethyl acetate	(470)[a]			79 (96)	
ethyl lactate				100 (250)	
diacetone alcohol				28 (64)	
1-ethoxy propanol				11 (17)	
acetone	220	N S	N S	164	17
ethanol				57	
1-propanol				57	
dichloromethane				15	
Methanol	N S	6	83	5	27
		42 (135)[b]	38 (52)[b]	16 (70)[b]	
t-butanol		20 (14)	10 (19)	2 (2 7)	
acrylonitrile		0 77	97 6	0 76	
		43	40	17	
benzene		1 2	58	0 7	
		4 (10)	33 (40)	1 3 (4)	

Note N S not stated ([a]) values in parentheses refer to measurements at the higher loading ([b]) values in parentheses refer to results from lab-scale biofilter

isopropanol, ethyl acetate, ethyl lactate, diacetone alcohol and 1-ethoxy-2-propanol, the results of which are presented in Table 4 9

The results from a pilot-scale biofilter study were reported by Ottengraf *et al* (27) for the removal of various VOCs (acetone, ethanol, i-propanol, dichloromethane) from the waste gas of an industrial cleaning process The elimination capacities (and removal efficiencies) of the pilot-biofilter for the various contaminants were reported to be lower than the elimination capacities of a lab-scale biofilter for the same compounds, see Table 4 9 It was concluded that the reduced removal efficiencies of the pilot-biofilter were due to its poorer humidification system and the lower operational temperatures of the bed

Jol and Dragt (37) examined the elimination of a mixture of rapidly degraded VOCs from the waste gases of three different industrial sites In the first test site, part of the waste gas stream from a muffle furnace (50 to 150 m^3 h^{-1}) was led to a pilot biofilter The industrial process was reported to use four different kinds of lacquering agents, namely epoxyfenol, alkydamino, alkydureaformaldehyde, and alkyd-amino-epoxy, and in addition the following solvents, alcohols, alkylcellosolves, esters, and alkylated aromatics The total organic concentration of the waste gas entering the biofilter was between 200 to 3,000 mg-C m^{-3}, corresponding to an odour concentration of 1,000 to 3,000 OU m^{-3}, see Table 4 10 The ability of the biofilter to reduce the contaminant content of the waste gas was reported in terms of the reduction in the odour content of the waste gas The outlet odour concentration for all the loadings tested was between 300 to 800 OU m^{-3} The alcohols, alkylcellosolves and esters were easily degraded, but the addition of nutrients was required to increase the elimination of the hydrocarbons From this initial study it was calculated that for a full scale installation, a removal efficiency of 70 to 90 % would require a loading between 50 and 100 m^3 m^{-2} h^{-1} to the biofilter Under these circumstances it was calculated that the alcohols, alkylcellosolves and esters would be eliminated at an efficiency of 90 to 95 %, while the hydrocarbons, which comprised mainly of alkylated aromatics, would have a removal efficiency between 30 to 50 %

In the second study by Jol and Dragt (37), the removal of water soluble lacquer components from a waste gas stream was examined, see Table 4 10 It was found that part of the elimination occurred in the humidifier unit leading to the biofilter The total odour removal efficiency was 95 % at a gas load of 350 m^{-3} h^{-1} With a lacquer containing alcohols, esters and toluene the maximum elimination capacity was calculated to be 35 g-C m^3 m^{-2} h^{-1} It was determined that the critical concentration of this system was 0 75 g-C m^{-3} And finally, a pilot scale biofilter for

a pharmaceutical plant gave elimination efficiencies of between 90 to 100 % for the compounds acetone, ethanol and 1-propanol dichloromethane The acetone and alcohols were the most biodegradable compounds, see Table 4 11

Table 4.10 Results of Pilot Biofilters for the Elimination of Mix Solvent Vapours from Exhaust Gases of Lacquering Industry (37)

Compound eliminated	Load $m^3\ m^{-2}\ h^{-1}$	Gas concentration g-C m^{-3}	Elimination capacity	
			%	g-C $m^{-3}\ h^{-1}$
lacquering agents (see text) plus alcohols, alkycellosolves, esters, alkylated aromatics	50 to 150	200 to 3,000 TOC	40	3 3
water soluble lacquers	350	N S	95	N S
lacquer containing alcohols, esters and toluene	N S	0 1 to 1 0	N S	35

Note NS not stated

Table 4 11 Elimination of Mixed Solvents Containing Gas Stream from a Pharmaceutical Plant (37)

Compound eliminated	Gas concentration (mg m^{-3})	
	Inlet	Outlet
acetone	41	1
ethanol	2200	33
1-propanol	1500	<10
dichloromethane	2450	730

Weckhuysen *et al* (23) examined the elimination of butanal with a wood bark biofilter This study reported on the influence of humidity, nutrient supply, pH, and loading of butanal to the bed, on the performance of the biofilter It was found that a minimum humidity between 32 9 and 47 6 % was required for biological activity to be detected in the bed For subsequent experiments an optimum humidity of 57 %

was chosen This value was high enough to ensure that adequate biological activity was occurring, but was not too high to create a large pressure drop across the bed Weckhuysen *et al* (23) reported that the addition of $CaCO_3$, to stabilise the pH of the bed, resulted in an 8 % increase in the elimination efficiency of the biofilter, see Table 4 12 An increase in the elimination efficiency by 11 % was found to occur when inorganic nutrients were supplied to the biofilter Both a higher maximum elimination capacity and a higher critical concentration for butanal removal were observed for a nutrient supplied biofilter (maximum elimination capacity 90 4 g m^3 h^{-1}, critical load 120 0 m^3 h^{-1}) compared to a biofilter without nutrient supply (maximum elimination capacity 74 5 g m^3 h^{-1}, critical load 99 0 m^3 h^{-1}) Analysis of the microbes present in the biofilter found that a heterogeneous population was responsible for the elimination of the butanal

Table 4.12 Comparison of Biofilter Performance for the Removal of a Butanal Containing Gas Stream (23)

Parameter Adjusted	Unadjusted biofilter	Adjusted biofilter
Nutrient supply	86 %	97 %
pH	72 %	80 %

Note Butanal concentration of 10 ppm (v/v) and a loading of 100 m^3 m^{-2} h^{-1} The percentage values refer to the elimination efficiency of the biofilters

Other reports concerning the biofiltration of the rapidly degraded VOCs include the elimination of methanol by Shareefdeen *et al* (38) who determined that a peat/perlite bed gave an elimination capacity of up to 112 8 g (methanol) m^{-3} h^{-1} The biofiltration of mixed solvents from industrial sources were studied by Dalouche *et al* (4) and Beerli and Rotman (39), and aldehyde elimination by Don (20), the results are compiled in Table 4 13

4 4 2 Slowly Degraded VOCs

This group consists of the aliphatic and aromatic hydrocarbons, phenols and dichloromethane

Sly *et al* (30) examined the feasibility of using biofiltration for the removal of methane, which can be present at dangerously high concentrations in coal mine ventilation atmospheres Glass tubing was used as the packing material for the

Table 3.13 Compiled Results for the Biofiltration of Various Compounds

Application	Compound removed	Packing	Loading $m^3\ m^{-2}\ h^{-1}$	Inlet concentration	Elimination capacity %	Elimination capacity	Comment	Ref
spray plant	1-propanol pentoxone triethylamine (and others)	peat	80	10 mg m^{-3} 10-20	80-90 " "	N S	>95 % reduction in the odour concentration achieved	4
spray plant	ethyl glycol butyl glycol ethyl hexanol hexyl glycol	peat	100	30-75 10-20 50-100 30-80	75-90 " 50-75 "	N S	-	4
experimental biofilter	aldehydes	N S	50	3 g m^{-3}	N S	40 g-C $m^{-2}\ h^{-1}$	begun with stepwise increase in concentration	20
print factory	n-propanol	peat	4.8-9.6	790-2050 ppm	90	N S	3 m bed height required for 90 % reduction	39

Continued next page

Table 3 13

Continued

Application	Compound removed	Packing	Loading $m^3\ m^{-2}\ h^{-1}$	Inlet concentration	Elimination capacity		Comment	Ref
					%			
print factory	alcohol mix ethanol, methanol, methyl ether ketone, ethyl acetate		4 8-9 6	525-2800 ppm	90		2 5 m bed height required for 90 % reduction	39
print factory	solvent mix ethanol methanol, naphtha		4 8-9 6	440-2400 ppm	90		4 5 m bed height required for 90 % reduction	39
experimental biofilter	methanol	peat\ perlite	6 42-12 75	6 5 g m^{-3}	N S	12 8 g $m^{-3}\ h^{-1}$		41

Note N S not stated

biofilter, and the bed was seeded with *Metylomonas fodinarum*, a bacterium capable of oxidising methane It was observed that for a methane concentration range of 0 25 to 1 0 % in air, greater than 70 % removal was achieved with a residence time of 15 minutes, and that greater than 90 % removal occurred with a residence time of 20 minutes In addition, it was determined that for long term use, the biofilter required a nutrient supply of KNO_3 to maintain methane removal It was observed that in the methane concentration range studied, the rate of methane elimination was directly proportional to its concentration, see Table 4 14, which indicated that the biofilter was operating in the diffusion control region

Table 4.14 Linear Dependence of Removal Rate with Methane Concentration (30)

Inlet methane concentration (%)	Elimination rate (mg h^{-1})
0 25	12 2
0 5	34 8
1 0	66 1

Note At a gas flow rate of 210 ml min^{-1}

Cox *et al* (21, 31, 40) has examined the biofiltration of styrene Cox *et al* (21) proposed that the use of fungal species for styrene elimination would be advantageous in a biofilter, because

(i) fungal species are much more tolerant to lower pH and humidity conditions than are bacteria Thus, their use in biofiltration would require less stringent controls on such parameters, and would also reduce the pressure drops across the filter bed,

(ii) there would be better mass transfer of compounds of low water solubility such as styrene due to the high specific surface area of the mycelium

Cox *et al* (21) set out to enrich styrene degrading fungi from a garden soil sample under conditions similar to those found in industrial treatment of waste gasses Several biofilters were set up, each with a different packing material, and innoculated with the soil suspension The packing materials used were polyurethane cubes, perlite granules, and activated carbon (six types) It was observed that the efficiency of styrene degradation was dependent on the type of support material used The polyurethane and perlite filter beds were found to be better at styrene elimination than the carbon beds, see Table 4 5 Styrene degrading fungi were readily isolated

from the polyuretane and perlite supports, whereas bacterial isolates dominated in the activated carbon beds In addition, it was found that the pH of the water run-off from the carbon supports were much less acidic (pH 5 6 to 5 8) than those from the polyurethane and perlite material (pH 2 6 to 2 7) It was concluded that the fungi were more tolerant of the lower pH environments than the bacteria No correlation could be found between the different carbon supports and the elimination capacities observed It was postulated that the activated carbon materials adsorbed any acids produced which in turn favoured the growth of the bacteria

In the initial growth studies with *E jeanselmei* (in flasks) Cox *et al* (31) reported that the bacterium was capable of growth on styrene as its sole carbon and energy source up to a maximum styrene concentration of 0 36 mM *E jeanselmei* was also able to degrade several styrene related compounds namely styrene oxide, 2-phenylethanol, 1-phenylethanol, phenylacetic acid, acetophenone, phenol, benzoic acid and styrene glycol (very slow growth) No growth was observed with either phenylacetaldehyde or α-methylstyrene However, it was found that the presence of glucose did repress the oxidation of styrene and its related compounds Some of the styrene derived compounds were postulated to be intermediates in the pathway of styrene degradation, indicating that *E jeanselmei* has a wide substrate specificity Thus, Cox *et al* (31) suggested that the use of this bacterium for styrene elimination would not lead to the formation of harmful or non-degradable intermediates in a biofilter

The removal of styrene was studied further by Cox *et al* (40) using a pilot-scale biofilter composed of perlite The bed was seeded with pre-adapted fungi (identity not stated) which was found to reduce the start-up time of the biofilter, styrene elimination began within two days of start-up Removal efficiencies of between 73 to 98 % were reported, corresponding to a maximum elimination capacity of between 60 to 70 g m^{-3} h^{-1} The results for the biofilter are shown in Table 4 15 The effluent levels of the styrene fell below the maximum emission level of 107 mg m^{-3} for styrene recommended by the Dutch government The fungi proved to be tolerant to the low acidity of the bed Within 15 days of start up, the pH fell from pH 6 to pH 3 and remained at this level until operation of the biofilter was stopped (> 80 days) A minimal water content of 40 % was required for the maximum elimination capacity to be achieved, a reduction in the water content to 25 % resulted in a 50 % reduction in the elimination capacity of the biofilter

Hartmans *et al* (15) reported on the removal of styrene with a compost filter At a loading of 50 to 100 m^3 m^{-2} h^{-1} and an inlet concentration of 100-600 mg m^{-3}, Hartmans *et al* (15) determined the maximum elimination capacity of the biofilter to be 50 g m^{-3} h^{-1} However, there was an eventual decline in the elimination capacity of the biofilter due to exhaustion of the nutrients in the compost bed by the micro-organisms

Table 4.15 Results of Styrene Elimination using a Fungi Seeded Biofilter (40)

Load		Gas concentration		Maximum elimination capacity	
m^3 m^{-2} h^{-1}	g m^{-3}	Inlet mg m^{-3}	Outlet mg m^{-3}	%	g m^{-3} h^{-1}
105	27	253	5	98	26
105	38	356	4	99	37
120	81	678	20	97	79
149	91	608	164	73	66

Zilli *et al* (32) examined the elimination of phenol from waste gas From batch growth experiments, it was found that a pure culture of *Pseudomonas putida* gave better elimination rates for phenol, 0 97 to 8 50 mg g^{-1} (biomass) h^{-1}, than a mixed culture of *Pseudomonas* species, 1 6 to 2 95 mg g^{-1} h^{-1} Thus, the specificity of the mixed culture to phenol was judged to be less than that of the pure culture of *Ps putida* From this initial observation, Zilli *et al* (32) proceeded to seed a lab-scale biofilter, composed of a bed of mixed peat and glass, with a pure culture of *Ps putida*, at a surface loading of 20 m^3 m^{-2} h^{-1}, and a phenol concentration up to 2,000 mg m^{-3} Over an experimental period of one year, an average degree of phenol conversion of 0 93 to 0 996 (i e 93 to 99 6 %) was achieved with no apparent decline in the performance of the biofilter Even after a 10 day shut down period full elimination capacity was regained within 24 hours of starting up A linear relationship between concentration and phenol conversion was observed up to a phenol concentration of 1,800 mg m^{-3} The maximum elimination capacity of the biofilter was calculated to be 124 g m^{-3} h^{-1} at the loading of 133 2 g m^{-3} h^{-1}

There is little detail to be found in the literature concerning the biofiltration of other slowly degraded VOCs However, some which have been mentioned include benzene (27), xylene (27), dichloromethane (16, 15, 27) and toluene (16, 27, 36, 41) These reports are concerned with the isolation of a species capable of degrading the

compound in question, such as *Nocardia* sp for xylene and styrene, or the seeding of the bed with *Hyphomicrobium* sp for dichloromethane (16, 17)

4 4 3 Very Slowly Degraded VOCs

This class of VOCs consist principally of the chlorinated hydrocarbons other than dichloromethane (which has already been discussed) The most common compounds of this group found in waste gases are 1,2-dichloroethane, 1,1,1-trichloroethane, and trichloroethene Other compounds which are grouped under this classification include the polycyclicaromatic hydrocarbons (PAHs) and CS_2 As previously discussed in Section 4 2 the biodegradation of these compounds is difficult since they belong to the xenobiotic class of compounds As a result, there are very few examples to be found in the literature concerning the use of biofiltration for the elimination of such compounds Most references are primarily concerned with the isolation and identification of microbial species capable of degrading these compounds

For the degradation of CS_2, Ottengraf *et al* (17) reported that microbes from activated sludge could only degrade CS_2 if a second substrate was also present, such as glucose, methanol or formic acid It was concluded that CS_2 was used only as a sulphur source Plas *et al* (33) isolated a *Thiobacillus* species capable of utilising CS_2 as its sole energy source This species could survive CS_2 concentrations of up to 150 mg l^{-1}, with a removal rate of 2 5 mg g h^{-1}(protein) min^{-1}, thus suggesting the *Thiobacillus* sp as an ideal candidate for the biofiltration of CS_2

Hartmans *et al* (44) reported growth studies with two microbial species capable of degrading chlorinated hydrocarbons *Mycobacterium aurum*, capable of degrading vinly chloride (VC), and *Xanthobacter autotrophicus* which can degrade 1,2-dichloroethane (DE), were characterised The main conclusions from their study were

(i) elimination of VC and DE in the biofilter should be feasible VC vapour concentrations up to 125 g m^{-3} had no affect on the growth of *M aurum* on VC or *X autotrophicus* on DE DE vapour concentrations of 22 g m^{-3} had no effect on the growth of *X autotrophicus* on DE, but, there was a 50 % reduction in the growth of *M aurum* on VC, and no growth of the *M aurum* on VC was observed at a DE vapour concentration of 45 g m^{-3},

(ii) the principal end product was found to be HCl which was neutralised with NaOH to form NaCl NaCl concentrations of 100 mM were found to reduce the growth of *X autotrophicus* Thus, the prevention of NaCl build up in the bed would be required to ensure microbial growth

4 5 Biofiltration of Nitrogen and Sulphur Containing VICs and VOCs

This section discusses the literature concerned with the use of biofiltration for the elimination of nitrogen (Section 4 5 1) and sulphur (Section 4 5 2) containing compounds In particular it discusses the elimination of NH_3 and H_2S which are two of the principle VICs present in waste gases

4 5 1 Nitrogen Containing Compounds

Togashi *et al* (18) examined the elimination of NH_3 from a gas stream using a peat biofilter The initial tests examined the removal of NH_3, at a concentration of 70 ppm, using an unseeded peat bed It was observed that the time taken for breakthrough of the NH_3 depended on its loading to the bed The breakthrough varied from one day (with a loading of 7 01 g-NH_3 kg^{-1} (dry peat) day^{-1} to 20 days (0 701 g-NH_3 kg^{-1} day^{-1}) Once breakthrough had occurred the outlet concentration of NH_3 rapidly reached that of the inlet concentration of the gas stream, thus, elimination was only transient, and indicated that only physical sorption was occurring on the unseeded peat bed This conclusion was supported when the peat was analysed after the experimental runs It was found that there was an increase in microbial numbers from 9 $x10^7$ to 2 $x10^9$ cells g^{-1} However, there was no associated increase in the levels of nitrates/nitrites, which would indicate oxidation of the NH_3 thus it was concluded that nitrifying bacteria did not naturally inhabit the peat used

The NH_3 initially removed by the peat was considered to be retained by physical sorption on the peat surface, due to

(i) absorption into the aqueous layer surrounding the peat particles,

(ii) adsorption of NH_3 onto the humic functional groups present in the peat (i e onto COOH, phenolic-OH, etc)

The total amount of NH_3 retained by the various sorption mechanisms varied from 10 to 20 g-N g^{-1} (dry weight)

Seeding of the bed with nitrifying bacteria was required for continuous elimination of NH_3 from the gas stream The addition of $Ca(OH)_2$, to adjust the pH of the bed to about pH 7 was reported to improve the elimination capacity of the biofilter (values not given) For an NH_3 inlet concentration of 20 ppm, the maximum elimination capacity of the biofilter was calculated to be 0 18 g-N kg^{-1} day^{-1} It was determined that the inlet loading should not exceed 70 % of the elimination capacity of the bed, as above this value overloading of the biofilter ocurred leading to an irreversible decline in the nitrifying capacity of the peat bed

The removal of NH_3 from the ventilated air of a piggery was examined by van Langenhove *et al* (45) using a wood bark biofilter The bed did not require seeding for NH_3 elimination to occur The volume of waste gas entering the biofilter was varied from 50 to 500 m^3 h^{-1}, and contained an NH_3 concentration of 6 to 17 ppm An elimination efficiency of 90 % was reported for NH_3 loadings below 2 g-N m^{-3} h^{-1} (i e the critical gas concentration) The maximum elimination capacity of the biofilter was calculated to be between 2 5 to 3 g-N m^{-3} h^{-1}

Martin *et al* (46) examined the removal of NH_3 using a peat biofilter, and an inlet NH_3 concentration of 20 to 30 mg m^{-3} at a gas velocity of 50 to 125 m h^{-1} It was found that the initial high removal of ammonia was again due to sorption by the peat However, by day 30 this had levelled off to a steady removal efficiency of about 50 %, which coincided with an increase in microbial numbers to about 10^{11} cells g^{-1} by day 30 Also, Martin *et al* (46) reported the results from a pilot-scale biofilter used to reduce odours emanating from an animal rendering plant It was found that for a gas residency time of under 2 minutes, 90 % of NH_3 and 100 % of amines were removed

Dragt *et al* (25) compared a pilot-scale biofilter for the removal of NH_3 from the exhaust air of a piggery to that of lab-scale biofilter Both biofilters used compost as the filtering material Under similar operating conditions, namely a gas flow rate of 500 m^3 m^{-2} h^{-1} with an inlet NH_3 concentration of 10 ppm (10 to 50 ppm in the case of the lab-scale biofilter), both biofilters eliminated up to 90 % of the NH_3 passing through the bed The elimination capacity of the lab-biofilter was found to be 9 g-N m^{-3} h^{-1}, whereas the pilot-biofilter had a lower value of 2 g-N m^{-3} h^{-1} The lower elimination capacity for the pilot-biofilter was determined to be due to

(i) operating the biofilter near the critical concentration for NH_3 for this system (which was calculated to be 8 ppm), thus, operating in the diffusion limitation regime (Section 4 3),

(ii) the build up of inhibitory concentrations of nitrates/nitrites in the compost bed Gently flushing the bed with water over a 2 day period was reported to remove most of the nitrate/nitrite build up and to have a minimal effect on both the pressure drop and the elimination capacity

As previously mentioned, Don (20) reported that a peat/heather mix gave better removal of NH_3 than a wood bark/compost biofilter Don does not explain the higher results with the peat/heather mix It was also found that the biofilter became overloaded at NH_3 concentrations above 50 mg m^{-3}, due to the build up of toxic levels of ammonium in the biofilter Subsequent studies with a pilot-scale biofilter containing a peat/heather mix reported a removal efficiency of 90 % for NH_3, at a surface load of 400 m^3 m^{-2} h^{-1}

There are few detailed examples in the literature on the elimination of nitrogen containing organic compounds However, there are several reports that mention the elimination of various nitrogen compounds by biofiltration, such as triethyl amine (4), trimethyl amine (47), and acrylomtrile (27) Ottengraf *et al* (17) reported that methyl acrylate, dimethylformamide and acrylomtrile are biodegradable compounds, though the microbial species responsible were not identified Shoda (6) briefly discussed the degradation of trimethyl amine by a compost biofilter The mam end product was found to be NH_3 Therefore, seeding of the biofilter with nitrifying bacteria was required to ensure complete elimination of all odorous compounds from the gas stream

4 5 2 Sulphur Containing Compounds

A large amount of work has been done on the biofiltration of H_2S from exhaust gases, and increasingly on the elimination of other sulphur containing organic compounds Furusawa *et al* (26) reported on an in-depth study on the removal of H_2S by a peat biofilter The biofilter was pre-treated at an inlet H_2S concentration of 60 ppm and an air flow rate of 3 6 to 36 m^{-3} kg^{-1} (dry peat) day^{-1} Under these conditions, Furusawa *et al* (26) noted that an acclimatisation period of up to 15 days (increasing with the loading) was required before steady state conditions were reached in the bed An initial rate of H_2S elimination of 0 44 g-S kg^{-1} (dry peat) day^{-1} was reported irrespective of the inlet H_2S concentration Analysis of sulphur compounds in the peat after experimental runs showed that large amounts of sulphates and sulphites were present, the oxidised end product of H_2S Comparing the elimination capacity of the untreated bed to an irradiated peat bed (i e a sterilised peat bed), Furusawa *et al* (26) found that there was minimal removal of

H_2S by the sterilised peat Thus, it was concluded that microbiological activity in the untreated bed was responsible for the removal and the oxidation of the H_2S

Following on from the initial work done by Furusawa *et al* (26), Wada *et al* (48) identified *Thiobacillus intermedius* as the bacterium principally responsible for the elimination of H_2S in the peat biofilter Characterising a biofilter innoculated with *T intermedius*, Wada *et al* observed that the elimination of H_2S from the gas stream was only a transient phenomenon The eventual build up of sulphates caused the pH of the bed drop below pH 3 This dramatically reduced the microbial numbers present in the peat bed, which in turn reduced the elimination capacity of the biofilter A steady state of H_2S elimination was obtained with the addition of $Ca(OH)_2$ to prevent the pH of the bed becoming too acidic The specific rate of uptake of H_2S by *T intermedius* was calculated to be $1\ 4 \times 10^{-13}$ g-S $cell^{-1}$ $hour^{-1}$

Clark and Wnorowski (49) reported on the use of a grass/compost filter mixture for the elimination of H_2S For concentrations of up to 48 ppm and flow rates of 13 dm^3 min^{-1}, they found that the basic filtering material used did not sustain an acceptable level of H_2S removal The addition of activated sludge was required to supply the biofilter with additional microbial species capable of oxidising the H_2S, and that $CaCO_3$ had to be mixed into the bed to prevent the build up of acidic end products Treatment of the biofilter in this manner resulted in a removal efficiency of greater than 99 %, see Table 4 16

Table 4.16 The Removal of H_2S by a Biofilter Packed with a Compost/Grass Bed Mixture (49)

Day	1	5	10	15	20	25	30	35	40
Inlet concentration (ppm)	20	20	45	48	23	22	22	22	22
Outlet concentration (ppm)	0 1	0 1	0 8	7	1 5	1 5	1 6	1 6	1 6

Note H_2S removal with the addition of $CaCO_3$ and activated sludge

Clark and Wnorowski (49) also studied the elimination of SO_2 using a mixture of compost and grass as their basic filtering material This is the only other example of the elimination of a sulphur containing VIC by biofiltration other than that of H_2S They found that SO_2 could be removed at efficiencies of greater than 95 % for an inlet concentration of up to 1000 ppm (v/v) at an air flow rate of 13 dm^3 min^{-1} (see Table 4 17)

Table 4.17 **The Removal of SO_2 by a Biofilter Packed with a Compost/Grass Bed Mixture (49)**

Day	1	3	5	7	9	11	13	16	20	22
Inlet concentration (ppm)	36	36	20	65	136	148	191	82	72	123
Outlet concentration (ppm)	0 3	0 3	0 2	0 2	0 2	3 0	0 2	2 6	12	23

A number of workers have proceeded to examine the removal of several sulphur containing organic compounds, namely methanethiol (MT) (35, 50-54), dimethyl sulphide (DMS) (34, 35, 50, 53-56), and dimethyl disulphide (DMDS) (50, 52, 53) Most of the work reported on the biofiltration of these compounds has consisted of characterising the removal of H_2S, MT, DMS, and DMDS by biofiltration, with the emphasis on isolating and identifying new microbial strains capable of oxidising these compounds at higher removal rates

Hirai *et al* (50) studied the removal capacity of peat biofilters seeded with activated sludge for the elimination of H_2S, MT and DMS in single and mixed gas streams Initially, they determined the maximum elimination capacity of peat beds acclimatised on a single gas It was found that of the three gases, H_2S had the highest elimination capacity, followed by MT then DMS, the results are compiled in Table 4 18 The saturation constant (corresponding to the critical gas phase concentration) for the single gases were calculated to be 55 ppm for H_2S,10 ppm for MT, and 10 ppm for DMS The inlet gas was then changed over to a second gas, i e different to the one that the peat bed was acclimatised on, to see what effect bed acclimatisation had on the elimination capacity It was found that H_2S and MT were eliminated by peat beds irrespective of the original gas used to acclimatise the bed, with little affect on their maximum elimination capacity (Table 4 18) However, DMS proved to be the most difficult gas to be eliminated by the biofilters There was poor elimination of DMS on MT or H_2S acclimatised beds It was concluded that DMS could only be eliminated on beds initially acclimatised on DMS

Hirai *et al* (50) proceeded to compare the elimination of co-supplied gases (H_2S and MT, MT and DMS, and DMS and H_2S) to their elimination as single gases on the same gas-acclimatised beds as the previous experiment The results are presented in Table 4 19

Table 4.18 **The Elimination of H_2S, MT and DMS Supplied as Single Gases to Acclimatised Peat Beds (50)**

Gas peat acclimatised on	Elimination rate of single gas (g-S kg^{-1} day^{-1})		
	H_2S	MT	DMS
H_2S	5 0	0 4	0
MT	4 8	0 9	0
DMS	4 6	1 3	0 38

Note Acclimatisation conditions
H_2S 80-150 ppm, space velocity 90 h^{-1}, load 2-3 63 g-S kg^{-1} day^{-1}
MT 3 33-46 1 ppm, space velocity 30 h^{-1}, load 0 0282-0 390 g-S kg^{-1} day^{-1}
DMS 5 05-57 1 ppm, space velocity 30 h^{-1}, load 0 0468-0 535 g-S kg^{-1} day^{-1}

Table 4.19 **The Influence of Acclimatisation on the Elimination of Mixed Gases Supplied to a Peat Biofilter (50)**

Gas peat acclimatised on	Maximum elimination of mixed gases (g-S kg^{-1} day^{-1})					
	H_2S and MT		MT and DMS		DMS and H_2S	
H_2S	H_2S	4 0			H_2S	5 3
	MT	0 8			DMS	0
MT	MT	0 5	MT	0 6		
	H_2S	4 1	DMS	0		
DMS			DMS	0 17	DMS	0 31
			MT	1 1	H_2S	4 2

The results presented in Table 4 19 can be summarised as follows

(i) on H_2S-acclimatised peat, it was observed that for the mixture of H_2S and MT both gases were eliminated at about 80 % of their individual elimination values, with saturation constants of 64 ppm for H_2S and 35 ppm for MT For the H_2S and DMS mix, there was negligible removal of DMS and only a slight change in the removal rate and saturation constant for H_2S elimination,

(ii) on the MT-acclimatised peat, the co-supply of H_2S and MT showed a 43 % decrease in the elimination of MT and a smaller decrease (18 %) in the elimination of H_2S compared to the H_2S-acclimatised peat The saturation

constants were calculated to be 113 ppm for H_2S, and 21 ppm for MT For the mixture of MT and DMS, there was negligible elimination of DMS,

(iii) on DMS-acclimatised peat, for the supply of DMS and H_2S, the removal of H_2S had little influence on the removal of DMS For the MT and DMS gases, MT was removed at a similar rate to that of the single gas supply of MT on DMS-acclimatised peat There was up to a 39 % decrease in the elimination of DMS

Hirai *et al* (50) explain their results by suggesting that different bacterial populations with different substrate specificities in the acclimatised beds were responsible for the elimination of the gases Thus, for example, the dominant bacteria in the H_2S-acclimatised bed could eliminate both H_2S and MT but not eliminate DMS because it could only oxidise S-H groups DMS proved to be the most difficult gas to be removed and was influenced by the presence of other gases The overall order of decreasing biodegradability was established to be H_2S > MT > DMS

The removal of DMDS was examined by Cho *et al* (55) using a peat biofilter seeded with aerobically "digested night sludge" For a loading of 36 m^3 m^{-2} h^{-1} and a DMDS concentration of 5 to 40 ppm a maximum removal rate of 0 68 g-S kg^{-1} h^{-1} was calculated The saturation constant was determined to be 1 ppm Cho *et al* concluded that species such as *Thiobacilli* were responsible for the degradation of the DMDS

Cho *et al* (51) identified the dominant bacterial strain from H_2S-acclimatised peat isolated from Hirai *et al* (50) as *Thiobacillus* sp strain HA43 Biofilters seeded with strain HA43 began removing H_2S immediately, and had an increased elimination capacity for H_2S (up to a 6 fold increase for seeded beds compared to non seeded beds), and MT compared to the results obtained by Hirai *et al* (50), see Table 4 20 But strain HA43 was found not to be able to degrade either DMS or DMDS

Table 4 20 The Elimination of H_2S and MT by a Biofilter Seeded with *Thiobacillus* sp HA43 (51)

Maximum elimination capacity (g-S kg^{-1} day^{-1})			
As single gases		As mixed gases	
H_2S	MT	H_2S	MT
11 3-33 0	0 21-0 27	8 6	0 25

Cho *et al* (53,57,58) report on work carried out with a *Xanthamonas* species with high capacity for oxidising H_2S The microbium isolate, *Xanthomonas* strain DY44, was proposed as a good candidate for H_2S removal because

(i) it has a faster growth rate (thus, shorter acclimatisation time) compared to most of the other known H_2S degrading microbial strains,

(ii) the final end products of H_2S oxidation are polysulphates and not sulphates Thus, pH drops in the bed are not as severe, avoiding adverse effects on microbial activity,

In batch cultures and in biofilter systems strain DY44 was found to eliminate H_2S at a rate of 3 92 mmol g^{-1} (dry cells) h^{-1}, irrespective of the presence of other gases such as MT, DMS and DMDS In a paper which is discussed below Cho *et al* (53) used *Xanthomonas* strain DY44 as part of a mixed culture systems for the elimination of a mixture of sulphur compounds

The most difficult gas to remove by biofiltration has been DMS particularly in the presence of other sulphur compounds such as H_2S or MT To improve the removal of DMS from biofilters, Zhang *et al* (35) isolated the bacterium *Hyphomicrobium* sp strain I55 from a DMS-acclimatised peat bed A biofilter seeded with strain I55 was capable of degrading DMS supplied as a single gas at a maximum rate of 0 59 g-S kg^{-1} (dry peat) day^{-1}, and a saturation constant of 6 3 ppm The maximum elimination rate of this biofilter seeded with strain I55 was an increase of 1 5 fold over the removal of DMS by the biofilter seeded with digested sludge studied by Hirai *et al* (50) On beds acclimatised with DMS, strain I55 rapidly eliminated either H_2S or MT when supplied as single gases to the bed But, with the re-introduction of DMS, a lag time of up to a day was observed before DMS elimination occurred However, it was found that DMS removal by strain I55 was inhibited when H_2S and MT were also present in the gas supply to the biofilter This was explained in terms of the pathway of dimethyl sulphoxide (DMSO) metabolism by *Hyphomicrobium* sp , which is simplified as follows

$$DMSO \rightarrow DMS \rightarrow MT \rightarrow H_2S \rightarrow \rightarrow SO_4^{2-}$$

The above biochemical pathway shows that both MT and H_2S are further down the degradative pathway than DMS Thus, strain I55 would favour the degradation of either H_2S of MT before DMS The use of *Hyphomicrobium* strain I55 as part of a mixed culture seeded onto a biofilter bed for increasing the elimination of DMS in single (56), and mixed gases (53) is discussed later on in this section

Cho *et al* (53) isolated the bacterium *Thiobacillus thioparus* strain DW44 from peat previously acclimatised on DMDS (55) The gases H_2S, MT, DMS, and DMDS, were degraded by a biofilter inoculated with strain DW44 when supplied as single gases, the results are presented in Table 4 21 For a mixture of the three gases supplied to the biofilter, they found that H_2S and MT were completely removed However, the elimination of DMS was inhibited by the presence of MT but stimulated by the presence of H_2S

T thioparus strain DW44 was subsequently seeded onto a pilot-scale biofilter by Cho *et al* (54) to reduce odorous compounds emanating from a sewage treatment plant The removal of sulphur compounds by the biofilter was found to be very good over the trial period For a space velocity of 46 2 h^{-1} removal ratios of 99 8 % for H_2S, 99 0 % for MT, 89 5 % for DMS, and 98 1 % for DMDS were obtained (gas inlet concentrations were not stated)

Table 4.21 The Elimination of H_2S, MT, DMS, and DMDS by a Biofilter Seeded with *T. thioparus* Species DW44 (53)

Gas	Maximum elimination capacity (g-S kg^{-1} day^{-1})
H_2S	5 52
MT	1 16
DMS	0 50
DMDS	1 02

Note For singly supplied gases, H_2S supplied at a concentration of 150-200 ppm, SV 30 h^{-1}, conditions for other gases not stated

Zhang *et al* (34) isolated *Pseudomonas acidovorans* strain DMR11 from DMS-acclimatised peat, which was found to be capable of oxidising DMS Growth experiments with the bacterium showed that DMS elimination could only occur in the presence of a second carbon source such as sodium gluconate or sodium malate The removal rate of DMS in glucose medium was calculated as 1 12 $x10^{-17}$ mole $cell^{-1}$ h^{-1} The sole product of DMS oxidation was DMSO, thus strain DMR11 differed in metabolism from previous isolates which oxidised DMS to sulphate through MT and H_2S intermediates This difference in metabolism was taken advantage of by Zhang *et al* (56) to improve the removal of DMS A peat biofilter seeded with a mixture of *Hypomycrobium* sp strain 155 and *Ps acidovorans* strain DMR11 was found to have a higher removal rate for DMS than the sum of the

individual removal rates of the separate inoculants, see Table 4 22 This was due to the fact that strain DMR11 oxidised DMS to DMSO which in turn induced a much faster DMSO oxidising pathway in strain I55 than strain I55 had for DMS oxidation solely

Table 4 22 The Influence of Microbial Species on the Removal of DMS in a Biofilter (56)

Strain	Maximum elimination capacity (g-S kg^{-1} day^{-1})
I55 only	0 43
DMR11 only	0 73
I55 and DMR11	1 19

Cho *et al* (53) attempted to enhance the elimination of DMS in the presence of H_2S and MT by inoculating biofilters with combinations of different microbial species As previously stated the ability of *Hyphomicrobium* sp I55 to degrade DMS is inhibited by the presence of H_2S or MT (35) To overcome this inhibition, and thus, to improve the removal of DMS in mixed gas supplies, Cho *et al* combined I55 with *Thiobacillus* sp HA43 or with *Xanthomonas* sp DY44, both of which are only capable of degrading H_2S or MT The general conclusion is that the presence of either strains HA43 or DY44 with I55 enhances the removal of all three gases, but in particular the removal of DMS is greatly increased, see Table 4 23 The DMS removal rate of 0 091 g-S kg^{-1} day^{-1} by strain I55 alone was most closely approached by the value of 0 801 g-S kg^{-1} day^{-1} by the mixed culture of I55 and DY44

Table 4 23 A Comparison of the Removability of H_2S, MT, and DMS By Strain I55 Alone and With Either Strain HA44 or DY44 (53)

Gas	Load	Maximum elimination capacity (g-S kg^{-1} day^{-1})			
	g-S kg^{-1} day^{-1}	I55	I55 Single[a]	I55, DY44	I55, HA44
H_2S	0 586	0 545	0 513	0 584	0 586
MT	0 145	0 096	0 131	0 136	0 125
DMS	0 093	0 023	0 091	0 081	0 049
Total	0 827	0 664	0 735	0 801	0 760

Note [a] I55 single gas supply removal rates

A second attempt to improve the removal of DMS in mixed gas supplies by Cho *et al* (53) was not as successful *Thiobacillus thioparus* stain DW44, a second species able to degrade DMS in single gas supplies was mixed with *Xanthomonas* sp DY44 Again the objective was for strain DY44 to remove H_2S and MT and allow DW44 to eliminated DMS However, the removal of all the three gases in the mixed culture system could only be attributed to strain DY44, the presence of strain DW44 had no influence on gas removal It was concluded that the presence of H_2S and MT inhibited the ability of DY44 to remove DMS

4 6 Summary

There is an increasing need to control the emissions of waste gases from industrial and agricultural sources Such waste gases contain contaminants which may pose a general nuisance value or could pose a serious health risk to local populations There are several methods available for the treatment of waste gases, but increasingly to-day biological methods of waste gas treatment are favoured Among the biological methods available is biofiltration, which consists of a filter bed of material inhabited by micro-organisms As the waste gas flows through the filter bed the gaseous contaminants are simultaneously absorbed by the filter material and degraded by the micro-organisms which use the contaminants as a carbon and/or energy source In the case of organic compounds, the contaminants are ultimately degraded to CO_2 and H_2O

There are several parameters which govern the efficient operation of a biofilter, these include the temperature, pH, moisture content, loading and filter type of material In the case of the filter material, materials such as peat fibre or heather are favoured because of their fibrous nature which resist compacting

A wide variety of VOCs and to a lesser extent VICs can be eliminated by biofilters The efficiency of elimination of VOCs is dependent on their biodegradability VOCs such as alcohols, esters and ketones which have high aqueous solubilities are readily eliminated within the biofilter In contrast VOCs with low water solubilites, particularly chlorinated organic compounds, are poorly eliminated The elimination of very slowly degraded compounds can be increased by seeding the biofilter with micro-organisms which have been isolated and identified as having a greater ability to degrade the compound in question

4.7 Aims of Experimental Work

The aim of this work was to set up a lab-scale biofilter for the elimination of ethanol vapour from an artificial waste gas stream The filter material used was peat fibre which is used by Bord na Mona as part of the mix of filter material in its BioPure^{TM} biofiltration system (the other components used consist of heather and buffering materials) The choice of ethanol as the organic vapour to be eliminated was based partly on its availability and because it is a relatively biodegradable compound which would pose no difficulty to the micro-organisms inhabiting the peat bed

4.7.1 Experimental Details

(a) Biofiltration Apparatus and its Operation

The biofiltration apparatus used in the experiment was comprised of two units, the biofilter itself and a solvent vaporiser unit, see Figure 4 7 Both of these units were made of glass, and teflon tubing and fittings were used throughout the apparatus The biofilter unit consisted of a cylindrical column, with an internal diameter of 0 095 m, and a total unit height of about 0 60 m (the actual height of the biofilter column occupied 0 35 m of this) A glass sintered plate was positioned about 10 cm above the base of the unit The function of the plate was to support the peat bed while allowing excess water to drain from the peat A water sprinkling unit was positioned above the top of the bed for the periodic addition of water Air inlet and outlet taps were located at the bottom and top of the unit respectively Thus, the artificial gas stream entered at the base of the biofilter, passed up through the filter bed and exited at the top

The vaporiser unit was packed with 5A molecular sieve which was saturated with liquid ethanol A lagging jacket surrounding the vaporiser was connected to a low temperature circulator (LTC) This allowed the temperature of the unit to be varied from -60° to 20°C The air entered at the base of the vaporiser unit and became saturated with ethanol vapour as it passed up through the molecular sieve bed The concentration of the ethanol vapour was controlled by varying the temperature of the vaporiser unit with the LTC Once the desired ethanol concentration had been established the artificial gas stream was switched onto the biofilter line

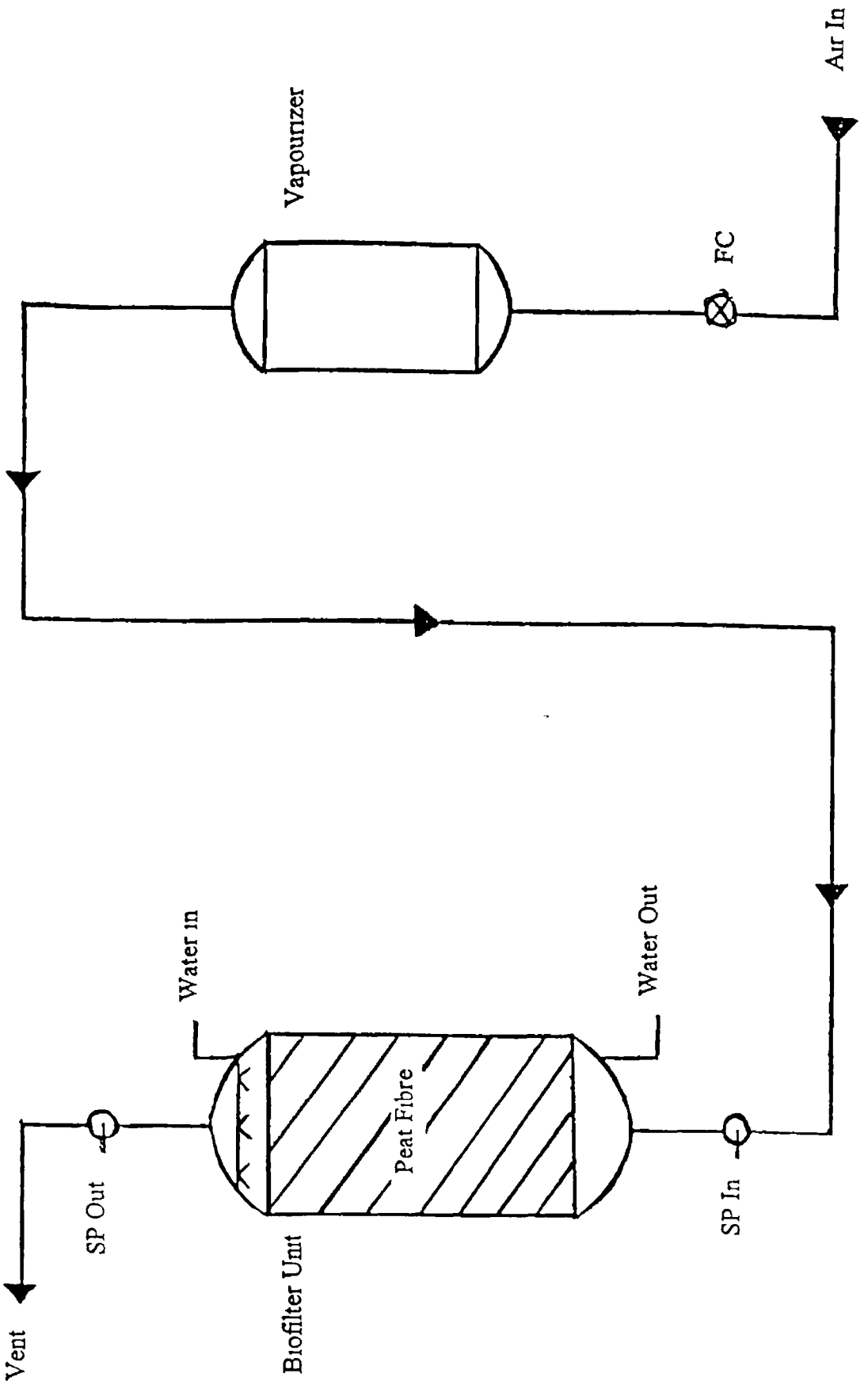

Figure 4.7 Schematic Diagram of the Biofiltration Apparatus used for the Elimination of Vaporous Ethanol

The peat fibre used in the biofilter has been previously described in Section 2 5 2 The peat material was used as supplied by Bord na Mona, the only pre-treatment carried out on the peat before packing the bed was to gently thrash it to remove any fine materials present This was done to prevent the fine materials from clogging the sintered glass support during the operation of the biofilter The biofilter column was then packed with the peat to a bed height of about 0 35 m, which corresponded to a density of 117 29 kg (dry weight) m^{-3} The air flow through the biofilter was adjusted by means of a mass flow controller (FC) to 40 ± 1 cm^3 min^{-1} as measured at the biofilter exit During the course of the experiment the temperature of the biofilter varied from 18° to 25°C

A Perkin-Elmer GC F11 incorporating an FID was used to measure the vapour concentration of ethanol at the inlet and outlet gas sampling ports (SPin and SPout respectively in Figure 4 7) The GC column used was 5 % DC-710 liquid stationary phase on Chromosorb W AW The GC conditions used were nitrogen carrier gas flow rate 40 ± 1 cm^3 min^{-1}, injection block setting 3½, attenuation 1 x 10^4, and oven temperature 100°C The ethanol concentration was measured periodically as follows a gas sampling bulb, c 600 cm^3 volume, was connected to one of the gas sampling ports (SPin, SPout) of the biofilter and the diverted air stream allowed to flow through the bulb for about 10 minutes The bulb was then sealed and transferred to the GC unit, then using a gas-tight syringe, gas volumes of 0 5 cm^3 were injected onto the GC column, the chromatographic peaks were recorded using a chart recorder The concentration of the ethanol was determined by reference to a calibration curve of peak height versus vapour concentration

(b) <u>Humidity, pH, and Biological Measurements</u>

Peat samples were taken from the top of the peat bed and tested for humidity, pH, and microbial cell numbers The humidity and pH measurements were carried out as previously described in Section 2 5 2 The microbial counts were carried out by the School of Biological Sciences at DCU, the procedure was as follows One gram of the fresh peat sample was stirred in 100 cm^3 of Ringer's solution for about 5 minutes The solution was then diluted decimally from 10^{-3} to 10^{-5}, and 1 cm^3 aliquots of each dilution was plated out on petridishes For bacterial selection the media used was PCA containing 0 2 mg cm^{-1} cyclohexamid For the selection of fungi, MEA containing 0 1 mg cm^{-1} chloramphenicol was used Samples were incubated for 3 days at 20°C for bacteria and 25°C for fungi, before cell numbers were counted The microbial cell numbers were expressed as number of colony forming units per gram of fresh peat fibre

4 7 2 Results and Discussion

The biofilter was in operation for a total of 1897 hours, or 79 days The parameters of the biofilter and the initial conditions of the peat fibre used are presented in Table 4 24

Table 4 24 The Biofilter and the Fibrous Peat Parameters at the Start of the Experimental Run

Parameter	Value
Biofilter	
Biofilter bed height	0 350 m
Internal diameter	0 095 m
Bed volume	2 481 x 10^{-3} m^{-3}
Bed temperature	20°C
Peat	
Humidity	52 4 %
pH	4 3 ± 0 2
Amount of peat used	0 550 kg (fresh weight)
	0 291 kg (dry weight)
Packing density of peat	221 68 kg (fresh) m^{-3}
	117 29 kg (dry) m^{-3}
Air flow rate	2 4 x10^{-3} m^3 h^{-1}
Filter volume load (space velocity)	0 967 m^3 m^{-3} h^{-1}
Inlet ethanol concentration (initial)	39 2 ± 1 8 g m^{-3}

The air flow rate was set at 2 4 x10^{-3} m^{-3} h^{-1} (40 cm^3 min^{-1}) which corresponded to a space velocity (SV) of slightly less than 1 m^3 m^{-3} h^{-1} This SV value is quite low when compared to the typical SV values of 50 to 300 m^3 m^{-3} h^{-1} which are cited in the literature (12) However, it was not feasible to achieve higher volume flow rates in this experimental set up

The results of the biofilter experiment are presented in Table 4 25, and a breakthrough curve for the ethanol are shown in Figure 4 8

Table 4 25 **The Results for the Elimination of Vapour Phase Ethanol by the Peat Biofilter**

Hours running	Inlet[a]	Outlet[a]
2	40 1 (4 7)	0
3	39 8 (4 3)	-
21	38 8 (5 9)	0
26	-	0
46	36 9 (5 5)	0
69	37 2 (4 0)	0
74	-	0
76	-	0
81	42 2 (5 6)	0
98	-	0
100	39 1 (7 2)	-
104	63 3 (5 6)	-
126	67 7 (10 3)	0
148	59 3 (5 3)	0
220	62 8 (7 1)	0
227	63 7 (5 4)	0
244	60 8 (7 1)	0
250	80 5 (4 7)	0
254	82 3 (5 8)	-
270	81 7 (6 8)	0
296	-	0
298	82 0 (9 0)	-
318	71 9 (5 6)	0
390	66 8 (8 2)	0
414	69 2 (6 1)	0

Hours running	Inlet[a]	Outlet[a]
438	79 1 (7 3)	0
442	71 2 (6 1)	-
460	69 3 (5 6)	0
486	-	0
487	72 2 (6 9)	0
558	83 8 (9 3)	0
584	63 5 (5 6)	0
607	68 4 (6 6)	0
630	-	0
654	-	0
726	75 3 (5 7)	0
772	74 1 (5 5)	0
894	72 5 (5 1)	0
966	-	6 1 (3 3)
990	-	7 3 (4 6)
1062	74 1 (8 7)	9 8 (3 7)
1132	-	14 3 (2 7)
1229	76 3 (5 4)	11 2 (0 7)
1253	-	13 4 (4 2)
1282	79 1 (6 3)	10 4 (4 0)
1326	-	10 9 (4 6)
1569	77 4 (7 3)	13 6 (5 4)
1729	96 4 (4 5)	12 5 (6 2)
1897	77 3 (5 6)	17 3 (4 0)

Note [a] Inlet and outlet values are in g m^{-3}, values in parentheses are ± values

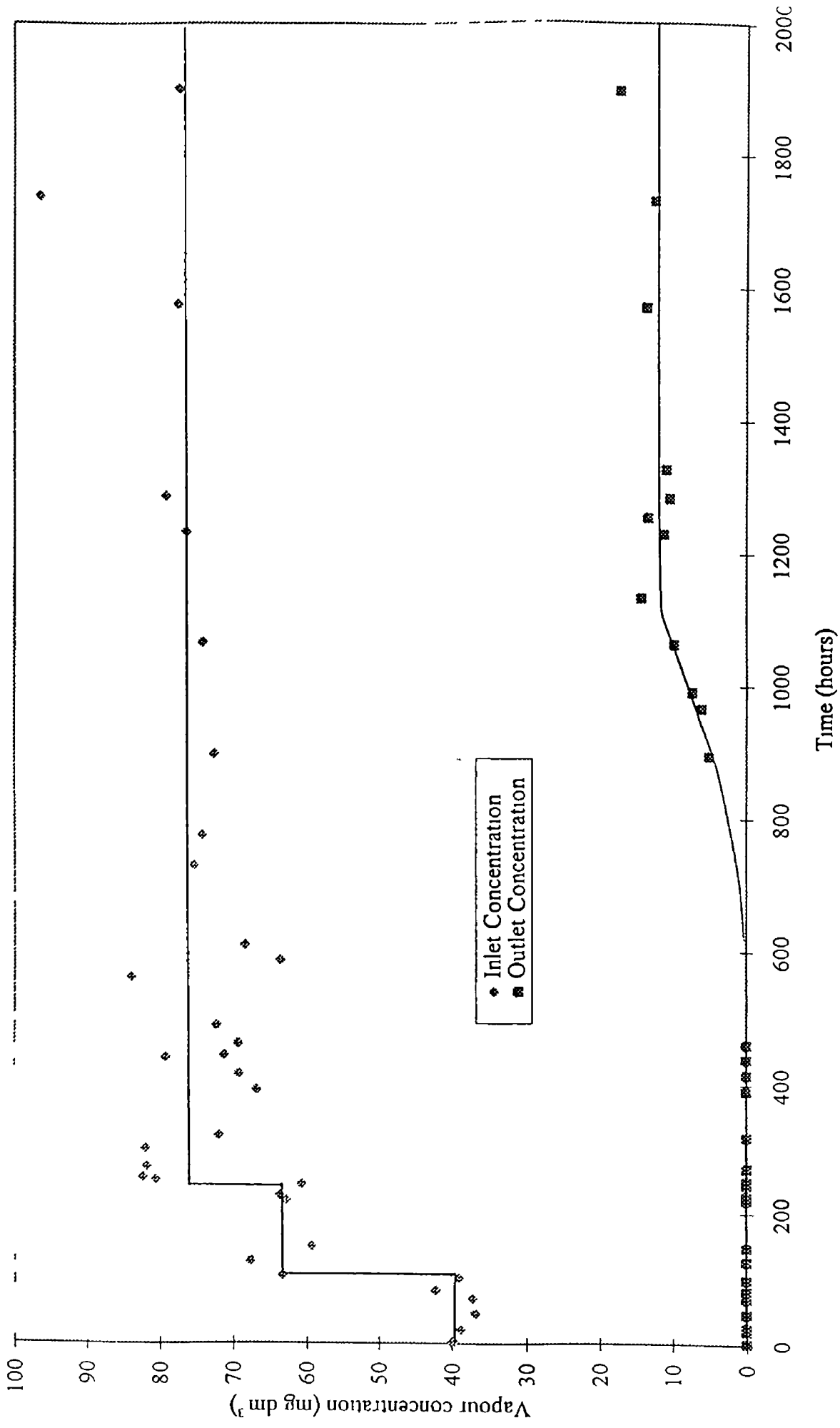

Figure 4.8 The Breakthrough Curve for Ethanol Removal by the Peat Biofilter

The mean value for the initial concentration of the ethanol vapour entering the biofilter was 39 2 ± 1 8 g m^{-3}, corresponding to a loading of about 38 g m^{-3} h^{-1} After 100 hours of operation no ethanol vapour was detected in the gas stream exiting the biofilter, see Figure 4 8 Therefore, the inlet concentration was increased at this time to 62 9 ± 2 9 g m^{-3}, and further increased to 75 9 ± 7 0 g m^{-3} after 250 hours of operation This final inlet concentration was maintained to the end of the run Breakthrough of the ethanol vapour was detected at the exit of the biofilter after 486 hours of operation Over the next 700 hours the outlet concentration of the ethanol gradually increased and eventually levelled of to a steady state value after about 1200 hours of operation The outlet concentration remained at about 12 6 ± 2 3 g m^{-3} until the end of the experimental run after 1900 hours of operation

The elimination capacity, and the percentage elimination capacity of the biofilter were calculated using Equations 4 2 and 4 3, see Table 4 26 From a graph of the elimination capacity of the biofilter as a function of the inlet concentration (Figure 4 9), the maximum elimination capacity of the biofilter was tentatively determined to be about 61 g m^{-3} h^{-1}, and the critical gas concentration to be about 60 g m^{-3} The maximum elimination value reported here is in good agreement with the elimination capacity of 57 g m^{-3} h^{-1} for ethanol reported by Ottengraf *et al* (17)

Above the critical gas concentration the biofilter was operating at its maximum elimination capacity, which has been previously described by Ottengraf *et al* (24) The biodegredation of the ethanol was at its maximum, and a further increase in the inlet concentration to the bed did not lead to an increase in the elimination capacity Below 60 g m^{-3} the biofilter was operating in its linear range, the elimination capacity being controlled by the rate of transfer of the ethanol to the biolayer

Table 4 26 **Elimination Capacity of the Biofilter as a Function of Specific Filter Loading**

Inlet concentration	Elimination capacity	
g m^{-3}	g m^{-3} h^{-1}	%
39 2	37 9	100
62 9	60 8	100
75 9	61 2	83 4

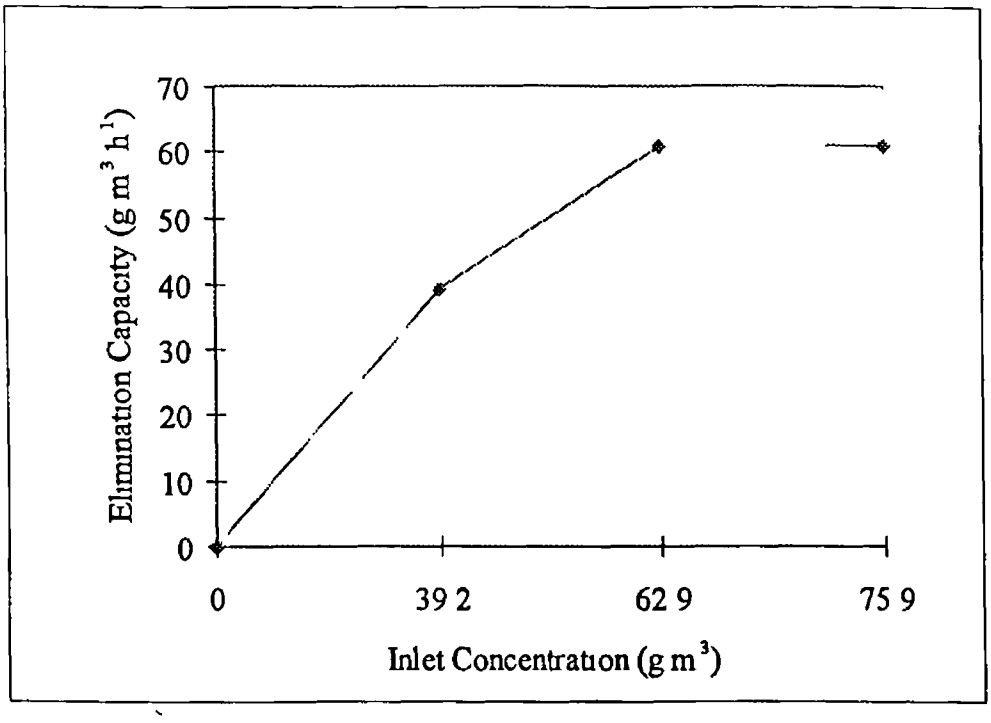

Figure 4.9 The Elimination Capacity of the Biofilter for the Removal of Ethanol as a Function of The Ethanol's Inlet Concentration Note, flow rate was 2 4 x10^{-3} m^3 h^{-1}

Physical parameters were determined at the start of the experimental run and after 1300 hours of operation The results are shown in Table 4 27

Table 4 27 The pH, Humidity, and Microbial Numbers During the Course Of the Experimental Run

Hours	Microbial numbers x10^6 cells g^{-1}		Humidity	pH
	Bacteria	Fungi	%	
Start up	2 31	1 97	52 4	4 3
1300	2 27	2 68	70 0	4 2

Two observations on the results presented in Table 4 27 can be made and are as follows

(i) the overall numbers of micro-organisms present remain at about $x10^6$ cells per gram, this value is low when it is considered that cell numbers of 10^9 to 10^{11} cells per gram have been reported elsewhere (18,46) The bacterial cell numbers remain virtually unchanged from the start up of the biofilter to 1300 hours, when equilibrium conditions within the bed were established Over the same time period there was only a 1 4 fold increase in the numbers of fungi present,

(ii) the levels of fungi and bacteria in the biofilter were similar, in mixed populations of bacteria and fungi, it is expected that bacteria should greatly out-number the levels of fungi present in the bed (59)

Both observations may be attributed to the low pH of the peat bed, which remained at about pH 4 3 during the operation of the biofilter It is possible that the acidity of the peat inhibited the growth of the bacteria, while encouraging the growth of fungal species This conclusion is supported by Wada *et al* (48) who reported that increasing acidity levels in the peat bed caused the bacterial cell numbers to decrease dramatically once the pH of the bed fell below pH 3 Weckhuysen *et al* (23) reported that the addition of inorganic nutrients to a wood bark biofilter for the elimination of butanal increased the elimination efficiency by 11 % In this study no such nutrient was added to the biofilter during the course of the experiment Therefore, it is also possible that the low cell numbers may be due to a lack of inorganic nutrients which are required by the ethanol degrading micro-organisms

The degradation of the ethanol within the biofilter was assumed to be due to the action of the micro-organisms inhabiting the peat bed, and that the ethanol was ultimately oxidised to the mineral end products H_2O and CO_2 The similar levels of fungi and bacteria which were measured once equilibrium had been reached in the biofilter, would suggest that the elimination of the ethanol was most likely due to a heterogeneous population of micro-organisms which may have included both bacteria and fungi

It was noted that as the experiment progressed there was an increase in the numbers of small animals such as worms and insects in the peat bed The development of such a micro-ecology within the bed was expected to occur, and indeed, is considered to be advantageous in the operation of the biofilter (59) It has been suggested that the presence of small animals grazing on the biolayer prevent its overgrowth, and as a result clogging of the filter bed is prevented and the back pressure of the bed is kept low

The maximum elimination capacity of the biofilter could be raised by increasing the cell numbers present in the bed The two most obvious conditions which can be changed to improve the elimination capacity are the pH of the peat, and the addition of inorganic nutrients to the biofilter The pH can be increased to a more favourable level by mixing the peat with basic materials such as $CaCO_3$, or NaOH, at the time of start up of the biofilter The ideal pH for the biofilter would probably be about pH 7 (2, 59) At this pH value the largest increase in cell numbers would be expected to be among the bacteria which out-compete the fungi at higher pHs The addition of inorganic nutrients to the bed would also increase the cell numbers This has been demonstrated by Weckhuysen *et al* (23), the addition of inorganic nutrients can result in a marked increase in the elimination capacity of the biofilter

4.7 3 Conclusion

In summary, this study demonstrated that ethanol vapour can be removed readily and continuously from an artificial gas stream passing through a peat biofilter The elimination of the ethanol from the gas stream was assumed to be due to its degradation by the micro-organisms inhabiting the peat bed, and that the ethanol was ultimately converted to H_2O and CO_2 The maximum elimination capacity of the biofilter was calculated to be c 61 g m^{-3} h^{-1}, and the critical gas concentration to be c 60 g m^{-3} The low pH of the bed was considered to strongly influence the growth of the micro-flora The acidic nature of the unadjusted peat used was concluded to inhibit the growth of the bacteria while favouring the growth of fungi during the operation of the biofilter

4 8 References

(1) Bohm, H , Chem. Engineering Progress, 88(4), 34-40 (1992)

(2) Leson, G and Winer, A M , J. Air Waste Manage. Assoc., 41(8), 1045-1054 (1991)

(3) Pomeroy, R D , Journal WPCF, 54(12), 1541-1545 (1982)

(4) Dalouche, A , Gillet, M , Lemasle, M , Martin, G and Orain, L (in French), Pollution Atmospherique, 92, 317-322 (1981)

(5) Koch, W, "Findings with operation of biofilters for reduction of odour-intensive emissions" (original in German), Die Fleischmehl-Indusrtie, 8, 165-175 (1982)

(6) Shoda, M , in Biological Degredation Of Wastes, Martin, A M (Ed), Elsevier Applied Science, pp 31-46 (1991)

(7) Van Langenhove, H , Bendinger J K and Oberthur, M C , "Organic Sulphur Compounds Persistent Odurants in the Biological Treatment of Waste Gas", In Dragt, A J , van Ham, J (Eds), Biotechniques For Air Pollution Abatement And Odour Control Policies, Elsevier Science Publishers, 177-182 (1992)

(8) Kiss, A and Shelton, Manual Of Environmental Law, Grotius Publications, pp 331-392 (1993)

(9) Ottengraf, S P P , TIBTEC, 5, 132-136 (1987)

(10) Ottengraf, S P P and Diks, R M M , In Dragt, A J , van Ham, J (Eds), Biotechniques For Air Pollution Abatement And Odour Control Policies, Elsevier Science Publishers, 17-31 (1992)

(11) Cesario, M T , Beeftink, H H and Tramper, J , "Biological treatment of waste gases containing poorly water soluble pollutants", In Dragt, A J , van Ham, J (Eds), Biotechniques For Air Pollution Abatement And Odour Control Policies, Elsevier Science Publishers, 135-140 (1992)

(12) VDI-3477 (in German and English), Biologische Abgas-/Abluftreinigung-Biofilter (Biological Waste Gas/Waste Air Purification-Biofilters, Verein Deutscher Ingenieure, Dusseldorf (1991)

(13) van Langenhove, H , Wuyts, E and Schamp, N , Water Res., 20(12), 1471-1476 (1986)

(14) Lehtomaki, J , Torronen, M and Laukkarinen, A , "A feasibility study of biological waste-air purification in a cold climate", In Dragt, A J , van Ham, J (Eds), Biotechniques For Air Pollution Abatement And Odour Control Policies, Elsevier Science Publishers, 131-134, (1992)

(15) Hartmans, S , Tramper, J and de Bont, J A M , European Congress on Biotechnology, 5, 659-662 (1990)

(16) Ottengraf, S P P, "Exhaust Gas Purification", In Rehm, H-J, Reed, G (Eds), Biotechnology, VCH Verlagsgesellschaft, Weinheim, 8, 425-452 (1986)

(17) Ottengraf, S P P, Meesters, J J P, van den Oever, A H C and Rozema, H R, Bioprocess. Bioengineering, 1, 61-69 (1986)

(18) Togashi, I, Suzuki, M, Hirai, M, Shoda, M and Kubota, H, J. Ferment. Technol., 64(5), 425-432 (1986)

(19) Zeisig, H D, "Experiences with the use of biofilters to remove odours form piggeries and hen houses", In Nicsen, V C, Voorburg, J H, L'Hermite, P (Eds), Volatile Emissions From Livestock Farming And Sewage Operations, Elsevier Applied Science, London/New York (1988)

(20) Don, J A, VDI Berichte, 561, 63-73 (1985)

(21) Cox, H H J, Houtman, J H M, Doddema, H J and Harder, W, Biotechnology Letters, 15(7), 737-742 (1993)

(22) van Lith, C, "Designe criteria for biofilters", in Air and Waste Management Association, 82nd Annual Meeting and Exhibition, Anaheim, California, June 25-30, 2-13 (1989)

(23) Weckhuysen, B, Vriens, L and Verachter, H, Appl. Microbiol. Biotechnol., 39, 395-399 (1993)

(24) Ottengraf, S P P and Disks, R, Chimicaoggi, 8(5), 41-45 (1990)

(25) Dragt, A J, Jol, A and Ottengraf, S P P, In Neijssel, O M, van der Meer, R R, Luyben, K C A M (Eds), Proc. 4th Euro. Congrs. on Biotechnology, Elsevier Science Publishers, 2, 600-603 (1987)

(26) Furusawa, N, Togashi, I, Hirai, M, Shoda, M and Kubota, H, J.Ferment. Technol, 62(6), 589-594 (1984)

(27) Ottengraf, S P P, Graafland, T F and Dragt A J, In Neijssel, O M, van der Meer, R R, Luyben, K C A M (Eds), Proc 4 th European Congress on Biotechnology, Elsievier Science Publishers, 2, 596-599 (1987)

(28) van Langenhove, H, Lootens, A and Schamp, N, Water, Air and Soil Pollut., 47, 81-86 (1989)

(29) Alexander, M, Science, 211, 132-138 (1981)

(30) Sly, L I, Bryant, L J, Cox, J M and Anderson, J M, Appl Microbiol Biotechnol., 39, 400-404 (1993)

(31) Cox, H H J, Houtman, J H M, Dodderma, H H and Harder, W, Appl. Microbiol. Biotechnol, 39, 372-376 (1993)

(32) Zilli, M, Converti, A, Lodi, A, del Borghi, M and Ferraiolo, G, Biotechnology and Bioengineering, 41, 693-699 (1993)

(33) Plas, C, Wimmer, K, Holubar, P, Mattanovich, D, Danner, H, Jelinek, E, Harant, H and Braun, R, Appl. Microbiol. Biotechnol, 38, 820-823 (1993)

(34) Zhang, L., Kuniyoshi, I., Hirai, M. and Shoda, M., Biotechnology Letters, 13(3), 223-228 (1991).

(35) Zhang, L., Hirai, M. and Shoda, M., J. Ferment. Bioengineering, 72(5), 292-296 (1991).

(36) Ottengraf, S. P. P. and van den Oever, A. H. C., Biotechnology and Bioenginering, 25, 3089-3102 (1983).

(37) Jol, A. and Dragt, A. J., DECHEMA Biotechnology Conference, 2, 373-389 (1988).

(38) Shareefdeen, Z., Baltzis, B. C., Oh, Y.-S. and Bartha, R., Biotechnology and Bioengineering, 41, 512-524 (1993).

(39) Beerli, M. and Rotman, A. "Use of peat biofilter for the removal of organic solvent odors", in "Peat As A Raw Material", Fuchsman, C. H., (Ed.), Proceecings of a Seminar At Bord na Mona, New Bridge, Co. Kildare, 24-25 May, 55-83 (1990).

(40) Cox, H. H. J., Doddema, H. J. and Harder, W., Med. Fac. Landbouww.Univ. Gent, 58(4a), 1741-1748 (1993).

(41) Salemink, R., Med. Fac. Landbouww. Univ. Gent, 56(4a), 1535-1541, (1991).

(44) Hartmans, S., Kaptein, A., Tramper, J. and de Bont, J. A. M., Appl. Microbiol. Biotechnol., 37, 796-801 (1992).

(45) Van Langenhove, H., Lootens, A. and Schamp, N., Med. Fac. Landbouww. Univ. Gent, 53(4b), 1963-1969 (1988).

(46) Martin, G., Lemasle, M. and Le Cloirec, P. "The use of peat to deodorise industrial and animal wastes in the presence and absence of large bacterial populations", in "Peat As A Raw Material", Fuchsman, C. H., (Ed.), Proceecings of a Seminar At Bord na Mona, New Bridge, Co. Kildare, 24-25 May, 84-100 (1990).

(47) Charbonnier, M. and Blesson, G. (in French), Fonderie-Fondeur D'Aujourd'hui, 59, 7-11 (1986).

(48) Wada, A., Shoda, M., Kubota, H., Kobayashi, T., Katayama-Fujimura, Y., and Kuraishi, H., J. Ferment. Technol., 64(2), 161-167 (1986).

(49) Clark, R. C. and Wnorowski, A. U. "Biofilters for sewer pump stations: influence of matrix formulations on the capacity and efficiency of odorant removal by an experimental biofilter", In: Dragt, A. J., van Ham, J. (Eds.), Biotechniques For Air Pollution Abatement And Odour Control Policies, Elsevier Science Publishers, 183-186 (1992).

(50) Hirai, M., Ohtake, M. and Shoda, M., J. Ferment. Bioengineering, 70(5), 334-339 (1990).

(51) Cho, K.-S., Zhang, L., Hirai, M. and Shoda, M., J. Ferment. Bioengineering, 71(1), 44-49 (1991).

(52) Cho, K -S , Hırai, M and Shoda, M , J. Ferment. Bioengineering, 71(6), 384-389 (1991)
(53) Cho, K -S , Hırai, M and Shoda, M , J. Ferment. Bioengineering, 73(3), 219-224 (1992)
(54) Cho, K -S , Hırai, M and Shoda, M , J. Ferment. Bioengineering, 73(1), 46-50 (1992)
(55) Cho, K -S , Hırai, M and Shoda, M , J. Ferment. Bioengineering, 71(4), 289-291 (1991)
(56) Zhang, L , Hırai, M and Shoda, M , J. Ferment Bioengineering, 74(3), 174-178 (1992)
(57) Cho, K -S , Kunıyoshı, I , Hırai, M and Shoda, M , Biotechnology Letters, 13(12), 923-928 (1991)
(58) Cho, K -S , Hırai, M and Shoda, M , Appl. Environ. Microbiol., 58(4), 1183-1189 (1992)
(59) Bord na Mona, personal communication

Appendix A Common Names and Chemical Names for Organic Compounds Mentioned in the Text

Common name	Chemical name
β-BHC	1,2,3,4,5,6-Hexachloro-cyclohexane, β isomer
2,4-D	2,4-Dichlorophenoxy-acetic acid
Diuron	3-(3,4-Dichlorophenyl)-1,1-dimethylurea
DDT	2,2-bis (p-Chlorophenyl)-1,1-dichloroethene
DMDS	Dimethyl disulphide
DMS	Dimethyl sulphide
DMSO	Dimethyl sulphoxide
MT	Methanthiol
Lindane (also γ-BHC)	1,2,3,4,5,6-Hexachloro-cyclohexane, γ isomer
Parathion	O,O-Diethyl O-p-nitro-phenyl phosphorothioate

Appendix B Exclusion Volume and Its Relationship to the Surface Area of a Solid

The exclusion volume equation (Equation 3 10) is

$$|Z_1| C_1 V_{ex} = \frac{|Z_1| C_1 V - |Z_1| C_{01} V}{m_S} \qquad \text{Equation C 1}$$

The development of negative adsorption method from measuring the surface area is based on the additional definition

$$V_{ex} = S_E d_{ex}(c_i) \qquad \text{Equation C 2}$$

where $d_{ex}(c_i)$ is the exclusion distance, which is a function of the concentration, c_i, and S_E is the surface area from which the ion i is repelled The parameter d_{ex} is the mean distance over which the ion i is depleted near the surface of the solid It is evaluated conventionally as a function of c_i with the help of the diffuse double layer theory of a swarm of ions near a charged planar surface According to the double layer theory the surface charge density neutralised by a swam of 1 1 electrolyte ions is

$$\sigma_\delta = -\{2 \varepsilon_o DRTc[\exp(-F\psi_\delta/RT) + \exp(F\psi_\delta/RT) - 2]\}^{1/2} \qquad \text{Equation C 3}$$

where σ_δ is the surface charge density (coulombs per square metre), ε_o is the permittivity of vacuum, D the dielectric constant of liquid water, R the molar gas constant, T the absolute temperature, c is the same as c_i, F is the Faraday constant, and ψ_δ is the electric potential (volts) at the plane where the diffuse ion swarm comes into contact with the solid Often the condition $-F\psi_\delta/RT >> 1$ is met and Equation C 3 can be approximated to

$$\sigma_\delta \approx -(2\varepsilon_o DRTc)^{1/2} \exp(-F/RT) \qquad \text{Equation C 4}$$

Equation C 4 and the standard double layer relationship,

$$\sigma_\delta = \varepsilon_o D(d\psi/dx)_{x=\delta} \qquad \text{Equation C 5}$$

then lead to the differential equation

$$(d\psi/dx) = (2RTc/\varepsilon_0 D)^{1/2} \exp(-F\psi/2RT) \quad (x = \delta) \qquad \text{Equation C 6}$$

where δ is the distance between the two planes that where $\psi = -\infty$ and that where σ_δ is evaluated The solution of Equation C 6 is

$$\exp(F\psi_\delta/2RT) = F(2c/\varepsilon_0 DRT)^{1/2}\ \delta/2 \qquad \text{Equation C 7}$$

The definition of $d_{ex}(c)$ in the double layer theory is

$$d_{ex}(c) = \int_{\delta}^{\infty} [1-\exp(F\psi\,(x)/RT)]\ dx \qquad \text{Equation C 8}$$

The right hand side of Equation C 8 is the relative probability that a univalent anion will not be found at a point x near a negatively charged planar surface, integrated over all x values from δ outward Thus, the mean exclusion distance is equal to the probability that an ion is excluded from the region between x and x + dx, summed over all such regions The integral of Equation C 8 can be calculated with the help of a transformation based on Equations C 3 and C 5

$$\begin{aligned} d_{ex}(c) &= \int_{\psi_\delta}^{0} \frac{1-\exp(F\psi/RT)}{d\psi/dx}\, d\psi \\ &= 1/(\beta)^{1/2} \int_{y_\delta}^{0} \frac{(1-e^{y})\, dy}{[ce^{-y}+e^{y}-2]^{1/2}} \\ &= 1/(\beta c)^{1/2} \int_{y_\delta}^{0} e^{y/2}\, dy \\ &= 2/(\beta c)^{1/2}\ [1-\exp(y_\delta/2)] \\ &\approx 2/(\beta c)^{1/2} - \delta \end{aligned} \qquad \text{Equation C 9}$$

where $\beta = 2F^2/\varepsilon_0 DRT = 1\ 084 \times 10^{16}$ m mol^{-1} (at T = 298 15 K) and $y = F\psi$ RT The last step of calculations is made with the help of Equation C 7 The introduction of Equation C 9 into Equation C 2 produces the double layer model equation for the exclusion volume in a 1 1 electrolyte

$$V_{ex} = 2S_E/(\beta c)^{1/2} - \delta S_E \qquad \text{Equation C 10}$$

thus a plot of V_{ex} versus $c^{-1/2}$ will be a straight line with a slope proportional to the exclusion area S_E

Appendix C Derivation of the Single Point BET Method

The BET equation has the general form

$$\frac{P/Po}{V(1-P/Po)} = \frac{1}{Vm\,C} + \frac{(C-1)}{Vm\,C}\frac{P}{Po} \qquad \text{Equation B 1}$$

where V is the volume (at STP) of the gas adsorbed at pressure P, Po the saturation pressure which is the vapour pressure of liquefied gas at the adsorbing temperature, Vm the volume of gas (STP) required to from an adsorbed monolayer and C a constant related to the energy of adsorption

The surface area (S) of a solid giving the monolayer adsorbed gas volume Vm (at STP) is then calculated from

$$S = Vm\,A\,N \qquad \text{Equation B 2}$$

where A is Avogadro's number, M the molar volume of the gas and N the area occupied by each adsorbed gas molecule

For the single point surface area measurement, the constant C in Equation B 1 is recognised to be generally very large, i e $C >> 1$ Thus, Equation B 1 can be reduced to

$$\frac{P/Po}{V(1-P/Po)} = 1/Vm\ (1/C + 1/Po) \qquad \text{Equation B 3}$$

Since the term $1/(Vm/C)$ is also generally small, Equation B 3 can be further simplified to the following

$$Vm = V / (1-P/Po) \qquad \text{Equation B 4}$$

Substituting Equation B 4 into Equation B 2 yields the following equation

$$S = V\,A\,N\,\frac{(1-P/Po)}{M} \qquad \text{Equation B 5}$$

from which the surface area can be readily calculated once the volume V of gas adsorbed is determined

Appendix D Calculation of Co Values for Alcohol Vapours

The saturation pressure values for the alcohol vapours at 20°C were calculated from the vapour pressure values given in the CRC Handbook using the ideal gas equation

$$PV = nRT \qquad \text{Equation D 1}$$

where P is pressure (atm), V is volume (dm^3), n the mole fraction, R the ideal gas constant (8 2058 $x10^{-2}$ L atm mol^{-1} K^{-1}) and T the absolute temperature (K) Rearranging Equation D 1

$$n = PV/RT \qquad \text{Equation D 2}$$

the mole fraction n can be found from

$$C_0 \text{ (mg dm}^{-3}) = nM/10^{-3} \qquad \text{Equation D 3}$$

where M is the molecular weight of the alcohol The C_0 values for the alcohol vapours at 20°C were calculated to be,

Alcohol	C_0 (mg dm^{-3})
Ethanol	110 00
2-Propanol	103 96
1-Butanol	21 77
1-Pentanol	1 16

As an example, the vapour pressure of 1-pentanol at 293 K was calculated to be 0 224 mmHg This is converted to atmospheres by dividing the value by 760 mmHg (since 1 atm ~ 760 mm Hg)

$$0\ 224 / 760 = 3\ 155 \times 10^{-4} \text{ atm}$$

inserting this value into Equation D 2, and taking V to be 1 L, the mole fraction of 1-pentanol can be calculated

$$n = \frac{(3\ 155 \text{x} 10\text{-}4)(1)}{(8\ 2058 \text{x} 10\text{-}2)(293)} = 1\ 3122 \text{x} 10^{-5} \text{ moles}$$

The C_o of 1-pentanol can then be calculated by inserting the mole fraction value into Equation D 3

$$(1\ 3122\ x10^{-5})(88\ 15)/\ 10^{-3} = 1\ 16\ mg\ dm^{-3}$$

Thus, the C_o for 1-pentanol is 1 16 mg dm^{-3}